FORMATION OF CORROSION RESISTANT ORGANIC POLYMER COATINGS BY AN ELECTROCHEMICAL PROCESS

FINAL REPORT

TO

THE OFFICE OF NAVAL RESEARCH, ONR

Grant No. N00014-95-1-0485

Investigators: Jude O. Iroh and Wencheng Su
Department of Materials Science and Engineering
University of Cincinnati
Cincinnati, Ohio 45221-0012

REPORT DOCUMENTATION PAGE

Form Approved
OMB No. 0704-0188

1. AGENCY USE ONLY (Leave blank)	2. REPORT DATE	3. REPORT TYPE AND DATES COVERED
	June 24, 1999	Final 6/1/95 - 2/28/99

4. TITLE AND SUBTITLE
"Formation of Corrosion Resistant Organic Polymer Coatings by an Electrochemical Process"

5. FUNDING NUMBERS
N00014-95-1-0484

6. AUTHOR(S)
Jude O. Iroh, Wencheng Su

7. PERFORMING ORGANIZATION NAME(S) AND ADDRESS(ES)
Dept. of Materials Science and Engineering
University of Cincinnati
P.O. Box 210012
Cincinnati, OH 45221-0012

8. PERFORMING ORGANIZATION REPORT NUMBER

9. SPONSORING/MONITORING AGENCY NAME(S) AND ADDRESS(ES)
Program Office (Dr. John Sedriks)
Office of Naval Research
800 North Quincy Street
Arlington, VA 22217-5660

10. SPONSORING/MONITORING AGENCY REPORT NUMBER

11. SUPPLEMENTARY NOTES

12a. DISTRIBUTION/AVAILABILITY STATEMENT
Approval for public release; distribution unlimited

12b. DISTRIBUTION CODE

13. ABSTRACT *(Maximum 200 words)*

This project dealt with the formation, characterization and properties of corrosion resistant polypyrrople and substituted polypyrrole coatings. Aqueous electropolymerization was used to apply polypyrrole coatings onto low carbon steel (99.9% (Fe), 0.1% C). Galvanostatic electropolymerization was used throughout the course of this project. The progress of electropolymerization was followed by tracing the potential time (E-t) curve as a function of the reaction variables. Aqueous electropolymerization of pyrrole and methylpyrrole occurred instantaneously in basic medium (pH $\geq$ 8.4). However, three distinct reactions occurred in acidic medium (pH $\leq$ 6.0). These reactions were identified as the oxidation of steel, passivation of steel and polymerization. Polymerization commenced after steel was completely covered by the passive coatings. The transition of steel from a reactive substrate to a passive substrate is marked by the change in the electrode potential from negative values (~-0.44 vs SCE) to positive values > 0.65 vs SCE. The passivation time decreased with increased applied current. In acidic medium, the passivation time was minimum at pH 2.4. The adhesion strength of the polypyrrole coated steel was determined to be about 56% higher than that for uncoated steel. The adhesion strength varied with the electrochemical process parameters. Low pH and low current densities produced coatings with highest adhesion strength ~23 MPa. The corrosion rate of the polypyrrole coated steel was shown to be very low 2.9-0.16 mpy compared to that for the control of about 41.36 mpy.

14. SUBJECT TERMS
Electrochemical polymerization, passivation polypyrrole coatings, corrosion resistant coatings

15. NUMBER OF PAGES

16. PRICE CODE

17. SECURITY CLASSIFICATION OF REPORT	18. SECURITY CLASSIFICATION OF THIS PAGE	19. SECURITY CLASSIFICATION OF ABSTRACT	20. LIMITATION OF ABSTRACT
Unclassified	Unclassified	Unclassified	UL

FORMATION OF CORROSION RESISTANT ORGANIC POLYMER COATINGS BY AN ELECTROCHEMICAL PROCESS

FINAL REPORT

to

THE OFFICE OF NAVAL RESEARCH, ONR

Grant No. N00014-95-1-0485

Investigators: Jude. O. Iroh and Wencheng Su
Department of Materials Science and Engineering
University of Cincinnati
Cincinnati, Ohio 45221-0012

ABSTRACT

This project dealt with the formation, characterization and properties of corrosion resistant polypyrrople and substituted polypyrrole coatings. Environmentally friendly aqueous electrochemical polymerization was used to apply polypyrrole coatings to low carbon steel (99.9% (Fe), 0.1% C) substrates. Constant current electrochemical polymerization was used throughout the course of this project. The progress of the electrochemical reactions was followed by tracing the potential time (E-t) curve as a function of the reaction variables. The E-t traces showed that while the electrochemical polymerization of pyrrole and methylpyrrole occurred instantaneously in basic medium (pH $\geq$ 8.4), three distinct reactions occurred in acidic medium (pH $\leq$ 6.0). These reactions were identified as the dissolution/oxidation of steel, formation and precipitation of passive iron(II)oxalate on steel and electropolymerization. Electropolymerization commenced after steel was completely covered by the passive coatings. The transition of steel from a reactive substrate to a passive substrate is marked by the change in the electrode potential from negative values (~-0.44 vs SCE) to positive values > 0.65. The passivation time varied with the pH of the medium and the applied current. Increasing the applied current decreased the passivation time. In acidic medium, the passivation time was minimum at pH 2-3 and maximum at pH 6.

The surface structure and chemical composition of the passive coatings and the extent of doping of polypyrrole coatings were studied SEM, XRD, XPS and RAIR. It was shown that the passive coatings was iron(II)dihydrate and that polypyrrole coatings contained about 0.33 mole fraction of the oxalate ions.

The adhesion strength of the polypyrrole and poly(N-methylpyrrole) coatings to steel was determined by Lap joint shear test using EPON 828/polymeric curing agent adhesive system. The adhesion strength of the polypyrrole coated steel was about 56% higher than that for uncoated steel. The adhesion strength varied with the electrochemical process parameters. Low pH and low current densities produced coatings with highest adhesion strength ~23 MPa. The corrosion rate of the polypyrrole coated steel was shown to be very low 2.9-0.16 mpy compared to that for the control 41.36 mpy.

TABLE OF CONTENTS

PREFACE

This report contains the results obtained from the Young Investigator Program Grant N00014-95-1-0485 which was concerned with the formation of corrosion resistance coatings by Electrochemical polymerization. All the reaction performed in this project were carried out in solutions prepared in environmentally friendly deionized water. Electropolymerization was carried out galvanostatically in an attempt to keep the properties of the coatings constant. It was shown that both the pretreatment and coating of steel occurred during electrochemical polymerization. Furthermore, the formation, structure and properties of the passive films and coatings were found to be dependent on the electrochemical process variables.

Most of the results obtained from this project have been extensively published in peer reviewed journals and conference proceedings. These papers are included in this report. The articles which are still in preparation are also included in this report. An extended summary of these papers is also provided. The list of the papers is as follows:

1. "Formation of Polypyrrole Coatings onto Low Carbon Steel by Electrochemical Process", J. Appl. Polym. Sci., 65, 417-424 (1997).

2. "Kinetics and Efficiency of Aqueous Electropolymerization of Pyrrole onto Low-Carbon Steel", J. Appl. Polym. Sci., 65, 617-624 (1997).

3. "Effects of Electrochemical Process Parameters on the Synthesis and Properties of Polypyrrole Coatings on Steel", Synthetic Metals 95, 159-167 (1998)

4. "Electropolymerization of Pyrrole on Steel Substrates in the Presence of Oxalic acid and Amines", Electrochemica Acta, 44, 2173-2184 (1999).

5. "Characterization of the Passive Inorganic Interphase and Polypyrrole Coatings Formed on Steel by the Aqueous Electrochemical Process", J. Appl. Polym. Sci., 71, 2075-2086 (1999).

6. "Morphology and Structure ofthe Passive Interphase Formed During Aqueous Electrodeposition of Polypyrrole Coatings on Steel", Electrochemica Acta (accepted– not included)

7. "Formation of Polypyrrole Coatings on Stainless Steel in Aqueous Benzene Sulfonate Solution", Electrochemica Acta, 42(17), 2685-2694 (1997).

8. "Effect of Process Parameters on the Electropolymerization Potential and Rate of Formation of Polypyrrole on Stainless Steel", J. Appl. Polym. Sci., 66, 2433-2440 (1997)

9. "One Step Electrochemical Process for the Formation of Poly(N-methylpyrrole) Coatings on Steel in Different Media", Synthetic Metals, 97, 73-80 (1998).

10. "Electrodeposition of Poly(N-methylpyrrole) Coatings on Steel from Aqueous Medium", J. Appl. Polym. Sci., 71, 1293-1302 (1999).

11. "IR and XPS Studies on the Interphase and Poly(N-methylpyrrole)Coatings Electrodeposited on Steel Substrates", Electrochemica Acta, 44, 3321-3332 (1999)..

12. "Adhesion of Polypyrrole Coatings to Low-Carbon Steel", (in preparation)

13. "Corrosion Performance of Polypyrrole Coatings formed on Steel by Electrodeposition", (in preparation).

Papers 1-4 are concerned with aqueous electrochemical polymerization of pyrrole on low-carbon steel, while papers 5 and 6 deal with the analysis of the coatings by SEM, XPS and XRD. Papers 7 and 8 discuss the formation of polypyrrole on 304 stainless steel. Papers 9-11 describe the electrodeposition and characterization of Poly(N-methylpyrrole) on steel. Finally Papers 12 and 13 focus on the properties of the electrodeposited coatings. Adhesion strength (measured by lap joint shear test) and corrosion resistance (Tafel test and EIS) of the coatings were compared with those of the control samples containing no coatings.

SUMMARY OF RESULTS

Steel is susceptible to corrosion in a wet and an oxidizing condition. Conventional approaches to protection of steel include phosphating, chromating, sacrificial metal and polymeric coatings. Due to environmental concerns, escallating cost for part replacement and poor adhesion of conventional polymeric coatings, alternative methods are highly desired. Conducting polymers such as polypyrrole, polyaniline and polythiophene and their copolymers are excellent candidates for protection of reactive metals because of the polar nature of the monomers, and the electronic stability of the tutomeric structures. It is also believed that a conductive polymer coating could be a more efficient sacrificial coating when compared with zinc, because the conductive polymer can reversibly redo-oxidize without a significant degradation in the physical, electrochemical and mechanical properties. However, most conductive polymers are only spiringly soluble in water, the preferred medium for environmentally safe processing. Additionally, synthesis of conducting polymers is performed by oxidation and growth process. When steel is used as the substrate, the aqueous electrochemical synthesis of the conducting polymers competes with the oxidation of the substrate. Though pretreatment of steel prior to electropolymerization could prevent the oxidation of steel, it may not only minimize the wettability of the substrate by the monomers, but may render the substrate impermeable to the reactants. Consequently a process that could lead to in-situ passivation and electropolymerization is desired. The following subsections describe the synthesis, characterization and properties of polypyrrole and poly(N-methylpyrrole) coatings formed steel by aqueous electrochemical process.

Electropolymerization of pyrrole was carried out galvanostatically in a one-compartment electrochemical cell. An EG&G Princeton Applied Research Potentiostat /Galvanostat Model 273A was used as the source of power supply. A 0.5mm thick QD low carbon steel panel purchased from the Q-panel Company was used as the working electrode. The working electrode was degreased with tetrachloroethylene for about an hour prior to electrochemical polymerization. The counter electrodes comprised of two titanium alloy plates. Saturated Calomel elelectrode (SCE), manufactured by Corning Company was used as reference electrode. The current densities used in this study ranged from 0.56 to 11.26 mA/cm^2. The initial concentration of oxalic acid was varied from 0.05 to 0.4 M, while the initial monomer concentration was varied from 0.1 to 0.8 M. was performed for 300 - 2400 seconds.

Aqueous electropolymerization of pyrrole on steel in oxalic acid solution occurred in three distinct stages (Fig.1); (i) dissolution of steel, followed by (ii) passivation of steel and finally (iii) deposition of polypyrrole. Passivation time decreased with increased applied current (Tables 1). The passivation charge varied between 335 (2.7) and 180 (1.4) mC/cm^2(C) as the applied current was changed between 5 and 90 mA.

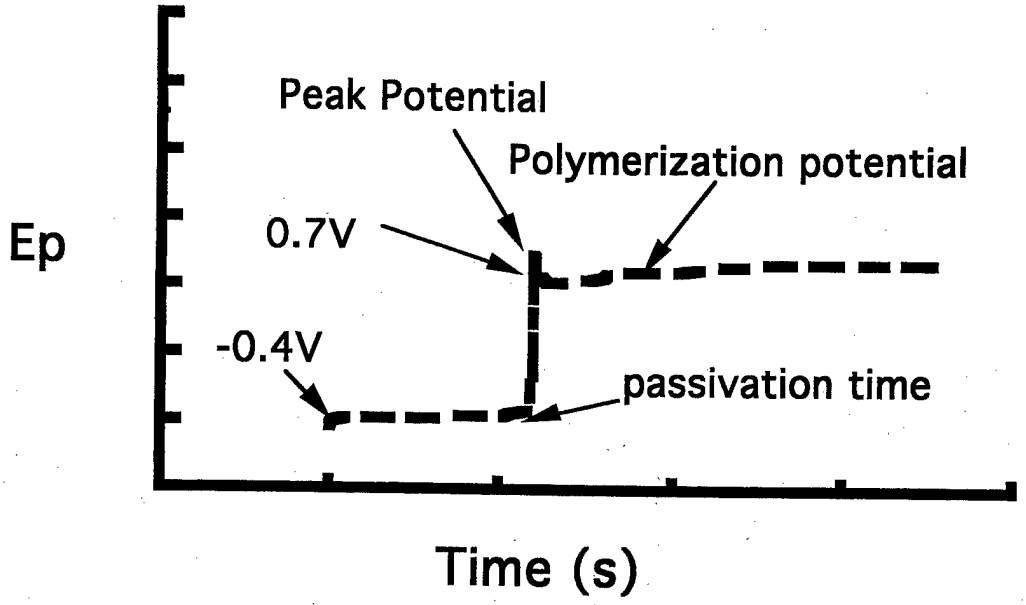

Scheme 1. E-t curve showing passivation time, peak potential and polymerization potential

Current density (mA/cm^2)	Passivation time (s)	Passivation charge (mC/cm^2)
0.56	598	335
1.13	287	324
2.25	109	245
3.38	67	226
4.50	47	211
5.63	38	214
7.88	28	220
11.26	16	180

Table 1. Dependence of passivation time and charge on the applied current

The electropolymerization potential of pyrrole increased linearly with current density and decreased slightly with pyrrole concentration in accordance with equations 1 and 2:

$$E_p = 0.62 + 0.041\,[Cd] \qquad (1)$$

$$Ep = E_{ox}\exp^{-}[M] \qquad (2)$$

The amount of polypyrrole coatings formed on steel increased proportionately with current density and electropolymerization time and increased slightly with initial pyrrole concentration.

The rate of electropolymerization of pyrrole on steel increased linearly with the applied current, $Rp \alpha i^{1.1}$ and increased slightly with the initial pyrrole concentration, $Rp \alpha [M]^{0.2}$. However, the rate of electropolymerization was found to be independent of oxalic acid concentration, $Rp \alpha [Ox]^{0}$.

1. EFFICIENCY OF ELECTROPOLYMERIZATION

The conversion, P and current efficiency, η, for the aqueous electropolymerization of pyrrole on low carbon steel were investigated. The conversion of pyrrole into polypyrrole, $P = \{W_P\}/\{W_M\}$, increased with electropolymerization time, the applied current and decreased with the initial monomer concentration (Figures 1-3). The oxalic acid concentration had no significant effect on conversion. The current efficiency for electropolymerization of pyrrole performed under high applied current, I ($I \geq 40$ mA) and high pyrrole concentration [M] ≥ 0.5 M, rose to its highest value at short polymerization times, $t < 300$ s (Figs. 4-6). It then decreased and levelled off at longer times, $t \geq 1000$ s. At low applied current, $I \leq 20$ mA and low pyrrole concentration, $[M] \leq 0.25$ M, the current efficiency increased gradually with increased reaction parameters ([M], I and t) and reached a maximum value at $t = 1000$ s (Figs. 4-6). A retrogression of the current efficiency occurred at $t \geq 1000$ s, for the reaction performed under an applied current of 10 mA. Overall the current efficiency varied between 39 to 130 % with the higher values occurring at high pyrrole concentration and high applied current (Figs. 4-6). The current efficiency was determined from the ratio of the experimental and theoretical electrochemical equivalent for polypyrrole.

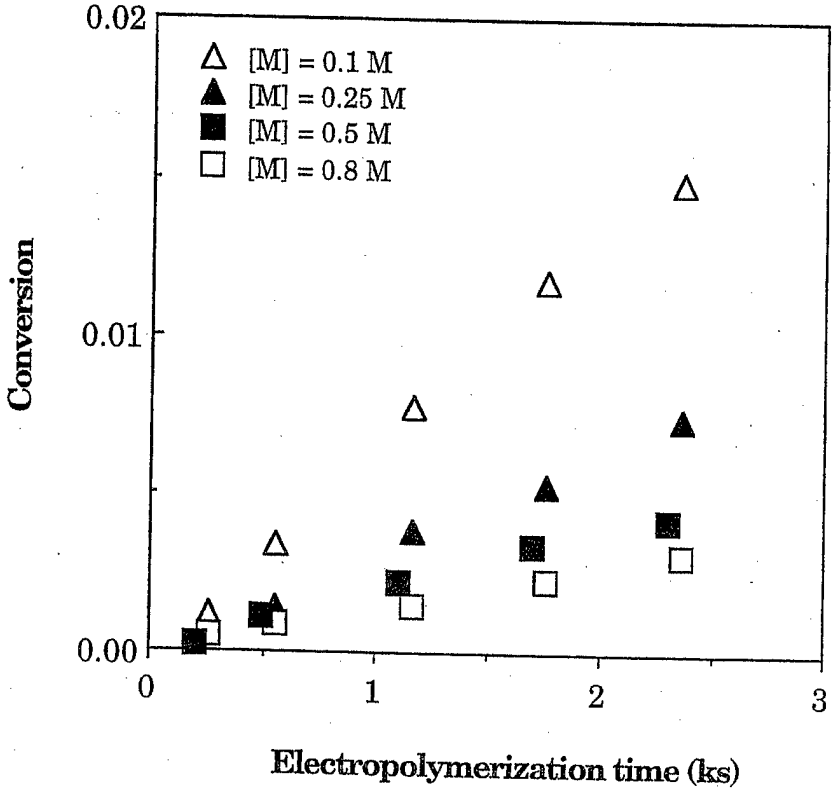

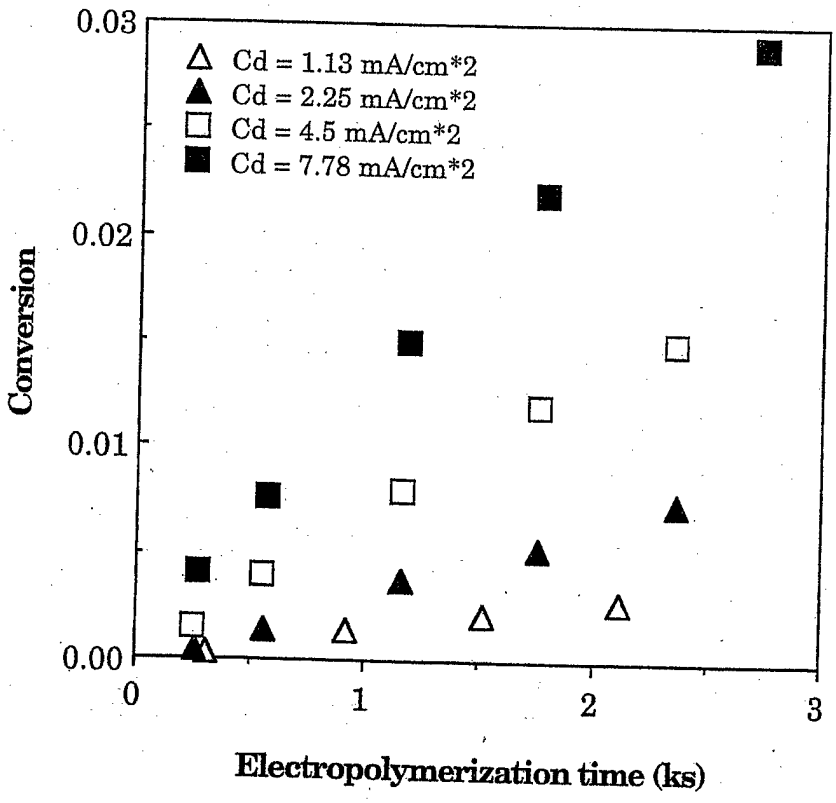

Figure 1. Dependence of conversion on initial pyrrole concentration and time (top).
Figure 2. Dependence of conversion on the applied current (bottom).

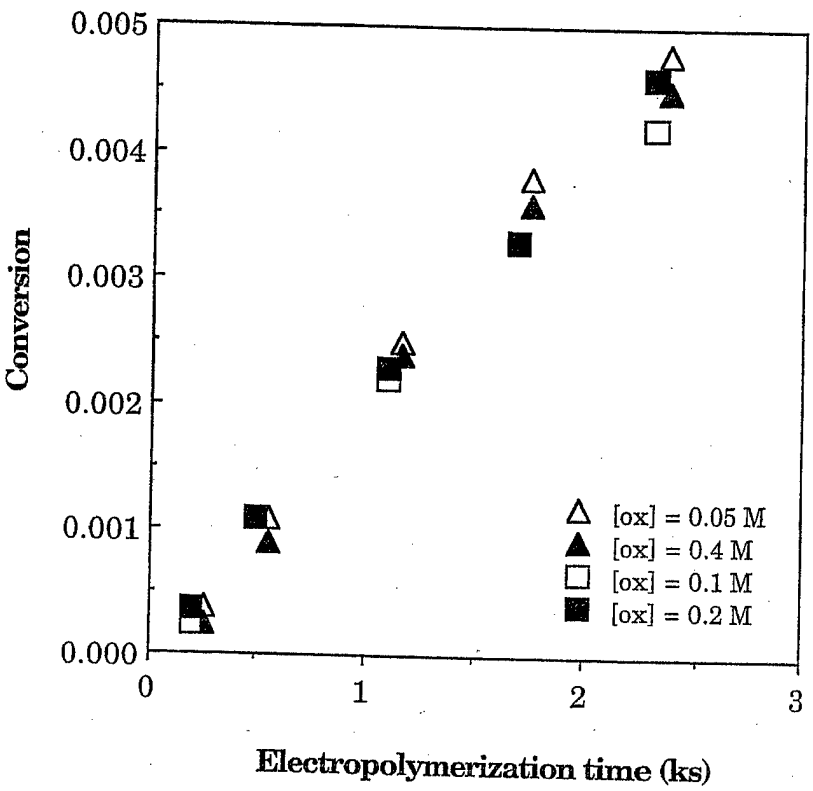

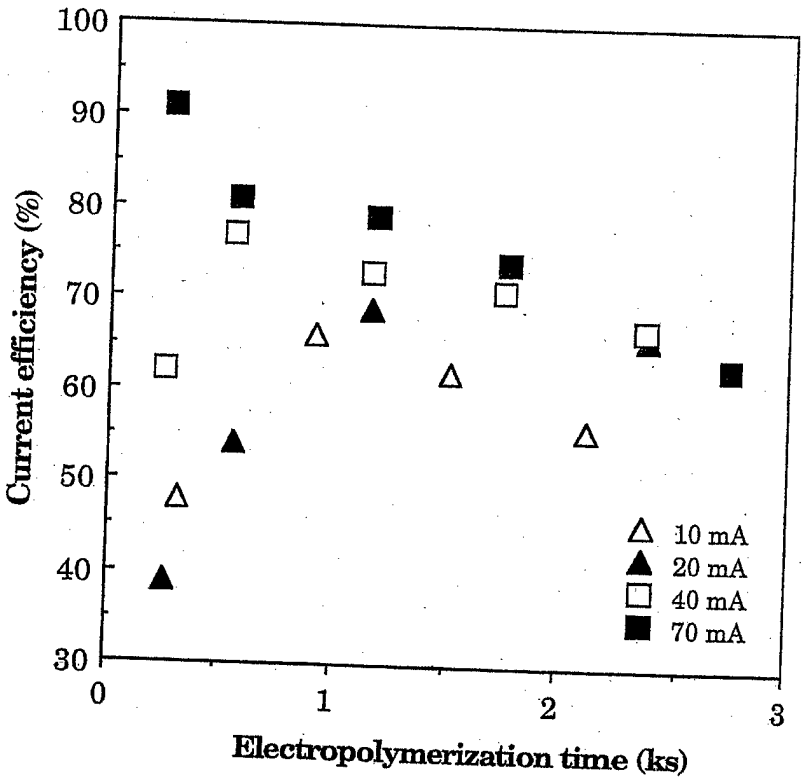

Figure 3. Dependence of conversion on oxalic acid concentration (top).
Figure 4. Dependence of current efficiency on the applied current and time (bottom).

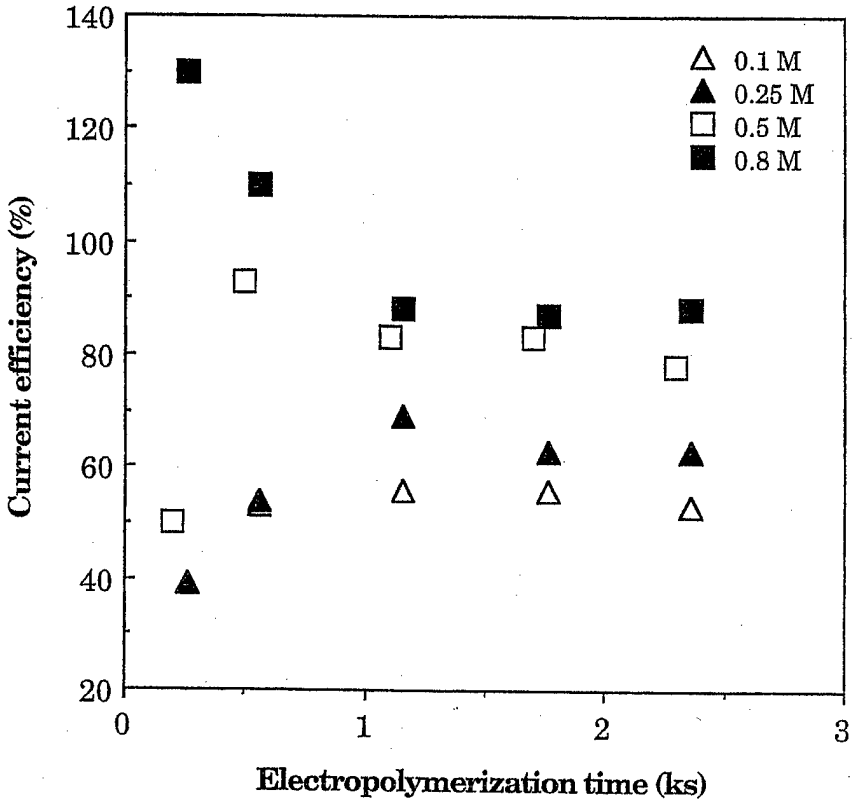

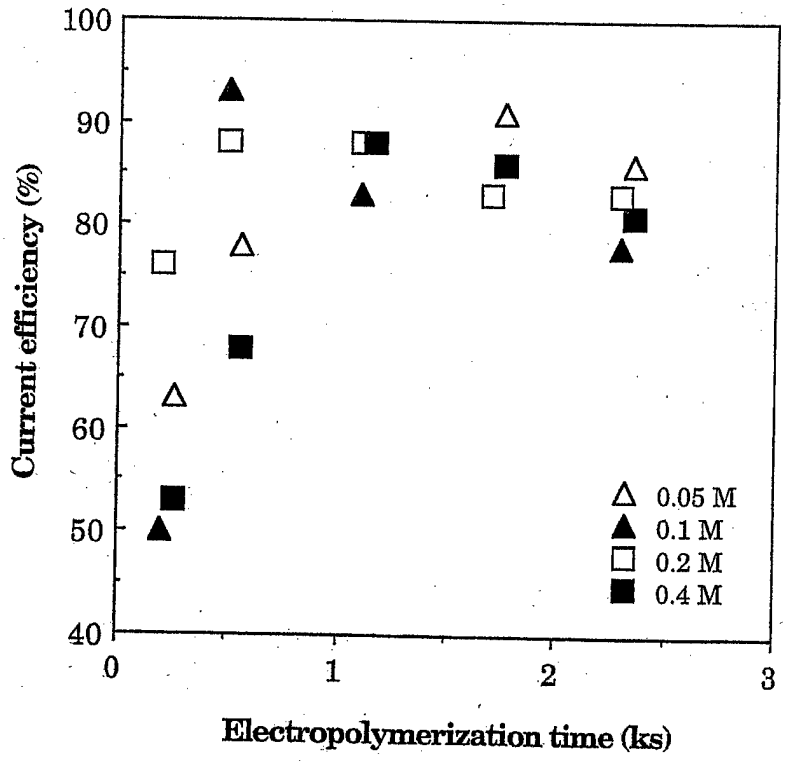

Figure 5. Dependence of current efficiency on initial pyrrole concentration (top).
Figure 6. Dependence of current efficiency on oxalic acid concentration (bottom).

2. EFFECT OF PROCESS VARIABLES ON PASSIVATION

Effects of pH and applied current density

The pH of the reaction medium and the applied current density(i) were systematically varied over a wide range of values while the initial monomer and electrolyte concentrations were kept constant at 0.25M and 0.1M respectively.

Figures 7 and 8 show the potential-time curves for the formation of polypyrrole coatings in different reaction medium at two different applied current densities. The electrode potential varies with pH and time of reaction. At low pH (pH $\leq$ 6), the induction/passivation time(τ) decreased with increasing applied current density, i. At pH 2.4, the passage of a current density of 0.56 mA/cm^2 resulted in an induction time of about 354 s, however, the induction time was decreased to about 24 s at 5.63 mA/cm^2.

The effect of applied current can be clearly understood by considering the reactions that occur at pH 6.0. For i < 1.13 mA/cm^2, τ was so large that passivation of steel did not occur even after 30-minutes of reaction. However, increasing i to 5.63mA/cm^2 reduced τ to 82 s (Fig. 10). Figures 11 and 12 show the relationship between τ and **i** for pH $\leq$ 6. Increasing the applied current decreased the passivation time. Empirical relationships between τ and **i** were developed as shown below:

$$\mathbf{pH = 1.4:} \quad \mathbf{Ln\ \tau = 5.72 - 1.22\ Ln\ i} \qquad \mathbf{(3)}$$

$$\mathbf{pH = 2.4:} \quad \mathbf{Ln\ \tau = 5.22 - 1.16\ Ln\ i} \qquad \mathbf{(4)}$$

$$\mathbf{pH = 4.1:} \quad \mathbf{Ln\ \tau = 5.98 - 1.42 Ln\ i} \qquad \mathbf{(5)}$$

$$\mathbf{pH = 6.0:} \quad \mathbf{Ln\ \tau = 9.95 - 3.15\ Ln\ i} \qquad \mathbf{(6)}$$

The passivation time (τ) was also shown to be dependent on the pH of the reaction medium. Keeping the applied current, τ was shortest at pH 2.4 and was maximum at pH 6.0. Overall, τ varied with pH according to following inequalities:

$$\tau_{pH=6.0} > \tau_{pH=4.1} > \tau_{pH=1.4} > \tau_{pH=2.4} \quad (7)$$

It was observed that the variation of τ with pH is very large at low current density, however, at high applied current densities, τ attains a minimal value which is independent pH. For example, at $\mathbf{i} = 0.56$ mA/cm^2; $\tau = 350$ seconds at pH 2.4, however, $\tau \sim \infty$ at pH=6.0.

When $\mathbf{i}$ was increased to 2.25 mA/cm^2, τ obtained at pH 2.4 was similar to that obtained at pH $\leq$ 4.1. The τ obtained at pH=6.0, however, remained much higher than those obtained at lower pH. Additional increase of $\mathbf{i}$ to 5.63 mA/cm^2, resulted in very short τ.

Figure 13 shows the dependence of the passivation charge on the applied current. The passivation passed remained relatively constant and virtually independent of pH for pH< 6.0. However, much higher passivation charge were needed at pH 6.0 but the former expectedly decreased with increased $\mathbf{i}$.

It is believed that the passivation of the iron in the presence of oxalate ions, is due to the formation of the iron(II) oxalate interlayer. We notice that the formation of the iron oxalate passive layer is also highly dependent on the applied current density and pH of the reaction medium.

The steady-state positive electrode potential obtained at the end of passivation is associated with the formation of polypyrrole. Figures 14 and 15 show the relationship between the steady-state electropolymerization potential and the applied current density for pH $\leq$ 6. The electropolymerization potential increases linearly with the applied current density and follows the following relationships:

$$\mathbf{pH = 1.4:} \quad \mathbf{E_p = 0.62 + 0.038\, i} \quad (8)$$

$$\mathbf{pH = 2.4:} \quad \mathbf{E_p = 0.58 + 0.094\, i} \quad (9)$$

$$\mathbf{pH = 4.1:} \quad \mathbf{E_p = 0.53 + 0.088\, i} \quad (10)$$

$$\mathbf{pH = 6.0:} \quad \mathbf{E_p = 0.25 + 0.22\, i} \quad (11)$$

This change of the electrode potential with current density may have something to do with the deficiency of electron transfer on the surface of the electrode. More electrons are removed from the electrode when the applied current density is high. Due to the slow reaction of the monomer,

the electron deficiency cannot be compensated immediately by the reaction, thus the deficiency of electron will result in a positive potential change. It can also be seen from Figure 14 that higher current densities, resulted in high electropolymerization potentials.

The E-t curves obtained during the formation of polypyrrole in alkaline medium differs from those obtained in acidic medium. As shown in Figure 15 passivation occurs instantaneously at pH 8.4 in agreement with the Pourbaix diagram, which proposes instantaneous passivation of the iron in basic media. Except for the E-t curve traced at i = 5.63 mA/cm2, all the other E-t curves show a maximum value, followed by gradual decrease of the electrode potential with time. It is believed that the passive interlayer formed at lower current density at pH ~ 8.4 is not very stable. For the same applied current density, the electropolymerization potential of pyrrole in alkaline medium was much higher than that in acidic medium.

Effect of initial pyrrole and electrolyte concentration

The effect of initial pyrrole and electrolyte concentration on the anodic polymerization of pyrrole on steel was investigated at pH 1.4. The oxalic acid concentration and the applied current density were kept constant at 0.1M and 2.25mA/cm^2, respectively. Electrochemical synthesis was performed at four different monomer concentrations: 0.1M, 0.25M, 0.5M and 0.8M. As shown in Figures 16 and 17, the concentration of pyrrole did not significantly affect the passivation time. The electropolymerization potential, however, decreased slightly with increasing monomer concentration. This phenomenon may be associated with the nature of electorchemcial reaction. The electropolymerization of pyrrole generally consists of two continuous steps. The first step is the diffusion of pyrrole monomer to the electrode surface, the rate of tdiffusion and adsorbtion of pyrrole on steel is determined by the pyrrole concentration. The second step is the oxidation reaction of pyrrole at the electrode-electrolyte solution interface. Since the applied current density and the electrolyte concentration were kept constant, the rate of passivation and polymerization is dependent on the monomer concentration at the interface per unit time. At high monomer concentration, the positive charge at the working electrode is rapidly consumed by pyrrole, there-by reducing the accumulation of charge on the electrode and decreasing the

electrode potential. At lower monomer concentration, the positive charge may not be completely consumed by pyyrole, thus some charge may accumulate on the working electrode, resulting in a higher reaction potential.

The effect of electrolyte concentration was investigated with 0.5M pyrrole concentration and applied current density of 2.25mA/cm^2. Electrochemical reactions were carried out at four different electrolyte concentration: 0.05M, 0.1M, 0.2M and 0.4M. The results are shown in Figures 18 and 19. It can be seen that the τ is not significantly affected by the electrolyte concentration. However, the electropolymerization potential decreased gradually with increasing electrolyte concentrations. This phenomenon is expected since the increasing the electrolyte concentration can reduce the overall resistance of the system.

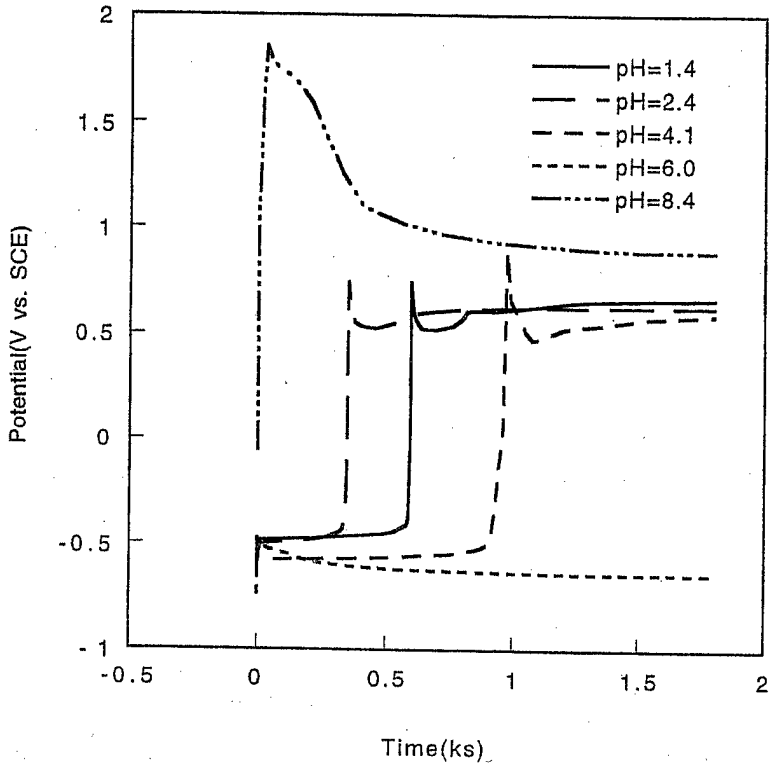

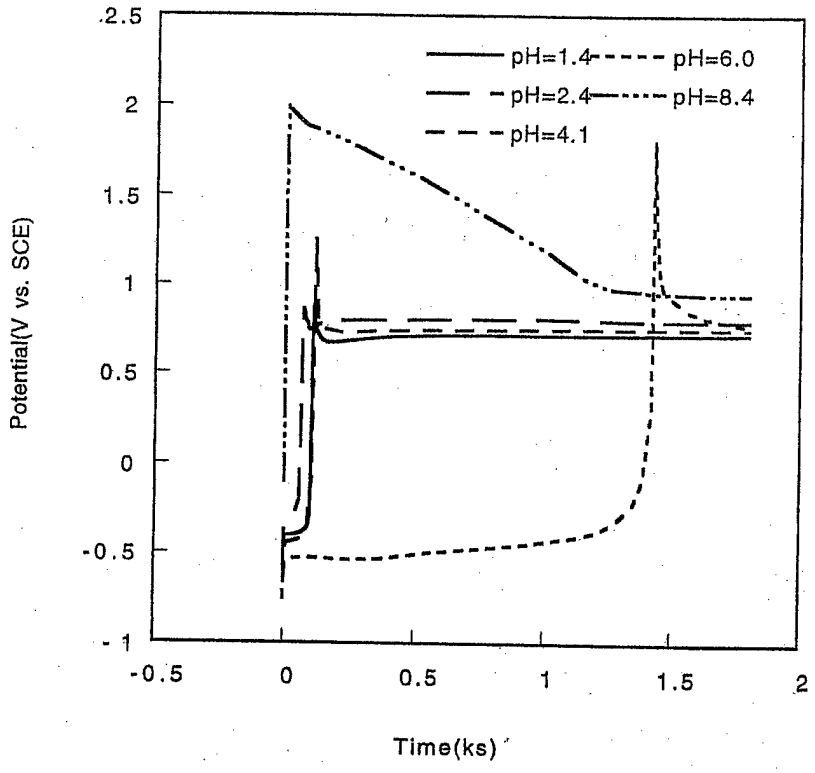

Figure 7. Dependence of the electrode potential on pH, (i=0.56mA/cm^2 (top)
Figure 8. Dependence of the electrode potential on pH, (i=2.25mA/cm^2 (bottom)
[Py]=0.25M, [RX]=0.1M).

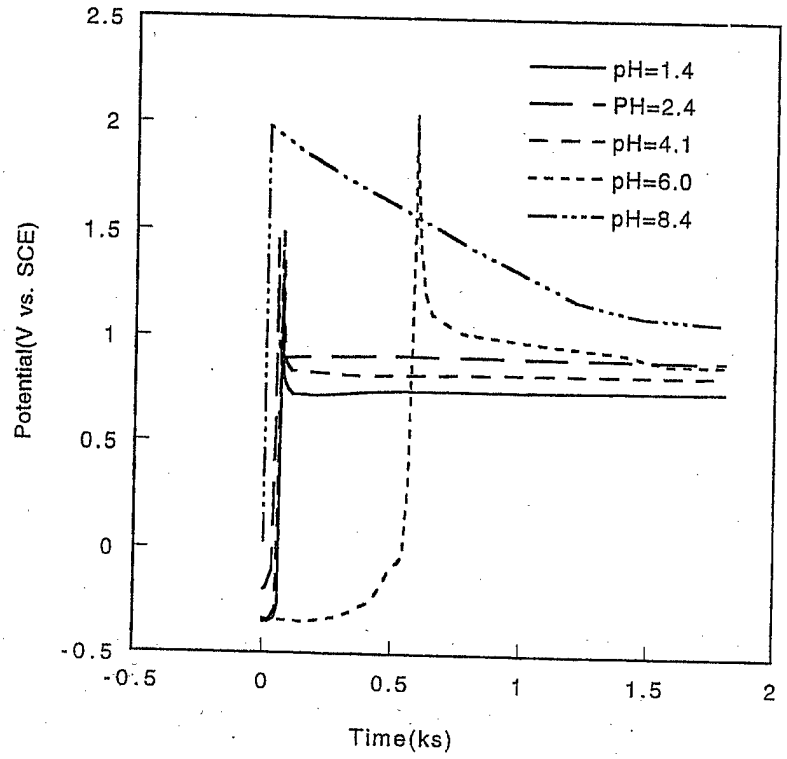

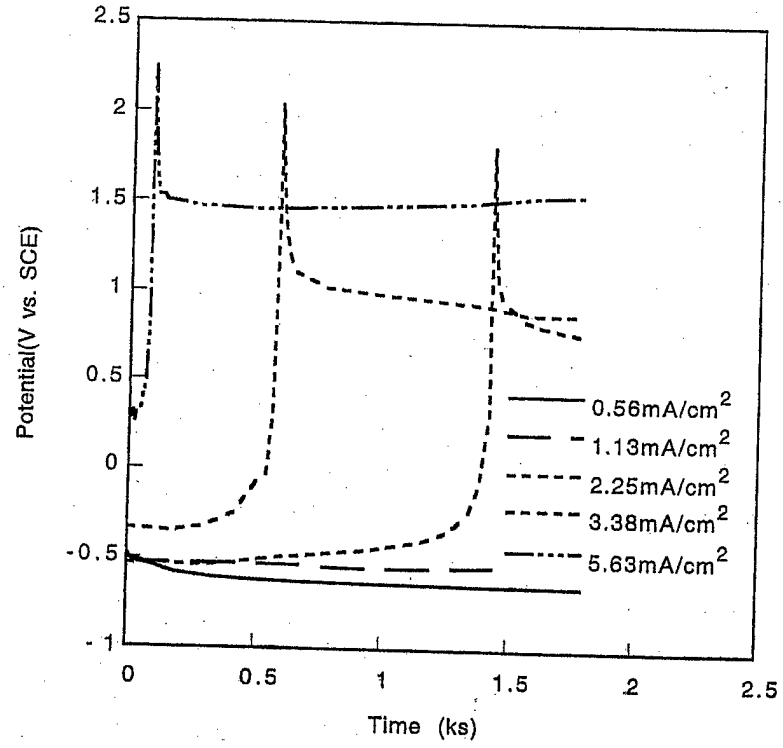

Figure 9. Dependence of the electrode potential on pH, (i=3.38 mA/cm^2 (top)
Figure 10. Dependence of the electrode potential on the applied current (pH = 6.0 (bottom)
[Py]=0.25M, [RX]=0.1M).

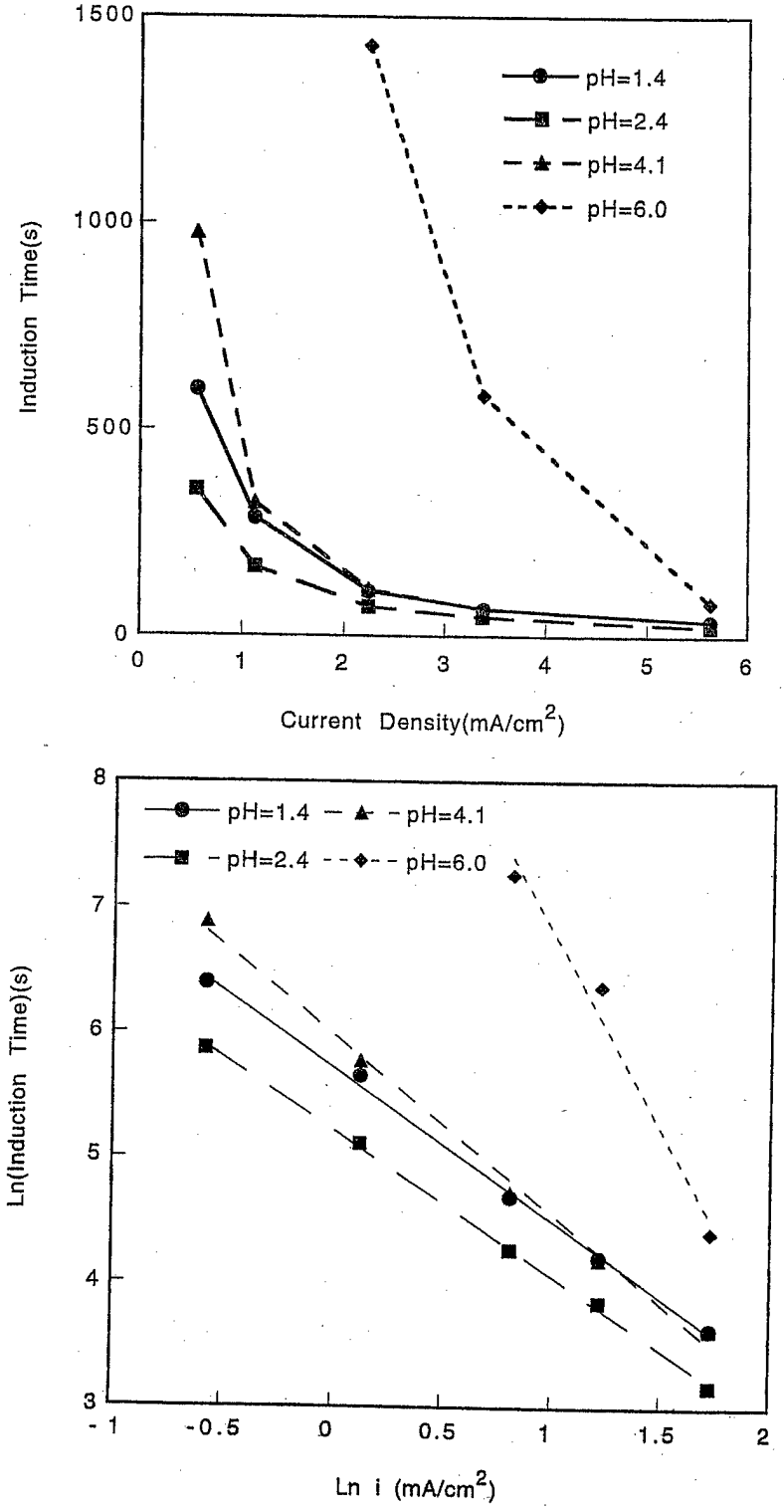

Figure 11. Dependence of passivation time on applied current and pH (top)
Figure 12. Log-log plot of t vs i and pH (bottom); ([Py]=0.25M, [RX]=0.1M)

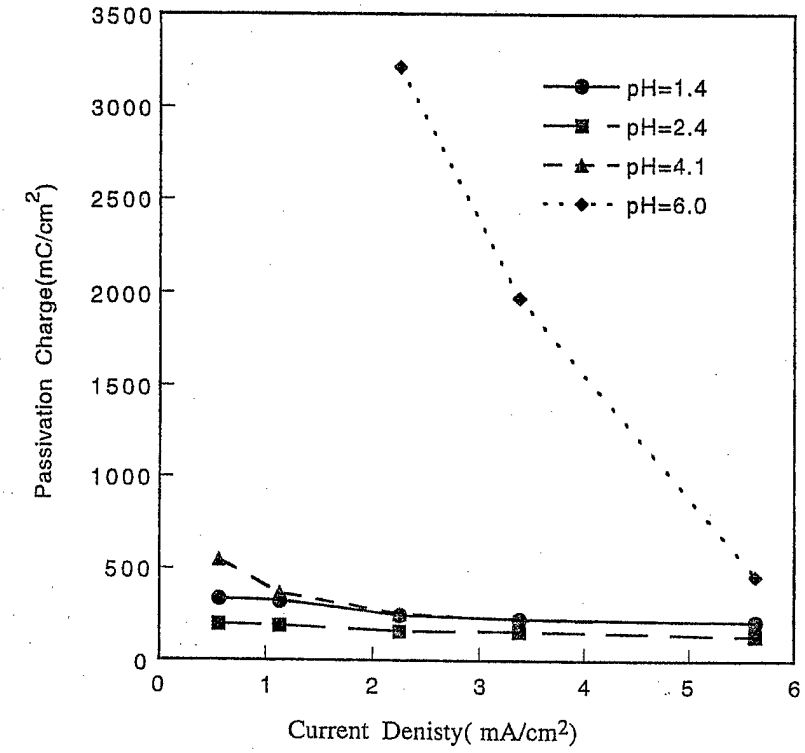

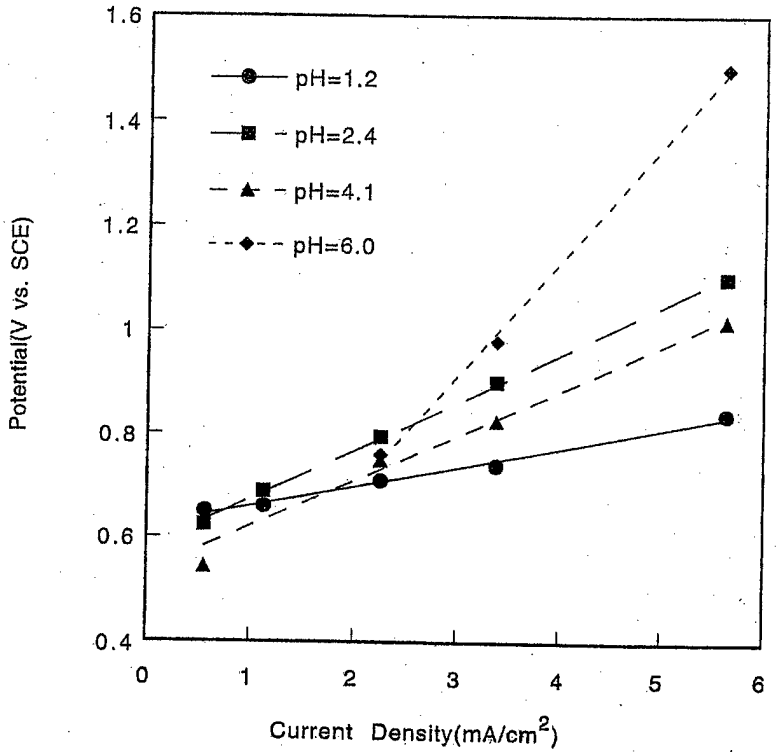

Figure 13. Dependence of passivation charge on applied current and pH (top)
Figure 14. Dependence of polymerization potential on applied current and pH (bottom)
([Py]=0.25M, [RX]=0.1M)

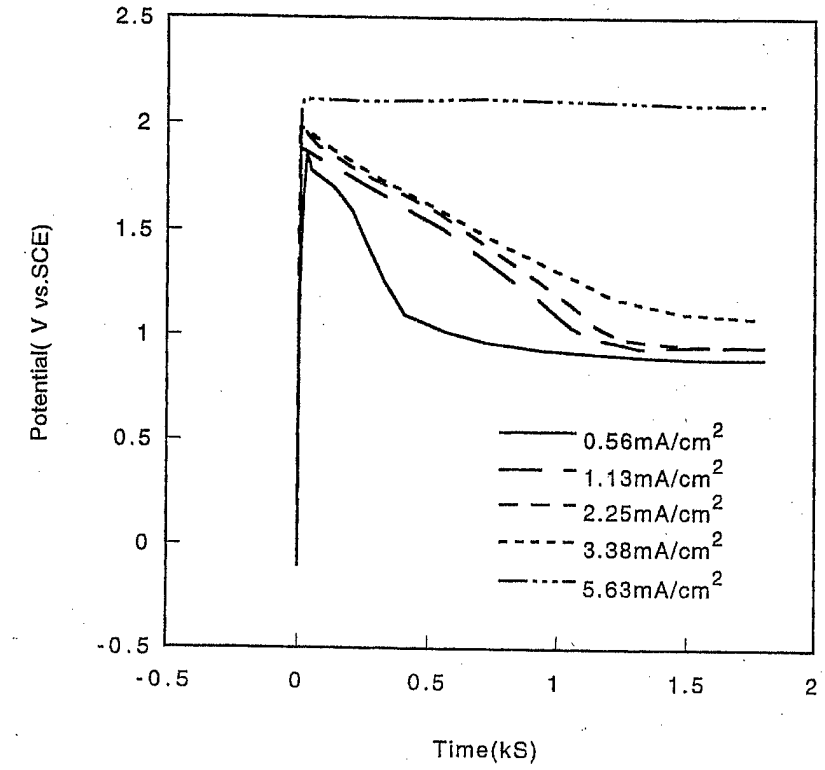

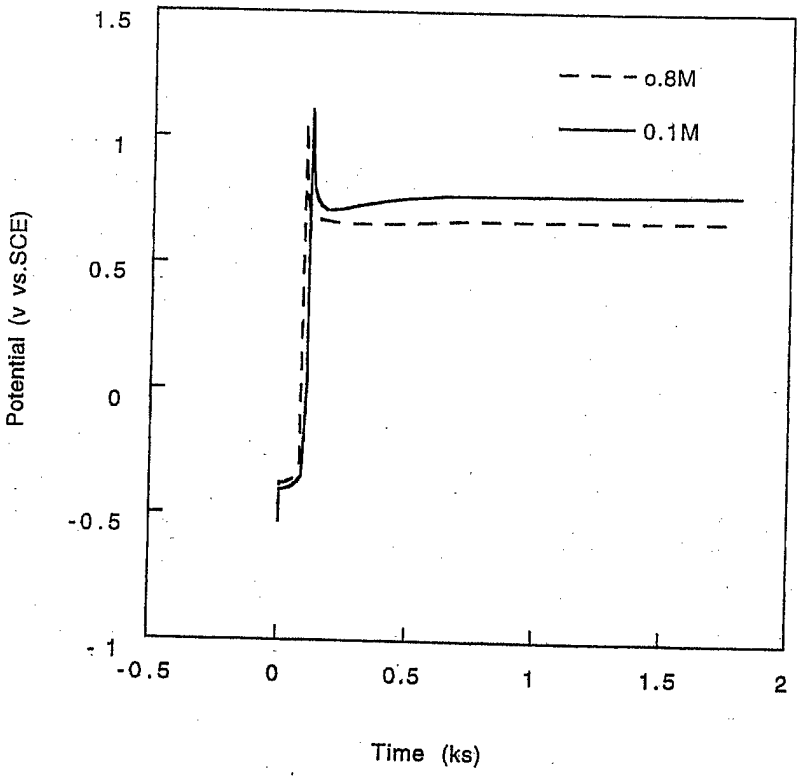

Figure 15. Dependence of electrode potential on applied current (top), pH=8.4 ([Py]=0.25M, [RX]=0.1M).

Figure 16. Dependence of electrode potential on the initial pyrrole concentration (bottom) (i=2.25mA/cm^2, [OA]=0.1M).

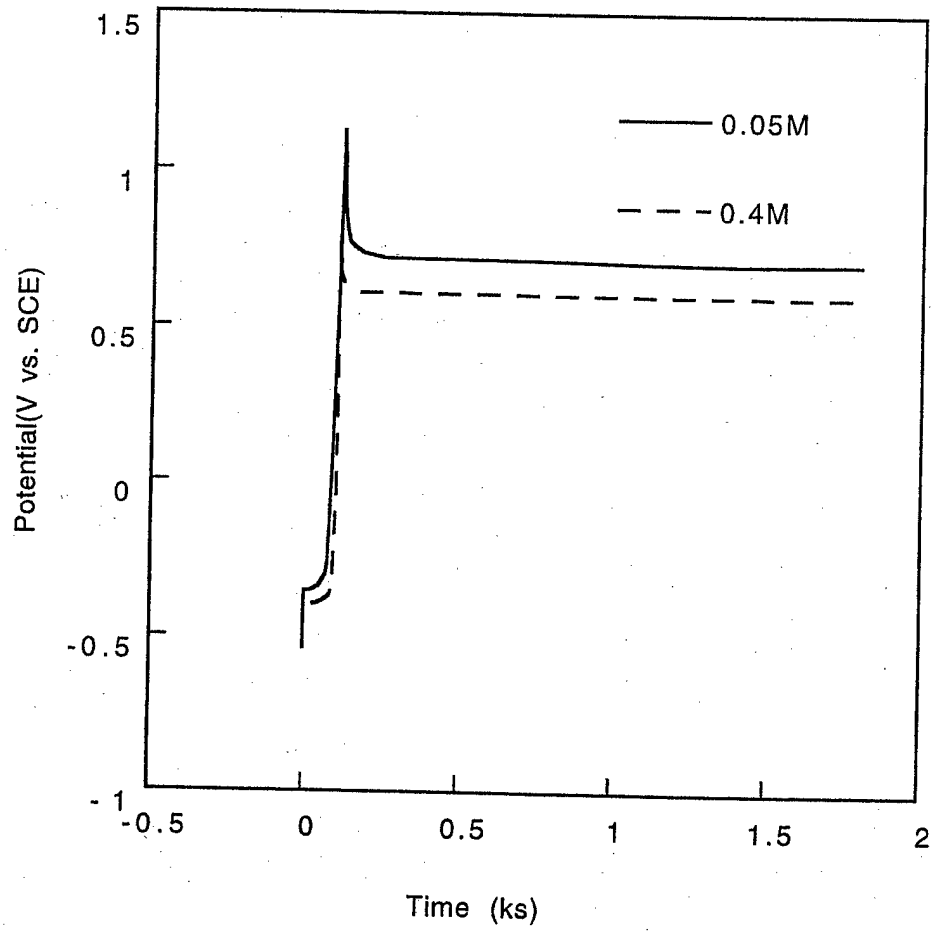

Figure 17. Dependence of electrode potential on oxalic acid concentration (top) (i=2.25mA/cm^2, [OA]=0.1M).

3. MORPHOLOGY AND STRUCTURE OF THE PASSIVE COATINGS

Characterization. The morphology of the coated and control samples was examined by a Hitachi S-4000 scanning electron microscope (SEM). X-ray diffraction patterns of the passive interphase were obtained by using a Philips X'pert diffractometer with Cu K_a radiation source. The diffractometer was operated at 40 kV and 50 mA. A scanning step of 0.04° in 2θ with a 10 second dwell time per step was used. The samples used for X-ray measurements were prepared by using polished steel sheets.

In order to have a better understanding of the formation of the passive interphase, a series of samples were prepared by applying i= 0.56 mA/cm^2 at pH 1.4 as a function of time. Figure 18 shows the SEM micrographs of these samples. Numerious fine inorganic crystals were deposited on the steel after about 100 seconds of reaction (Figure 18a). Note that the crystals are distributed uniformly on the steel surface, but only about 10% of the surface was covered by the crystals. The number and size of crystals deposited on the substrate increased significantly after 200 seconds of reaction (Figure 18b). The surface coverage was increased to about 25%. Additional crystals were deposited on the substrate surface after 400 seconds of reaction, however, the size of the crystals was not uniform (Figure 18c). Some of the crystals were larger than those formed at 200 s, other crystals were much smaller in size. This suggests that most of the crystals grew directly from the substrate surface rather than growing over other crystals. The degree of coverage of the substrate surface was estimated to be about 65% after about 400 seconds of reaction. At the end of the first stage(598 s), the entire surface of the substrate was covered by the closely packed crystals (Figure 18d). It can be seen that the crystals were impinged on each other. Some of the crystals also interlocked each other. It seems that most crystals, especially the larger crystals, tended to grow in such a way that their largest surface was in contact with the substrate surface. From above observation, it appears that the interphase consists of only a monolayer of a closely packed crystals. As shown in Figure 1, the reaction potential rose sharply to a positive value when the substrate was completely covered by the passive interphase, indicating that the passivation of the steel was established at this time. This is very important for

the electropolymerization of pyrrole. Since the formation of polypyrrole occurs by an oxidation reaction, it requires a positive electrode potential.

Figure 19 shows the SEM micrographs of the interphase formed by applying i = 0.56 mA/cm^2 at pH 2.4 and 4.1, respectively. The passive interphase formed at pH 2.4 and 4.1, respectively, also consists of closely packed crystals. Generally, the crystals formed in acidic medium (pH of 1.4 - 4.1) have irregular rectangular shape with tetragonal cross-section. The crystals were oriented in a nearly random fashion on the substrate surface plane and the size of the crystals is not uniform. The size of crystals seems to vary with the pH of the reaction medium for an applied current density of 0.56mA/cm2. The crystals formed at pH 1.4 and 2.4 are longer than those formed at pH 4.1. For the crystals formed at pH 1.4 and 2.4, the dimension of the tetragonal cross-section vary from about 0.9 to 4.1 μm and from about 0.2 to 3.5 μm, respectively. For the crystals formed at pH 4.1, the dimension of the tetragonal cross-section varied from about 0.4 to 1.7 μm.

Figure 20 shows the SEM micrographs of the interphase formed by applying i = 3.38 mA/cm^2 in at pH 1.4 to 4.1. It can be seen that all the interphase coatings also consists of closely packed fine crystals. The crystals formed by applying i= 3.38mA/cm2 are much smaller than those formed at lower current density. Most of the crystals also show tetragonal cross-section. The dimension of the cross-section varied from 0.2 to 1.2 μm.

Figure 21 compares the SEM micrographs of the samples formed at pH 6.0 at two different current densities. At an applied current density of 0.56 mA/cm^2, passivation of steel was not established even after 30 min reaction. As shown in Figure 21a, no crystals are observed on the substrate surface. When the current density was increased to 2.25 mA/cm^2, the passivation of the steel was established even though the passivation time was very long. It can be seen from Figure 21b that larger crystals were deposited on steel substrate under this condition. The dimension of the tetragonal cross-section of the crystals varies from 1.7 μm to 2.8 μm. These observations further demonstrate that passivation of steel is due to the formation of the closely packed crystals on the substrate surface .

It is believed that $FeC_2O_4 \cdot 2H_2O$ passive interphase is formed according to following reactions:

$$Fe - 2e \longrightarrow Fe^{2+} \qquad (12)$$

$$Fe^{2+} + C_2O_4^{2-} + 2H_2O \longrightarrow FeC_2O_4 \cdot 2H_2O \qquad (13)$$

The anodic dissolution of iron produced Fe^{2+} ions, these Fe^{2+} ions further react with the oxalate ions on the electrode surface to form insoluble iron(II) oxalate dihydrate, which precipitates on the substrate surface. When the substrate is completely covered by the small crystals, it becomes insulative, there-by preventing further oxidation of steel.

The crystallization of the iron(II) oxalate dihydrate on the steel substrate involves two steps: nucleation and growth. It can be accelerated by increasing the applied current. High applied current density, results in a high rate of formation of Fe^{2+} ions, and a concomitant high rate of formation of $FeC_2O_4 \cdot 2H_2O$. Both the nucleation rate and growth rate of the crystals are higher at higher current density, resulting in smaller crystal size and shorter formation time of the interphase. The effect of pH of the reaction medium on the crystallization of iron(II) oxalate dihydrate is more complicated. It is believed that the pH of the reaction medium has a significant effect on the nucleation of iron(II) oxalate. Nucleation will occur on the steel substrate when the solubility of $FeC_2O_4 \cdot 2H_2O$ is very low. The pH of the reaction medium might influence the solubility of $FeC_2O_4 \cdot 2H_2O$. It has been reported that iron(II) oxalate can be converted into soluble complexes $M_2[Fe(C_2O_4)_2]$ in the presence of excess alkali metal oxalate. Perhaps the solubility of the $FeC_2O_4 \cdot 2H_2O$ is lowest at pH 2.4, resulting a higher nucleation rate. The solubility of $FeC_2O_4 \cdot 2H_2O$ may be very high at pH 6.0, hence, it takes very long time for nucleation to occur.

Structure of The Passive Crystalline Interphase

Figure 22 compares the X-ray diffraction patterns of the bare steel substrate and the steel substrate coated with the passive interphase. The passive interphase was formed at 0.56 mA/cm^2 in the reaction medium of pH of 1.4. No diffraction peaks are observed for the bare steel substrate in the 2θ range of 10° to 40°. The steel substrate coated with the passive interphase shows four diffraction peaks in this region. Since the steel substrate doesn't show any diffraction peaks in above 2θ range, all the diffraction peaks can be attributed to the crystals of the passive interphase. It should be noted that the passive interphase does not show any strong diffraction peaks in the 2θ range of 40° to 90°.

Figure 23 shows the X-ray diffraction patterns of the interphase formed at 0.56 mA/cm^2 as a function of pH. The passive interphases formed at pH ≤ 4.1 show similar diffraction peaks. The steel substrate that was coated at pH 6.0 by applying i = 0.56 mA/cm2 shows no diffraction peaks, indicating that no $FeC_2O_4 \cdot 2H_2O$ crystals were formed on steel under this condition.

Figure 24 shows the x-ray diffraction patterns of the interphase formed at 3.38 mA/cm^2 in as a function of pH. It can be seen that all the passive interphases formed in the acidic medium show strong diffraction peaks. At this applied current density, the interphase formed at pH 6.0 shows much stronger diffraction peaks compared to other samples. In addition to the four main peaks shown in other three interphase, it also shows two additional weak diffraction peaks.

Chemically prepared $FeC_2O_4 \cdot 2H_2O$ is reported to crystallize in two slightly different structures, a monoclinic α–phase and an orthorhombic β–phase, depending on the conditions of preparations. In this compound, the Fe^{2+} ion is surrounded by a distorted octahedron of oxygen atoms. Two of them are provided by water molecules while the other four belong to two oxalate groups which serve to link each Fe^{2+} ion with two others to form a chain. The structure of α–phase belongs to the space groups C2/c and has unit cell dimensions a=12.00Å, b=5.57Å, and C=9.91Å with $\beta=128.43^{o}$. The space group of the β–phase structure is Cccm with unit cell dimensions a=12.26Å, b=5.57Å, and c=15.48Å. The difference between the two structure is merely in the relative displacement of adjacent chains in the direction of extension which coincides with b-axis.

Figure 25 compares the x-ray diffraction pattern of the interphase with that of the monoclinic $FeC_2O_4 \cdot 2H_2O$. It can be seen that their x-ray diffraction patterns are different, therefore, the interphase doesn't crystallize in monoclinic crystal structure.

Table 2 lists the d spacing and the relative intensities of the main diffraction peaks of the passive interphase formed under different experimental conditions. The corresponding data for the chemically prepared orthorhombic $FeC_2O_4 \cdot 2H_2O$ are also listed in Table 2 for the purpose of comparison. It can be seen that d values of the interphase are very close to the corresponding values of the chemically prepared orthorhombic $FeC_2O_4 \cdot 2H_2O$, indicating that the passive interphase crystallizes in orthorhombic structure. For both the electrodeposited interphase and the chemically prepared powder sample, (2 0 2) reflection corresponds to the strongest diffraction peak. The relative intensities of the other three main peaks change with experimental conditions

and their values are smaller than the corresponding values of the chemically prepared powder sample. For example, the relative intensity of the (4 0 0) reflection of the interphase varied from 8 to 30 while it is 50 for the chemically prepared powder sample. The relative intensity of the (0 2 2) reflection of the passive interphase varied from 2 to 13, but the corresponding value is 35 for the chemically prepared powder sample. It should be pointed out here that chemically prepared powder iron (II) oxalate dihydrate also shows some other diffraction peaks in the 2θ range of 10° to 40°, such as, d=3.61Å (rel. int. 2), 3.22 Å (2), 2.77 Å (2), 2.64 Å (18), 2.40 Å 2.37 Å (20), 2.29 Å. These peaks are absent in the x-ray diffraction patterns of the passive interphase. For all the interphases formed, only the interphase prepared by applying i = 3.38 mA/cm^2 in the medium at pH 6.0 shows two other additional weak diffraction peaks. These phenomena perhaps indicates that the preferred orientation of the crystals on the steel substrate is maintained.

Table 2. Position and relative intensity of the diffraction peaks of the interphase

Sample	d spacing (Å) (relative intensity)					
	(1 1 0)	(2 0 2)	(112)	(0 0 4)	(4 0 0)	(0 2 2)
Power β–$FeC_2O_4 \cdot 2H_2O$	5.06(2)	4.80(100)	4.23(4)	3.87(14)	3.06(50)	2.61(35)
pH=1.4, i=0.56 mA/cm^2		4.84(100)		3.85(4)	3.11(8)	2.61(2)
pH=1.4, i=3.38 mA/cm^2		4.86(100)		3.85(8)	3.12(8)	2.61(5)
pH=2.4, i=0.56 mA/cm^2		4.83(100)		3.85(7)	3.13(8)	2.61(5)
pH=2.4, i=3.38 mA/cm^2		4.86(100)		3.85(3)	3.12(14)	2.62(7)
pH=4.1, i=0.56 mA/cm^2		4.84(100)		3.86(5)	3.11(13)	2.61(2)
pH=4.1, i=3.38 mA/cm^2		4.85(100)		3.84(3)	3.13(18)	2.61(13)
pH=6.0, i=3.38 mA/cm^2	5.09(5)	4.85(100)	4.24(2)	3.85(11)	3.13(30)	2.61(9)

For an orthorhombic crystal structure, the relationship between the unit cell dimensions (a, b, c) and the index (h k l) can be expressed as follows:

$$1/d^2 = h^2/a^2 + k^2/b^2 + l^2/c^2 \qquad (14)$$

By means of the above equation, the unit cell dimensions of the pasive interphase formed under different experimental conditions were calculated and the results are listed in Table 3. It can be seen that b values of all the interphase are basically same and that they are very close to the corresponding literature value. The calculated a values of the interphase change with experimental conditions and are about 0.15 to 0.25 Å larger than the corresponding literature value. The calculated c values of the interphase vary a little bit with experimental conditions, but they are 0.07 to 0.1 Å smaller than the corresponding literature value. Based on the calculated unit cell dimensions, the unit cell volumes of the interphase are also calculated and the results are listed in Table 3. It can be seen that the unit cell volumes of the interphase are a little bit larger than the corresponding literature value.

Table 3. Unit cell dimension of the interphase and power β–$FeC_2O_4 \cdot 2H_2O$

Sample	a(Å)	b(Å)	c(Å)	V(Å^3)
Power β–$FeC_2O_4 \cdot 2H_2O$	12.26	5.57	15.48	1057
pH=1.4, i=0.56 mA/cm^2	12.51	5.54	15.41	1068
pH=1.4, i=3.38 mA/cm^2	12.51	5.54	15.41	1068
pH=2.4, i=0.56 mA/cm^2	12.41	5.54	15.41	1059
pH=2.4, i=3.38 mA/cm^2	12.46	5.54	15.41	1064
pH=4.1, i=0.56 mA/cm^2	12.45	5.55	15.42	1065
pH=4.1, i=3.38 mA/cm^2	12.49	5.55	15.38	1066
pH=6.0, i=3.38 mA/cm^2	12.51	5.55	15.40	1069

(a)

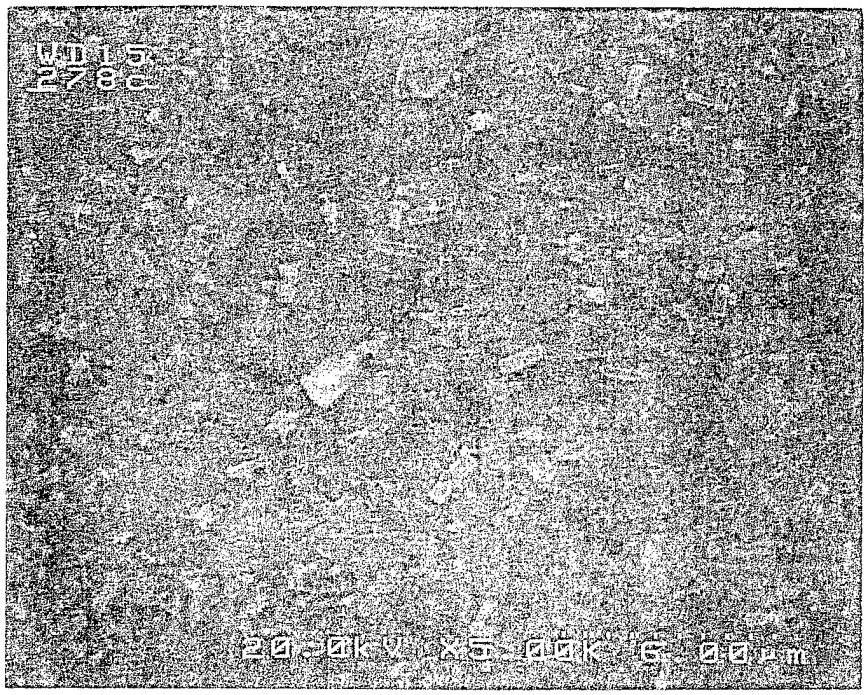

(b)

(c)

(d)

Figure 18. SEM micrographs of the samples prepared at 0.56 mA/cm^2 at pH 1.4 for; (a) t=100 s, (b) t=200 s, (c) t=400 s, (d) t=598 s.

(a)

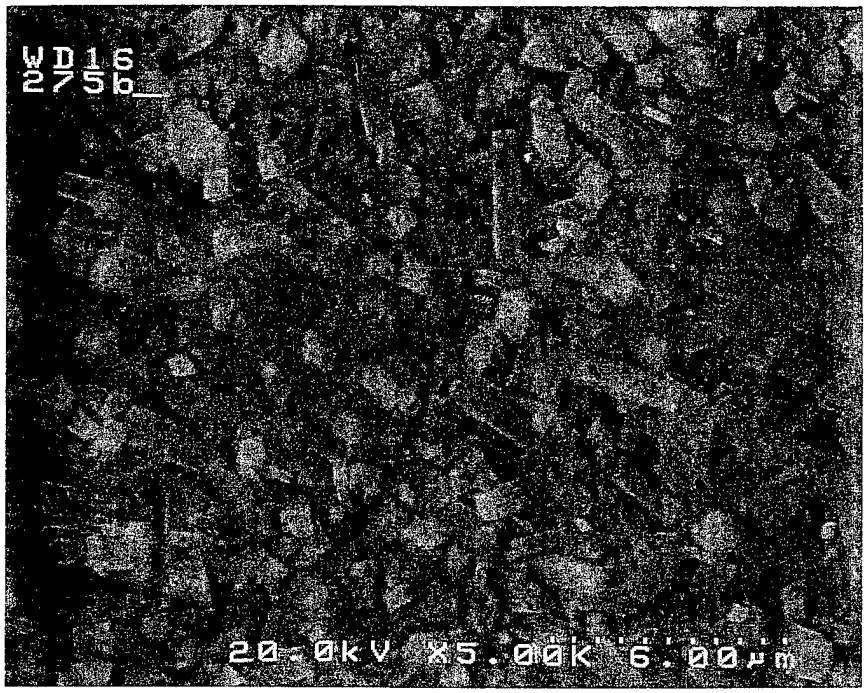

(b)

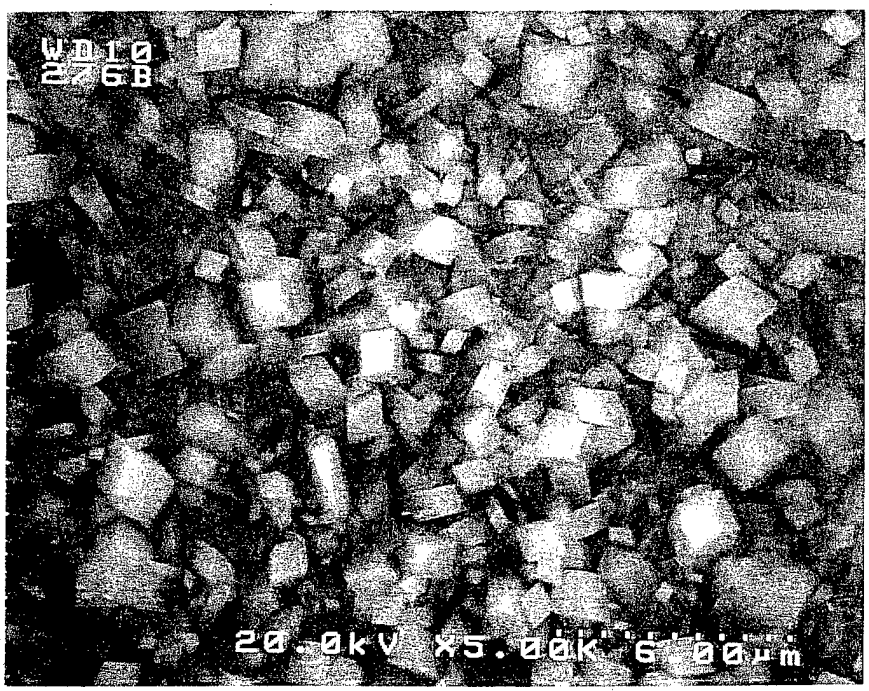

Figure 19. SEM micrographs of the interphase formed at 0.56 mA/cm^2 in the reaction medium of pH of 2.4 and 4.1. (a) pH=2.4, (b) pH=4.1.

(a)

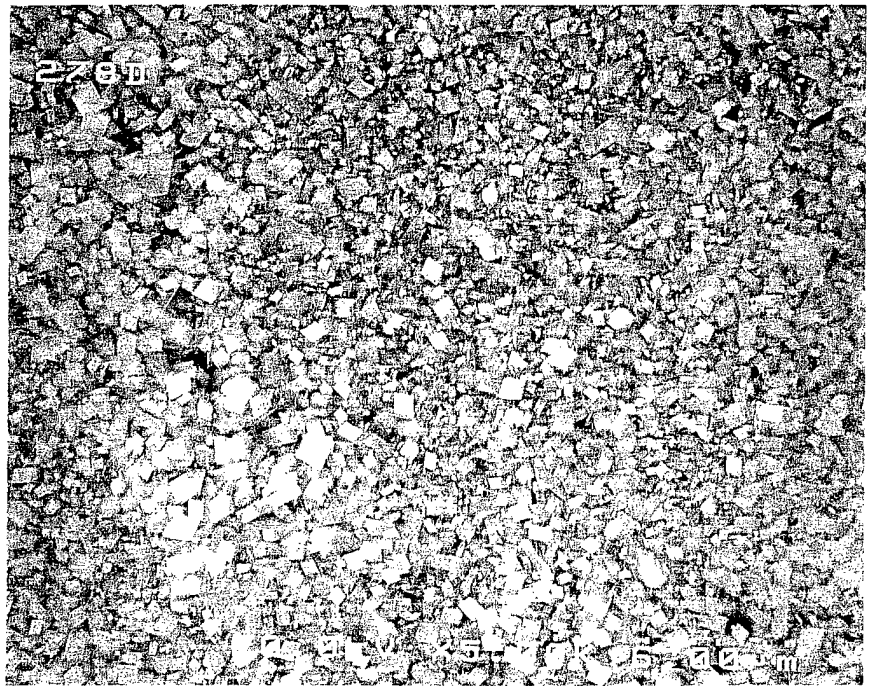

(b)

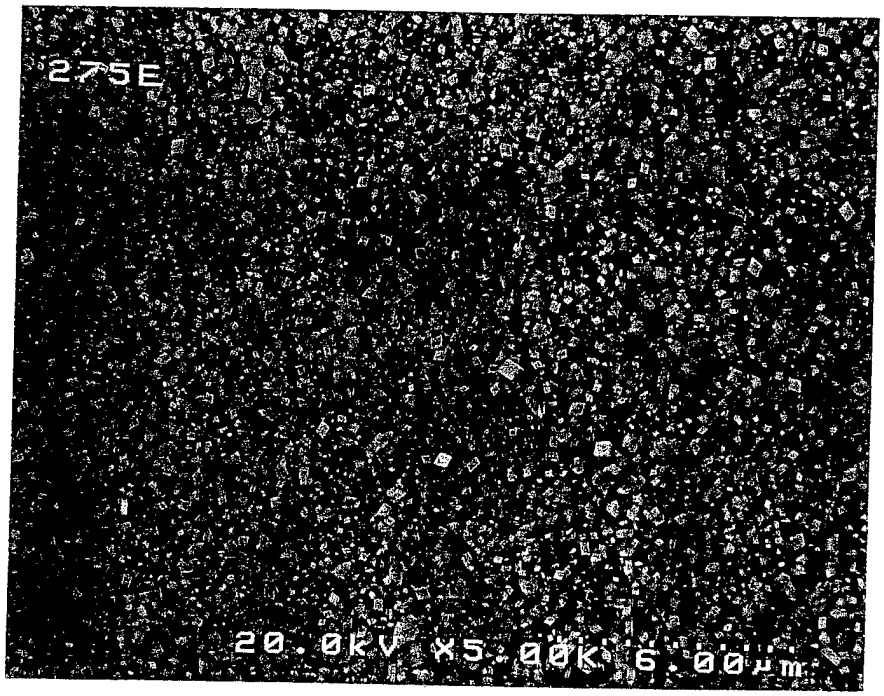

(c)

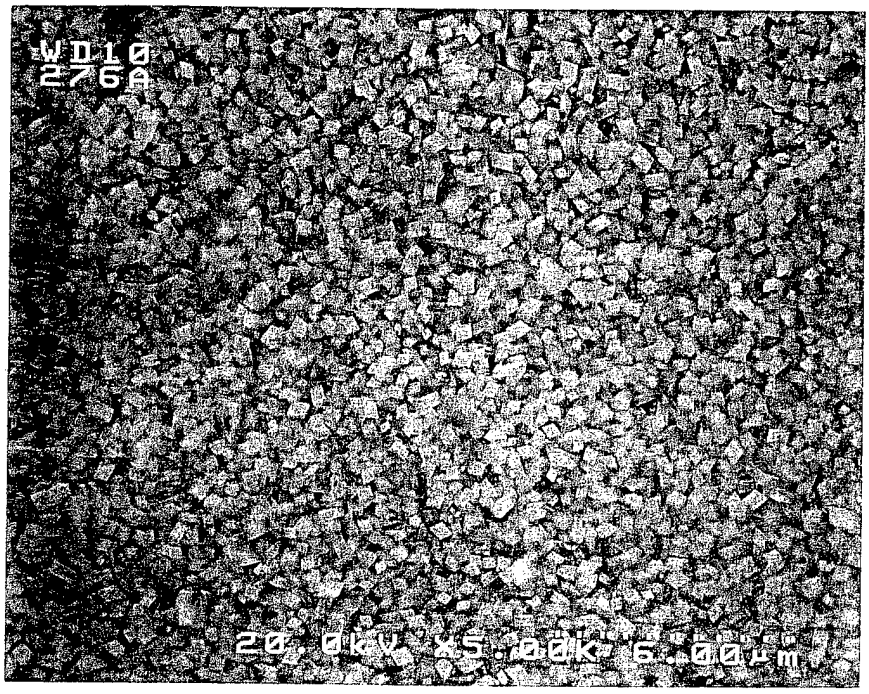

Figure 20. SEM micrographs of the interphase formed at 3.38 mA/cm^2 for; (a) pH=1.4, (b) pH=2.4, (c) pH=4.1.

(a)

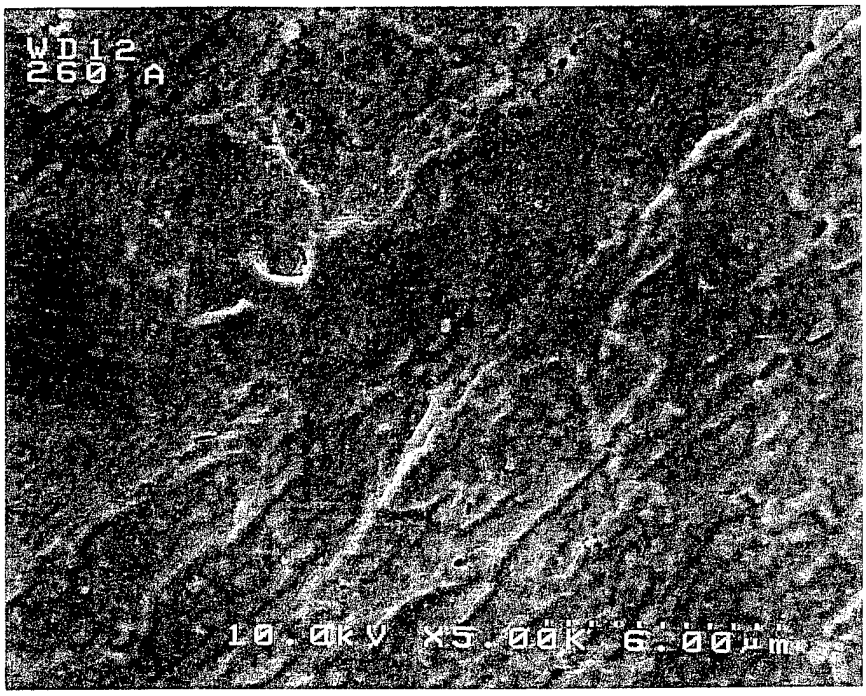

(b)

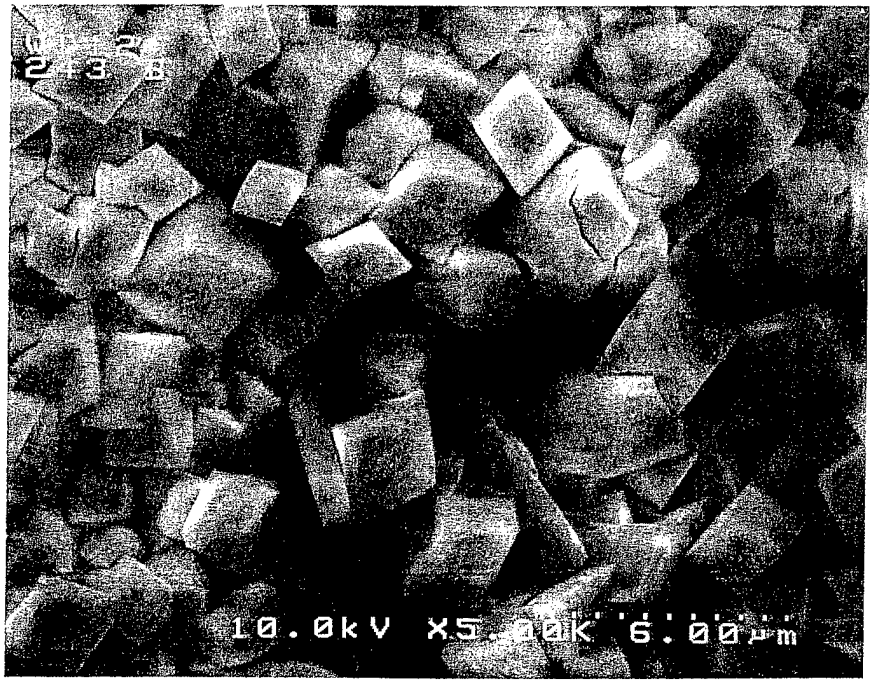

Figure 21. SEM micrographs of the samples formed in the medium of pH of 6.0 at ; (a) i=0.56 mA/cm^2, (b) i=2.25 mA/cm^2.

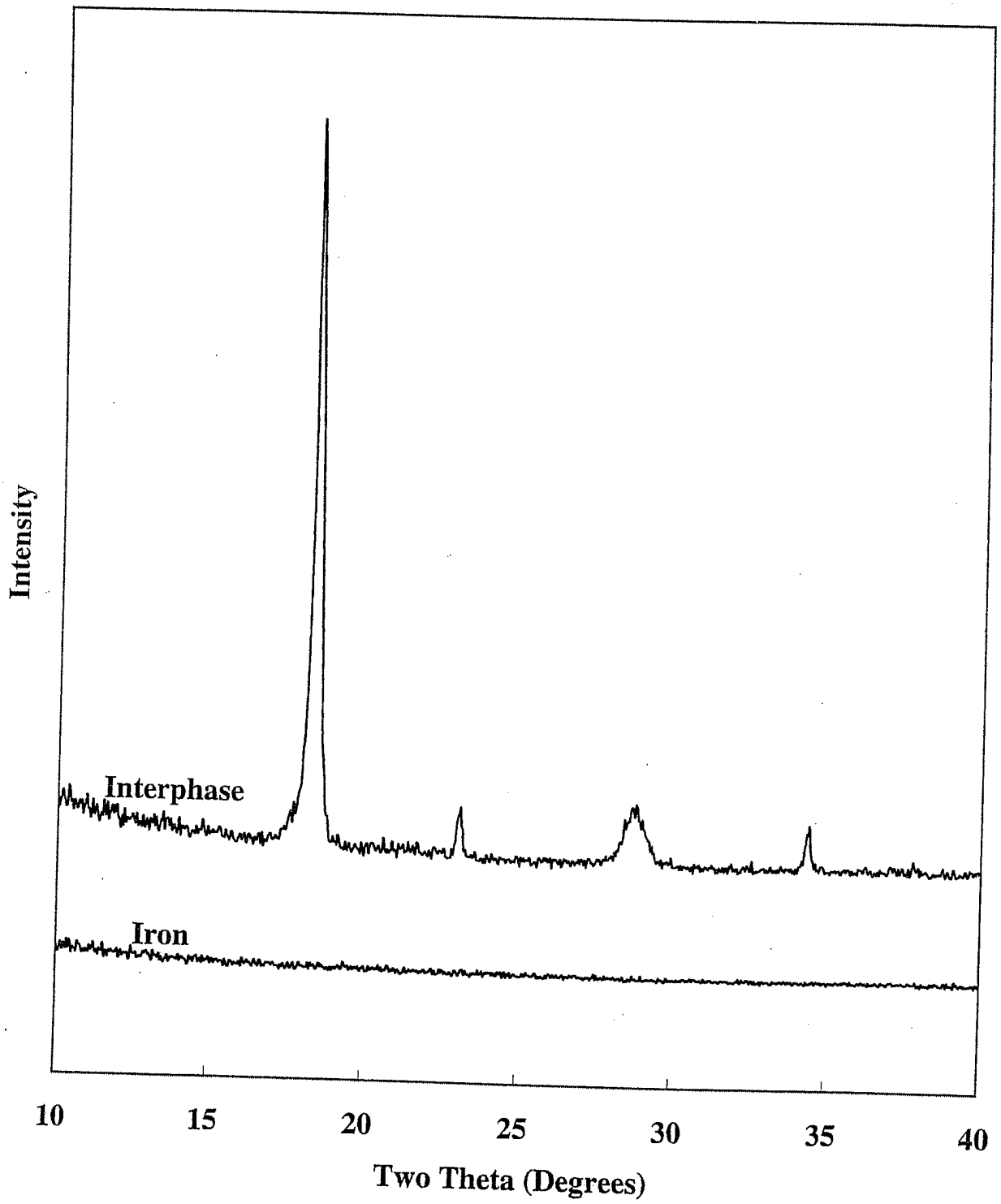

Figure 22. X-ray diffraction pattern of bare steel and steel covered by the passive interphase

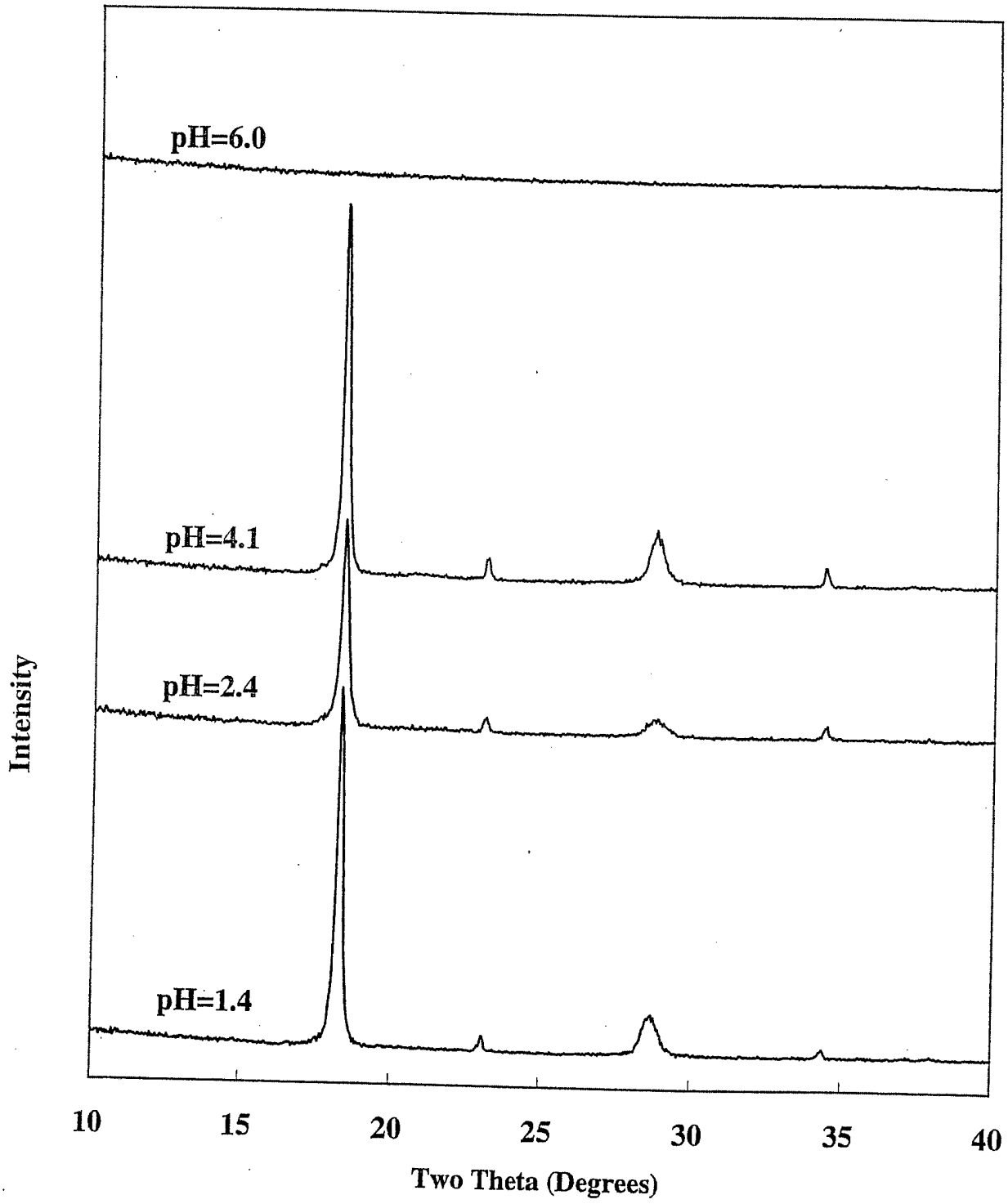

Figure 23. X-ray diffraction pattern of steel covered by the passive interphase as a function of pH; i = 0.56 mA/cm^2

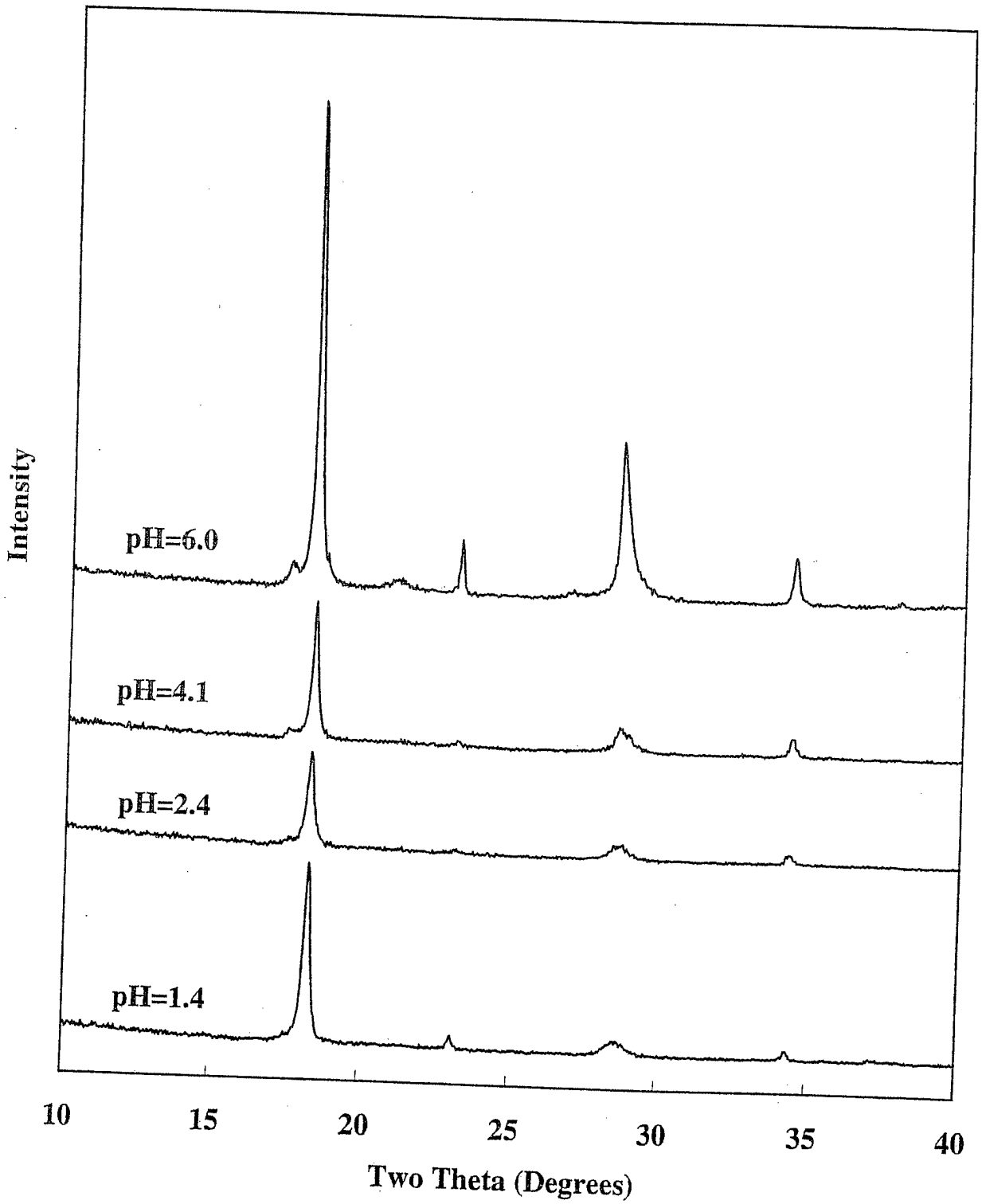

Figure 24. X-ray diffraction pattern of steel covered by the passive interphase as a function of pH; i = 3.38 mA/cm^2

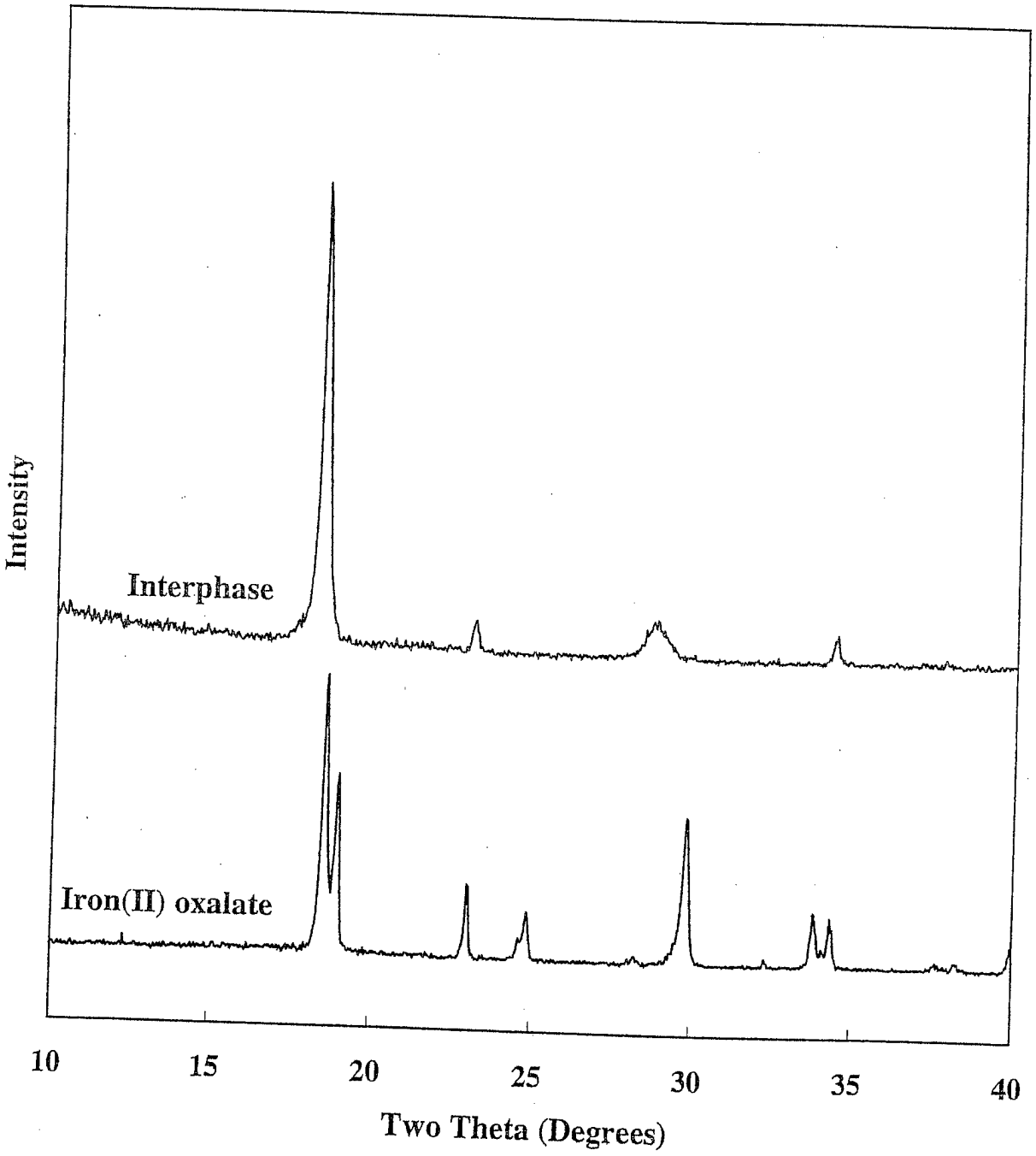

Figure 25. X-ray diffraction pattern of monoclinic iron(II) oxalate (bottom) and the passive interphase (top).

4. COMPOSITION OF THE PASSIVE FILMS AND POLYPYRROLE COATINGS: INFRARED SPECTROSCOPY, IR AND ELEMENTAL ANALYSIS

Reflection-Absorption Infrared Spectroscopy (RAIR)

The reflection-absorption infrared spectra(RAIR) of the sample were measured by a BIO-RAD FTS-40 FIIR spectrometer. An angular specular reflectance attachment was set to an incident angle of 65°. Spectra were obtained using a resolution of 4 cm^{-1} and were averaged over 128 scans. A background spectrum of a bare polished steel substrate was subtracted from the acquired spectra in all cases. In the case of transmission IR, the spectra were obtained by the means of the potassium bromide(KBr) pellets.

Figure 26 shows the RAIR spectra for the interlayer formed at end of the induction time in different pH solutions. No obvious IR peaks were observed for interlayer formed in basic medium. However, the interlayer formed in basic medium have similar spectra. Figure 27 shows the RAIR spectra of the interlayer formed at different time during the induction time at pH=1.4 and Figure 28 shows the RAIR spectra of the interlayer formed at different current density at pH=1.4. No significant difference is observed between the spectra for the interlayer obtained at different reaction time or different applied current density.

It is well known that two kinds of iron oxalate compounds exist, $FeC_2O_4 \cdot 2H_2O$ and $Fe_2(C_2O_4)_3 \cdot 2H_2O$. Figure 29 compares the IR spectra of these two model compounds with the interlayer. The IR spectra of the two model compounds were obtained by the transmission mode. The two iron oxalate model compounds show different IR spectra. The spectrum for $Fe_2(C_2O_4)_3 \cdot 2H_2O$, shows a very strong C-O stretch peaks around 1264 cm^{-1}, which is not observed in the spectrum for $FeC_2O_4 \cdot 2H_2O$. The O-H stretch peak of $Fe_2(C_2O_4)_3 \cdot 2H_2O$ occurs around 3558cm^{-1}, which is about 200cm^{-1} higher than that of $FeC_2O_4 \cdot 2H_2O$. It can be seen that the IR spectrum of the interlayer is very similar to that of $FeC_2O_4 \cdot 2H_2O$. The assignment of the main absorption bands for the model compounds and the interfaces are given in Tables 4 -6.

Figure 30 shows the IR spectra for pyrrole, the interlayer and the polypyrrole coatings obtained at pH=1.4. The IR spectrum of pyrrole was obtained by transimission mode. IR spectra also show

that the passive interlayer and polypyrrole were expectedly different. However, the N-H and O-H stretch peaks associated with pyrrole and oxalic acid, respectively were absent in the IR spectra of polypyrrole. Figure 31 shows the RAIR spectra of polypyrrole coatings formed at different pH. The coatings prepared in different pH medium shows silimar spectra. The assignment of the major bands for pyrrole and polypyrrole are listed in Table 7 and Table 8. For polypyrrole, the carbonyl —C=O peak stretch around 1710 and 1660cm^{-1} is associated with the passive interlayer, the oxalate dopant ions or overoxidation of polypyrrole. The —C-O peak stretch around 1360 and 1310cm^{-1} may also be due to the passive interlayer or overoxidation of polypyrrole. The C-O stretch peak around 1170cm^{-1} may be due to the oxalate dopant ions.

Elemental analysis shows the presence of oxygen in the coatings (Tables 9-11), indicating that the counter ion derived from the electrolyte is incorporated into polypyrrole. Using $HC_2O_4^-$ as the counter ion from oxalic acid system and sodium hydrogen oxalate and $C_2O_4^{2-}$ as the counter ion for the sodium oxalate, the degree of insertion of the counter ions was calculated to be 0.23 for the first two systems and 0.31 for the third system respectively. When the reaction medium was alkaline, the degree of insertion of the counter ions was found to be higher. This may be due to overoxidation of polypyrrole in alkaline medium.

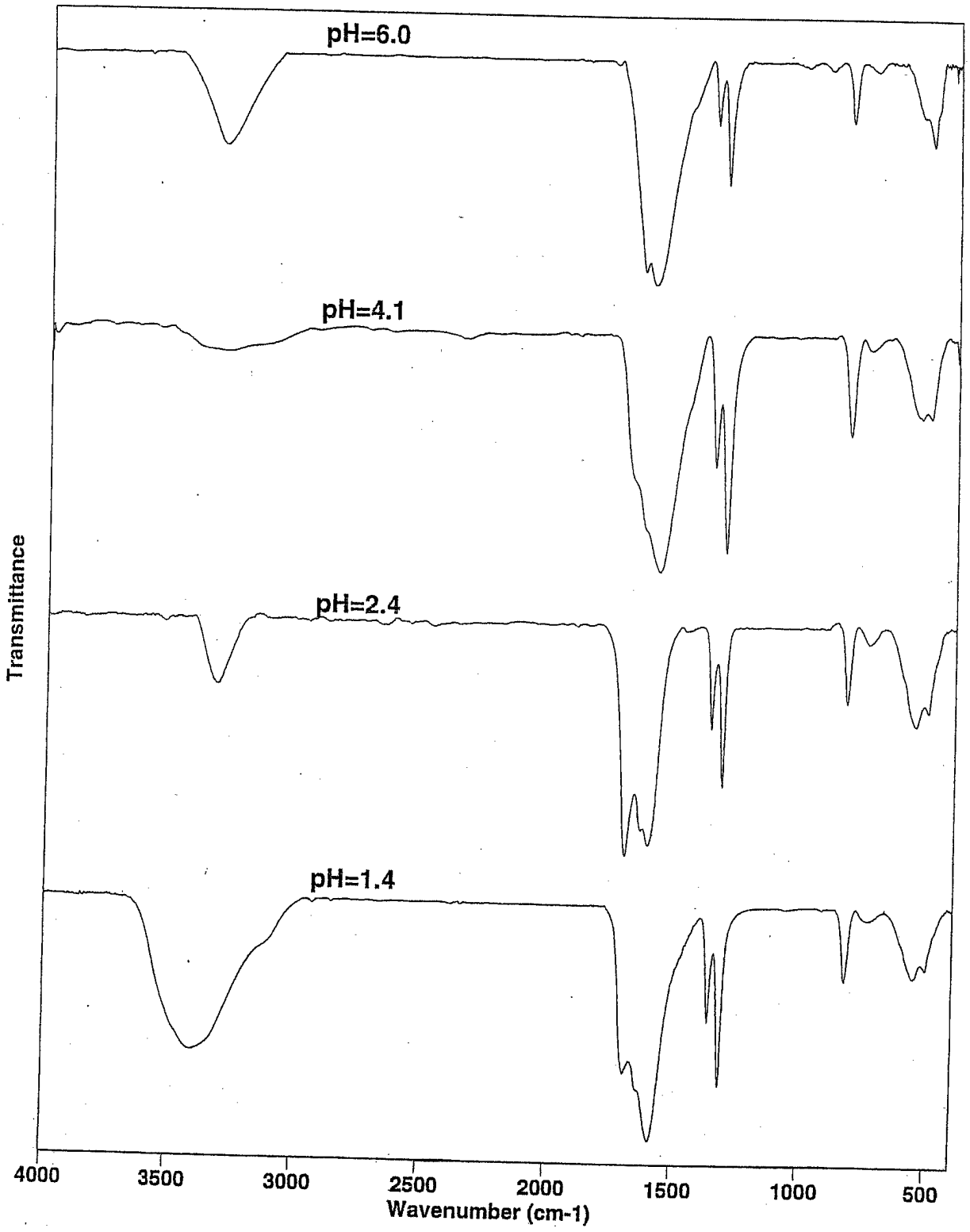

Figure 26. RAIR spectra for the passive coatings as a function of pH (i = 0.56 mA/cm^2)

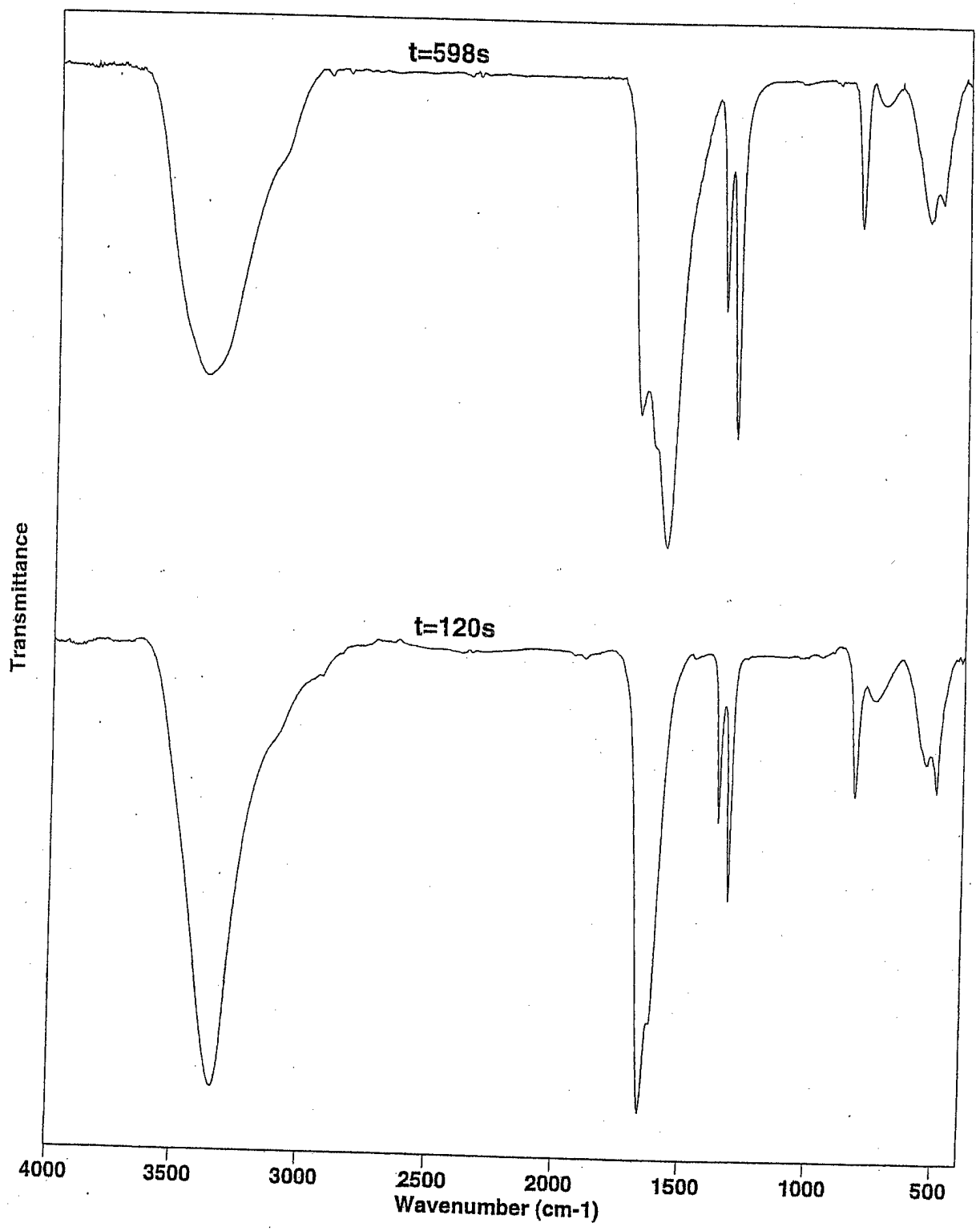

Figure 27. RAIR spectra for the passive coatings as a function of reaction time (pH = 1.4)

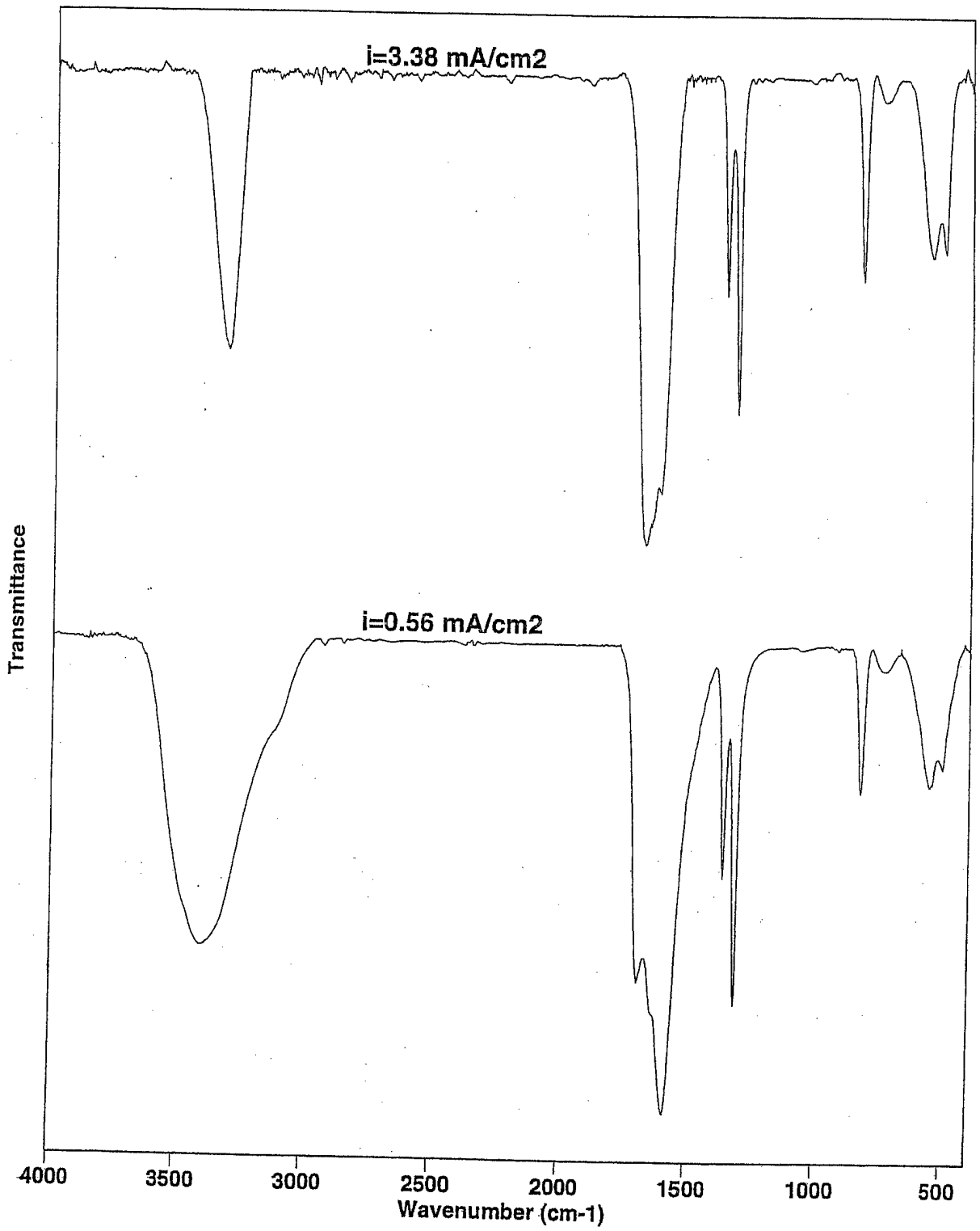

Figure 28. RAIR spectra for the passive coatings as a function of applied current (pH = 1.4)

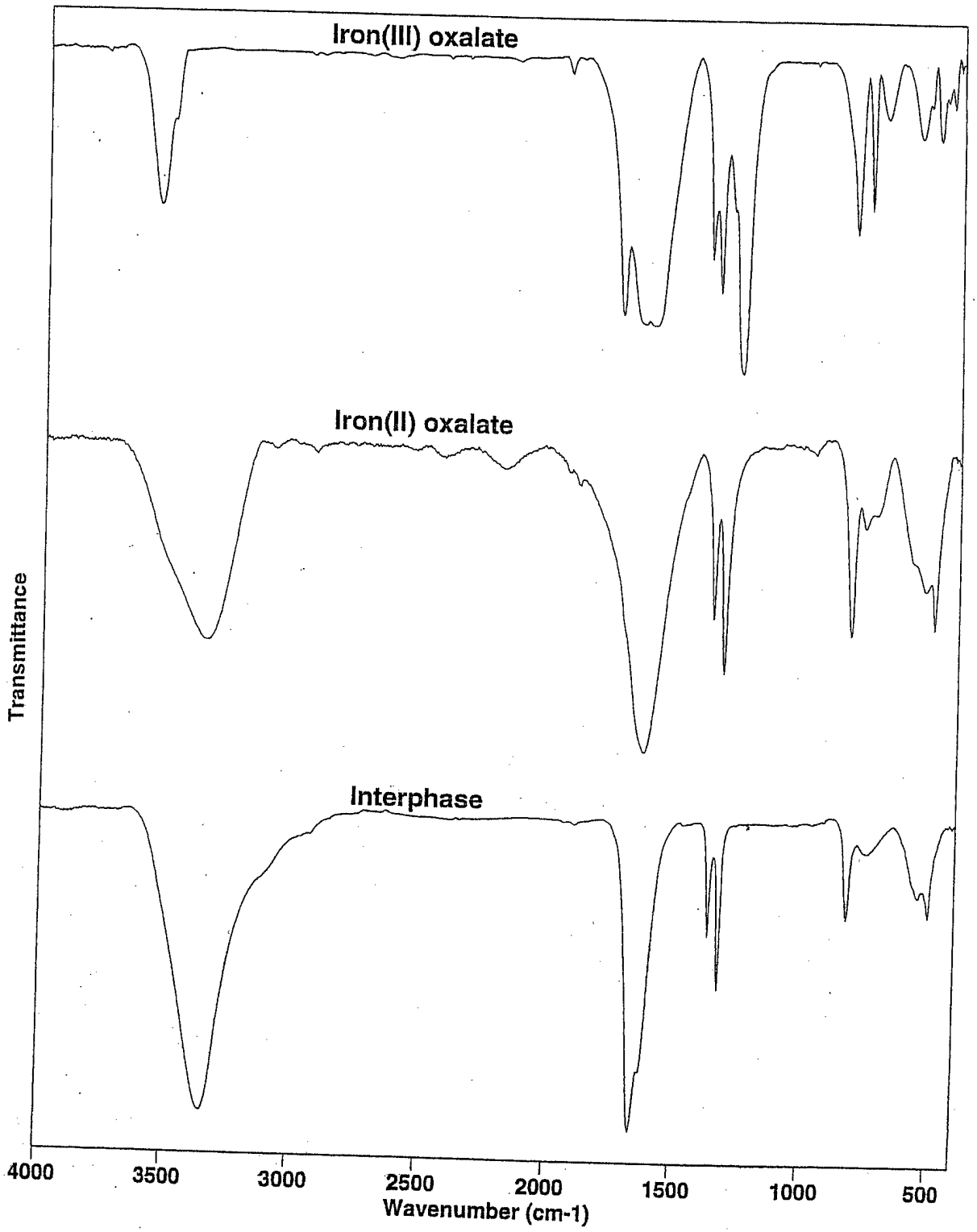

Figure 29. RAIR spectra for the passive coatings and iron (II/III) oxalate model compounds

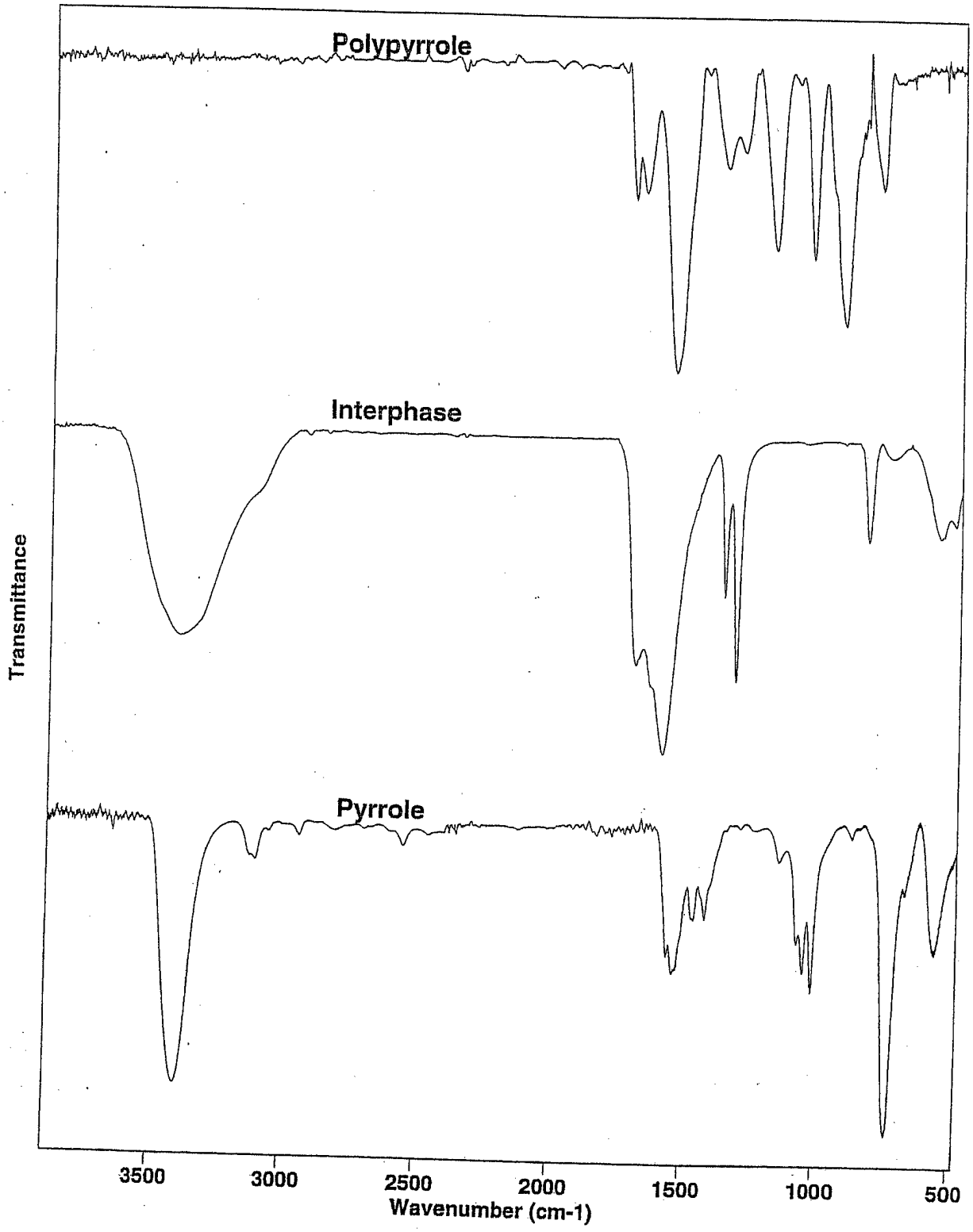

Figure 30. RAIR spectra for polypyrrole, passive coatings and pyrrole

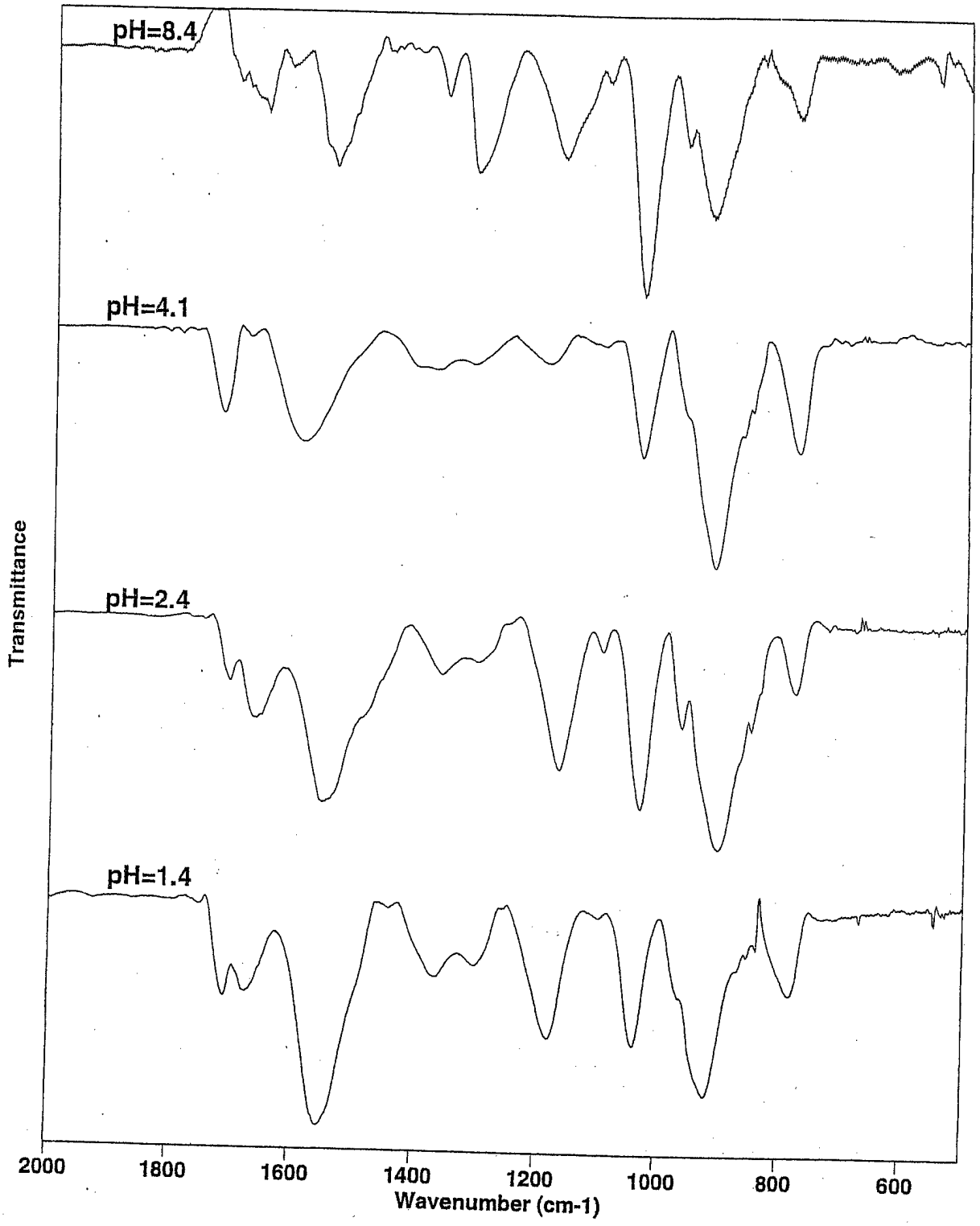

Figure 31. RAIR spectra for polypyrrole coatings as a function of pH

Table 4. **Assignment of infared absorption bands for model compound $FeC_2O_4.2H_2O$ (Transmission IR)**

Wavenumber(cm^{-1})	Assignment
3352	O-H stretch
1631	C=O stretch
1361	C-O stretch
1318	C-O stretch
823	O-C=O in-plane deformation
771	O-C=O in-plane deformation
727	? Fe-O
530	C-C-O in-plane deformation
493	C-C-O in-plane deformation

Table 5. **Assignment of infared absorption bands for model compound $Fe_2(C_2O_4)_3.6H_2O$ (Transmission IR)**

Wavenumber(cm^{-1})	Assignment
3558	O-H stretch
1735	C=O stretch
1649	C=O stretch
1610	C=O stretch
1384	C-O stretch
1349	C-O stretch
1264	C-O stretch
818	O-C=O in-plane deformation
758	O-C=O in-plane deformation
710	? Fe-O
566	C-C-O in-plane deformation
490	C-C-O in-plane deformation

Table 6. **Assignment of infrared absorbtion bands for the interface (RAIR)**

Wavenumber(cm^{-1})	Assignment
3403-3294	O-H stretch
1700-1670	C=O stretch
1658-1617	C=O stretch
1602-1575	C=O stretch
1364-1359	C-O stretch
1321-1314	C-O stretch
826-821	O-C=O in-plane deformation
747-729	?O-C=O in-plane deformation + Fe-O
554-540	C-C-O in-plane deformation
506-502	C-C-O in-plane deformation

Table 7. Assignment of infared absorption bands for pyrrole(Transmision IR)

Wavenumber(cm^{-1})	Assignment
3400	N-H stretch
3122	C-H stretch
3107	C-H stretch
1558	Ring C=C stretch
1538	Ring C=C stretch
1466	Ring stretch
1419	Ring stretch
1073	C-H in-plane deformation
1048	C-H in-plane deformation
1014	C-H in-plane deformation
763	C-H out--of-plane deformation
556	N-H wag

Table 8. Assignment of infrared absorbtion bands for polypyrrole(RAIR)

Wavenumber(cm^{-1})	Assignment
1721-1709	C=O stretch
1673-1652	C=O stretch
1591-1541	Ring C=C stretch
1367-1361	C-O stretch
1310-1301	C-O stretch
1178-1166	C-O stretch
1099-1096	C-H in-plane deformation
1037-1032	C-H in-plane deformation
925-903	C-H out-of-plane deformation
783-777	C-H out-of plane deformation

Table 9. **Results of the elemental analysis of the coating formed from oxalic acid electrolyte(pH=1.4)**

Elements	Composition(%)
C	58.67
H	3.70
N	16.85
O	17.47

Table 10. **Results of the elemental analysis of the coating formed from sodium hydrogen oxalate electrolyte(pH=2.4)**

Elements	Composition(%)
C	58.08
H	3.87
N	16.87
O	17.92

Table 11. **Results of the elemental analysis of the coating formed from sodiun oxalate electrolyte(pH=8.4)**

Elements	Composition(%)
C	55.76
H	4.22
N	15.82
O	22.64

5. STRENGTH OF ADHESION

The adhesion between the polypyrrole coatings and steel was determined by Lap Shear Joint test in accordance with ASTM standard procedure D-1002-72. Pairs of coupons were bonded together to form lap joints with an overlap length of 0.5 in. The adhesives consisted of an epoxy resin (EPON 828) and a polyamide curing agent (EPI-CURE 3140). An Instron universal mechanical tester was used and the test was performed at 1.27 mm/min.

Figure 32. compares the adhesion strength of polypyrrole coatings and the passive interphase as a function applied current. The adhesion strength of polypyrrole coated steel is about twice that of passive interphase coated steel. The adhesion strength decreases slightly with applied current. Increasing the current density from 1.13 to 3.38 mA/cm2 decreased the adhesion strength from 23 to 21, 20 to 19 and 3 to 2 MPa, at pH 1.4, 2.4 and 8.4, respectively.

The dependence of the adhesion strength on the pH of the monomer-electrolyte solution is shown in Figure 33. Increasing the pH from 1.4 to 8.4, resulted in a decrease in adhesion strength from 23 MPa at pH 1.4 to 3 MPa at pH 8.4. Note that for any given pH, lower adhesion strength is obtained at higher current density.

Figure 34 shows the comparison between the adhesion strength of Poly(N-methylpyrrole) coated steel and the control sample. No significant improvement in the adhesion strength was obtained by applying poly(N-methylpyrrole) coatings on steel.

An attempt was made to determine the strength of adhesion for polypyrrole-poly(N-methylpyrrole) copolymer coatings. It was shown that the adhesion strength of the copolymer lie between that of polypyrrole and poly(N-methylpyrrole). Infact increasing the mole % of polypyrrole in the copolymer, increased the adhesion strength (Figure 35).

It is believed that the —NH group in polypyrrole may be responsible for the enhanced adhesion strength obtained for the polypyrrole based systems over that of Poly(N-methylpyrrole) system. The —N-CH3 is less polar and cannot bond effectively to the substrate.

The fracture surface of the failed lap joints (Fig. 35), show cohesive failure for polypyrrole coated steel formed at pH 1-4 and adhesive failure for the passive interphase systems, poly(N-methylpyrrole) and control samples.

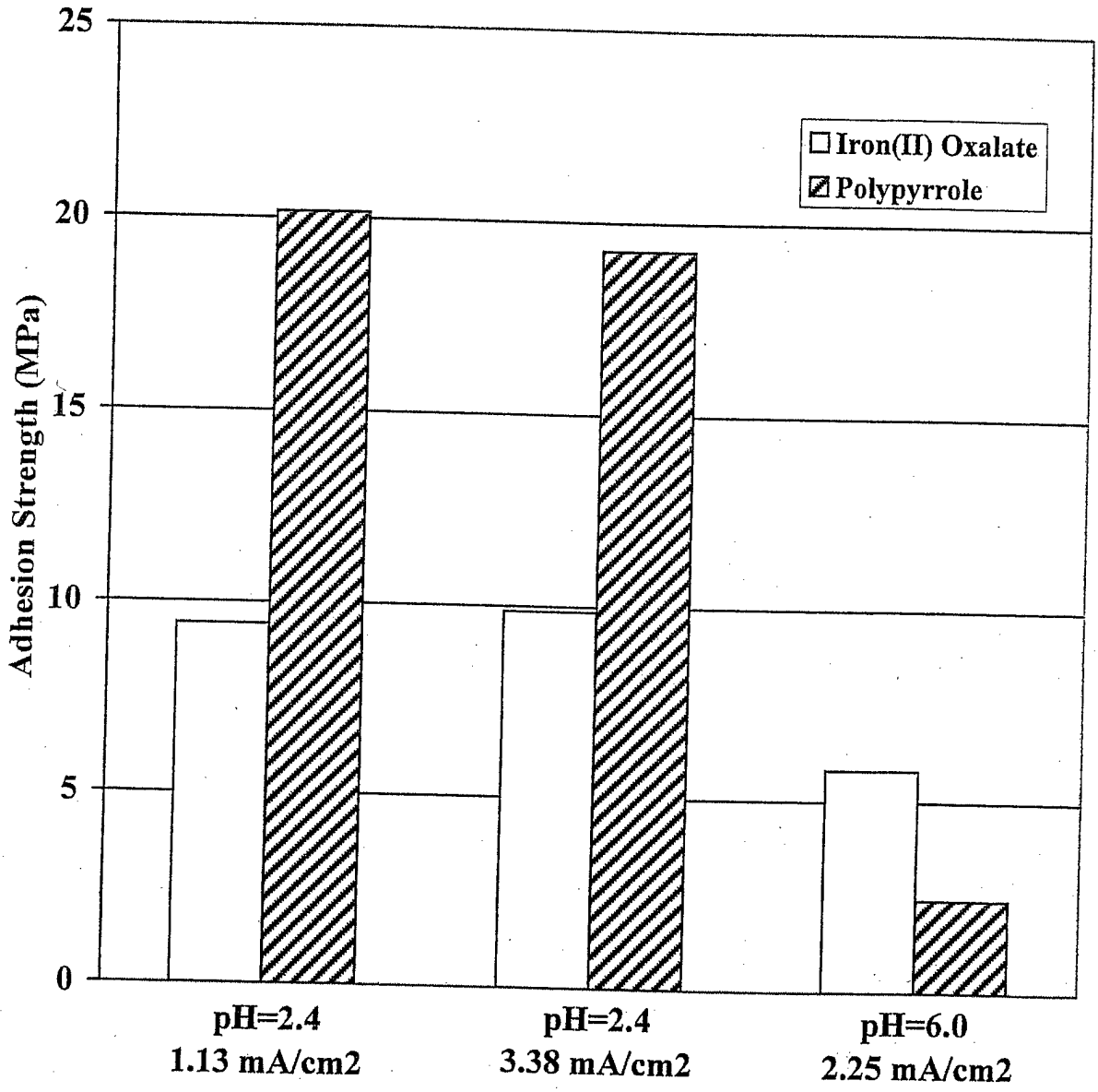

Figure 32. **The adhesion strength of steel coated with the passive interlayer and steel coated with polypyrrole as a function of pH and applied current**

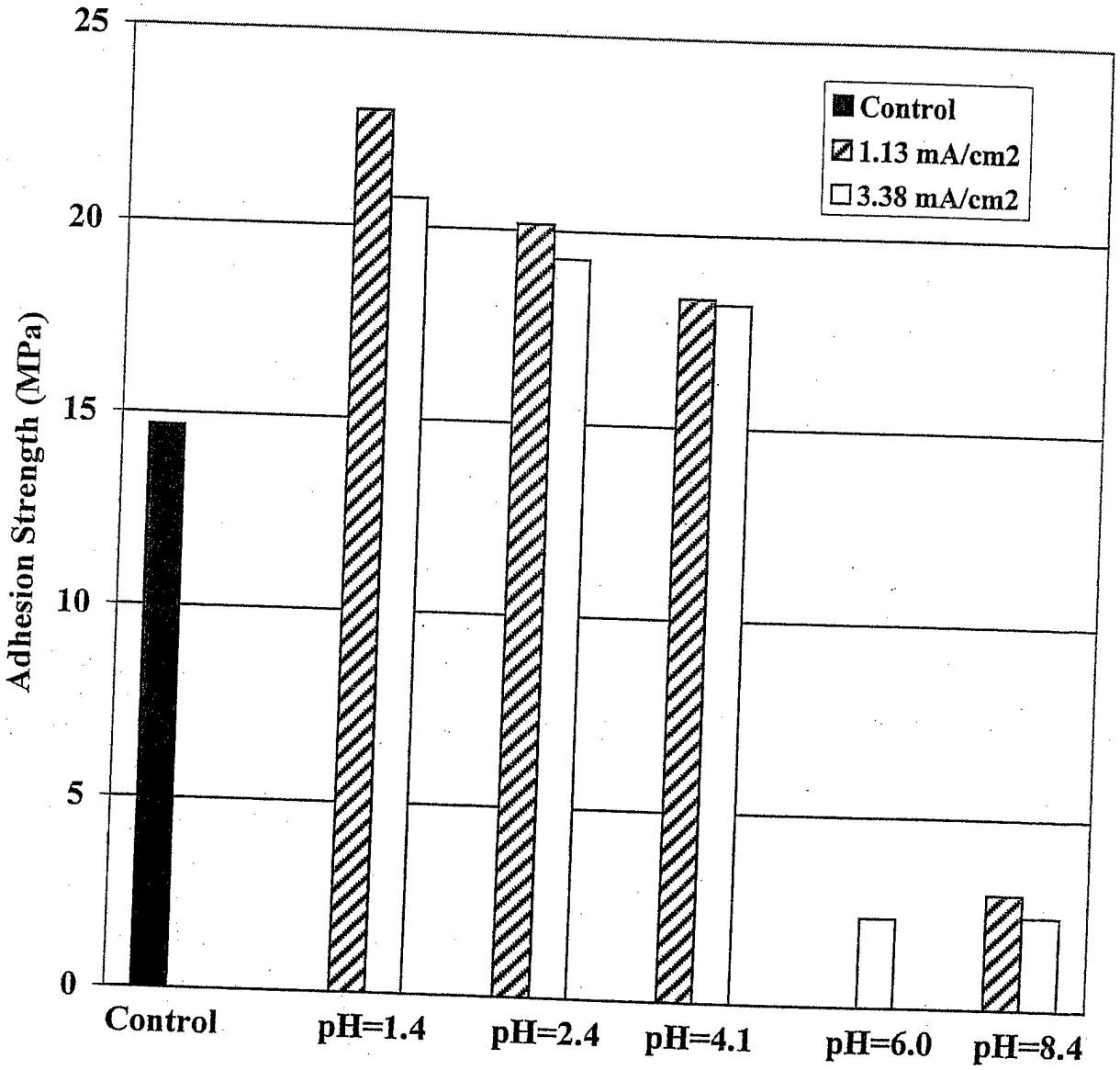

Figure 33. **The adhesion strength of steel coated with polypyrrole as a function of pH and applied current**

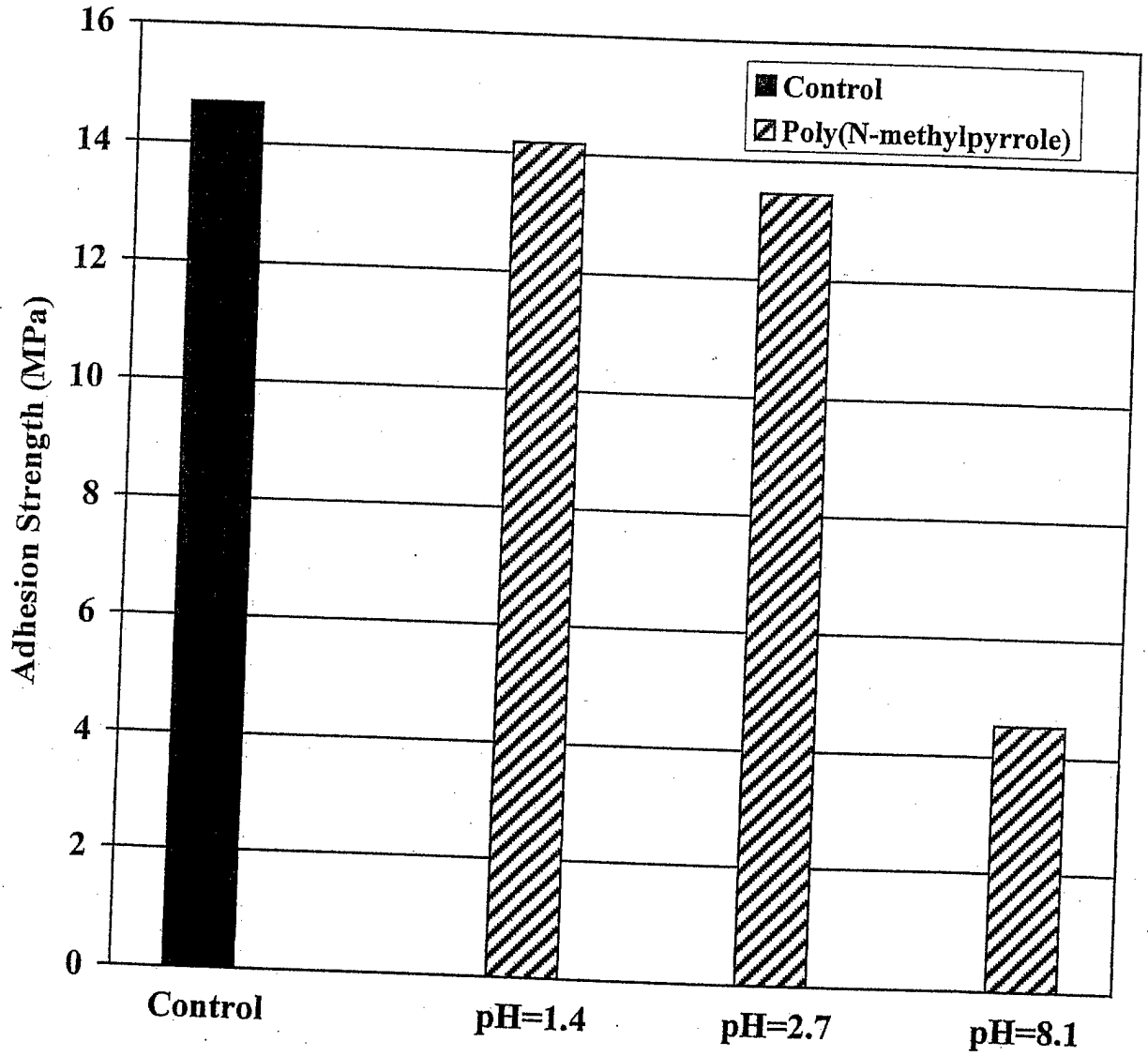

Figure 34. The adhesion strength of steel coated with poly(N-methylpyrrole) as a function of pH

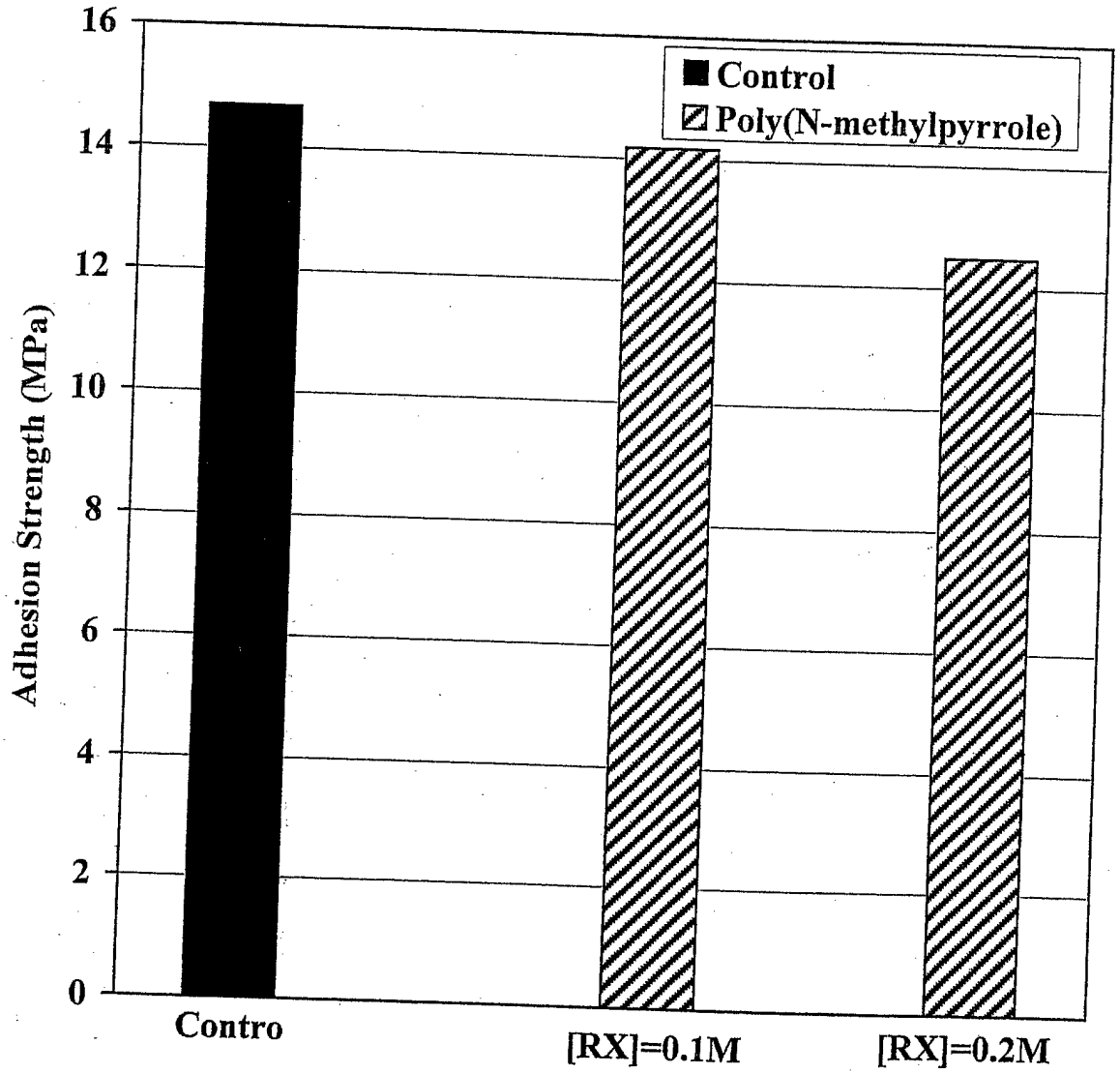

Figure 35. The adhesion strength of steel coated with poly(N-methylpyrrole) as a function of oxalic acid concentration.

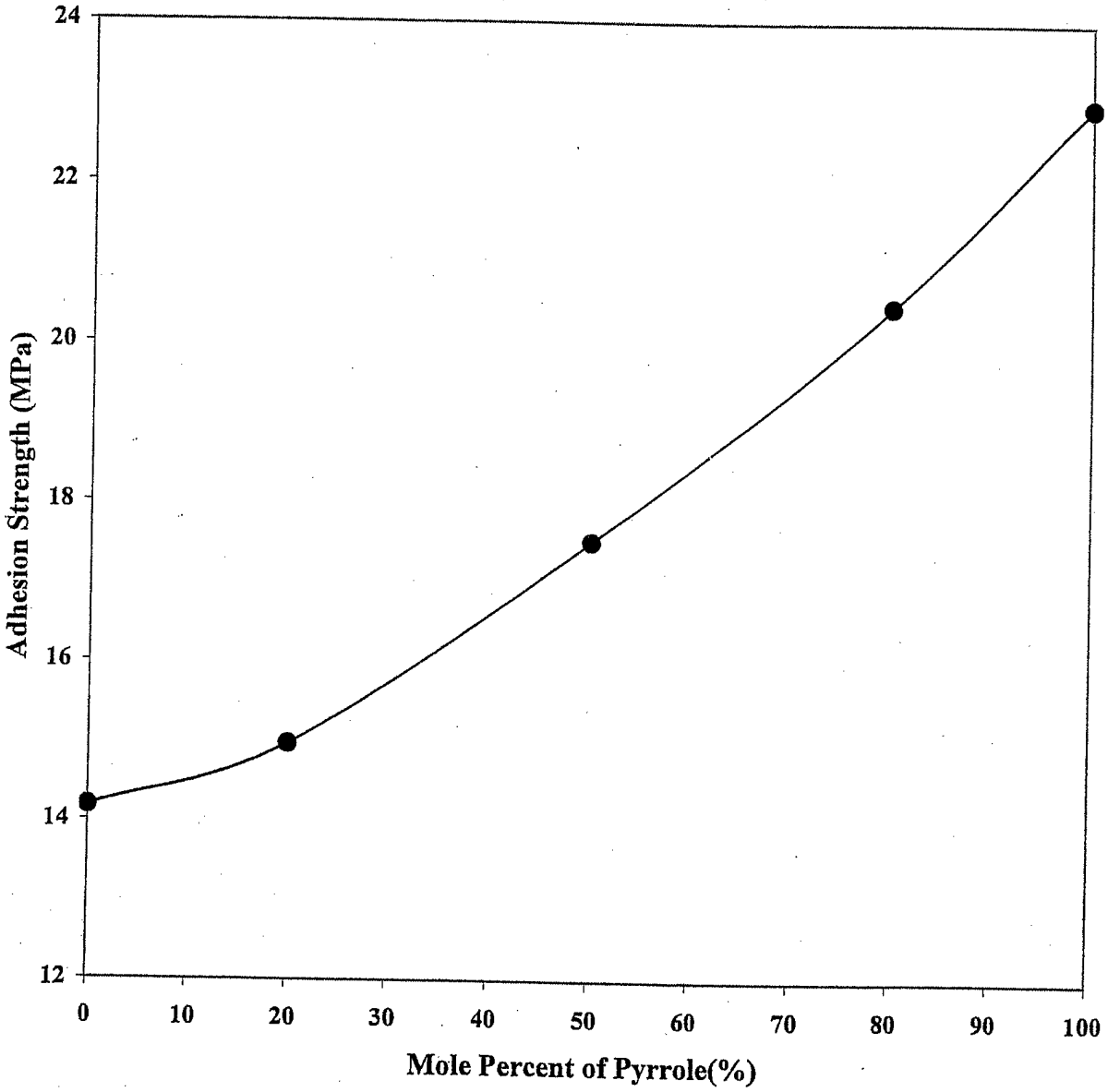

Figure 36. Dependence of the adhesion strength of steel coated with polypyrrole-co-poly(N-methylpyrrole) as a function of mole % of pyrrole in the feed

6. CORROSION PERFORMANCE OF THE COATINGS

Tafel Tests

The corrosion resistance of the coatings was determined by Tafel tests and electrochemical impedance spectroscopy, EIS. The corrosion current, corrosion potential and corrosion rate were obtained from the Tafel test. The Tafel test was conducted with a CMS 100 corrosion measurement system. 1 M NaCl solution was used as the corrosion media. The NaCl solution was saturated with air by aeration. A test spot with a diameter of 1 cm was immersed into the solution during the test. The polypyrrole coatings used for the Tafel test were 2.1 μm thick. The thickness of the poly(N-methylpyrrole) coatings varied from 1.0 to 1.5 mm. Figure 37 shows a typical Tafel plot. The Tafel plot shows a linear horrizontal region which eventually splits into two diverging (anodic and cathodic) curves. Tafel analysis was performed by extrapolating the horrizontal (linear) portion of the potential vs log current plot. to the point of intersection/convergence of the split curves. At this point both the corrosion potential Ecorr and corrosion current Icorr are obtained.

The corrosion rate is obtained by using the following expression.

CR(mpy) = [1.288x105Icorr (EW)]/(Ad)

Where CR is the corrosion rate in milliinches per year, $\mathbf{I_{corr}}$ is the corrosion current in amperes per square centimeters, EW is the equivalent weight of the oxidized element in grams/equivalent, A is the surface area of the specimen in square centimeters and d is the density of the specimen in g/cm3.

The Tafel test results are shown on Table 12. Note that the passive interphase showed a lower corrosion potential E_{corr} and higher corrosion current I_{corr} than bare steel (control), indicating that they cannot protect the latter. The polypyrrole coatings, however, showed a much higher corrosion potential and significantly lower corrosion current. Consequently, the corrosion rate of the polypyrrole coated steel is significantly reduced, showing that the coatings can effectively protect steel against corrosion. The coatings formed at pH 2.4 showed the least corrosion rate. Poly(N-methylpyrrole) also showed excellent corrosion resistance (Table 12).

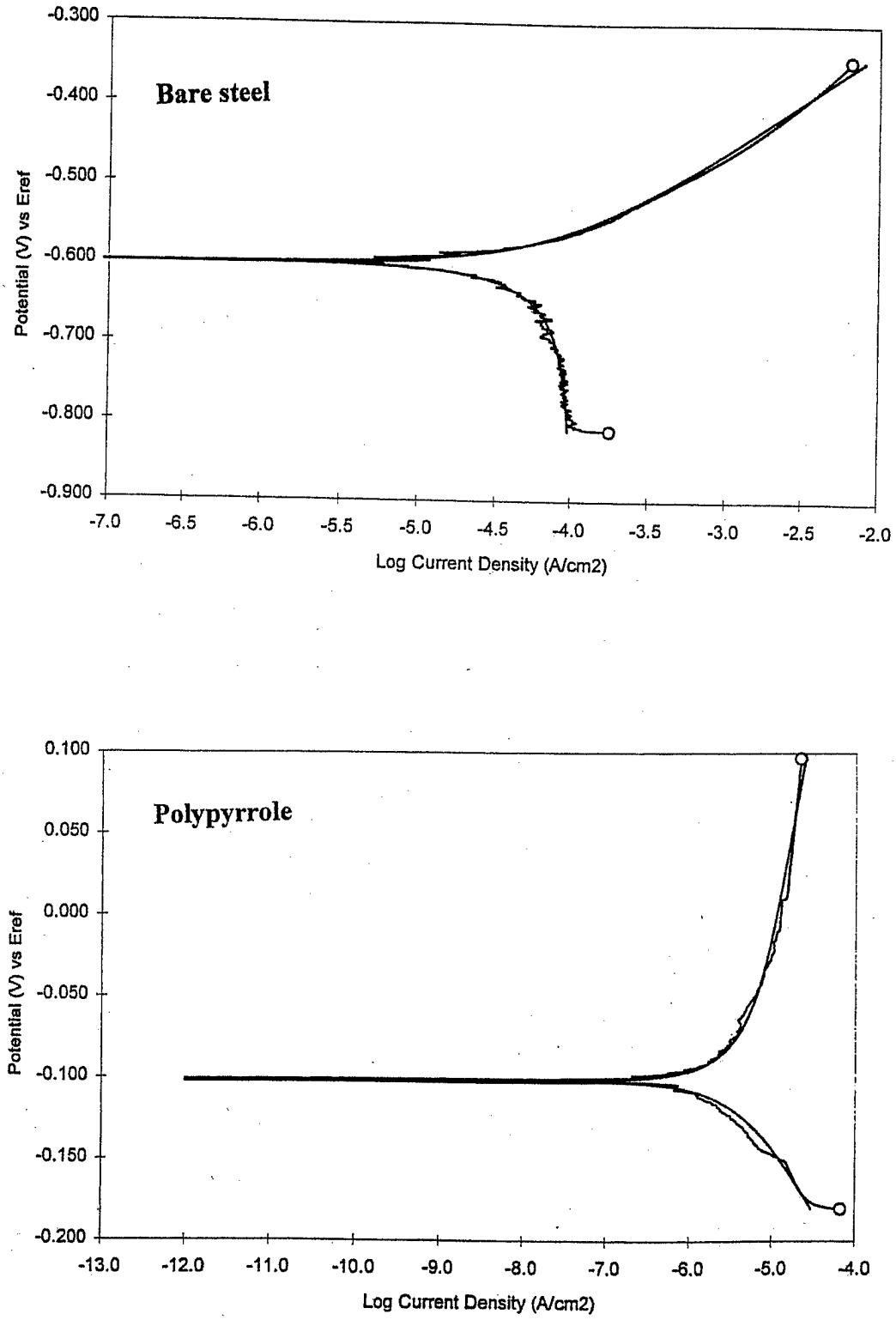

Figure 37. A typical Tafel plot

Sample	E_{corr}(mV)	I_{corr}(A/cm^2)	Corr. Rate(mm/yr)
Bare Steel	-600.6	9.05E-05	1.05
$FeC_2O_4 \cdot 2H_2O$, pH=1.4 $FeC_2O_4 \cdot 2H_2O$, pH=2.4	-698.8 -692.6	1.44E-04 1.20E-04	1.67 1.40
PPy, pH=1.4 PPy, pH=2.4 PPy, pH=4.1	-101.9 -15.7 -188.5	5.45E-06 3.60E-07 3.07E-06	0.063 0.0041 0.036
MPPy, pH=1.4 MPPy, pH=2.7	-429.5 -580.1	4.31E-06 6.37E-06	0.050 0.074

Table 11. Tafel results for steel coated with the passive coatings, polypyrrole and poly(N-methylpyrrole), as a function of pH (i = 1.13 mA/cm^2)

Electrochemical Impedance Spectroscoipy (EIS)

The corrosion resistance of the coated and control steel substrate was also evaluated by electrochemical impedance spectroscopy (EIS). EIS is an attractive technique for evaluation of corrosion resistance. It is a non-destructive technique and the mechanism of corrosion control by thin polymer films can be predicted by this technique. Experimentally, the substrates were immersed in an electrolytic solution and an alternating was applied. The alternating current response is measured. An electrode-electrolyte interface undergoing electrochemical reaction is analogous to an electronic circuit and can be represented by an electronic circuit model.

EIS readings was be taken every 2.5 min for 30 min in the frequency range of $1\text{-}10^4$ Hz. Nyquist plots will be constructed for a given current density and appropriate equivalent circuit model was used to correlate the impedance Z to the resistance, R (solution R_{sol} and electrode resistance R_e), current density, j and the capacitance of the film, C; For one depressed capacitance loop:

$$Z = R_{sol} + \frac{R_e}{1 + (j\,\omega\,R_e C)^{\alpha}}$$

Where a is a constant and has a value of 0.9. C is calculated by using the frequency corresponding to the apex of the capacitive loop while R_e is obtained from the chord of the capacitance loop. A correlation between the process variables, film porosity and corrosion resistance was made and further insight into corrosion protection was gained.

By comparing the impedance of an equivalent electrical circuit with the actual impedance of the substrate, the ease with which corrosion propagates in the coating-substrate interface, Rp, will be determined.

The polarization resistance of steel with, R_{pc} and without coatings, Rp, was determined and the inhibition efficiency, IE% was calculated by using the expression:

$$IE\% = \left(\frac{R_{pc} - R}{R_{pc}}\right) x\ 100$$

Figure 38 shows the equivalent circuit model used to analyze the EIS spectra. The circuit consists of a working electrode, areference electrode, electrolyte resistance, Rs, pore resistance Rpo, coatings capacitance Cc, polarization resistance Rp, double layer capacitance Cdl and a Warburg impedance W. The EIS results are shown on Figures 39-41. Note that the polarization resistance of polypyrrole coated steel depends on the applied current and pH of the monomer-electrolyte solution. Inhibition efficiency of 90 and 80% were obtained for polypyrrole coatings formed by applying a current density of 1.13mA/cm2 at pH 2.4, 1.4 and 4.1, respectively. At a higher

respectively. At a higher applied current density of 3.38 mA/cm2, the inhibition efficiency was 30% at pH 1.4 and 2.4, respectively.

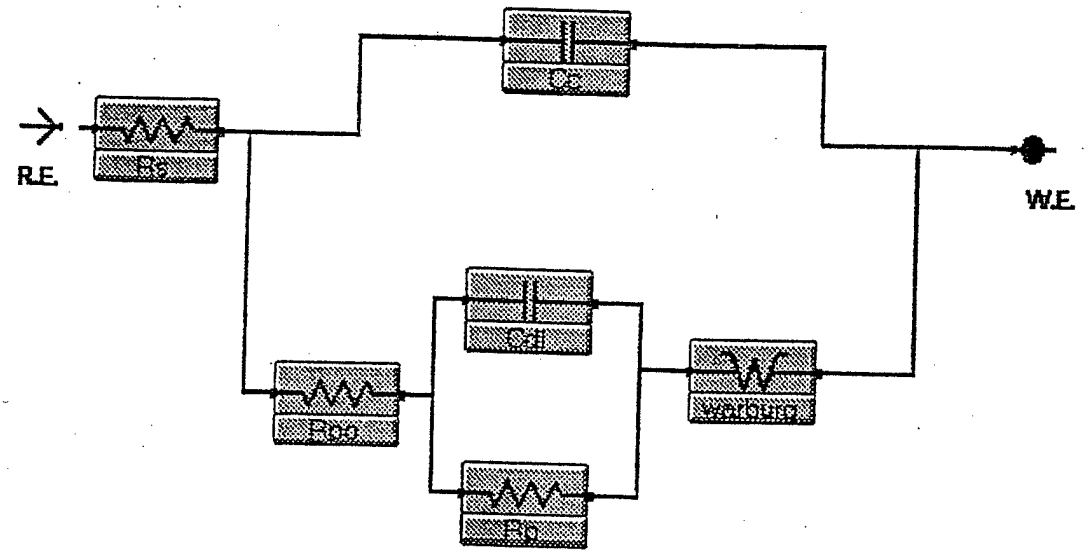

Figure 38. The equivalent circuit model for EIS analysis

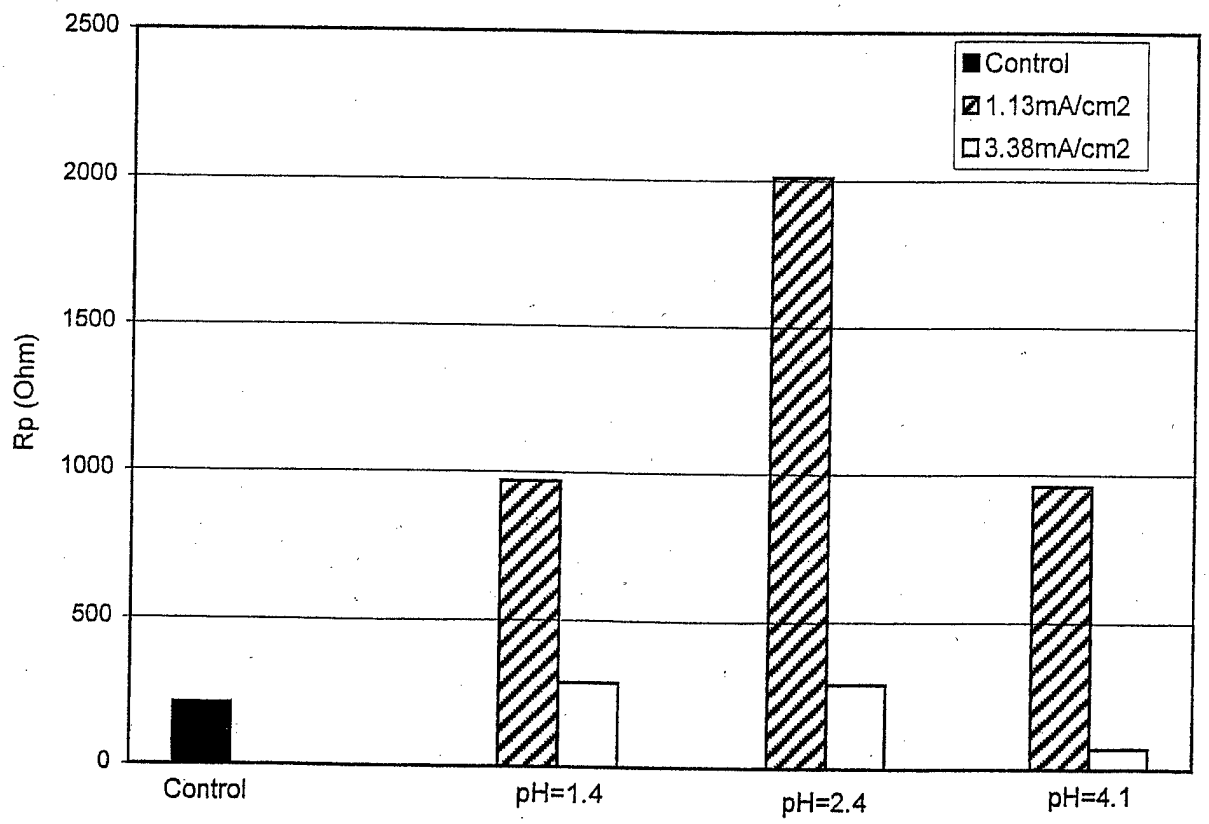

Figure 39. **Polarization resistance for polypyrrole coated steel as a function of pH and applied current.**

PUBLICATIONS AND DISSERTATION

DISSERTATION

1. Wencheng Su, "Electrochemical Synthesis and Characterization of Polypyrrole and Substituted Polypyrrole Coatings on Steel Substrates", University of Cincinnati, June 1999

PATENTS AND DISCLOSURES

1. "Passivation of Metals by pH and Electrochemical Process Parametric Control", UC Disclosure No. 96-033 (Patent application filed), with W. Su

2. "Formation of Conducting Composite and Conducting Elastomers on Steel by Electrochemical Process", Disclosure No. 99-026, with R. Rajagopalan

REFERRED PUBLICATIONS

Paper 1: "Formation of Polypyrrole Coatings onto Low Carbon Steel by Electrochemical Process", J. Appl. Polym. Sci., 65, 417-424 (1997).

Paper 2. "Kinetics and Efficiency of Aqueous Electropolymerization of Pyrrole onto Low-Carbon Steel", J. Appl. Polym. Sci., 65, 617-624 (1997).

Paper 3. "Effects of Electrochemical Process Parameters on the Synthesis and Properties of Polypyrrole Coatings on Steel", Synthetic Metals 95, 159-167 (1998).

Paper 4. "Electropolymerization of Pyrrole on Steel Substrates in the Presence of Oxalic Acid and Amines", Electrochemica Acta, 44, 2173-2184 (1999).

Paper 5. "Characterization of the Passive Inorganic Interphase and Polypyrrole Coatings Formed on Steel by the Aqueous Electrochemical Process", J. Appl. Polym. Sci., 71, 2075-2086 (1999).

Paper 6. "Morphology and Structure ofthe Passive Interphase Formed During Aqueous Electrodeposition of Polypyrrole Coatings on Steel", Electrochemica Acta (accepted).

Paper 7. "Formation of Polypyrrole Coatings on Stainless Steel in Aqueous Benzene Sulfonate Solution", Electrochemica Acta, 42(17), 2685-2694 (1997).

Paper 8. "Effect of Process Parameters on the Electropolymerization Potential and Rate of Formation of Polypyrrole on Stainless Steel", J. Appl. Polym. Sci., 66, 2433-2440 (1997).

Paper 9. "One Step Electrochemical Process for the Formation of Poly(N-methylpyrrole) Coatings on Steel in Different Media", Synthetic Metals, 97, 73-80 (1998).

Paper 10. "Electrodeposition of Poly(N-methylpyrrole) Coatings on Steel from Aqueous Medium", J. Appl. Polym. Sci., 71, 1293-1302 (1999).

Paper 11. "IR and XPS Studies on the Interphase and Poly(N-methylpyrrole)Coatings Electrodeposited on Steel Substrates", Electrochemica Acta, 44, 3321-3332 (1999).

Paper 12. "Adhesion of Polypyrrole Coatings to Low-Carbon Steel", (in preparation)

Paper 13. "Corrosion Performance of Polypyrrole Coatings formed on Steel by Electrodeposition", (in preparation).

Formation of Polypyrrole Coatings onto Low Carbon Steel by Electrochemical Process

WENCHENG SU, JUDE O. IROH

Department of Materials Science and Engineering, University of Cincinnati, Cincinnati, Ohio 45221-0012

Received 12 June 1996; accepted 17 October 1996

ABSTRACT: Thin polypyrrole coatings ($\sim 10\ \mu m$ thick) were formed on low carbon steel by an aqueous constant current electrochemical polymerization using oxalic acid as the electrolyte. The amount of polypyrrole coatings formed on steel increased with the applied current and monomer concentration. No significant change in the electropolymerization of pyrrole occurred as a result of increased electrolyte concentration. The induction time for electropolymerization decreased significantly with current density but was unaffected by the initial monomer and electrolyte concentration. The electropolymerization potential of pyrrole increased with increased current density (Cd), i.e., $Ep = 0.62 + 0.41$ [Cd], and decreased exponentially with increased monomer and electrolyte concentration, $Ep = E_0 \exp^{-[M]}$. Scanning electron microscopy (SEM) showed that the microstructure of the polypyrrole coatings formed on steel was dependent on the current density to the extent that smoother and more uniform coatings are formed at low current density. © 1997 John Wiley & Sons, Inc. J Appl Polym Sci **65:** 417–424, 1997

INTRODUCTION

Electropolymerization is an effective technique for applying polymer coatings of varying thickness onto conductive substrates. It combines an electrochemical reaction with polymerization.[1] Electropolymerization of pyrrole has been traditionally performed by using inert metals as the working electrode (WE).[2–10] Earlier attempts to electropolymerize pyrrole onto reactive metals was unsuccessful because of the preferred dissolution of the metals at a potential lower than the oxidation potential of pyrrole. The electropolymerization of pyrrole has been attempted on reactive metals such as steel, copper, and aluminum[11,12] in different electrolyte–solvent systems. Electropolymerization of pyrrole in acetonitrile and tetrafluoroborate medium onto reactive metals such as aluminum (Al), indium (In), silver (Ag), and steel (Fe) was investigated by Prejza.[11] It was shown that the dissolution of these metals occurred in preference to the electropolymerization of pyrrole. Cheung et al. investigated the electropolymerization of pyrrole on a wide range of metals using propylene carbonate as the solvent and tetraethylammonium perchlorate and toluenesufonate as the electrolytes.[12] They showed that polypyrrole–toluenesulfonate (PPy–TS) films could be formed on a wide range of metals. It was reported that the oxidation potential of pyrrole was increased while the current intensity decreased when titanium (Ti), steel (Fe), and Al were used as the working electrode. This behavior was attributed to the formation of a metal oxide layer which impeded electron transfer and electropolymerization. It was, however, noted that the presence of a metal oxide layer was necessary for the electropolymerization of pyrrole onto brass. The oxidation potential of PPy–TS films was also found to be dependent on the metal used as the

Correspondence to: J. O. Iroh.

Contract grant sponsor: Office of Naval Research.

working electrode. When platinum (Pt) was used as the working electrode, the electropolymerization of pyrrole appeared to be controlled by both diffusion and adsorption processes. In spite of these differences, the room-temperature electrical conductivity of fully oxidized free-standing PPy films ($\sim$ 20–50 s cm^{-1}) was reported to be independent of the nature of the working electrode. Janssen and Beck performed the electropolymerization of pyrrole on steel in an aqueous medium containing partially neutralized polyacrylate.[13] They reported that adherent PPy–polyacrylate composite film was formed at a low current density.

Schirmeisen and Beck performed galvanostatic electropolymerization of PPy from more than 20 nonaqueous and aqueous electrolytes containing different anions on Pt, gold (Au), copper (Cu), Ti, stainless steel (VA), and steel (Fe).[14] They showed that electropolymerization proceeded effectively in many aqueous electrolytes, when passive metals such as Pt, Au, V2A, or Ti were the working electrode. However, electropolymerization failed to occur when reactive metals such as Cu or iron were used. In acidic conditions (pH < 7), these metals actively dissolve and electropolymerization could not occur. In basic conditions (pH ≥ 10), the metals were passivated, but inorganic films were formed rather than polymer coatings. The only exception from this behavior was the electropolymerization of pyrrole onto steel using potassium nitrate as the electrolyte. Smooth, continuous, and adherent PPy coatings were formed on steel using electrolyte concentrations of 0.01–1*M* and current densities of 0.5–10 mA cm^{-2}. The degree of insertion of nitrate ions into the film was about 0.25.

Beck and Michaelis reported the formation of strongly adherent and smooth PPy coatings onto a steel working electrode by aqueous electropolymerization using oxalic acid as the electrolyte.[15] They showed that the adherence strength of the coatings was as high as 11.5 N mm^{-2} for 1 μm films but decreased with increasing coating thickness. The surface roughness of the PPy–oxalate film was found to be relatively low in comparison to other polypyrrole salts. The polymer films were essentially nonporous. The porosity of the film increased only slightly on elongation of the coating in the direction parallel to the iron substrate by 1–2%.

Hülser and Beck investigated the electropolymerization of PPy on Al from different aqueous electrolytes.[16,17] They showed that electropolymerization of adherent and homogeneous PPy coatings on Al occurred in these electrolytes. The electrolytes that were successful at initiating aqueous electropolymerization of pyrrole on Al include nitric acid, sulfuric acid, and oxalic acid. The ability to form an adherent PPy coating increased from left to right. Pretreatment of the Al by polishing (PD) or by anodic (galvanostatic) activation (GA) was found to be essential for the formation of a coherent and adherent PPy coatings. The presence of pores in the Al_2O_3 layer played an important role in the electrochemical process. In all cases, the Al_2O_3 layer containing pores, usually filled with electrolytes, were converted into Al_2O_3–PPy sandwich layers. The sandwich Al/Al_2O_3/PPy structure behaved as a condenser with electronically conducting Al and PPy plates. The Al_2O_3/PPy sandwich layers showed an unusually high permittivity of about 10^3. Ferreira et al. investigated the influence of solvent and electrolytes on the electropolymerization of pyrrole on steel.[18] They observed that the rate of corrosion of steel in acidic medium increased in the absence of pyrrole. Electropolymerization of pyrrole was shown to depend on the acidity of the medium. Electropolymerization of pyrrole in acetonitrile produced a PPy–ferric oxide composite film. However, in basic solvents, the coatings are composed of only PPy. In this article, we report the dependence of aqueous electropolymerization of pyrrole onto low carbon steel in an oxalic acid electrolyte on the electrochemical process variables such as the applied current, initial monomer concentration, electrolyte concentration, and reaction time.

EXPERIMENTAL

Materials

Pyrrole (98%) and oxalic acid (98%) were purchased from Aldrich Chemical Co. Tetrachloroethylene and methanol were also purchased from Aldrich. The reagents were dissolved in deionized water prepared in our department.

The working electrode was an 0.5 mm-thick QD low carbon steel panel purchased from the Q-panel Co. The working electrode was degreased with tetrachloroethylene for about 1 h prior to electrochemical polymerization. The counterelectrodes were composed of two Ti alloy plates. A saturated Calomel electrode (SCE), manufac-

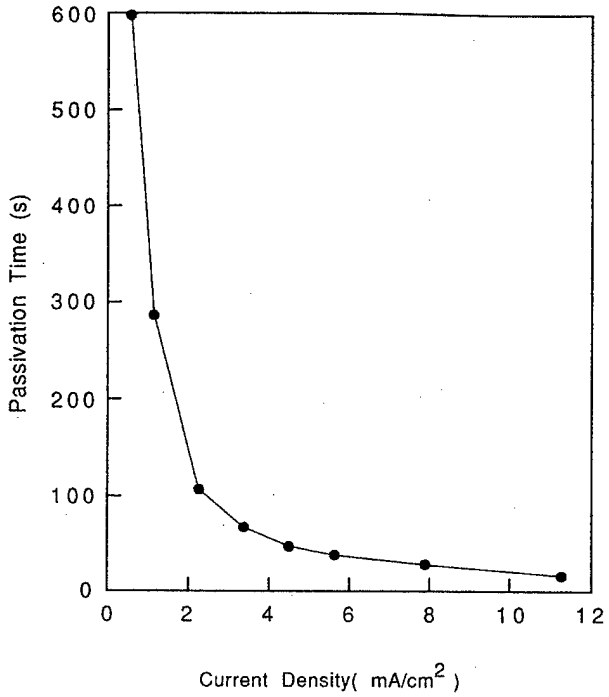

Figure 1 Dependence of induction time for electropolymerization of pyrrole onto steel (passivation time) on the applied current density.

tured by Corning Co., was used as the reference electrode. Galvanostat electropolymerization of pyrrole was performed by an EG&G Princeton Applied Research Potentiostat/Galvanostat Model 273A.

Electropolymerization

Electropolymerization of pyrrole was carried out in a one-compartment PPy cell. The current densities used in this study ranged from 0.22 to 11.26 mA/cm^2. The initial concentration of oxalic acid was varied from 0.05 to 0.4M, while the initial monomer concentration was varied from 0.1 to 0.8M.

The coated steel was rinsed with methanol and dried at 65°C in a vacuum oven to constant weight. The weight of the coatings was determined as the difference between the coated and noncoated steel (control).

Characterization

Elemental analysis of the coatings extracted from coated steel was performed by Galbraith Laboratories. The morphology of the coated and noncoated substrate was examined by scanning electron microscopy (SEM). The samples were shadowed with carbon to enhance their conductivity.

RESULTS AND DISCUSSION

Effect of Current Density

The concentration of pyrrole and oxalic acid were kept constant at 0.25 and 0.1M, respectively. The induction time for polymerization decreased with increased current density (Fig. 1). The decrease in the induction for electropolymerization was proportionate to the increment in the current density. Increasing the current density from 0.56 to 3.38 mA/cm^2 (500% increase) resulted in a sharp reduction in induction time from 598 to 67 s (90% reduction). A subsequent increase in the current density from 4.50 to 11.26 mA/cm^2 (150% increase) resulted in a more gradual decrease in the induction time from 47 to 16 s (66% reduction) (Table I). The induction time is the time expended during the dissolution of steel and ends at the onset of formation of iron oxalate (passivation time) (Fig. 2). At low current density (Cd) $\leq$ 0.22 mA/cm^2, the potential of the reaction remained constant and negative (Ep = −0.4 V vs. SCE), resulting in the dissolution of the steel (Fig. 2):

$$Fe - 2e \rightarrow Fe^{2+} \ (E_{ox} = -0.44 \text{ V})$$

The total charge passed during the passivation of steel remained nearly unchanged between 335 mC/cm^2 at 0.56 mA/cm^2 and 180 mC/cm^2 at 11.26 mA/cm^2 (Table II). An about 2000% change in the current density (0.56–11.26) caused only a 50% change in the passivation charge. The passivation of steel is accomplished by the formation of an iron oxalate (FeC_2O_4) interlayer (electropolymerization potential [Ep] $\geq$ 0.5 V)[14,15]:

Table I Dependence of Electropolymerization Potential and Induction Time for Polymerization on the Current Density

Current Density (mA/cm^2)	Induction Time (s)	Peak Potential (V vs. SCE)	Reaction Potential (V vs. SCE)
1.13	287	0.84	0.66
2.25	109	0.88	0.71
4.50	47	1.04	0.80
7.88	28	1.34	0.95

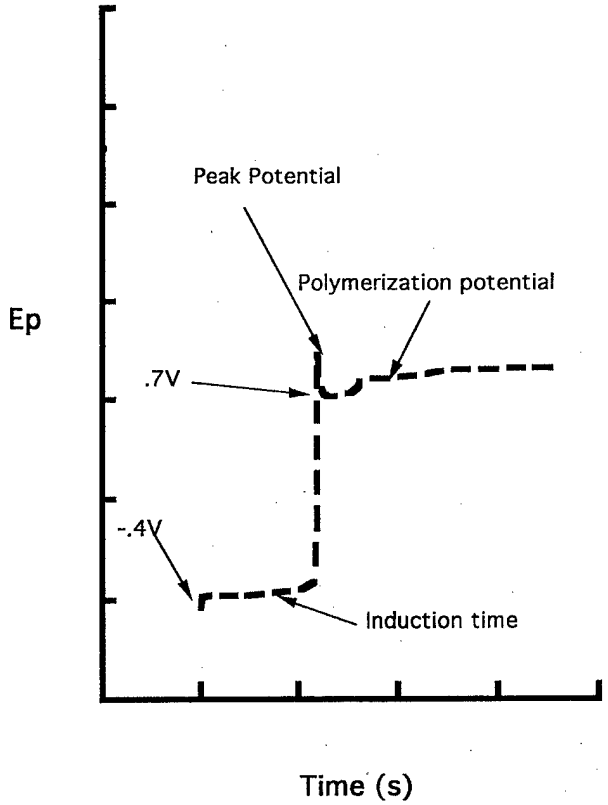

Figure 2 Induction time for electropolymerization of pyrrole onto steel using oxalic acid as the electrolyte.

$$Fe^{2+} + C_2O_4^{2-} + 2H_2O \rightarrow FeC_2O_4 \cdot 2H_2O$$

The electropolymerization of pyrrole is believed to commence at the end of the induction period at a positive potential value ($Ep \geq 0.5$ V vs. SCE) (Fig. 2). The electropolymerization potential of pyrrole increased linearly with current density (Cd) (Fig. 3) and followed the relationship

$$E_p = 0.62 + 0.041\ [Cd]$$

Table II Relationship Between Induction Time and Total Charges Passed During Induction Period

Current Density (mA/cm^2)	Induction Time (s)	Passivation Charge (mC/cm^2)
0.56	598	335
1.13	287	324
2.25	109	245
3.38	67	226
4.50	47	211
5.63	38	214
7.88	28	220
11.26	16	180

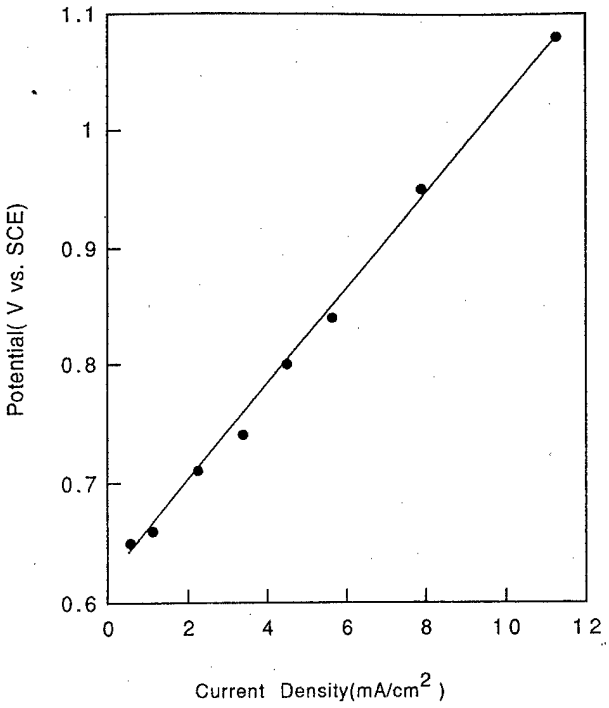

Figure 3 Dependence of polymerization potential on the current density.

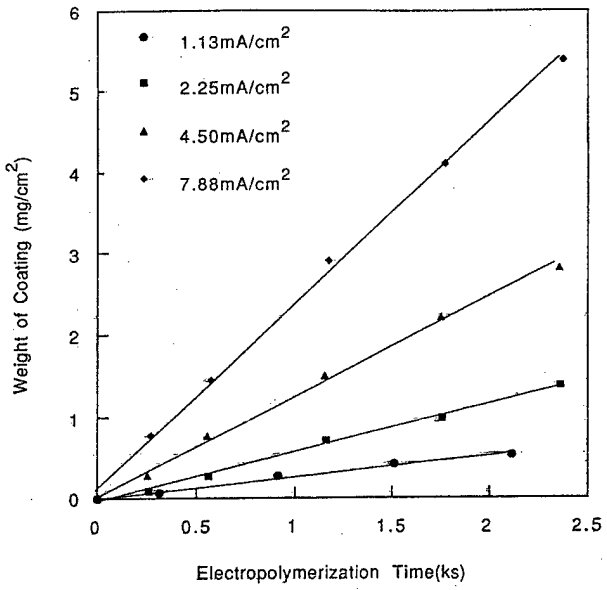

Figure 4 Dependence of PPy coating formation on current density. $[M] = 0.25M$; $[Ox] = 0.1M$; WE = low carbon steel.

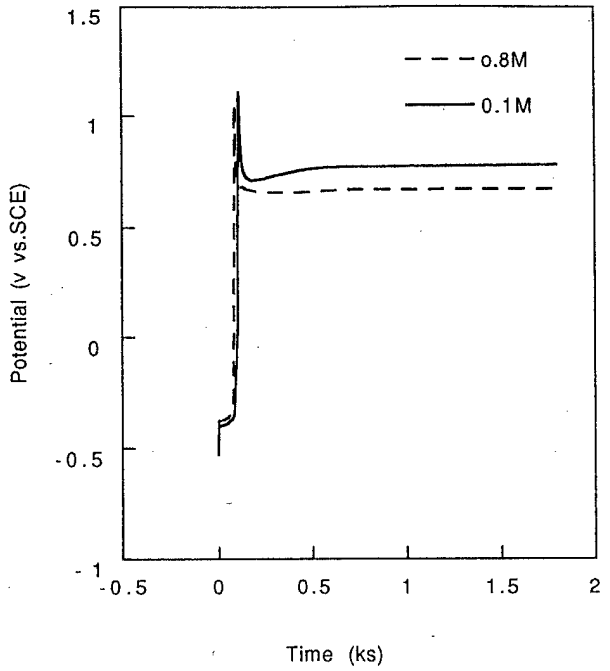

Figure 5 Dependence of induction time and electropolymerization potential on pyrrole concentration.

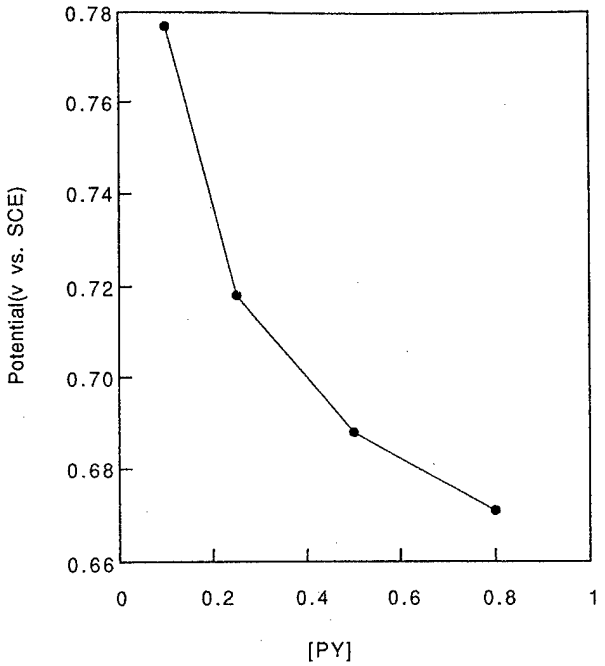

Figure 6 Dependence of polymerization potential on initial pyrrole concentration.

The amount of PPy coatings formed on steel increased with an increased electropolymerization potential in agreement with our earlier findings.[19] The weight of PPy coatings formed onto steel increased proportionately with current density and electropolymerization time (Fig. 4). The weight of the electrode before and at the end of induction time (passivation time) was determined and no significant change occurred. The passivation time was taken as the starting time for the electropolymerization of pyrrole.

Effect of Initial Monomer Concentration

The concentration of oxalic acid was kept constant at 0.1*M* and the current density was kept constant at 2.25 mA/cm^2, while pyrrole concentration was varied from 0.1 to 0.8*M*. The concentrations of pyrrole did not have any noticeable effect on the passivation time (Fig. 5). This suggests that pyrrole was not involved in the passivation of steel. The polymerization potential was found to decrease exponentially with increased pyrrole concentration:

$$Ep = E_{ox} \exp^{-[M]}$$

About a 14% decrease in the polymerization potential occurred when the monomer concentration was increased by 75% (Fig. 6). The lowering of the electropolymerization potential with in-

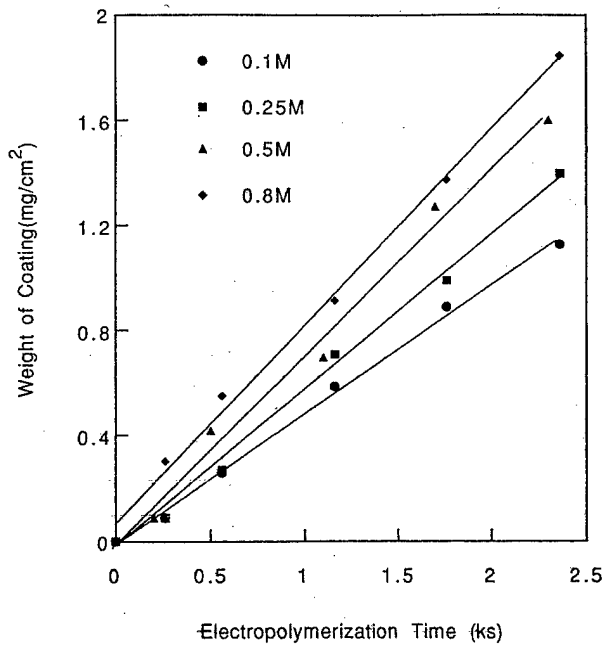

Figure 7 Dependence of coating formation on initial pyrrole concentration. Cd = 8.89 mA/cm^2; [Ox] = 0.1*M*; WE = low carbon steel.

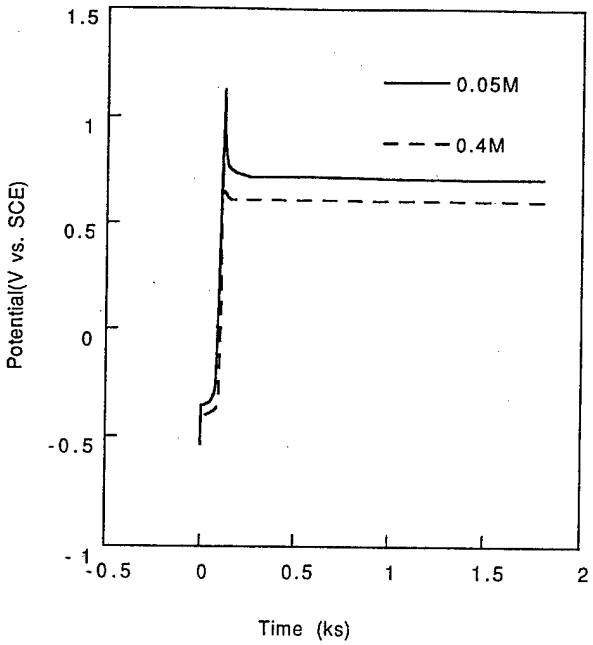

Figure 8 Dependence of polymerization potential on electrolyte concentration and electropolymerization time.

creased monomer concentration may be due to improved conductivity of the PPy-coated steel surface. It was reported that the FeC_2O_4 layer is more insulating than is the FeC_2O_4–(PPy–$(C_2O_4)_{.225}$)

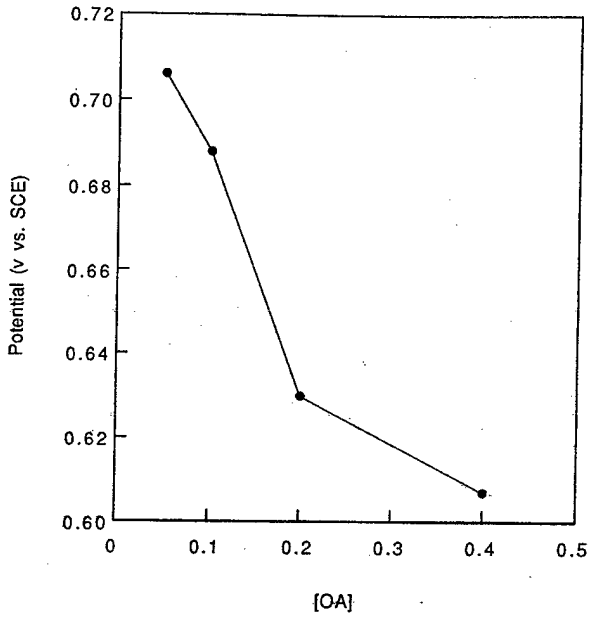

Figure 9 Dependence of polymerization potential on electrolyte concentration.

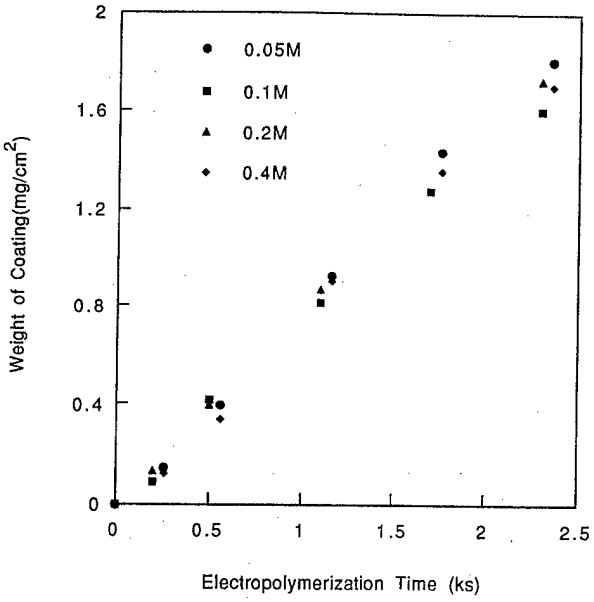

Figure 10 Dependence of polymerization of pyrrole on electrolyte concentration. Cd = 2.25 mA/cm^2; [M] = 0.5M; WE = low carbon steel.

composite interlayer.[15] The formation of PPy increased with pyrrole concentration and electropolymerization time (Fig. 7). The increment in the amount of PPy formed due to increased pyrrole concentration was, however, significantly lower than that obtained with an equivalent increase in the current density. For instance, doubling the current density from 2.25 to 4.5 mA/cm^2 resulted in the doubling of the amount of PPy formed from 12.4 to 25 mg (about a 102% increase) after 39 min of electropolymerization; however, doubling the monomer concentration from 0.1 to 0.2M resulted in only a slight increase in the amount of PPy formed from 14.2 to 15.3 mg ($\sim$ 7.8% increase) after 38 min of electropolymerization.

Effect of Electrolyte Concentration

The concentration of pyrrole was kept constant at 0.5M and the current density was maintained at

Table III Elemental Composition of PPy–Oxalate Coatings Formed on Low Carbon Steel

Elements	Content (%)
C	58.67
H	3.70
N	16.85
O	17.47

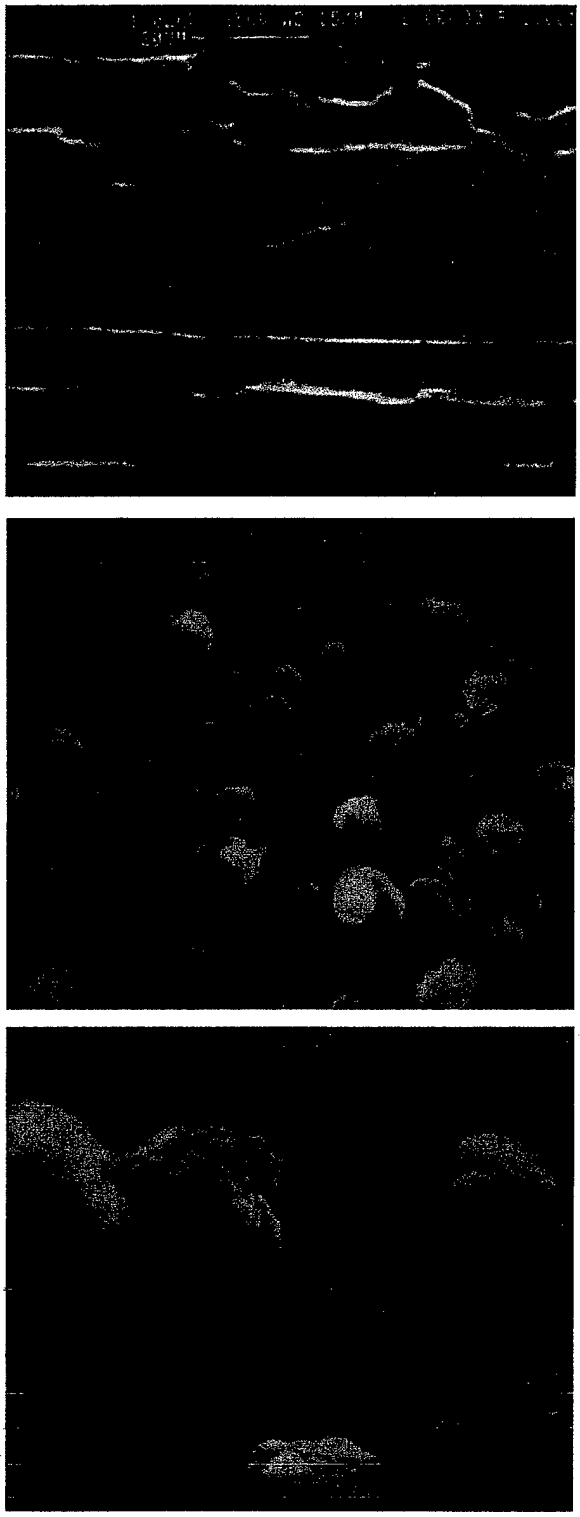

Figure 11 (Top) SEM micrograph of noncoated low carbon steel. SEM micrograph for low carbon steel coated with PPy formed by using (middle) low current density and (bottom) high current density.

2.25 mA/cm^2 while the concentration of oxalic acid was varied from 0.05 to 0.4*M*. The induction time for polymerization was unaffected by electrolyte concentration (Fig. 8), confirming that the electrolyte was not involved in the passivation of steel. The electropolymerization potentials of pyrrole decreased gradually with electrolyte concentration (Fig. 9). Subsequent addition of oxalic acid ($2H^+ + C_2O_4^{2-})_{aq}$ after the passivation of steel (formation of FeC_2O_4 interlayer) lowers the resistance of the steel–oxalate interlayer, resulting in a decreased electrode potential.[15] The amount of PPy formed onto the steel surface was independent of the electrolyte concentration (Fig. 10). Increasing the electrolyte concentration from 0.04 to 0.4*M* resulted in no significant change in the amount of PPy formed, irrespective of the electropolymerization time. The role of oxalic acid is to passivate steel, initiate electropolymerization, and dope the PPy coatings.

Composition and Morphology of the Coatings

The elemental composition of the PPy oxalate coatings formed on steel is shown in Table III. Elemental analysis confirms the presence of oxygen in the coatings and indicates that oxalic acid is incorporated into PPy. Using the oxalate monoanion as the counterion, a mol ratio of pyrrole to the oxalate monoanion of 4.41 : 1 was obtained.

The SEM pictures for low carbon steel and PPy-coated low carbon steel are shown in Figure 11. Overall, the surface of the PPy coatings is very smooth. The coatings formed by passing a lower current density for 30 min was smoother with fine microspheroidal grains. The PPy coatings formed at a higher current density (Cd = 7.88 mA/cm^2) had a larger microspheroidal grain size than that formed at a lower current density (Cd = 1.13 mA/cm^2). It is expected that the dependence of the morphology of the coatings on the current density would be reflected in the properties of the coatings.

REFERENCES

1. F. Beck, in *Encyclopedia of Materials Science and Engineering*, R. W. Cahn, Ed., Pergamon Press, New York, 1988, Suppl.
2. A. F. Diaz, A. Martinez, K. K. Kanazawa, and M.

Salmon, *J. Electroanal. Chem.*, **130,** 181–187 (1981).
3. A. F. Diaz, J. I. Castillo, J. A. Logan, and W. Lee, *J. Electroanal. Chem.*, **129,** 115–132 (1981).
4. A. F. Diaz, J. I. Castillo, K. K. Kanazawa, and J. A. Logan, *J. Electroanal. Chem.*, **133,** 233–239 (1982).
5. A. F. Diaz, K. K. Kanazawa, and G. P. Gardini, *J. Chem. Soc. Commun.*, 635 (1979).
6. K. K. Kanazawa, A. F. Diaz, W. D. Gill, P. M. Grant, G. B. Street, G. P. Gardini, and J. F. Kwack, *Syn. Met.*, **1,** 329 (1979).
7. A. F. Diaz, *Chem. Scr.*, **17,** 145 (1981).
8. G. Wegner, *Angew. Chem. Int. Ed.*, **20,** 361 (1981).
9. T. A. Skotheim, Ed., *Handbook of Conducting Polymers,* Macel Dekker, New York, 1986, Vols. 1 and 2.
10. J. Heinze, *Top. Curr. Chem.*, **152,** 1 (1989).
11. J. Prejza, I. Lundstrom, and J. E. Dubois, *J. Electrochem. Soc.*, **129,** 1685 (1982).
12. K. M. Cheung, D. Bloor, and G. C. Stevens, *Polymer,* **29,** 1709 (1988).
13. W. Janssen and F. Beck, *Polymer,* **30,** 353 (1989).
14. M. Schirmeisen and F. Beck, *J. Appl. Electrochem.*, **19,** 401 (1989).
15. F. Beck and R. Michaelis, *J. Coat. Technol.*, **64,** 59 (1992).
16. P. Hülser and F. Beck, *J. Appl. Electrochem.*, 596 (1990).
17. P. Hülser and F. Beck, *J. Electrochem. Soc.*, **137,** 2067 (1990).
18. C. A. Ferreira, S. Aeiyach, M. Delamar, and P. C. Lacaze, *J. Electroanal. Chem.*, **284,** 351 (1990).
19. S. Kuwabata, J. Nakamura, and H. Yoneyama, *J. Electrochem. Soc.*, **137,** 1788 (1990).

Kinetics and Efficiency of Aqueous Electropolymerization of Pyrrole onto Low-Carbon Steel

W. SU, JUDE O. IROH

Materials Science and Engineering Department, University of Cincinnati, Cincinnati, Ohio

Received 23 July 1996; accepted 30 December 1996

ABSTRACT: The effect of process parameters on the conversion, P, and current efficiency, η, for the aqueous electropolymerization of pyrrole on low-carbon steel has been investigated. The amount of polypyrrole coatings formed on steel, W_p, increased with the charge passed, Q, and the initial pyrrole concentration $[M]$, but was unaffected by the electrolyte concentration. The conversion of pyrrole into polypyrrole, $P = W_P/W_M$, increased with electropolymerization time, and the applied current, and decreased with the initial monomer concentration. The oxalic acid concentration had no significant effect on conversion. The current efficiency for the electropolymerization of pyrrole performed by using high applied current, $I(I \geq 40$ mA), and high pyrrole concentration, $[M] \geq 0.5M$, rose to its highest value at short polymerization times, $t < 300$ sec. It then decreased and leveled off at longer times, $t \geq 1{,}000$ sec. At low applied current, $I \leq 20$ mA, and low pyrrole concentration, $[M] \leq 0.25M$, the current efficiency increased gradually with increased reaction parameters ($[M]$, I, and t) and reached a maximum value at $t = 1{,}000$ sec. A retrogression of the current efficiency occurred at $t \geq 1{,}000$ sec, for the reaction performed by using applied current of 10 mA. Overall, the current efficiency varied between 39 and 130%, with the higher values occurring at high pyrrole concentration and high applied current. The current efficiency was determined from the ratio of the experimental and theoretical electrochemical equivalents for polypyrrole. © 1997 John Wiley & Sons, Inc. J Appl Polym Sci **65:** 617–624, 1997

Key words: kinetics; efficiency; aqueous-electropolymerization; polypyrrole-on-steel

INTRODUCTION

Electrochemical polymerization has the ability to form uniform and continuous coatings on conductive substrates. It is fast and inexpensive and allows *in situ* analysis and monitoring of the coating process. In this study, constant current electropolymerization is used. The total charge passed during electropolymerization, Q, is determined as the product of the applied current, I, and the time, t, of application. In constant potential coullometry, the total charge passed can be related to the concentration of the electroactive species in the cell (see reference 1).

Polypyrrole coatings are electrochemically formed on low-carbon steel with the intention to protect the substrate from corrosion. The process parameters, such as initial pyrrole concentration, oxalic acid concentration, applied current, and reaction time, are systematically varied. By determining the dependence of the coating process on the process parameters, we can control the coating formation process effectively and optimize the coating structure and properties. One area of the coating formation process of interest is the efficiency. The efficiency of electropolymerization

Correspondence to: J. O. Iroh.

 CCC 0021-8995/97/030617-08

refers to the amount of polymer formed with respect to the charge passed. The electrochemical formation of polypyrrole involves the conversion of pyrrole into polypyrrole by the transfer of electrons and the release of hydrogen ions.[2-5] As a result, by determining the weight of polypyrrole formed and comparing it with the initial weight of pyrrole in the feed, one can estimate the extent of conversion.

The first step in the electrochemical polymerization (oxidation) of pyrrole is the formation of radical cations. Dimerization of the radical cations is accompanied by the loss of two hydrogen ions from the 2,5 position of the pyrrole ring. The dimer has a lower half-wave oxidation potential than the monomer; hence, further oxidation of the dimer occurs preferentially.[2] The electrochemically formed polypyrrole can undergo further oxidation, resulting in a partial positive charge on the pyrrole ring.[6] As a result of this, the polymer associates with an anionic species (from the electrolyte salt) in order to maintain charge neutrality.[7]

The current efficiencies were determined in accordance with the method established by Schirmeisen and Beck.[8] The schematic representation of the formation of polypyrrole is shown below (Scheme I):

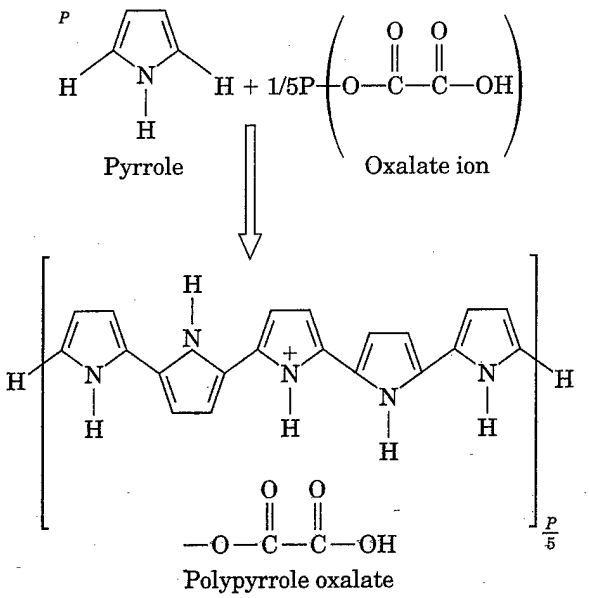

Scheme 1 Formation of doped polypyrrole.

P is the degree of polymerization; the counter ion is hydrogen oxalate, which is inserted into the coatings for charge compensation during electropolymerization; $\frac{1}{5}$ is the degree of insertion of the counter ion and was determined by elemental analysis. By use of the above model, the theoretical electrochemical equivalent, EE_{th}, for polypyrrole can be shown to be

$$EE_{\text{theory}} = M/(zF) = (M_M + yM_A)/[(2 + y)F] \quad (1)$$

where M_M is the molecular weight of the repeat unit ($M_M = 65$), M_A is the molecular weight of the oxalate ion, $y = \frac{1}{5}$, and F is Faraday's constant (96,500 coulombs per equivalent).

The experimental electrochemical equivalent can be determined from eq. (2):

$$EE_{\text{exp}} = W_p/Q \quad (2)$$

where W_p is the weight of polypyrrole coatings, and Q is the charge passed. Since the constant current method was used, the charge passed was determined as the product of applied current, I, and the electropolymerization time, t, i.e., $Q = I \times t$.

The current efficiency, η, is obtained from eq. (3):

$$\eta = EE_{\text{exp}}/EE_{\text{theory}} \quad (3)$$

The rate constant for the electropolymerization of pyrrole can be evaluated by recalling that the electropolymerization of pyrrole is preceded by the dimerization of the radical cation.

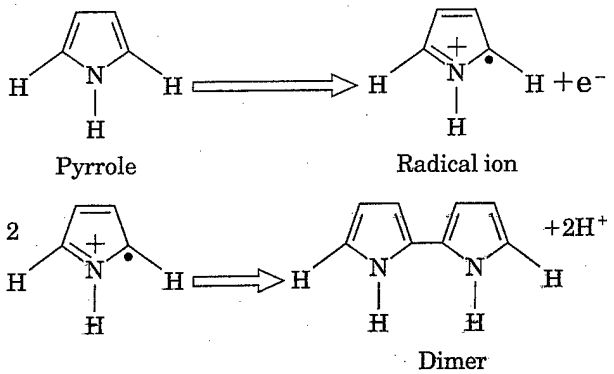

It was also reported that the dimer has a lower oxidation potential and should be oxidized in preference to the monomer.[2,9,10] The oxidized dimers will couple with each other to form a tetramer.

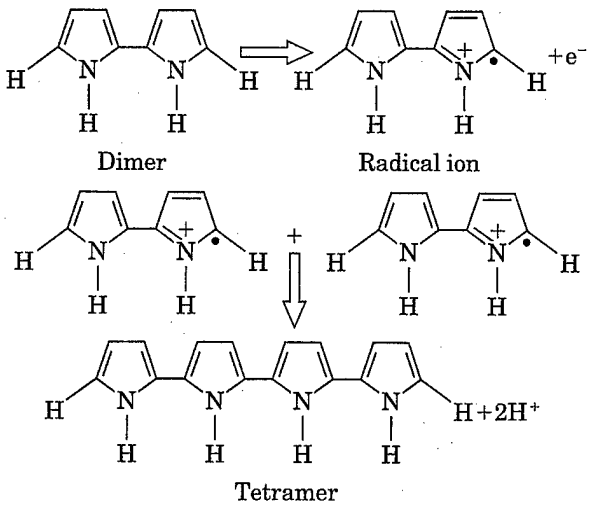

Further coupling could occur between the tetramer radical ion with itself or with a dimer. The possibility of a hexamer or octamer radical ion coupling with themselves or with a dimer or tetramer radical ion also exists. The coupling reaction will seize when the application of electric current is discontinued.

If the monomer is represented as M, then the reaction scheme can be written as follows[11-13]:

Initiation

$$M + I \xrightarrow{k_i} M^{\bullet +} + e^- \tag{4}$$

Coupling

$$2M^{\bullet +} \xrightarrow{k_c} M - M + 2H^+ \tag{5}$$

Oxidation of dimer

$$M - M + I \xrightarrow{k_i} M - M^{\bullet +} + e^- \tag{6}$$

Coupling of dimer radical cation

$$2M - M^{\bullet +} \xrightarrow{k_c} M - M - M - M + 2H^+ \tag{7}$$

The electrochemical polymerization can be approximated to a series of oxidation (initiation) and coupling (propagation) steps. The formation of the monomer radical cation, $M^{\bullet +}$, is the slowest of the initiation reactions. Recall that it was shown that the oxidation potential of the dimer is lower than that for pyrrole.[2,9,10] We can assume that the oxidation potential of the intermediate species (dimer, tetramer, hexamer, octamer or prepolymer) and the rate constant for coupling, k_c, are irrespective of the size of the species.

The rates of initiation, R_i, and propagation, R_p, can be written as follows:

Rate of initiation, R_i

$$R_i = \frac{d[M^{\bullet +}]}{dt} = \frac{k_i[M]I}{FV} \quad \text{for constant process} \tag{8}$$

Rate of coupling, $R_c = R_p$

$$R_c = -\frac{d[M^{\bullet +}]}{dt} = k_c[M^{\bullet +}]^2 \tag{9}$$

At steady state, $R_i + R_c = 0$

$$\text{i.e., } \frac{d[M^{\bullet +}]}{dt} = \frac{k_i[M]I}{FV} - k_c[M^{\bullet +}]^2 = 0 \tag{10}$$

$$[M^{\bullet +}] = \left(\frac{k_i I[M]}{VFk_c}\right)^{1/2} \tag{11}$$

$$R_p = k_c[M^{\bullet +}]^2 = \frac{k_i[M]I}{FV} = -\frac{d[M]}{dt} \tag{12}$$

where k_i is the rate constant for initiation, k_c is the rate constant for coupling (propagation), I is the applied current, F is the Faraday's constant (96,500 coulombs/mol), V is the volume of the monomer-electrolyte solution, $[M]$ is the monomer concentration, and $[M^{\bullet +}]$ is the concentration of the radical cation.

By solving eq. (12) and substituting $(1 - P)M_0$ for $[M]$, we obtain eq. (13):

$$-\ln(1 - P) = \frac{k_i It}{FV} \tag{13}$$

By substituting $I \times t = Q$, we obtain an expression that relates the conversion to the charge passed per unit volume

$$-\ln(1 - P) = \frac{k_i Q}{FV} \tag{14}$$

k_i can be determined from the slope of $\ln(1 - P)$ versus t or $\ln(1 - P)$ versus Q plot.

The conversion, P, is taken as the ratio of the

weight of the polymer coatings, W_P, to the initial weight of pyrrole, W_M, in the feed:

$$P = \frac{W_P}{W_M} \tag{15}$$

In this article, the effect of applied current, initial pyrrole concentration, electrolyte concentration, and reaction time on the current efficiency and conversion is presented. The dependence of the weight of the polypyrrole coatings formed on low-carbon steel on the charge passed and the process parameters, respectively, was also determined. It is hoped that by manipulating the electrochemical process parameters, optimal coating microstructure and coating properties will be established. Pyrrole was choosen for this study because the starting material is soluble in water and allows for controllable film formation in aqueous medium. The aqueous electrochemical polymerization of pyrrole is easy to control, cost effective, and environmentally safe. Polypyrrole is also one of the class of conducting polymers that have corrosion-resistant capability. The electropolymerization of pyrrole onto reactive metals such as steel and aluminum is believed to be an effective replacement for the hazardous chromate rinse process used to prime steel. The structure and properties of polypyrrole coatings are, however, dependent on the electrochemical process variables. Judicious control of the reaction variables is necessary in order to form pinhole-free, adherent, tough, and corrosion-resistant polypyrrole coatings.

EXPERIMENTAL

Materials

Pyrrole (98%) and oxalic acid (98%) were purchased from Aldrich Chemical Company, Inc. Tetrachloroethylene and methanol were also purchased from Aldrich Chemical Company. The reagents were dissolved in deionized water prepared in our department.

The working electrode is a 0.5-mm-thick QD low-carbon steel panel purchased from the Q-panel Company. The working electrode was degreased with tetrachloroethylene for about an hour prior to electrochemical polymerization. The counter electrodes were composed of two titanium alloy plates. A saturated calomel electrode (SCE), manufactured by Corning Company, was used as the reference electrode. Constant-current electropolymerization of pyrrole was performed with an EG & G Princeton Applied Research Potentiostat/Galvanostat, Model 273A.

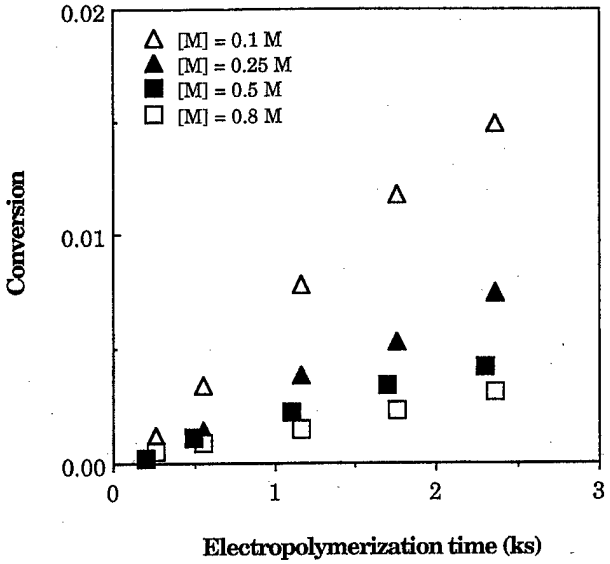

Figure 1 Dependence of conversion on initial pyrrole concentration and time.

Electropolymerization

The electropolymerization of pyrrole was carried out in a one-compartment polypropylene cell. The current densities used in this study ranged from 0.22 to 11.26 mA/cm^2. The initial concentration of oxalic acid was varied from 0.05 to 0.4*M*, while the initial monomer concentration was varied from 0.1 to 0.8*M*. Electropolymerization was performed for 300–2,400 sec.

The coated steel was rinsed with methanol and dried at 65°C in a vacuum oven to constant weight. The weight of the coatings was determined as the difference between the coated and noncoated steel (control).

Characterization

Elemental analysis of the coatings extracted from coated steel was performed by Galbraith Laboratories, Inc. The ratio of pyrrole to hydrogen oxalate ion was determined to be 5 : 1.

RESULTS AND DISCUSSION

Figures 1–3 show the variation of conversion {$P = (W_p/W_M)$} with the initial pyrrole concentra-

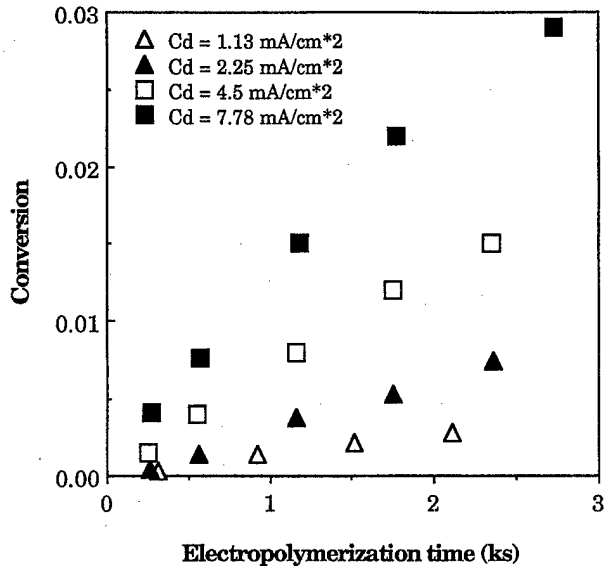

Figure 2 Dependence of conversion (Cd) on the applied current (working electrode area = 8.89 cm^2).

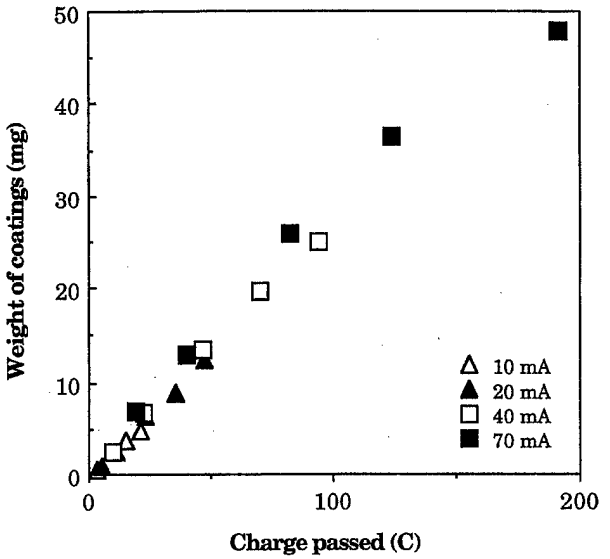

Figure 4 Dependence of the weight of polypyrrole coatings formed on steel on the charge passed and the applied current.

tion, the oxalic acid concentration and the applied current, respectively, as a function of electropolymerization time. The initial pyrrole concentration was varied between 0.1 and 0.8*M*, while the electrolyte concentration and applied current were varied between 0.05 and 0.4*M* and 10 to 70 mA, respectively. Electropolymerization time was varied between 200 and 3,000 sec. The conversion of polypyrrole varied inversely with initial pyrrole concentration (Fig. 1) and proportionately with applied current (Fig. 2) and reaction time (Figs. 1–3). Increasing the initial pyrrole concentration from 0.1 to 0.8*M* (700% increase) resulted in a decrease in the conversion from 1.5 to 0.31% (~ 80% decrease) for t = 40 min, [*OA*] = 0.1*M*, I = 20 mA, and working electrode area of 8.89 cm^2. The inverse relationship between pyrrole concentration and conversion was also confirmed at short reaction times. For example, increasing the pyrrole concentration from 0.1 to 0.8*M* (700% increase) resulted in a decrease in conversion from 1.2 to 0.05% (96% decrease) for t = 2.5 min (all other reaction conditions were maintained constant). The effect of applied current on conversion is shown on Figure 2. Increasing the applied current from 10 to 70 mA (600% increase) resulted in an increase in conversion from 0.36 to 2.9% (700% increase) (Figure 2) (t = 46 min, [*M*] = 0.25*M*, [*OA*] = 0.1*M*). Conversion was not dependent on the electrolyte concentration (Fig. 3). Increasing oxalic acid concentration from 0.05 to 0.4*M* (700% increase) resulted in only a slight change in conversion from 0.48 to 0.45% (6% change) at t ~ 40 min ([*M*] = 0.5*M*, I = 20 mA).

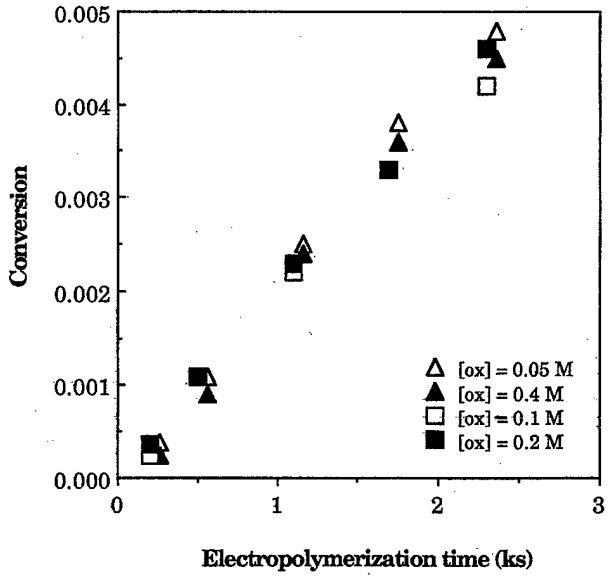

Figure 3 Dependence of conversion on oxalic acid concentration ([ox]).

The dependence of the weight of polypyrrole coatings formed on steel on the charge passed as a function of the reaction parameters (I, [*M*] and [*OA*]) is shown on Figures 4–6. The weight of polypyrrole coatings increased with the charge passed and was unaffected by the magnitude of

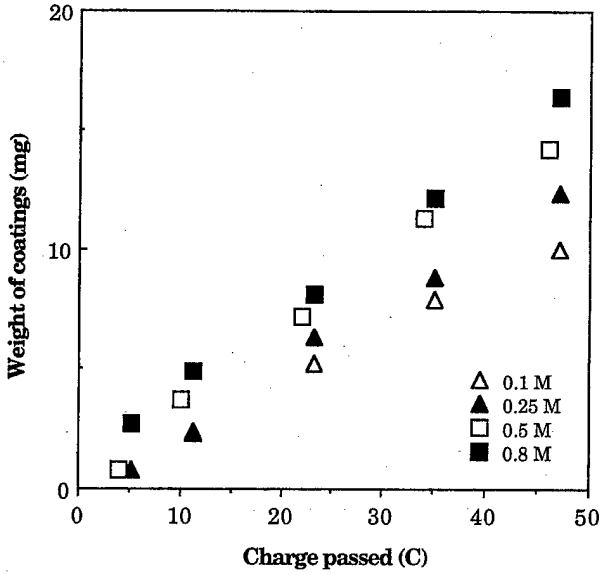

Figure 5 Dependence of the weight of polypyrrole coatings formed on steel on the charge passed and the initial pyrrole concentration.

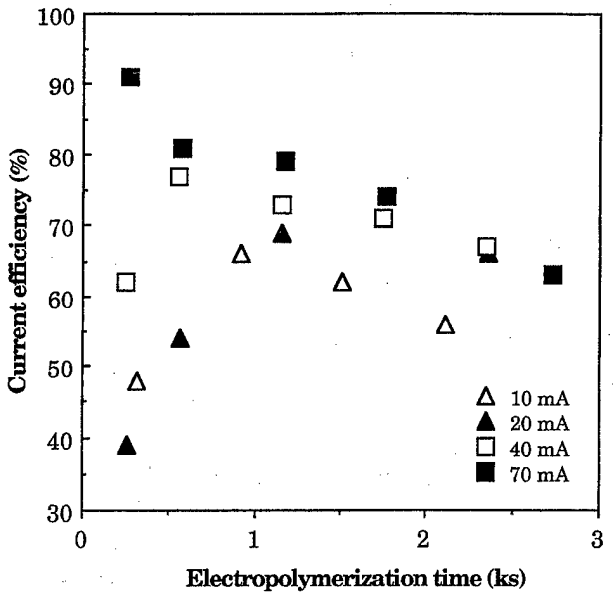

Figure 7 Dependence of current efficiency on the applied current and reaction time.

the applied current, as was expected (Fig. 4). The weight of polypyrrole coatings increased with pyrrole concentration per unit charge (Fig. 5). The weight of polypyrrole coatings increased from 0.8 to 2.7 mg as the pyrrole concentration was increased from 0.1 to 0.8*M*, for 23 coulombs of charge passed (Fig. 5). However, the weight of polypyrrole coatings per mole of pyrrole (monomer efficiency) decreased with increased pyrrole concentration. The weight of coatings per mole of pyrrole decreased from 8 to 3 mg/mol as the pyrrole concentration was increased from 0.1 to 0.8*M*. Increasing electrolyte concentration decreased the efficiency per mole of electrolyte (electrolyte efficiency). The weight of polypyrrole coatings was unaffected by the electrolyte concentration (Fig. 6), indicating that the electrolyte was not involved in the coupling reaction. The weight of polypyrrole coatings formed on steel increased with the charge passed and pyrrole concentration but was unaffected by the applied current or the oxalic acid concentration.

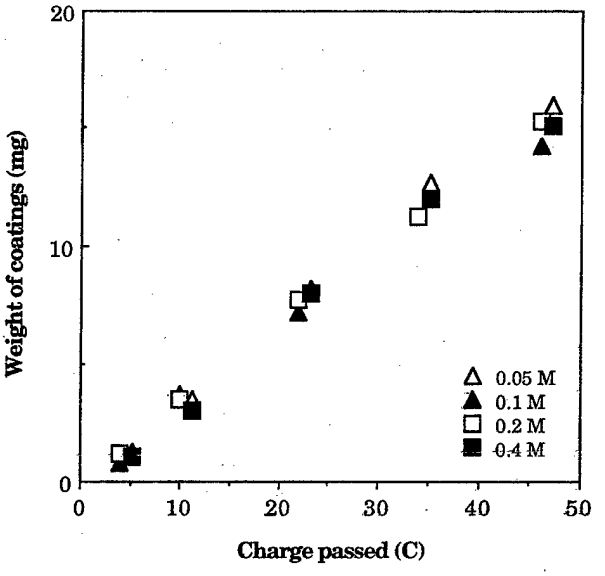

Figure 6 Dependence of the weight of polypyrrole coatings formed on steel on the charge passed and oxalic acid concentration.

The dependence of the current efficiency on the reaction parameters is shown on Figures 7–9. Generally, the current efficiency rose to a maximum value at low reaction time, followed by a gradual decrease before attaining a constant value that is invariant with time (Figs. 7–9). The effect of applied current and initial pyrrole concentration is shown on Figures 7 and 8, respectively. For the electropolymerization of pyrrole performed by using high applied current ($I \geq 40$ mA) and high pyrrole concentration ($[M] \geq 0.5M$), the current efficiency rose to its highest value at short reaction times, $t < 300$ sec. It then decreased and leveled off at longer times, $t \geq 1{,}000$ sec. At low applied current ≤ 20 mA and low pyr-

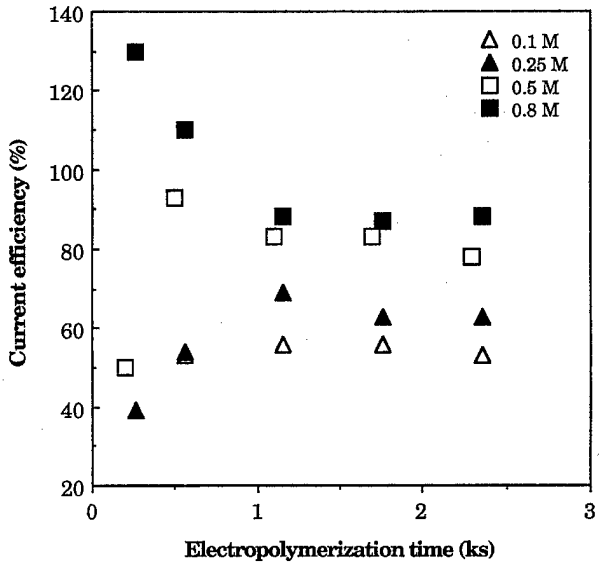

Figure 8 Dependence of current efficiency on initial pyrrole concentration.

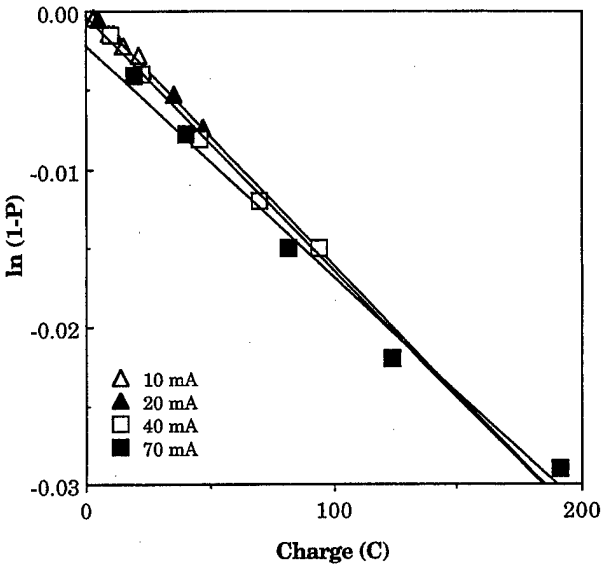

Figure 10 Variation of the rate constant for polymerization with applied current.

role concentration, $[M] \leq 0.25M$, the current efficiency increased gradually with increased reaction parameter (I, $[M]$, and t) and leveled off after 1,000 sec of electropolymerization. A retrogressive decrease in the current efficiency occurred at $t \geq 1{,}000$ sec for the reactions performed by using an applied current of 10 mA. Overall, the current efficiency varied between 39 and 130%, with the higher values occurring at high pyrrole concentration and high applied current. Figure 9 shows the dependence of the current efficiency on the electrolyte concentration and time. At low reaction times, $t < 600$ sec, the current efficiency increased with electropolymerization time, $t \leq 600$ sec, and leveled off at $t \geq 1{,}000$ sec. A subsequent increase in the reaction time above 1,000 sec resulted in no significant changes in the current efficiency (Fig. 9).

Figures 10–12 show a second-order kinetic

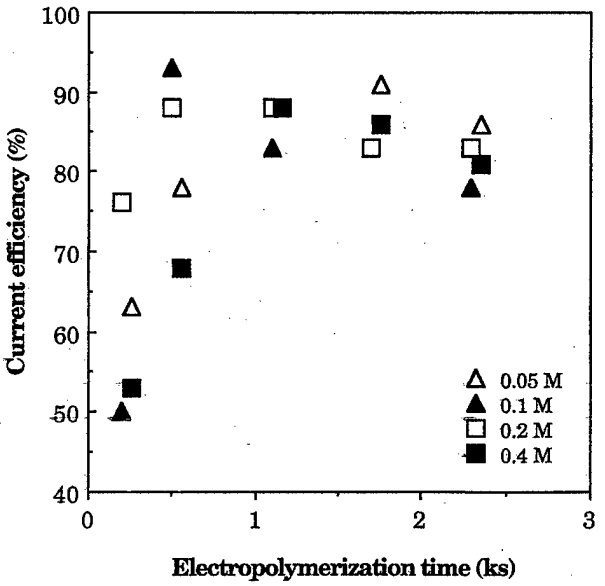

Figure 9 Dependence of current efficiency on oxalic acid concentration.

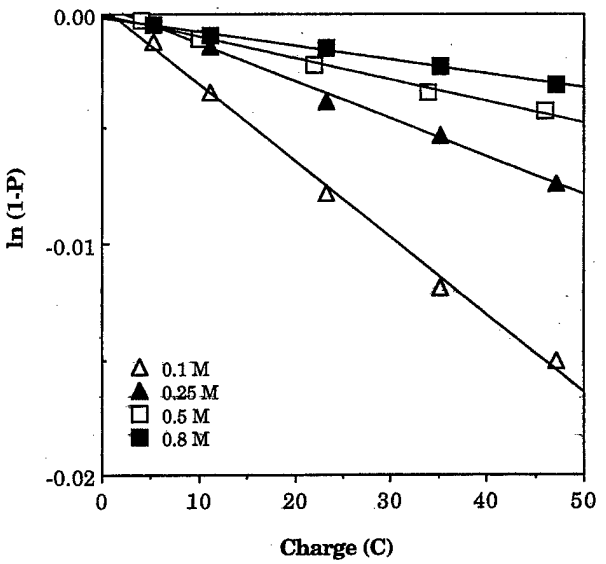

Figure 11 Variation of the rate constant for polymerization with initial pyrrole concentration.

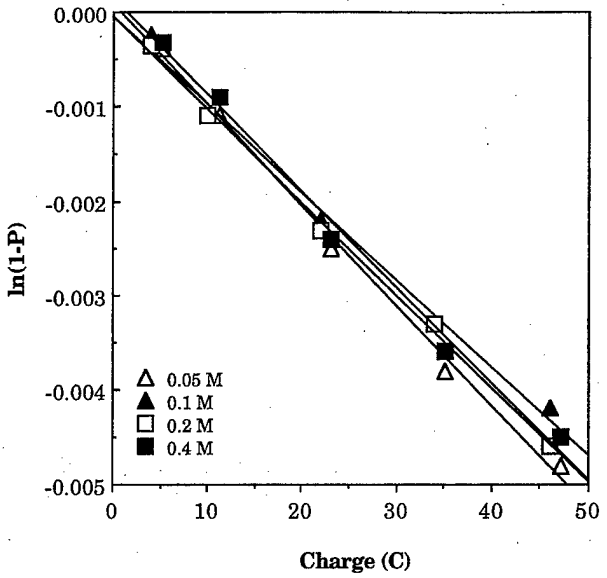

Figure 12 Variation of the rate constant for electropolymerization of pyrrole on oxalic acid concentration.

plot, $\ln(1 - P)$ versus Q, for the aqueous electropolymerization of pyrrole on low-carbon steel. The rate constant for electropolymerization can be estimated from the slope of Figures 10–12. The slope of $\ln(1 - P)$ versus Q plot was unaffected by the value of the applied current, as was expected. Increasing the applied current from 10 to 70 mA resulted in no significant change in the slope from 1.35×10^{-4} to 1.47×10^{-4} (Fig. 10). Increasing the initial pyrrole concentration, however, resulted in a decrease in the slope of $\ln(1 - P)$ versus Q (Fig. 11). Varying the pyrrole concentration from 0.1 to 0.8M resulted in a decrease in the rate constant from 3.30×10^{-3} to 6.1×10^{-5}. The electrolyte concentration has no significant effect on the rate constant. Changing the electrolyte concentration from 0.05 to 0.4M resulted in no change in the slope (Fig. 12).

CONCLUSION

The effect of electropolymerization reaction parameters on the conversion of polypyrrole and the efficiency of aqueous electropolymerization on steel has been investigated. The conversion of polypyrrole increased with the applied current and decreased with initial pyrrole concentration. There was no dependence of conversion on the electrolyte concentration. The amount of coatings formed on steel increased with the total charge passed but was unaffected by the applied current or the electrolyte concentration. It, however, increased with initial pyrrole concentration. The current efficiency was high at short reaction times. It declined gradually and remained unchanged after about 1,000 sec of electropolymerization. Very high current efficiency was obtained at high monomer concentration and high applied current at short reaction times $t < 1{,}000$ sec.

ACKNOWLEDGMENT

The financial support from the Office of Naval Research is gratefully acknowledged.

REFERENCES

1. EG&G Princeton Applied Research, Model 270/250 Research Electrochemistry Software User's Guide, 1992, EG&G Princeton Applied Research, Princeton, NJ.
2. E. M. Genies, G. Bidan, and A. F. Diaz, *J. Electroanal. Chem.*, **149,** 101 (1983).
3. H. F. Mark, N. M. Bikales, C. G. Overberger, G. Menges, and J. I. Kroschwitz, Eds., *Encyclopedia of Polymer Science and Engineering,* 2nd Ed., Vol. 13, Wiley, New York, 1988.
4. C. S. C. Bose, S. Basak, and K. Rajeshwar, *J. Phys. Chem.*, **96,** 9899 (1992).
5. B. Qian, Y. Li, B. Yan, and H. Zhang, *Synthetic Metals,* **28,** 51 (1989).
6. A. F. Diaz, J. I. Castillo, J. A. Logan, and W-Y. Lee, *J. Electroanal. Chem.*, **129,** 115 (1981).
7. A. Diaz, *Chemica Scripta,* **17,** 145 (1981).
8. M. Schirmeisen and F. Beck, *J. Appl. Electrochem.*, **19,** 401 (1989).
9. G. A. Wood, MS Thesis, University of Cincinnati, 1995.
10. G. A. Wood and J. O. Iroh, *Synthetic Metals* (1996).
11. J. H. Epsin, *Chemical Kinetics and Reaction Mechanisms, McGraw-Hill Series in Advanced Chemistry,* McGraw-Hill Book Company, New York, 1981, 30–34.
12. G. Odian, Principles of Polymerization, 2nd Ed., Wiley Interscience Publication, Wiley, New York, 1981, 46–72.
13. M. P. Stevens, *Polymer Chemistry,* 2nd Ed., Oxford University Press, Oxford, 1990, 332–334.

ELSEVIER

Synthetic Metals 95 (1998) 159–167

SYNTHETIC METALS

Effects of electrochemical process parameters on the synthesis and properties of polypyrrole coatings on steel

Wencheng Su, Jude O. Iroh *

Department of Materials Science and Engineering, University of Cincinnati, Cincinnati, OH 45221-0012, USA

Received 11 November 1997; accepted 12 November 1997

Abstract

Polypyrrole coatings have been successfully formed on low carbon steel by aqueous electrochemical process. The effects of electrochemical process parameters such as pH of the reaction medium, applied current density and initial monomer and electrolyte concentrations on the formation process of polypyrrole coatings were systematically investigated. The composition and morphology of the coatings were studied by FT-IR, elemental analysis and scanning electron microscopy (SEM). Our results show that passivation of the steel, electropolymerization of pyrrole, the morphology and properties of the coatings were all dependent on the electrochemical process parameters. By proper choice of the electrochemical process parameters, the passivation of the steel could be established within a short time and smooth, uniform, strongly adherent coatings could be formed on the steel substrate.

Keywords: Polypyrrole; Steel; Electrochemical process parameters; Synthesis; Coatings

1. Introduction

It is well known that corrosion is largely an electrochemical reaction occurring on the surface of the metals. One of the approaches to protect metals against corrosion is the application of polymeric coatings that are capable of inhibiting the oxidation of metals. However, in the traditional coating techniques, the hazardous and environmentally unsafe chromate rinse process is generally required [1–3]. Electropolymerization is an alternative process which can provide polymeric coatings without involving toxic chemicals. Other advantages of electropolymerization are that it can be easily automated and the chemical and physical properties of the coatings can be controlled by varying the reaction parameters such as the current density, monomer concentration, electrolyte type, electrolyte concentration, pH of the medium and the reaction time.

Polypyrrole is one of the most important conducting polymers and its free-standing films with high conductivity have been successfully prepared by electrochemical method [4–8]. Generally inert electrodes such as platinum are used to prepare the free-standing films. Recently, attempts have also been made to investigate the formation of polypyrrole on oxidizable iron electrode by electrochemical method. Cheung et al. [9] reported that fibrilar polypyrrole could be formed on iron in propylene carbonate and tetraethylammonium toluenesulfonate media. Ferreira et al. [10] investigated the electropolymerization of pyrrole on iron in different organic solvents and found that the formation of polypyrrole was dependent on the acidity of the medium. Beck et al. [11–13] also investigated many aqueous electrolytes and showed that potassium nitrate (KNO_3) and oxalic acid ($H_2C_2O_4$) could lead to the formation of polypyrrole on iron. It was found that polypyrrole coatings formed in aqueous oxalic acid medium had very strong adhesion to the steel surfaces. Su and Iroh [14,15] also investigated the kinetics and efficiency of electropolymerization of pyrrole on steel in aqueous oxalic acid medium. Recently, we found that the formation process and properties of this kind of coating were greatly influenced by the electrochemical process parameters. In this paper, we report the results of our preliminary investigation.

2. Experimental

All chemicals were Aldrich products except for sodium bicarbonate ($NaHCO_3$) which was purchased from Fisher Scientific. All aqueous solutions used in the experiments were made from deionized water.

Aqueous electropolymerization of pyrrole was performed in a one-compartment polypropylene cell. The working elec-

* Corresponding author. Tel.: +1 513 556 3115; fax: +1 513 556 2569.

0379-6779/98/$ - see front matter
PII S0379-6779(97)04112-X

trode was a 0.5 mm thick QD low carbon steel panel provided by Q-panel Company. The working electrode was degreased with tetrachloroethylene for about 1 h prior to the electropolymerization. The coated surface area of the electrode was 8.89 cm^2. The counter electrodes comprised two titanium alloy plates. A saturated calomel electrode (SCE) manufactured by Corning Company was used as reference electrode. The working electrode and the counter electrode were used as anode and cathode, respectively. The instrument used to electrochemically coat the low carbon steel sheets was an EG&G Princeton Applied Research model 273A potentiostat/galvanostat.

The constant current method was the technique used in this experiment. The applied current density (i) was varied from 0.5 to 6 mA/cm^2. The initial pyrrole (Py) concentration was varied from 0.1 to 0.8 M while the initial electrolyte concentration was changed from 0.05 to 0.4 M. The electrochemical reactions were carried out in media of five different pHs, which were 1.4, 2.4, 4.1, 6.0 and 8.4. The pH of the solution containing pyrrole (Py) and oxalic acid (OA) was adjusted by sodium bicarbonate. The electropolymerization time was fixed at 1800 s. After each experiment, the coated steel sheet was rinsed with water and methanol and dried in a vacuum oven at 65°C to constant weight.

Elemental analysis of the coatings scraped from the substrate was done by Galbraith Laboratories, Inc. The IR spectra of the coatings were measured by a BIO-RAD FTS-40 FT-IR spectrometer. The morphology of the coatings was examined by scanning electron microscopy (SEM). The samples were shadowed with gold to enhance their conductivity.

3. Results and discussion

3.1. Effects of pH and applied current density

In this part of the experiments, the pH of the reaction medium and the applied current density (i) were varied in a very wide range while the initial monomer and electrolyte concentrations were kept constant at 0.25 and 0.1 M, respectively.

Figs. 1 and 2 show the potential–time curves for the formation of polypyrrole coatings in different reaction media at two different applied current densities. It can be seen that the potential–time curves were different in media of different pH. In acidic medium, the formation process of polypyrrole was characterized by two distinct stages. In the first stage, the potential of the reaction was negative and no black polypyrrole was produced on the substrate. At the end of the first stage, the potential rose sharply to a positive maximum value, then decreased quickly, and at last reached a steady-state value. Black polypyrrole coatings began to form on the substrate during the second stage.

The first stage can be regarded as the induction period of the electropolymerization of pyrrole. As shown in Figs. 1–7, this induction period was greatly influenced by the applied

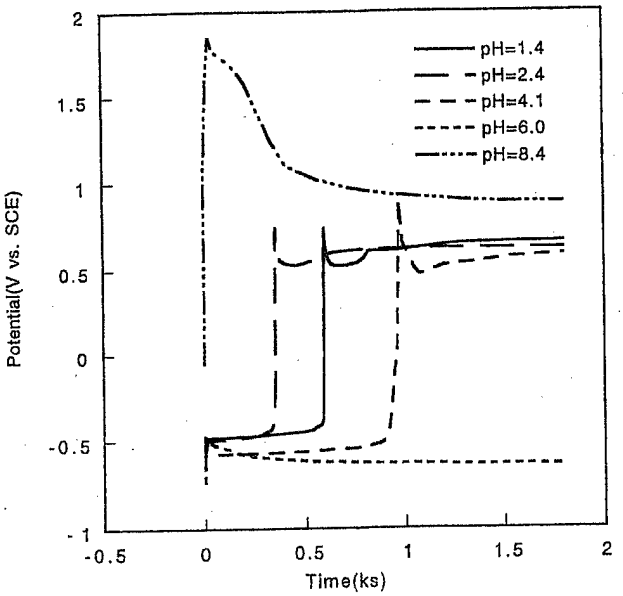

Fig. 1. Potential–time curves for the formation of polypyrrole coatings on steel at different pH (i=0.56 mA/cm^2, [Py] =0.25 M, [RX] =0.1 M).

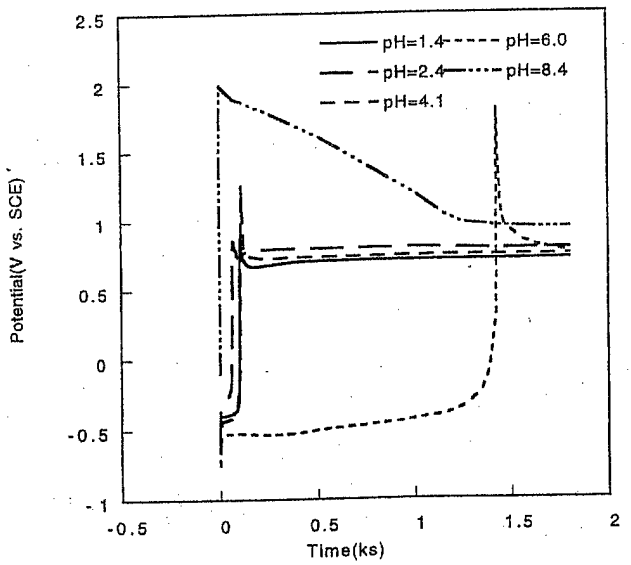

Fig. 2. Potential–time curves for the formation of polypyrrole coatings on steel at different pH (i=2.25 mA/cm^2, [Py] =0.25 M, [RX] =0.1 M).

current density and the pH of the reaction medium. For all the acidic media, the induction time (τ) decreased rapidly with increasing current density. For example, for the reaction medium of pH 2.4, application of current density of 0.56 mA/cm^2 resulted in an induction time of about 354 s; however, the induction time became only about 24 s at 5.63 mA/cm^2. The effect of applied current density was more significant for the reaction medium of pH 6.0. When current density was below 1.13 mA/cm^2, the induction time was so long that no passivation of steel was established even after 30-min reaction. Increasing the applied current density above 2.25 mA/cm^2 led to the passivation of the steel and the induction time was only 82 s at 5.63 mA/cm^2.

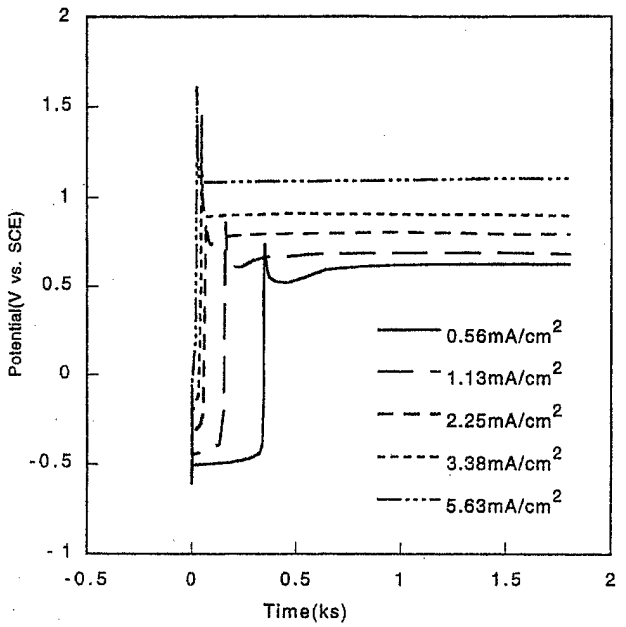

Fig. 3. Potential–time curves for the formation of polypyrrole coatings on steel at different current density at pH = 2.4 ([Py] = 0.25 M, [RX] = 0.1 M).

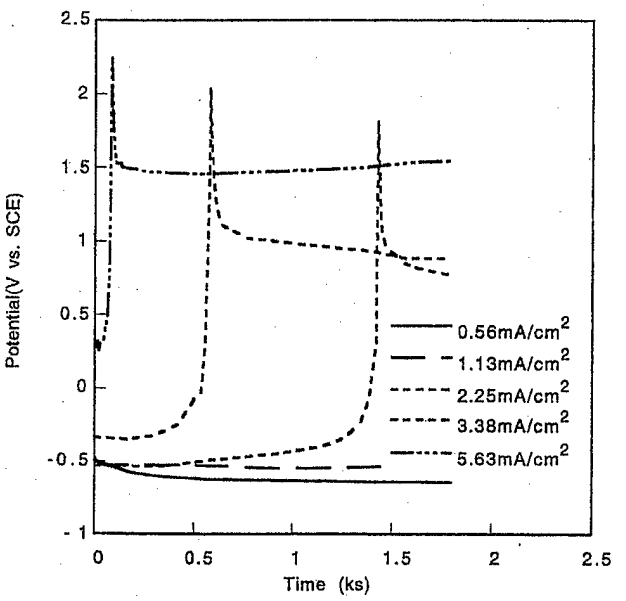

Fig. 4. Potential–time curves for the formation of polypyrrole coatings on steel at different current density at pH = 6.0 ([Py] = 0.25 M, [RX] = 0.1 M).

Fig. 6 shows the relationship between ln(induction time) and ln(current density) for the four acidic media. For each reaction medium, a linear relationship is obtained, which can be expressed by the following equations:

$$\text{pH}=1.4: \quad \ln \tau = 5.72 - 1.22 \ln i \tag{1}$$

$$\text{pH}=2.4: \quad \ln \tau = 5.22 - 1.16 \ln i \tag{2}$$

$$\text{pH}=4.1: \quad \ln \tau = 5.98 - 1.42 \ln i \tag{3}$$

$$\text{pH}=6.0: \quad \ln \tau = 9.95 - 3.15 \ln i \tag{4}$$

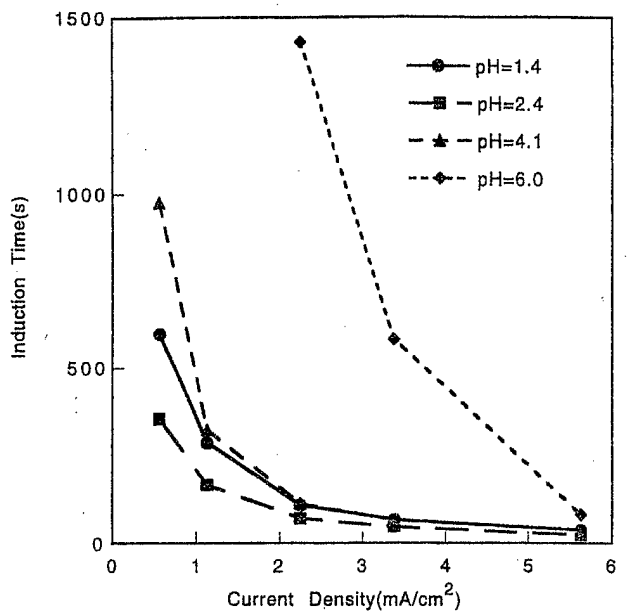

Fig. 5. Relationship between induction time and current density at different pH ([Py] = 0.25 M, [RX] = 0.1 M).

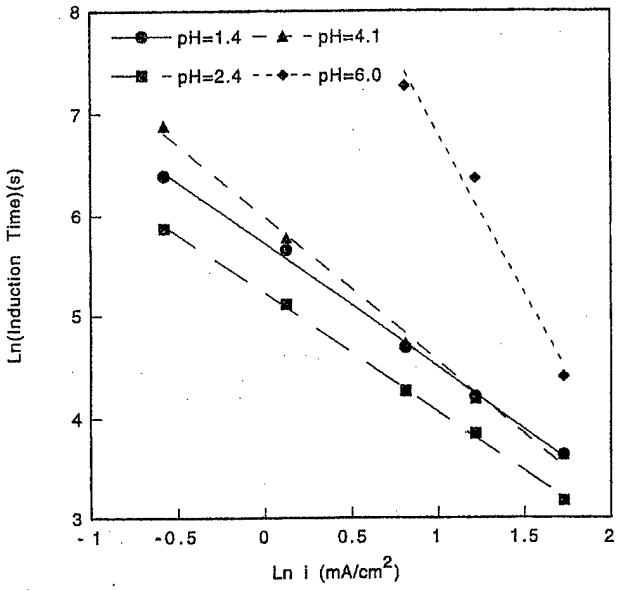

Fig. 6. Dependence of induction time on the applied current density at different pH ([Py] = 0.25 M, [RX] = 0.1 M).

Induction time was also changed with pH of the reaction medium. For the same applied current density, induction time was shortest in the medium of pH 2.4 while it became longest in the medium of pH 6.0. Overall, the induction time is varied according to following sequence:

$$\tau_{\text{pH}=6.0} > \tau_{\text{pH}=4.1} > \tau_{\text{pH}=1.4} > \tau_{\text{pH}=2.4} \tag{5}$$

For the acidic medium, the difference in induction time is very large at low current density, but the induction times tend to become very close to each other at higher current density. For example, at the current density of 0.56 mA/cm^2, the induction time at pH = 2.4 was about 350 s; however, no passivation of steel was observed at pH = 6.0 even after 30-

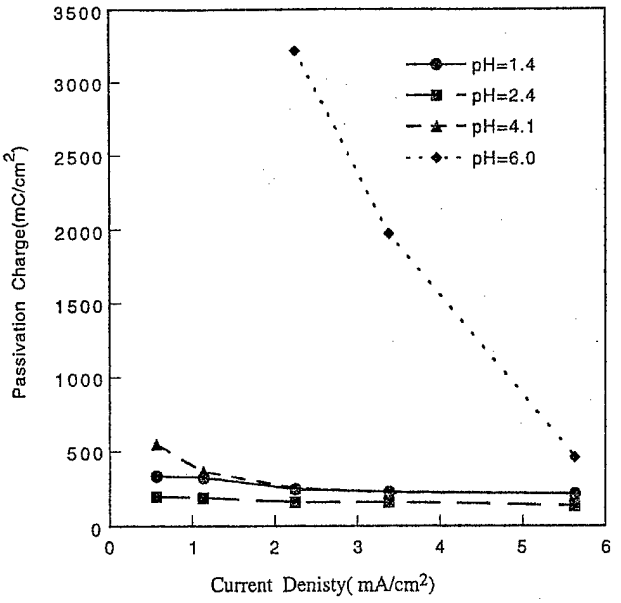

Fig. 7. Relationship between passivation charge and current density at different pH ([Py] = 0.25 M, [RX] = 0.1 M).

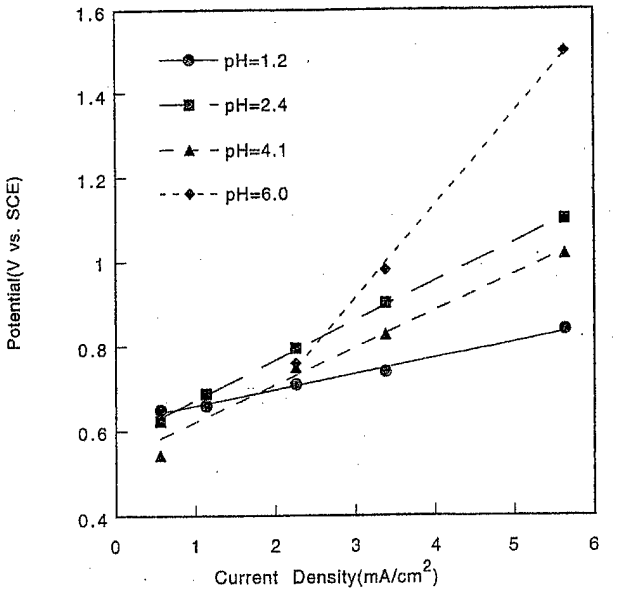

Fig. 8. Relationship between electropolymerization potential and current density at different pH ([Py] = 0.25 M, [RX] = 0.1 M).

min reaction. At the applied current density of 2.25 mA/cm^2, the induction time became very close for the reaction medium with pH below 4.1. The induction time at pH = 6.0 was still much higher than in those media of lower pH. When the applied current density was increased to 5.63 mA/cm^2, the induction times became close to each other for the four reaction media.

Fig. 7 shows the change of charge consumed during the induction period with applied current density for the acidic medium. Compared with the induction time, the passivation charge shows slightly different behaviour. When the pH of the reaction medium was below 4.1, the passivation charge only decreased very slowly with increasing current density. For example, the passivation charge was 198 mC/cm^2 at 0.56 mA/cm^2 for the medium of pH 2.4, but it only became 135 mC/cm^2 at 5.63 mA/cm^2. For the reaction medium of pH 6.0, it showed a much higher passivation charge than those of the other three systems at 2.25 mA/cm^2, but its passivation charge decreased very rapidly with further increase of current density. At 5.63 mA/cm^2, the passivation charge actually became very close to those of the other three systems.

Beck et al. [12,13] suggested that the passivation of the iron was due to the formation of the iron(II) oxalate interlayer when oxalic acid was the electrolyte. But it seems that the formation of the iron oxalate interlayer is dramatically dependent on the applied current density and pH of the reaction medium. The detailed mechanism is being studied in our lab.

The second stage of the formation process of polypyrrole is associated with the polymerization of pyrrole on the steel substrate. The first positive potential peak is perhaps related to the nucleation of polypyrrole on the steel electrode [16,17]. It has been reported that the nucleation and three-dimensional growth is the mechanism for the deposition of polypyrrole on platinum and pyrrole oxidizes more readily on polypyrrole than on platinum [16]. After the peak, the electropolymerization potential tended to become very steady during the rest of the reaction. Fig. 8 shows the relationship between the steady-state electropolymerization potential and the applied current density for the four acidic media. As shown in Fig. 8, the electropolymerization potentials all increase linearly with the applied current density and follow the relationships:

$$\text{pH}=1.4: \quad E_p = 0.62 + 0.038i \tag{6}$$

$$\text{pH}=2.4: \quad E_p = 0.58 + 0.094i \tag{7}$$

$$\text{pH}=4.1: \quad E_p = 0.53 + 0.088i \tag{8}$$

$$\text{pH}=6.0: \quad E_p = 0.25 + 0.22i \tag{9}$$

This potential change with current density may have something to do with the deficiency of electrons on the surface of the electrode. More electrons are removed from the electrode when the applied current density is increased. Due to the slow reaction of the monomer, the electron deficiency cannot compensate immediately by the reaction, thus the deficiency of electrons will result in a positive potential change. It can also be seen from Fig. 8 that higher current density has more significant effect on the electropolymerization potential of pyrrole. Asavapiriyanont et al. [16] have reported that the electropolymerization of pyrrole is independent of pH. Perhaps the voltage drop through the interlayer is different for different acidic media.

The formation process of polypyrrole in alkaline medium was quite different from that in acidic medium. It can be seen from Fig. 9 that no induction time was observed when the pH of the reaction medium was 8.4. These results are not unusual. According to a Pourbaix diagram, the application of an anodic potential to an iron sheet immersed in alkaline medium will

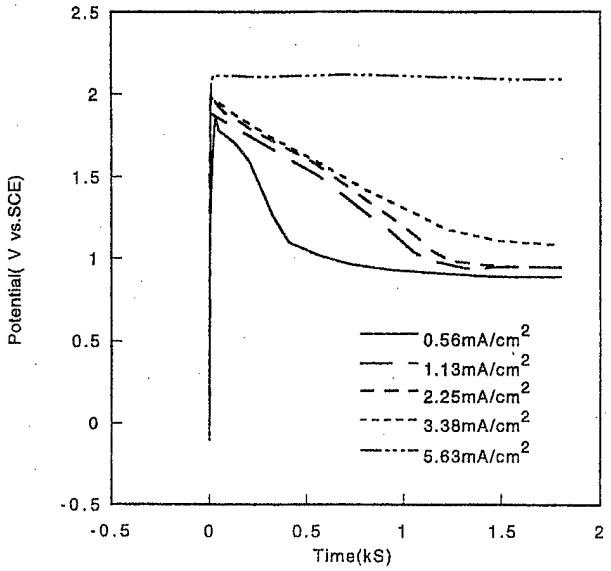

Fig. 9. Potential–time curves for the formation of polypyrrole coatings on steel at different current density at pH=8.4 ([Py]=0.25 M, [RX]=0.1 M).

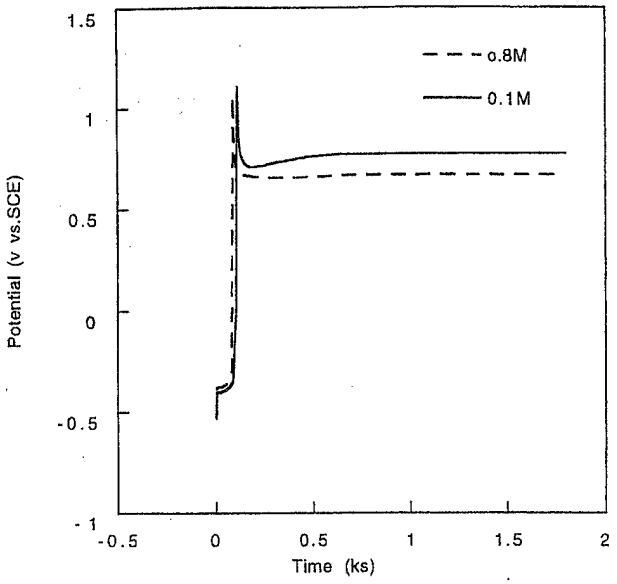

Fig. 10. Potential–time curves for the formation of polypyrrole coatings on steel at different monomer concentrations (i=2.25 mA/cm^2, [OA]=0.1 M).

bring about the passivation of the iron [18,19]. However, in alkaline medium, steady-state electropolymerization potential was only observed when the current density was 5.63 mA/cm^2. When the applied current densities were below 5.63 mA/cm^2, the potential first decreased with time, then tended to a steady-state value; the reproducibility of the potential–time curves was poor. The detailed mechanism of this phenomenon is not clear. Perhaps the interlayer formed at lower current density was not very stable. For the same applied current density, the electropolymerization potential of pyrrole in alkaline medium was much higher than that in acidic medium.

3.2. Effects of monomer and electrolyte concentrations

The effect of monomer and electrolyte concentrations on the anodic synthesis of polypyrrole coatings was investigated in a medium of pH 1.4. In order to determine the effect of initial monomer concentration, the concentration of oxalic acid and the applied current density were kept constant at 0.1 M and 2.25 mA/cm^2, respectively. The electrochemical reactions were performed at four different monomer concentrations: 0.1, 0.25, 0.5 and 0.8 M. As shown in Figs. 10 and 11, the concentration of pyrrole did not have any noticeable effect on the induction time. The electropolymerization potential, however, decreased slightly with increasing monomer concentration. This phenomenon may be associated with the process of an electrochemical reaction. The electropolymerization of pyrrole generally consists of two continuous steps. The first step is the diffusion of pyrrole monomer to the electrode surface, the rate of this step is determined by the pyrrole concentration. The second step is the oxidation reaction of pyrrole at the interface between the electrode and electrolyte solution. Since the applied current density and the

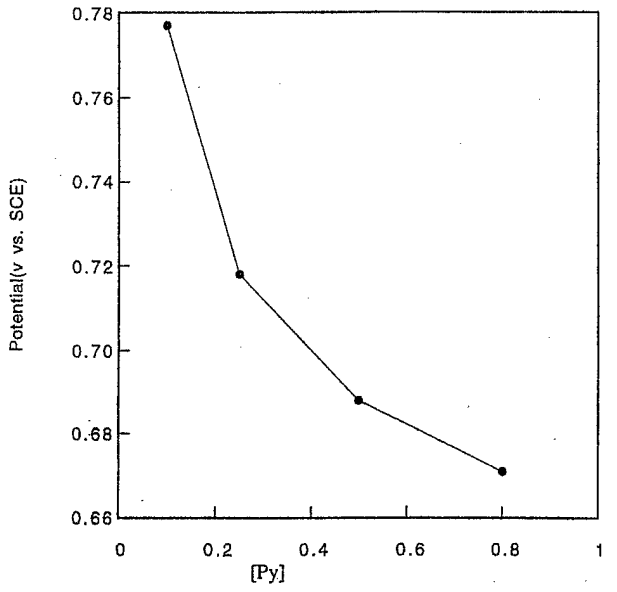

Fig. 11. Variation of electropolymerization potential with initial monomer concentration (i=2.25 mA/cm^2, [OA]=0.1 M).

electrolyte concentration were kept constant, the rate of the reaction was determined by the amount of monomer available at the interface at unit time. For higher monomer concentration, the positive charge at the working electrode is rapidly consumed by pyrrole, the accumulation of the charge at the electrode is lower, thus the corresponding reaction potential is lower. At lower monomer concentration, the positive charge cannot be consumed by pyyrole immediately, thus some charge will be accumulated at the working electrode, resulting in a higher reaction potential.

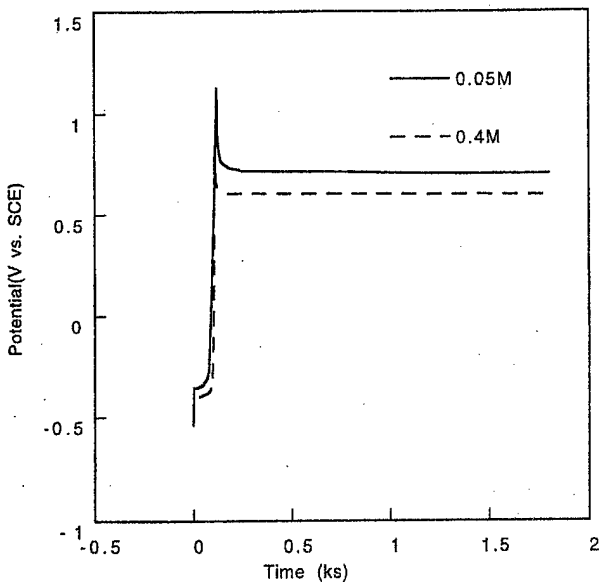

Fig. 12. Potential–time curves for the formation of polypyrrole coatings on steel at different electrolyte concentrations (i=2.25 mA/cm^2, [OA] = 0.1 M).

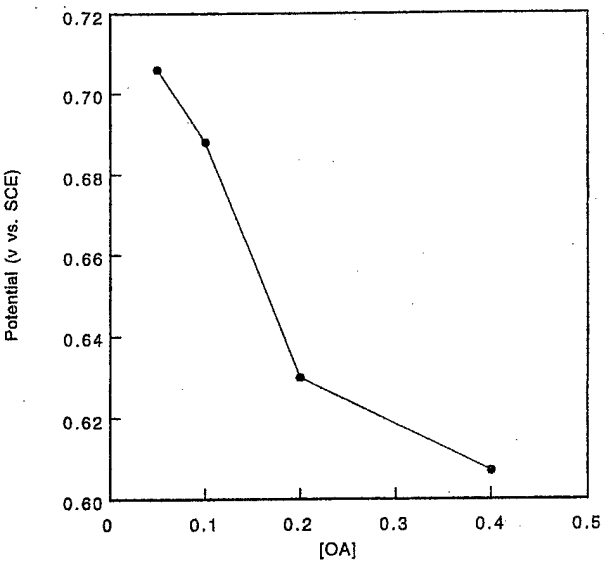

Fig. 13. Variation of electropolymerization potentials with initial electrolyte concentrations (i=2.25 mA/cm^2, [OA] =0.1 M).

The effect of electrolyte concentration was investigated with 0.5 M pyrrole concentration and 2.25 mA/cm^2 applied current density. Electrochemical reactions were carried out at four different electrolyte concentrations: 0.05, 0.1, 0.2 and 0.4 M. The results are shown in Figs. 12 and 13. It can be seen that the induction time was not significantly affected by the electrolyte concentration. However, the electropolymerization potential decreased gradually with increasing electrolyte concentration. This phenomenon is expected since the increasing electrolyte concentration can reduce the overall resistance of the system.

3.3. Composition and properties of the coatings

The composition of the coatings formed in different reaction media was first investigated by IR. Fig. 14 shows the IR spectra of the polypyrrole coatings formed in media of different pH. IR spectra of the coatings formed in different media are very similar and they show the characteristic peaks associated with pyrrole units and oxalate counterions [9,10,20–22]. The peaks occurring around 3433–3446 cm^{-1} correspond to the N–H stretch of the pyrrole ring and O–H stretch from the counterions. The peaks around 1699–1697 and 1653–1643 cm^{-1} are due to the C=O stretch from the counterions. The peaks located at 1558 and 1541 cm^{-1} come from the pyrrole ring C=C stretch and the peaks around 1466–1457 and 1417–1398 cm^{-1} are caused by pyrrole ring stretch. The peaks around 1244–1186 cm^{-1} may be due to C–O stretch. The peaks around 1033–1026 cm^{-1} correspond to C–H in-plane deformation of the pyrrole units. The peaks around 922–908 and 789–762 cm^{-1} are due to the C–H out-of-plane deformation of the pyrrole units. The peaks around 729–721 cm^{-1} may come from O–C=O in-plane deformation from the counterions. Thus, the IR results confirm the formation of polypyrrole and the presence of counterions in the coatings.

Three samples prepared in oxalic acid (pH = 1.4), sodium hydrogen oxalate (pH = 2.4) and sodium oxalate media (pH = 8.4), respectively, were analyzed by elemental analysis. The results are shown in Tables 1–3. Elemental analysis shows the presence of oxygen in the coatings, which indicates that electrolyte was incorporated into polypyrrole. Using $HC_2O_4^-$ as the counter ions for the oxalic acid system and sodium hydrogen oxalate system, and $C_2O_4^{2-}$ as the counter ions for the sodium oxalate system, the degree of insertion of the counter ions was calculated to be 0.23 for the first two systems and 0.31 for the third system, respectively. When the reaction medium was alkaline, the degree of insertion of the counter ions was slightly higher; this may be due to the overoxidation of polypyrrole in alkaline medium.

The properties of coatings obtained at different pH were very different. Coherent, tough and strongly adherent coatings could be obtained in media of low pH. The quality of the coatings was so excellent that no crack or detachment of the coatings was observed even after many times of bending. However, when the pH was increased to around 6, no coatings were formed at low applied current density (below 1.13 mA/cm^2). At higher applied current density, the coatings formed were brittle, non-uniform and poorly adherent to the substrate. In alkaline medium, the coatings obtained were all very brittle and could be easily peeled off from the substrate. It has been found that alkaline medium is not advantageous for the formation of good quality films of polypyrrole on platinum [14].

Applied current density has also great effect on the properties of the coatings. Coherent, tough and strongly adherent coatings were obtained at low current density, while the coatings became brittle and could be easily peeled off from the

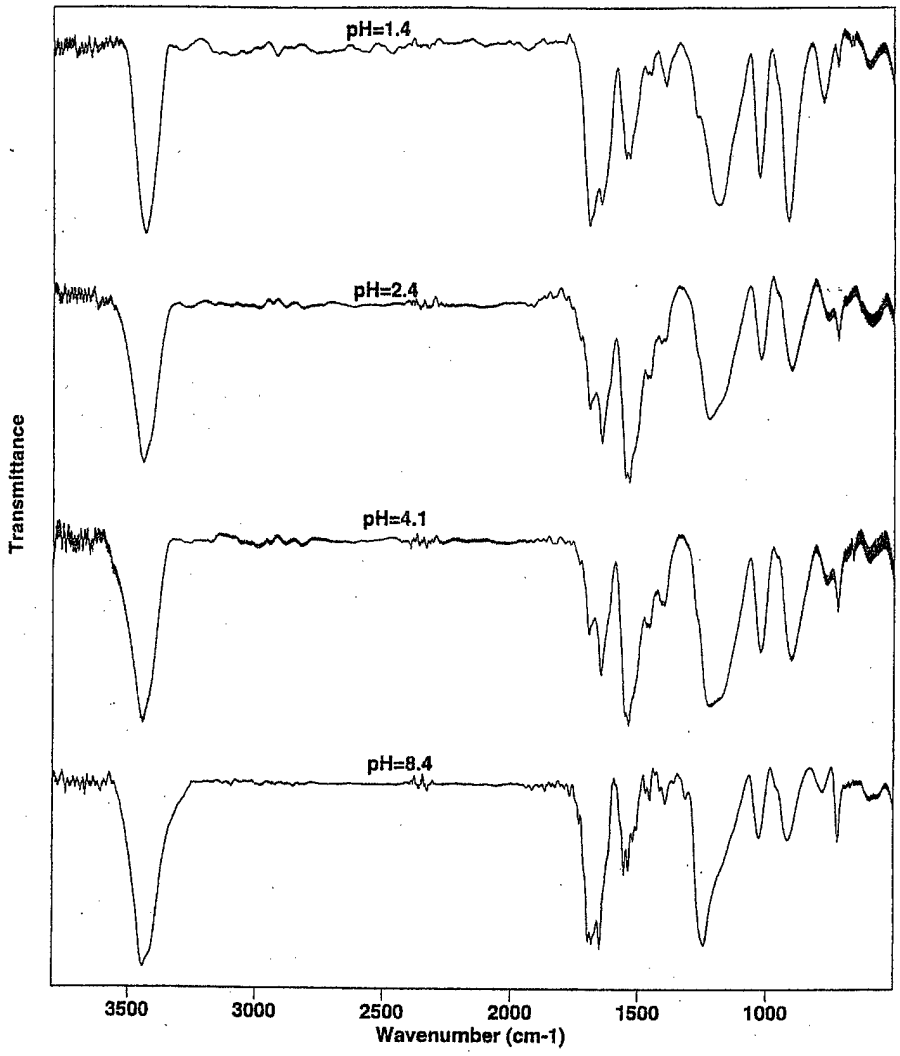

Fig. 14. IR spectra of the polypyrrole coatings formed at different pH.

Table 1
Results of the elemental analysis of the coating formed from oxalic acid electrolyte (pH = 1.4)

Element	Content (%)
C	58.67
H	3.70
N	16.85
O	17.47

Table 2
Results of the elemental analysis of the coating formed from sodium hydrogen oxalate electrolyte (pH = 2.4)

Element	Content (%)
C	58.08
H	3.87
N	16.87
O	17.92

substrate at higher current density. This phenomenon is perhaps because high applied current density induces some kind of side reaction, which may result in short chain length or lead to formation of defects along the chain.

The morphology of the coatings formed at low and high current density was also investigated by SEM and is shown in Figs. 15–17. Overall, the coatings formed at lower current density (0.56 mA/cm^2) for 30 min were very smooth with fine microspheroidal grains. Because the thickness of the coatings was very thin, the shape of the substrate could be seen. One exception was the coating formed at pH = 4.1; the surface of this coating was very flat and no microspheroidal grains were observed. This may be due to the relatively short electropolymerization time under the above reaction condition. The polypyrrole coatings formed at a higher current density (5.63 mA/cm^2) show rougher surface and had larger microspheroidal grain size. The SEM micrographs also showed some small cracks on the surface of these samples,

Table 3
Results of the elemental analysis of the coating formed from sodium oxalate electrolyte (pH = 8.4)

Element	Content (%)
C	55.76
H	4.22
N	15.82
O	22.64

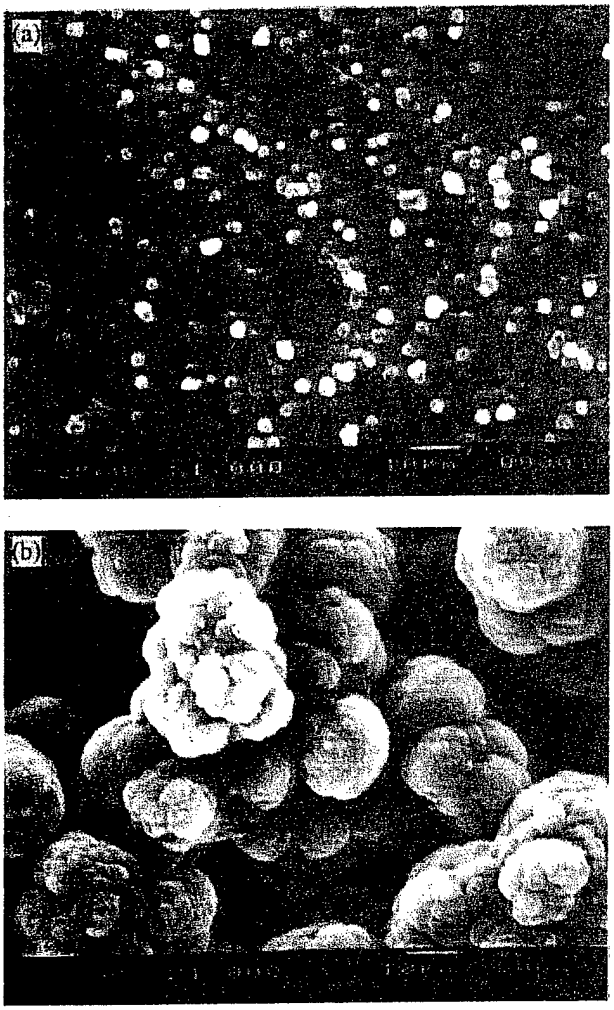

Fig. 15. SEM micrographs for the steel coated with polypyrrole at pH = 1.4: (a) $i = 0.56$ mA/cm^2; (b) $i = 5.63$ mA/cm^2.

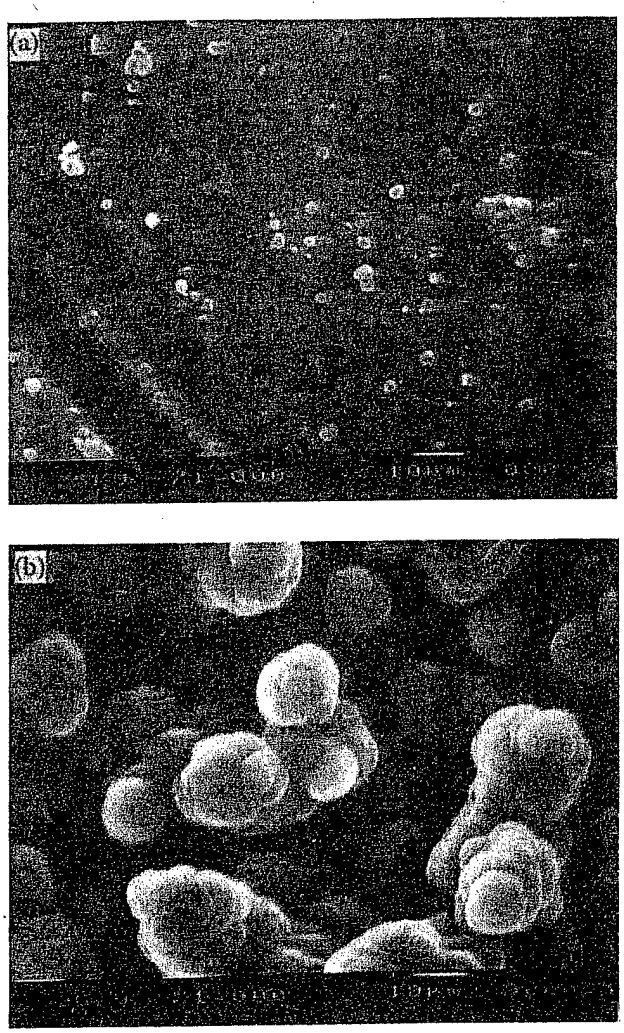

Fig. 16. SEM micrographs for the steel coated with polypyrrole at pH = 2.4: (a) $i = 0.56$ mA/cm^2; (b) $i = 5.63$ mA/cm^2.

which further demonstrated that high-quality coatings were formed at lower current density.

4. Conclusions

Polypyrrole coatings have been successfully formed on low carbon steel from aqueous oxalate solution by electrochemical method. Electrochemical process parameters were found to have great effect on the formation process and the properties of the coatings. In acidic medium, an induction period was shown before the electropolymerization of pyrrole took place, while no such period was observed in alkaline medium. In acidic medium, the shortest induction time was observed in the reaction medium of pH around 2.4. The induction time also decreased dramatically with increasing current density. For all the reaction media, the electropolymerization potential of pyrrole increased with increasing applied current density and a linear relationship was observed in acidic medium. Our results also revealed no significant dependence of induction time on the initial pyrrole concentration and electrolyte concentration. The electropolymerization potential, however, decreased with increasing pyrrole and electrolyte concentration, respectively. Coherent, smooth, tough and strongly adherent coatings were obtained in reaction media of low pH at low applied current density. High current density and/or

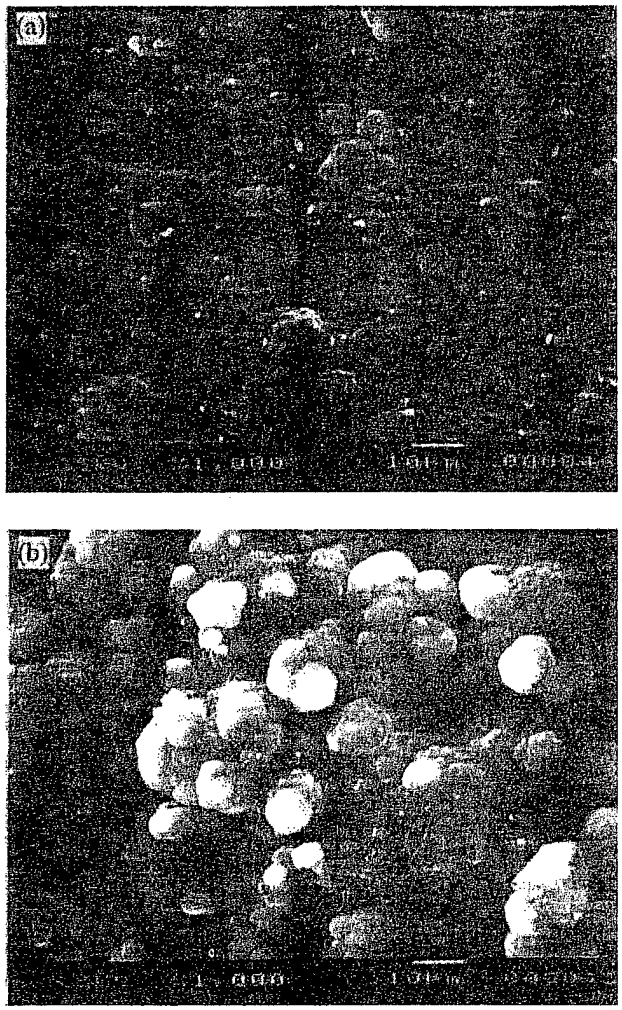

Fig. 17. SEM micrographs for low carbon steel coated with polypyrrole at pH = 4.1: (a) $i = 0.56$ mA/cm^2; (b) $i = 5.63$ mA/cm^2.

reaction media of high pH generally led to brittle and poorly adherent coatings.

Acknowledgements

Financial support from the Office of Naval Research's Young Investigators Program, Grant N00014-95-1-0485, is gratefully acknowledged.

References

[1] G.L. Burnside, G.E.F. Brewer, J. Paint Technol. 36 (1992) 96.
[2] G.E.F. Brewer, Electropolymerization of Coatings, American Chemical Society, Washington, DC, 1974.
[3] G.E.F. Brewer, J. Appl. Electrochem. 13 (1983) 269.
[4] A.F. Diaz, K.K. Kanazawa, J. Chem. Soc., Chem. Commun. (1979) 635.
[5] A.F. Diaz, J.I. Castillo, J. Chem. Soc., Chem. Commun. (1980) 397.
[6] M. Salmon, A.F. Diaz, A.J. Logan, M. Krounbi, J. Bargon, Mol. Cryst. Liq. Cryst. 83 (1982) 265.
[7] A.F. Diaz, B. Hall, IBM J. Res. Dev. 27 (1983) 342.
[8] E.M. Geniès, G. Bidan, A.F. Diaz, J. Electrochem. Soc. 149 (1983) 101.
[9] K.M. Cheung, D. Bloor, G.C. Stevens, Polymer 29 (1988) 1709.
[10] C.A. Ferreira, S. Aeiyach, M. Delamar, P.C. Lacaze, J. Electroanal. Chem. 284 (1990) 351.
[11] M. Schirmeisen, F. Beck, J. Appl. Electrochem. 19 (1989) 401.
[12] F. Beck, R. Michaelis, J. Coat. Technol. 64 (1992) 59.
[13] F. Beck, R. Michaelis, F. Schloten, B. Zinger, Electrochim. Acta 39 (1994) 229.
[14] W. Su, J.O. Iroh, J. Appl. Polym. Sci. 65 (1997) 417.
[15] W. Su, J.O. Iroh, J. Appl. Polym. Sci. 65 (1997) 617.
[16] S. Asavapiriyanont, G.K. Chandler, G.A. Gunawardena, D. Pletcher, J. Electroanal. Chem. 177 (1984) 229.
[17] T.F. Otero, E. Angulo, J. Appl. Electrochem. 22 (1992) 369.
[18] M. Pourbaix, Lectures on Electrochemical Corrosion, Plenum, New York, 1973.
[19] D.A. Jones, Principles and Prevention of Corrosion, Macmillan, London, 1992.
[20] R.A. Jones (ed.), Heterocyclic Compounds, Pyrroles, Vol. 48, Part 1, Wiley, New York, 1990.
[21] G. Socrates, Infrared Characteristic Group Frequencies, Wiley, New York, 2nd edn., 1994.
[22] P. Novak, B. Rasch, W. Wielstich, J. Electrochem. Soc. 138 (1191) 3300.

PERGAMON

Electrochimica Acta 44 (1999) 2173–2184

ELECTROCHIMICA Acta

Electropolymerization of pyrrole on steel substrate in the presence of oxalic acid and amines

Wencheng Su, Jude O. Iroh *

Department of Materials Science and Engineering, University of Cincinnati, 498 Rhodes Hall (ML 12), Cincinnati, OH 45221-0012, USA

Received 11 October 1997; received in revised form 15 May 1998

Abstract

Electropolymerization of pyrrole on steel substrate was carried out in aqueous oxalate solutions in the presence of amines. Triethylamine and allyamine were the amines used in this study. The electropolymerization process of pyrrole in acidic medium was found to be different from that in alkaline medium. In acidic medium, the reactions were characterized by an induction period while no such period was observed in alkaline medium. Our results show that the pH of the reaction medium and the applied current density had a great influence on the induction time. Effects of triethylamine and allyamine on the electropolymerization process of pyrrole were very similar. The composition of the coatings was studied by FTIR and elemental analysis. The coatings formed in different medium had a similar composition. Smooth, uniform, strongly adherent coatings could be formed on the steel substrate by proper choice of the reaction parameters. © 1999 Elsevier Science Ltd. All rights reserved.

Keywords: Pyrrole; Polymerization; Steel; Current density; PH

1. Introduction

The nature of the working electrode is a critical consideration for the preparation of polypyrrole. Since polypyrrole films are produced by an oxidative process, it is important that the electrode does not oxidize concurrently with the monomer. For this reason, most free-standing films of polypyrrole have been prepared using a platinum or a gold electrode [1–7]. However, recently the electropolymerization of pyrrole on oxidizable steel electrode was also investigated by several groups [8–13].

Cheung and Bloor studied the electrochemical polymerization of pyrrole on different metallic electrodes in propylene carbonate (PC) and tetraethylammonium toluenesulphonate (NEt_4Tos) medium [8]. Their results indicated that continuous polypyrrole-toluenesulphonate (PPy-TS) films could be formed on mild steel (Fe) electrodes in the above medium. The films obtained showed a fibrillar surface structure, but they were very brittle.

The electropolymerization of pyrrole on iron was also investigated in different organic solvents such as acetonitrile (ACN), propylene carbonate (PC), methanol (MeOH), tetrahydrofuran (THF), *N*,*N*-dimethylformamide (DMF) and dimethylsulfoxide (DMSO) in the presence of 0.1 M tetrabutylammonium hexafluorophosphate (NBu_4PF_6) or tetraethylammonium *p*-toluene sulfonate (NEt_4Tos) [9]. The electropolymerization of pyrrole was found to be dependent on the acidity of the medium. If the solvent was too acidic (such as ACN), iron dissolution was favoured, preventing polypyrrole deposition. If the solvent was too basic (DMF or DMSO), it could react with the radical cation and therefore hinder the polymerization of pyrrole. However, when PC, MeOH, EtOH or THF were used as the solvent, the formation of polypyrrole films on the electrodes occurred.

* Corresponding author. Tel.: +1-513-556-3096; fax: +1-513-556-3626.

PII: S0013-4686(98)00343-0

Troch-Nagels reported that polypyrrole could be electrocoated on mild steel in aqueous Na_2SO_4 medium [10]. However, the coatings obtained by this method were brittle and had poor adhesion to steel.

Beck and his coworkers also investigated the galvanostatic electrodeposition of polypyrrole on iron in aqueous medium [11–13]. They found that polypyrrole films could not be deposited on iron from aqueous electrolytes containing anions such as BF_4^-, ClO_4^-, HSO_4^-, SO_4^{2-}, Tos^-, HCO_3^-, $H_2PO_4^-$, HPO_4^{2-} and $H_2BO_3^-$. However, polypyrrole layers were obtained on iron when potassium nitrate and oxalic acid were used as the electrolyte. When potassium nitrate was used as the electrolyte, the adhesion of the coatings to the substrate was not very good. Smooth and strongly adherent polypyrrole coatings could be electrodeposited on iron from aqueous electrolyte containing oxalic acid [12, 13].

Triethylamine (TEA) and allyamine are well known as corrosion inhibitors for iron [14]. The presence of these two kind of amines in the aqueous oxalate medium may influence the passivation of the iron and electropolymerization of pyrrole. In this work, we investigated the electropolymerization of pyrrole on steel in aqueous oxalate medium in the presence of triethylamine and allyamine.

2. Experimental

Pyrrole and oxalic acid were purchased from Aldrich Chemicals. Triethylamine (TEA) was purchased from Fisher Scientific and allyamine was purchased from Fluka Chemika-BioChemika. All aqueous solutions used in the experiments were made from deionized water.

Aqueous electropolymerization of pyrrole was performed in a one-compartment polypropylene cell. The working electrode was made from a QD low carbon steel panel provided by Q-panel Company. The working electrode was degreased with tetrachloroethylene for about an hour prior to the electropolymerization. The coated surface area of the electrode was 8.89 cm^2. The counter electrodes comprised of two titanium alloy plates. A saturated calomel electrode (SCE) manufactured by Corning Company was used as the reference electrode. The instrument used to electrochemically coat the low carbon steel was an EG&G Princeton Applied Research Potentiostat/Galvanostat Model 273A. The working electrode and counter electrodes were used as anode and cathode, respectively.

The constant current method was the technique used in this experiment. The current density (i) was varied from 0.5 to 4 mA/cm^2. The pH of the solution containing pyrrole and oxalic acid was adjusted by triethylamine (TEA) and allyamine. In this study, the pH of the reaction medium was varied between 1 and 10. The initial monomer and electrolyte concentrations were kept constant at 0.25 and 0.1 M, respectively, and the electropolymerization time was fixed at 1800 s. After each experiment, the coated steel sheet was rinsed with deionized water and methanol and dried in an oven at 65°C to constant weight. Elemental analysis of the polypyrrole coatings scraped from the steel substrates was done by Galbraith Laboratories. The IR spectra of the coatings were measured by a Bio-rad FTS-40 FIIR spectrometer.

3. Results and discussion

3.1. Electropolymerization of pyrrole on steel in the presence of amine

The electropolymerization of pyrrole on steel substrates was first investigated in the presence of triethylamine (TEA). Figures 1–5 show the potential–time curves for the electropolymerization of pyrrole on steel in different pH medium. It can be seen that the potential–time curves obtained in acid medium were different from those obtained in basic medium. In acidic medium, the electropolymerization of pyrrole was characterized by two distinct stages. In the first stage, the reaction potential was negative. Because the electropolymerization of pyrrole was an oxidative process, the electropolymerization couldn't take place at such a low potential. However, the reaction potential rose sharply to a positive maximum value at the end of the first stage. After that, the potential decreased quickly and eventually reached a steady-state value. Black polypyrrole coatings began to form on the substrate during the second stage. Therefore the first stage of the reaction can be regarded as the induction period of the electropolymerization of pyrrole.

As shown in Figs. 1–4, the induction period was greatly influenced by the pH of the reaction medium. For the same applied current density, the induction time was shortest in the medium with a pH of 2.8 while it was longest in the medium with a pH of 6.0. Overall, the induction time was varied according to following sequence:

$$\tau_{pH=6.0} > \tau_{pH=4.4} > \tau_{pH=1.4} > \tau_{pH=2.8} \quad (1)$$

Fig. 6 shows the change in induction time with current density for each acidic medium. Since the passivation of steel was not observed in the medium of pH 6.0 at current densities below 1.13 mA/cm^2, only the induction time observed at a higher applied current density was shown in Fig. 6. It can be seen that the difference in induction time was very large at low current density,

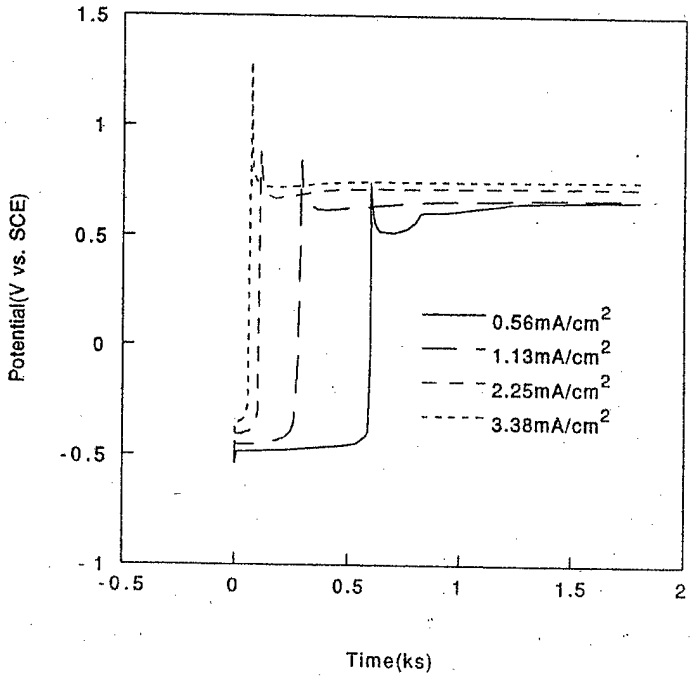

Fig. 1. Potential–time curves for electropolymerization of pyrrole on steel in the presence of TEA at different current density, pH = 1.4.

but the induction time tended to become close to each other at higher current density. For example, at the current density of 0.56 mA/cm^2, the induction time in the medium of pH 2.8 was about 363 s while the induction time in the medium of pH 4.4 was about 1257 s. When the applied current density was increased to 3.38 mA/cm^2, the induction time became very close for the reaction medium with a pH below

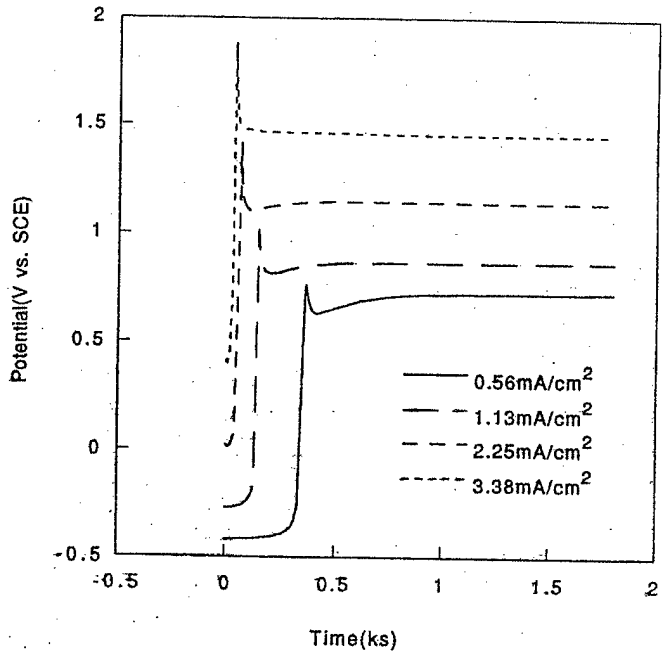

Fig. 2. Potential–time curves for electropolymerization of pyrrole on steel in the presence of TEA at different current density, pH = 2.8.

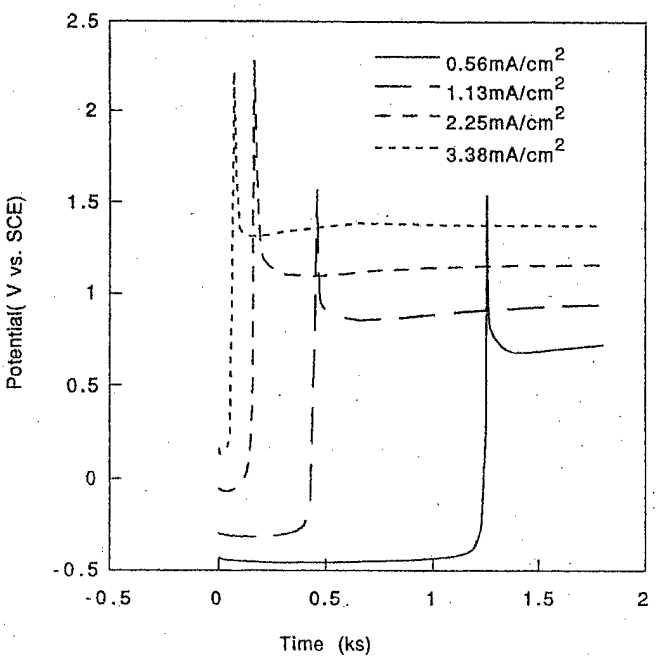

Fig. 3. Potential–time curves for electropolymerization of pyrrole on steel in the presence of TEA at different current density, pH = 4.4.

4.1. The induction time of the medium of pH 6.0 was still much longer than those of the lower pH mediums.

As shown in Fig. 6, the induction time (τ) also decreased dramatically with increasing current density. For example, when the pH of the reaction

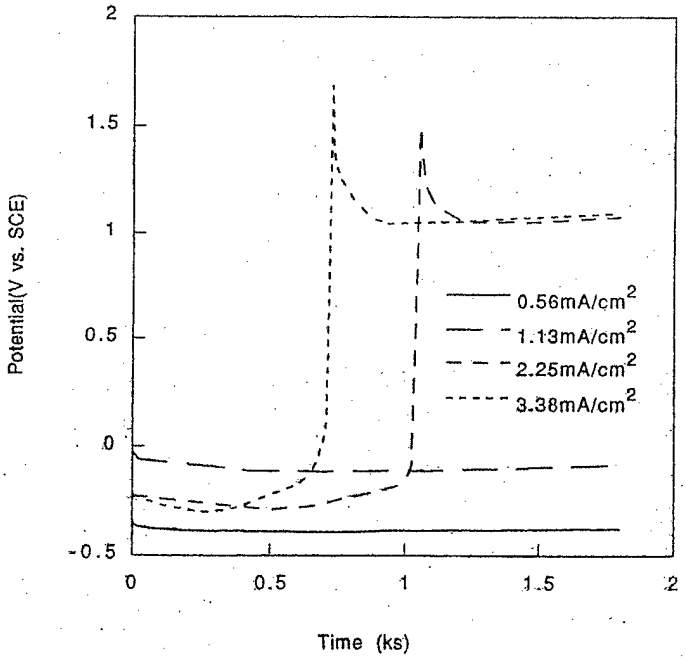

Fig. 4. Potential–time curves for electropolymerization of pyrrole on steel in the presence of TEA at different current density, pH = 6.0.

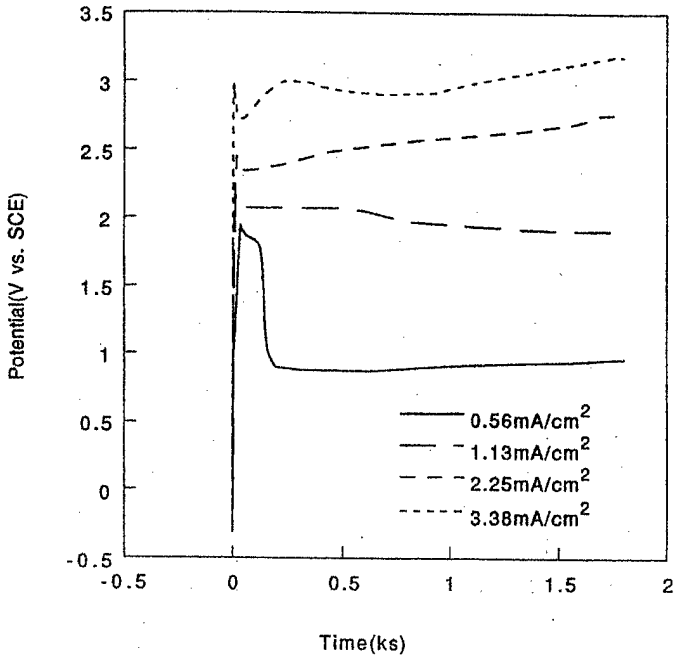

Fig. 5. Potential–time curves for electropolymerization of pyrrole on steel in the presence of TEA at different current density, pH = 9.5.

medium was about 4.4, the induction time was about 1257 s at current density of 0.56 mA/cm^2, however, the induction time became only about 73 s at 3.38 mA/cm^2. Fig. 7 shows the relationship between ln(induction time) and ln(current density) for the acidic medium. For each reaction medium, a linear relationship is obtained, which obeys the following equations:

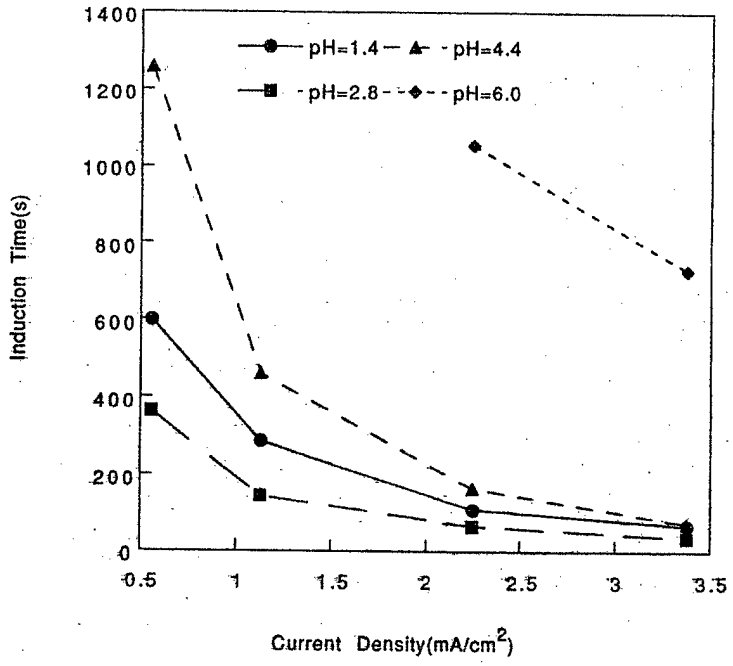

Fig. 6. Relationship between induction time and current density at different pH in the presence of TEA.

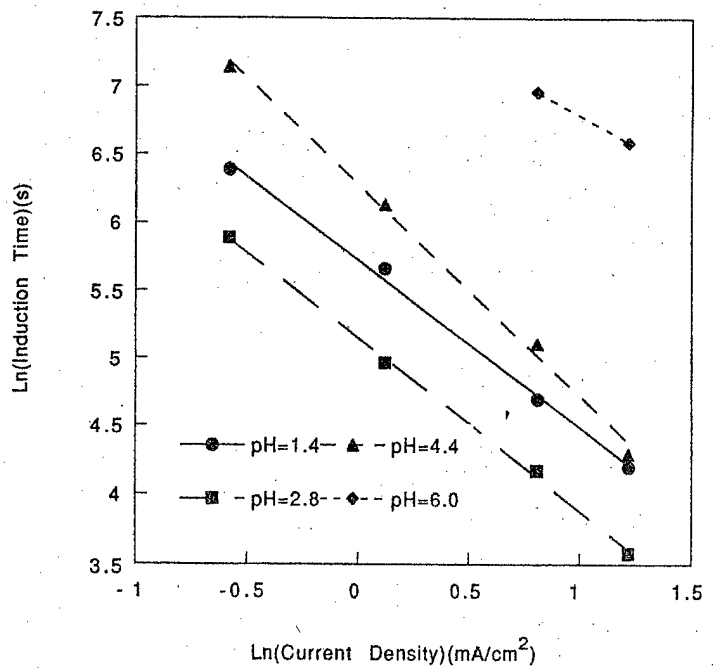

Fig. 7. Dependence of induction time on current density at different pH in the presence of TEA.

$$\text{pH} = 1.4: \ln\tau = 5.72 - 1.24 \ln i \quad (2)$$

$$\text{pH} = 2.8: \ln\tau = 5.15 - 1.26 \ln i \quad (3)$$

$$\text{pH} = 4.1: \ln\tau = 6.28 - 1.56 \ln i \quad (4)$$

$$\text{pH} = 6.0: \ln\tau = 7.69 - 0.90 \ln i \quad (5)$$

Fig. 8 shows the variation of the charge consumed during the induction period with the applied current density for all the acidic medium. Compared with the induction time, the passivation charge shows a

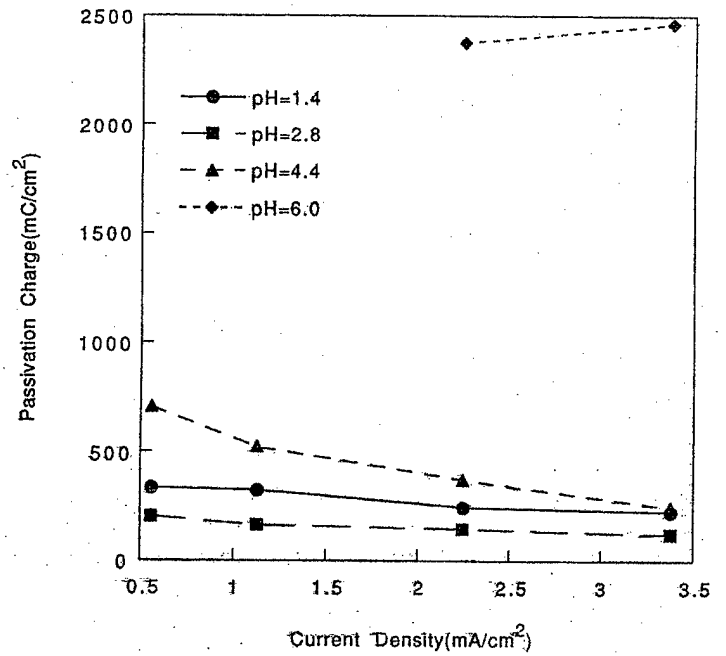

Fig. 8. Relationship between passivation charge and current density at different pH in the presence of TEA.

little difference in behaviour. For the reaction medium of pH 1.4 and 2.8, the passivation charge only decreased slightly with increasing current density. For example, the passivation charge was 335 mC/cm^2 at 0.56 mA/cm^2 for the medium of pH 1.4 and it was 226 mC/cm^2 at 3.38 mA/cm^2. For the reaction medium of pH 4.4, the passivation charge decreased gradually with increasing current density. However, for the reaction medium of pH 6.0, its passivation charge didn't change much between the two current densities.

Beck suggested that the passivation of the iron was due to the formation of the iron (II) oxalate interlayer when oxalic acid was as the electrolyte [12,13]. But it seems that the formation time of the iron oxalate interlayer is dramatically dependent on the applied current density and pH of the reaction medium. The detailed mechanism of the passivation of steel is now being studied in our laboratory.

When the passivation of steel was established, the electropolymerization of pyrrole began to occur on the steel substrate. The first positive potential peak is perhaps related to the nucleation of polypyrrole on the steel electrode [14,15]. It has been reported that the nucleation and three-dimensional growth is the mechanism for the deposition of polypyrrole on Pt and pyrrole oxidizes more readily on polypyrrole than on Pt [14]. After the peak, the electropolymerization potential tended to become very steady during the rest of the reaction. Fig. 9 shows the relationship between the steady-state electropolymerization potential and the applied current density for the acidic medium. As shown in Fig. 9, the electropolymerization potential increased linearly with the applied current density and can be expressed by the following relationships:

$$\text{pH} = 1.4: E_p = 0.63 + 0.03i \quad (6)$$

$$\text{pH} = 2.8: E_p = 0.57 + 0.26i \quad (7)$$

$$\text{pH} = 4.1: E_p = 0.59 + 0.24i \quad (8)$$

$$\text{pH} = 6.0: E_p = 1.08 - 0.01i \quad (9)$$

The variation of the electropolymerization with current density may have something to do with the deficiency of electrons on the surface of the electrode. More electrons were removed from the electrode when the applied current density was increased. Due to the slow reaction of the monomer, the electron deficiency could not be compensated immediately by the reaction, thus the deficiency of electrons would result in a positive potential change. It can also be seen from Fig. 9 that the electropolymerization potential also changed with pH for the same applied current density. The medium of pH 1.4 led to the lowest electropolymerization potential. The electropolymerization potential was very similar between the medium of pH 2.8 and 4.4. The electropolymerization potential for the medium of pH 6.0 almost maintained a constant value and the correspond-

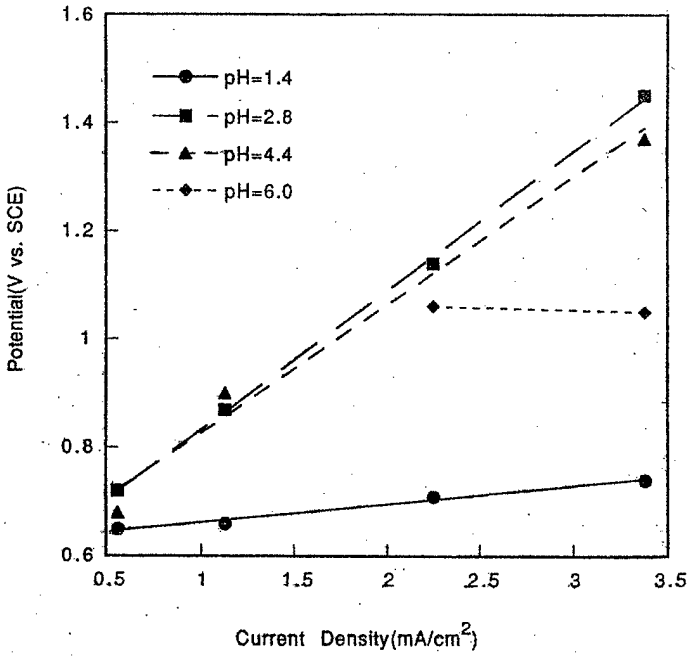

Fig. 9. Relationship between electropolymerization potential and current density at different pH in the presence of TEA.

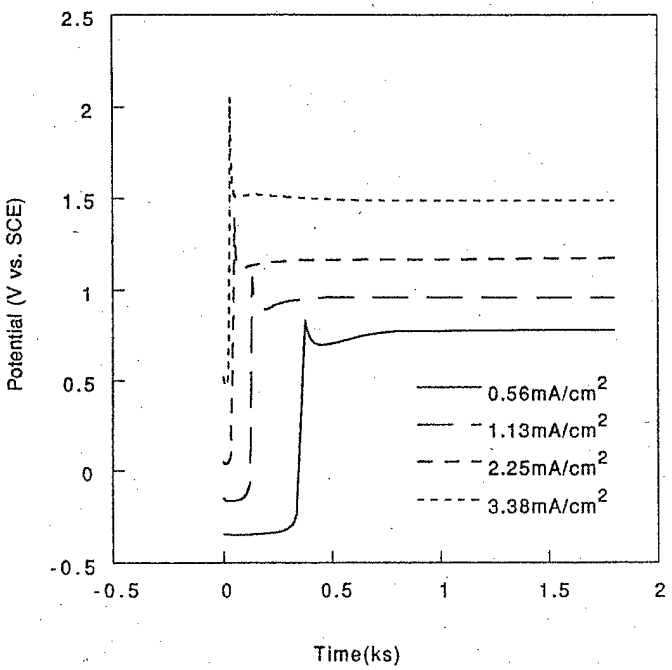

Fig. 10. Potential–time curves for electropolymerization of pyrrole on steel at different current density in the presence of allyamine, pH = 2.4.

ing electropolymerization potential was intermediate between those of pH = 1.4 and pH = 2.8. Asavapiriyanont et al. have reported that the electropolymerization of pyrrole is independent of pH [14]. Maybe the voltage drop through the interlayer is different for different acidic medium.

The formation process of polypyrrole in alkaline medium was quite different from that in acidic med-

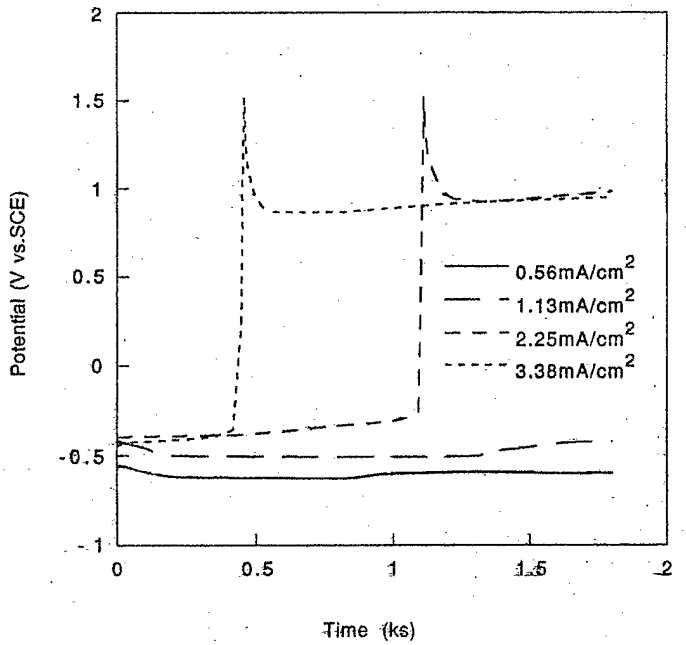

Fig. 11. Potential–time curves for electropolymerization of pyrrole on steel at different current density in the presence of allyamine, pH = 5.8.

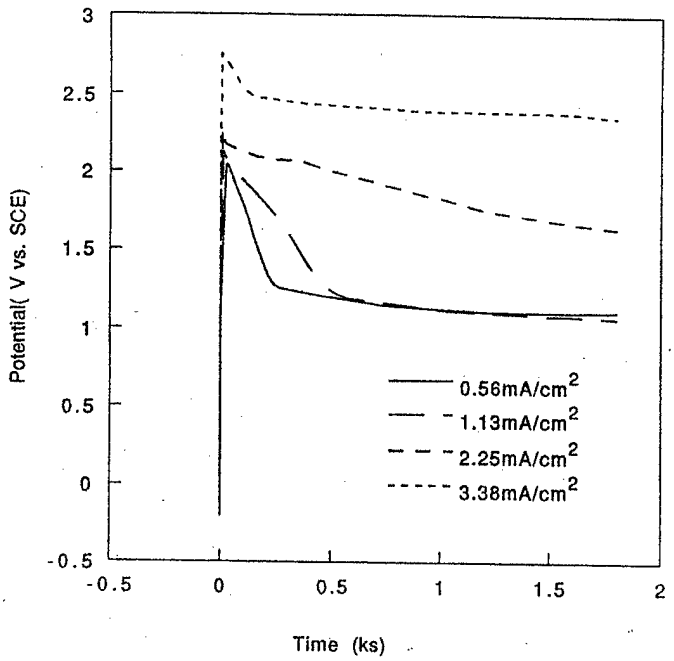

Fig. 12. Potential–time curves for electropolymerization of pyrrole on steel at different current density in the presence of allyamine, pH = 8.0.

ium. It can be seen from Fig. 5 that no induction period was observed when the pH of the reaction medium was 9.5. These results are not unusual. According to a Pourbaix diagram, the application of an anodic potential to an iron sheet immersed in alkaline medium, will bring about the passivation of the iron [16]. However, in alkaline medium, the electropolymerization potentials of pyrrole were not steady for all the applied current densities. For the same applied current density, the electropolymerization potential of pyrrole in alkaline medium was much higher than that in acidic medium. Perhaps the oxide interlayer formed in alkaline medium was not very stable and had a higher resistance than the interlayer formed in acidic medium.

The electropolymerization process of pyrrole on steel was also investigated with another corrosion inhibitor of steel, i.e. allyamine. The potential–time curves of the electropolymerization reactions of pyrrole are shown in Figs 10–12. The potential–time curves are very similar for the same electrochemical parameters between the triethylamine and allyamine systems. This may indicate that the mechanism of the passivation of the steel was the same for these two systems. Because TEA or allyamine could react with the hydrogen ions in the solutions to form ammoniumion, neutral TEA or allyamine molecules actually didn't exist in the solutions. Perhaps the role of TEA or allyamine was only to adjust the pH of the reaction medium.

3.2. Composition and properties of the coatings

The composition of the coatings formed in different reaction medium was first investigated by elemental analysis. The results of the elemental analysis are listed in Table 1. For all three samples, oxygen element was found present in the coatings, indicating that an electrolyte was incorporated into polypyrrole coatings.

Table 1
Results of elemental analysis of PPy coatings formed in different conditions

Sample	Elements	Content (%)
pH = 1.4	C	58.67
	H	3.70
	N	16.85
	O	17.47
pH = 9.5 (TEA)	C	55.71
	H	3.80
	N	15.82
	O	21.37
pH = 8.0 (allyamine)	C	56.72
	H	3.85
	N	15.91
	O	20.68

The degree of insertion of the counterions was calculated from the mole ratio of the nitrogen and oxygen elements. The degree of insertion of the counterions was calculated to be 0.23 when oxalic acid was used as the electrolyte (pH = 1.4). The degree of insertion was calculated to be 0.29 when the pH of the TEA reaction medium was 9.5. For allyamine system, the degree of insertion was calculated to be 0.28 when the pH of the reaction medium was 8.0. The degree of insertion for the coatings obtained in alkaline medium was a little bit higher than that in acidic medium. This is perhaps due to the overoxidation of polypyrrole in alkaline medium.

Figures 13 and 14 show the IR spectra of the polypyrrole coatings formed in different pH medium for two systems. The IR spectra of the coatings formed in different medium are very similar and they show the characteristic peaks associated with pyrrole units and oxalate counterions [8, 9, 17, 18]. The peaks occurring around 3572–3392 cm^{-1}, correspond to the N–H stretch of the pyrrole ring and maybe O–H stretch from the counterions. The peaks around 1700–1684 and 1660–1610 cm^{-1} are characteristic of a C=O

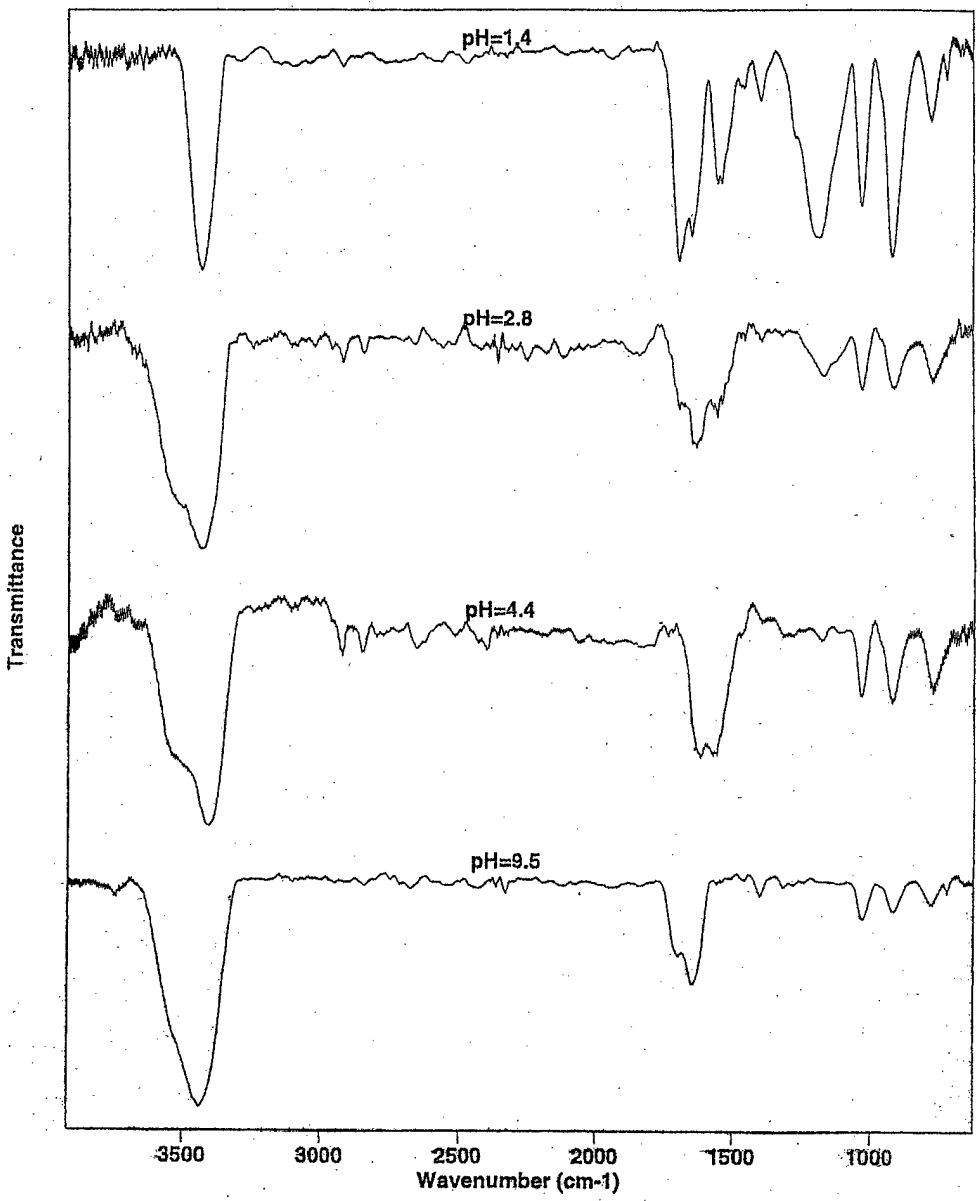

Fig. 13. IR spectra of PPy coatings formed in different pH medium in the presence of TEA.

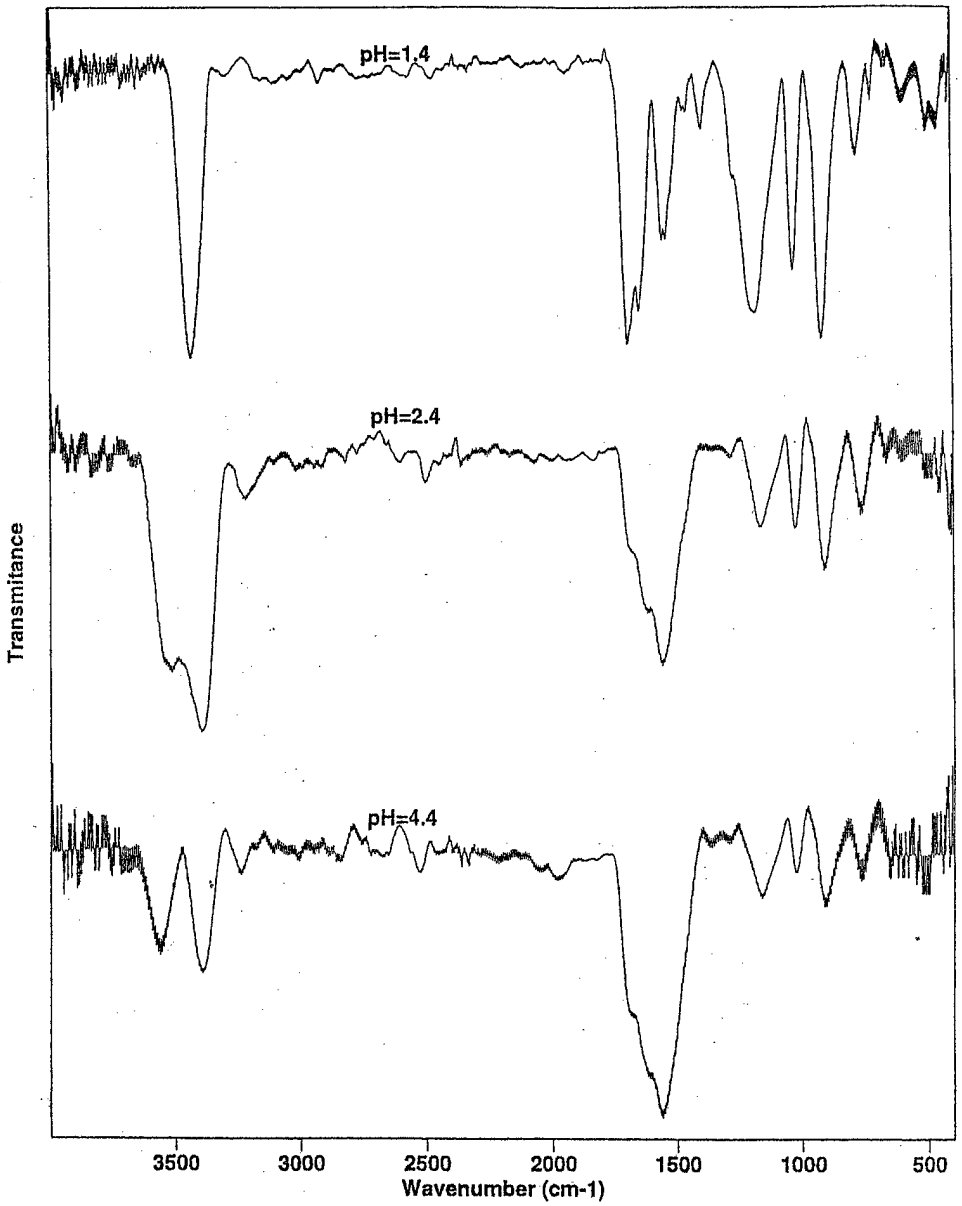

Fig. 14. IR spectra of PPy coatings formed in different pH medium in the presence of allyamine.

stretch from the counterions. The peaks located at 1561–1558 and 1545–1541 cm^{-1} are due to a pyrrole ring C=C stretch and the peaks around 1460–1458 and 1403–1399 cm^{-1} are caused by pyrrole ring stretch. The peaks around 1244–1186 cm^{-1} are maybe due to C–O stretch. The peaks at 1033–1023 cm^{-1} correspond to C–H in-plane deformation of the pyrrole units. The peaks at 922–906 and 782–766 cm^{-1} are due to the C–H out-plane deformation of the pyrrole units. The peaks at 722–721 cm^{-1} may come from O–C=O in-plane deformation from the counterions. Thus the IR results further confirm the formation of polypyrrole and the presence of counterions in the coatings.

The properties of coatings obtained at different pH were very different. Uniform and strongly adherent coatings could be obtained at low pH medium. However, when the pH was increased to around 6, no coatings were formed at current densities below 1.13 mA/cm^2. At higher applied current density, the coatings obtained were brittle, non-uniform and poorly adherent to the substrates. In alkaline medium, the coatings obtained were all very brittle and could be

easily peeled off from the substrates. Applied current density also had great effects on the properties of the coatings. Uniform and strongly adherent coatings were obtained at low current density while the coatings became brittle and could be easily peeled off from the substrate at higher current density.

4. Conclusion

Electropolymerization of pyrrole on steel was successfully performed in aqueous oxalate solutions in the presence of triethylamine and allyamine. These two kinds of amines were found to have similar effects on the electropolymerization process. Our results reveal that pH of the reaction medium and applied current density had great effects on the electropolymerization process and the properties of the coatings. In acidic medium, the shortest induction time was observed in the reaction medium of pH around 2.8. The induction time also decreased dramatically with increasing current density. For all the reaction medium, the electropolymerization potential of pyrrole increased with applied current density and a linear relationship was observed for each acidic medium. Uniform, smooth and strongly adherent coatings were obtained in low pH reaction medium at low applied current density. High current density and or high pH of the reaction medium generally led to brittle and poorly adherent coatings.

Acknowledgements

Financial support from the Office of Naval Research's Young Investigators Program, Grant N00014-95-1-0485, is gratefully acknowledged.

References

[1] A. Dall'Olio, G. Dascola, V. Varacca, C. R. 267 (1968) C433–C435.
[2] A.F. Diaz, K. Keiji Kanazawa, J. Chem. Soc. Chem. Commun. (1979) 635–636.
[3] A.F. Diaz, J.I. Castillo, J. Chem. Soc. Chem. Commun. (1980) 397–398.
[4] G.P. Gardini, Oxidation of monocyclic pyrrole, in: A. Katritzky, A.J. Boulton (Eds.), Advanced Heterocyclic Chemistry, vol. 15, Academic Press, New York, 1973.
[5] E.M. Genies, G. Bidan, A.F. Diaz, J. Electrochem. Soc. 149 (1983) 101.
[6] A.F. Diaz, J. Crowley, J. Bargon, G.P. Gardini, J.B. Torrance, J. Electroanal. Chem. 121 (1981) 355–361.
[7] M. Salmon, A.F. Diaz, A.J. Logan, M. Krounbi, J. Bargon, Mol. Cryst. Liquid Cryst. 83 (1982) 265–276.
[8] K.M. Cheung, D. Bloor, G.C. Stevens, Polymer 29 (1988) 1709–1717.
[9] C.A. Ferreira, S. Aeiyach, M. Delamar, P.C. Lacaze, J. Electroanal. Chem. 284 (1990) 351–369.
[10] G. Troch-Nagels, R. Winand, A. Weymeersch, L. Renard, J. Appl. Electrochem. 22 (1992) 756–764.
[11] M. Schirmeisen, F. Beck, J. Appl. Electrochem. 19 (1989) 401–409.
[12] F. Beck, R. Michaelis, J. Coat. Technol. 64 (808) (1992) 59–67.
[13] F. Beck, R. Michaelis, F. Schloten, B. Zinger, Electrochim. Acta 39 (1994) 229–234.
[14] S. Asavapiriyanont, G.K. Chandler, G.A. Gunawardena, D. Pletcher, J. Electroanal. Chem. 177 (1984) 229.
[15] T.F. Otero, E. Angulo, J. Appl. Electrochem. 22 (1992) 369.
[16] D.A. Jones, Principles and Prevention of Corrosion, Maxmillan Publishing Company, 1992.
[17] R.A. Jones (Ed.), Heterocyclic Compounds, Pyrroles, vol. 48, Part 1, John Wiley & Sons, 1990.
[18] G. Socrates, Infared Characteristic Group Frequencies, 2nd ed., John Wiley & Sons, 1994.

Characterization of the Passive Inorganic Interphase and Polypyrrole Coatings Formed on Steel by the Aqueous Electrochemical Process

JUDE O. IROH, WENCHENG SU

Department of Materials Science and Engineering, University of Cincinnati, Cincinnati, Ohio 45221-0012

Received 3 June 1998; accepted 8 June 1998

ABSTRACT: Polypyrrole coatings have been successfully formed on steel from aqueous oxalic acid-pyrrole solutions by electrochemical polymerization. Formation of the coatings was found to be dependent on the pH of the reaction solution and the applied current. In acidic medium, the formation of polypyrrole was characterized by an induction (passivation) period before electropolymerization of pyrrole. At the end of the induction period, a crystalline passive interphase was formed. The morphology and composition of the electrodeposited passive interphase and the resultant polypyrrole coatings were investigated by scanning electron microscopy, reflection-absorption infrared spectroscopy, and X-ray photoelectron spectroscopy. Our results reveal that the chemical composition of the passive interphase was similar to that of iron(II) oxalate dihydrate, $FeC_2O_4 \cdot 2H_2O$, crystals. Size and orientation of the crystalline passive interphase varied with electrochemical process variables. © 1999 John Wiley & Sons, Inc. J Appl Polym Sci 71: 2075–2086, 1999

Key words: polypyrrole coatings; interphase; low carbon steel; electrochemical method

INTRODUCTION

Polypyrrole is one of the important conducting polymers. Its free-standing films with high conductivity and good mechanical properties were first obtained by the electrochemical method,[1,2] and many papers have been published concerning various aspects of this materials.[3–6] For the preparation of polypyrrole, the nature of the working electrode is a critical consideration. Because polypyrrole films are produced by an oxidative process, it is important that the electrode does not oxidize concurrently with the monomer. For this reason, most free-standing films of polypyrrole have been prepared using a platinum or a gold electrode. But, recent interest has been shown in the formation of adherent polypyrrole coatings on oxidizable metals, such as iron for corrosion protection.[7–11]

Cheung and colleagues[7] studied the electrochemical polymerization of pyrrole on different metallic electrodes in propylene carbonate and tetraethylammonium *p*-toluene sulfonate medium.[7] Their results indicated that continuous polypyrrole films with fibrillar surface could be formed on mild steel electrodes in the above medium, but the films obtained were very brittle. The electropolymerization of pyrrole on iron was also investigated in different organic solvents in the presence of tetrabutylammonium hexafluorophosphate and tetraethylammonium *p*-toluene sulfonate.[8] The electropolymerization of pyrrole was found to be dependent on the acidity of the medium. When propylene carbonate, methanol,

Correspondence to: J. O. Iroh.

Journal of Applied Polymer Science, Vol. 71, 2075–2086 (1999)
 CCC 0021-8995/99/122075-12

and tetrahydrofuran were used as the solvent, the formation of polypyrrole films on the electrodes occurred.

Beck and his coworkers[9–11] also investigated the galvanostatic electrodeposition of polypyrrole on iron in aqueous medium. They found that polypyrrole films could not be deposited on iron from most aqueous electrolytes. However, polypyrrole coatings were formed on iron when potassium nitrate and oxalic acid, respectively, were used as the electrolyte. In the case of oxalic acid, they reported that smooth and strongly adherent coatings were obtained.

Recently our group have systematically investigated the effect of electrochemical parameters on the formation process of polypyrrole coatings on steel from the aqueous oxalate medium.[12–14] It was found that the formation of polypyrrole coatings on steel was dependent on the electrochemical parameters. Our preliminary results show that electropolymerization of pyrrole on steel in aqueous oxalic acid solution was preceded by the formation of crystalline passive inorganic interphase. It was also noticed that the size, orientation, and deposition rate of the passive interphase was affected by the electrochemical process variables. To get a better understanding of the formation and properties of polypyrrole coatings deposited on steel, we investigated the morphology and composition of the passive interphase and the resultant polypyrrole coatings, and our results are reported in this article.

EXPERIMENTAL

Materials

All chemicals used in this article were purchased from Aldrich Chemical Company, except for sodium bicarbonate ($NaHCO_3$), which was purchased from Fisher Scientific (Pittsburgh, PA). All aqueous solutions used in the experiments were made from deionized water. QD low carbon steel panels having a thickness of 0.5 mm were provided by the Q-panel Company (Cleveland, OH). For the purpose of characterization, steel sheets were mechanically polished to a mirror finish. The polishing sequence began with wet polishing on 320, 600-grit silicon carbide papers to grinding the surface. Additionally, the steel panels were wet-polished with 5.0 μm, 1.0 μm, 0.3 μm aluminum oxide abrasive slurries. Finally, the substrates were rinsed with distilled water and acetone and degreased with tetrachloroethylene for ~ 1 h before electropolymerization of pyrrole.

Electropolymerization

Aqueous electropolymerization of pyrrole was performed in a one-compartment polypropylene cell. QD low carbon steel sheets was used as the working electrode. Counter electrodes were comprised of two titanium alloy plates. A saturated calomel electrode (SCE) manufactured by Corning Company was used as the reference electrode. The instrument used to electrochemically coat the low carbon steel was an EG&G Princeton Applied Research Potentiostat/Galvanostat Model 273A. The working electrode and the counter electrodes were used as anode and cathode, respectively.

Constant current method was the technique used in this experiment. Current density (i) was varied from 0.5 to 6 mA cm^{-2}. The pH of the solution containing pyrrole and oxalic acid was adjusted by using sodium bicarbonate and varied from 1.4 to 8.4. The initial monomer and electrolyte concentrations were kept constant at 0.25M and 0.1M, respectively. After each experiment, the coated steel sheet was rinsed with water and methanol, and dried in an oven at 65°C to constant weight.

Characterization

Morphology of the samples was examined by a Hitachi S-4000 scanning electron microscope (SEM). Reflection-absorption infrared (IR) spectra (RAIR) of the sample were measured by a Bio-Rad FTS-40 FIIR spectrometer (Bio-Rad, Richmond, CA). An angular specular reflectance attachment was set to an incident angle of 65°. Spectra were obtained using a resolution of 4 cm^{-1} and were averaged over 128 scans. A background spectrum of a bare-polished steel substrate was subtracted from the acquired spectra in all cases. In the case of transmission IR spectroscopy, spectra were obtained by means of potassium bromide pellets. A Perkin–Elmer Model 5300 X-ray photoelectron spectrometer (XPS), with Mg Kα X-rays, operating at 300 W and 15 kV DC, was used to obtain XPS spectra. An Apollo computer system with Perkin–Elmer software was used for data acquisition and processing.

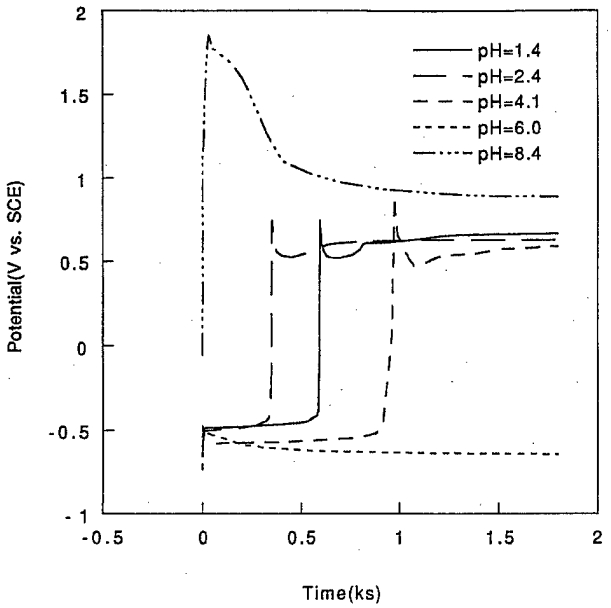

Figure 1 Potential-time curves for the formation of polypyrrole coatings on steel at a different pH (i = 0.56 mA cm^{-2}).

RESULTS AND DISCUSSION

Features of the Formation of Polypyrrole Coatings on Steel

Figure 1 shows the potential-time curves for the formation of polypyrrole coatings on steel at an applied current density of 0.56 mA cm^{-2} at different pH of the reaction medium. It can be seen that the formation of polypyrrole coatings is dependent on the pH of the reaction medium. In acidic medium, the formation of polypyrrole was characterized by three distinct stages. In the first stage of the reaction, the dissolution of steel occurred at a negative electrode potential. Dissolution of steel was terminated when steel was completely covered by crystalline passive interphase. Formation of the passive interphase is marked by a sharp rise in the electrode potential to a high positive value of ~ 1.2 V *vs.* SCE. Finally, a steady-state polymerization potential of ~ 0.6–0.8 V *vs.* SCE is attained. Dark-colored polypyrrole coatings are formed on the passivated steel in the final stage. The time it takes to form the passive interphase is regarded as the induction time for polymerization of pyrrole or the passivation time.

In acidic medium, the pH of the reaction medium has a dramatic effect on the induction time. For the same applied current density, induction time was shortest at pH 2.4 and was longest at pH 6.0. Overall, the induction time varied with the pH according to following sequence:

$$\tau_{pH6.0} > \tau_{pH4.1} > \tau_{pH1.4} > \tau_{pH2.4}$$

The effect of pH of the reaction medium on the induction time can be understood by the following example: the induction time was determined to be ~ 350 s for the reaction performed at pH 2.4. However, when the pH of the reaction medium was increased to 6.0, the induction time was so long that passivation was not established, even after a 30-min reaction.

Figure 2 shows the potential-time curves for the formation of polypyrrole coatings on steel at a different applied current density at pH 1.4. It can be seen that the induction time decreased dramatically with increasing current density. For example, the induction time was ~ 600 s at the current density of 0.56 mA cm^{-2}; however, the induction time was reduced to only ~ 70 s at a higher applied current density of 3.38 mA cm^{-2}.

Formation of polypyrrole coatings in basic medium showed a different trend from that in acidic medium. It can be seen from Figure 1 that no induction time was observed when the pH of the reaction medium was basic (pH 8.4). These results are not unusual. According to a Pourbaix

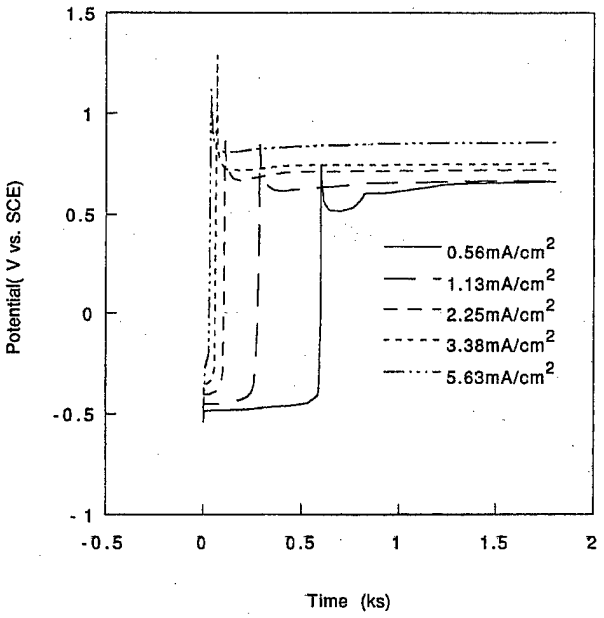

Figure 2 Potential-time curves for the formation of polypyrrole coatings on steel at a different current density at pH 1.4.

Figure 3 SEM micrograph of the interphase formed at 0.56 mA cm^{-2} in the medium of pH 1.4.

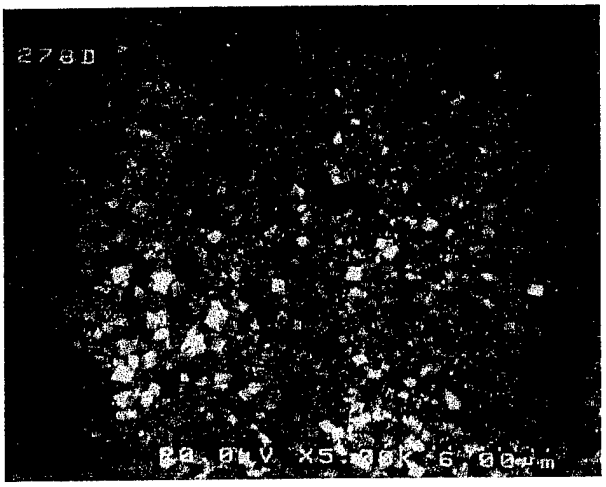

Figure 4 SEM micrograph of the interphase formed at 3.38 mA cm^{-2} in the medium of pH 1.4.

diagram, the application of an anodic potential to a iron sheet immersed in basic medium will bring about the passivation of the iron.[15,16]

In acidic medium, the third stage is associated with the polymerization of pyrrole on the substrate. The drop in electrode potential from ~ 1.2 V *vs.* SCE to 0.6–0.8 V *vs.* SCE is perhaps related to the nucleation and growth of polypyrrole on the steel electrode.[17,18] It has been reported that the nucleation and three-dimensional growth is the mechanism for the deposition of polypyrrole on Pt, and pyrrole oxidizes more readily on polypyrrole than that on Pt.[17] The electropolymerization of pyrrole occurred at the steady-state. In basic medium, however, the polymerization potential first decreased with time then tended to become steady, and the reproducibility of the potential-time curves was poor. For the same applied current density, the polymerization potential of pyrrole in basic medium was much higher than that in acidic medium. This may be due to the fact that the composition of the passive interphases is different for the two systems. The passive interphase formed in the basic medium is noncrystalline and may be composed of iron oxides rather than crystalline iron oxalates formed in acidic medium.

Morphology and Composition of the Interphase

Figures 3 and 4 show the SEM micrographs of the interphase formed at two different current densities at pH 1.4. It can be seen that the interphase is composed of many small crystals, and steel substrate was completely covered by the small crystals. The size of the crystals became much smaller at higher current density. Figure 5 shows the SEM micrograph of the sample prepared at 0.56 mA cm^{-2} at pH 6.0 in 30 min. In this case, passivation of the steel substrate was not established. No crystalline phases were observed on the surface of steel; however, it seems that there was a very thin film on the surface of the steel, which may be due to the formation of soluble iron oxides.

Figure 6 shows the RAIR spectra for the interphase formed at the end of the induction time at different pH. Although the induction time varied significantly with the pH (see Fig. 1), there were

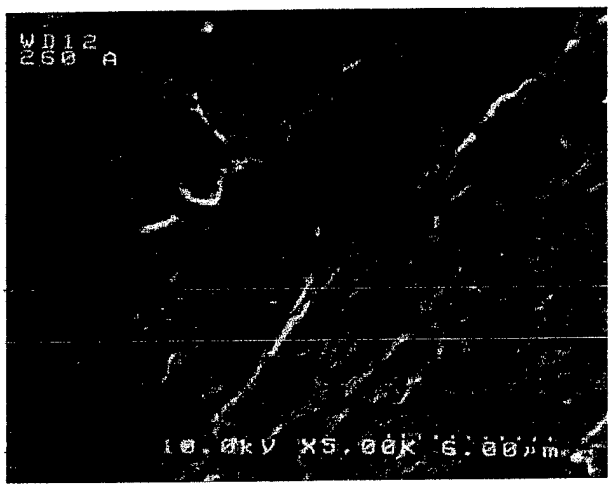

Figure 5 SEM micrograph of the sample formed at 0.56 mA cm^{-2} in the medium of pH 6.0 for 30 min.

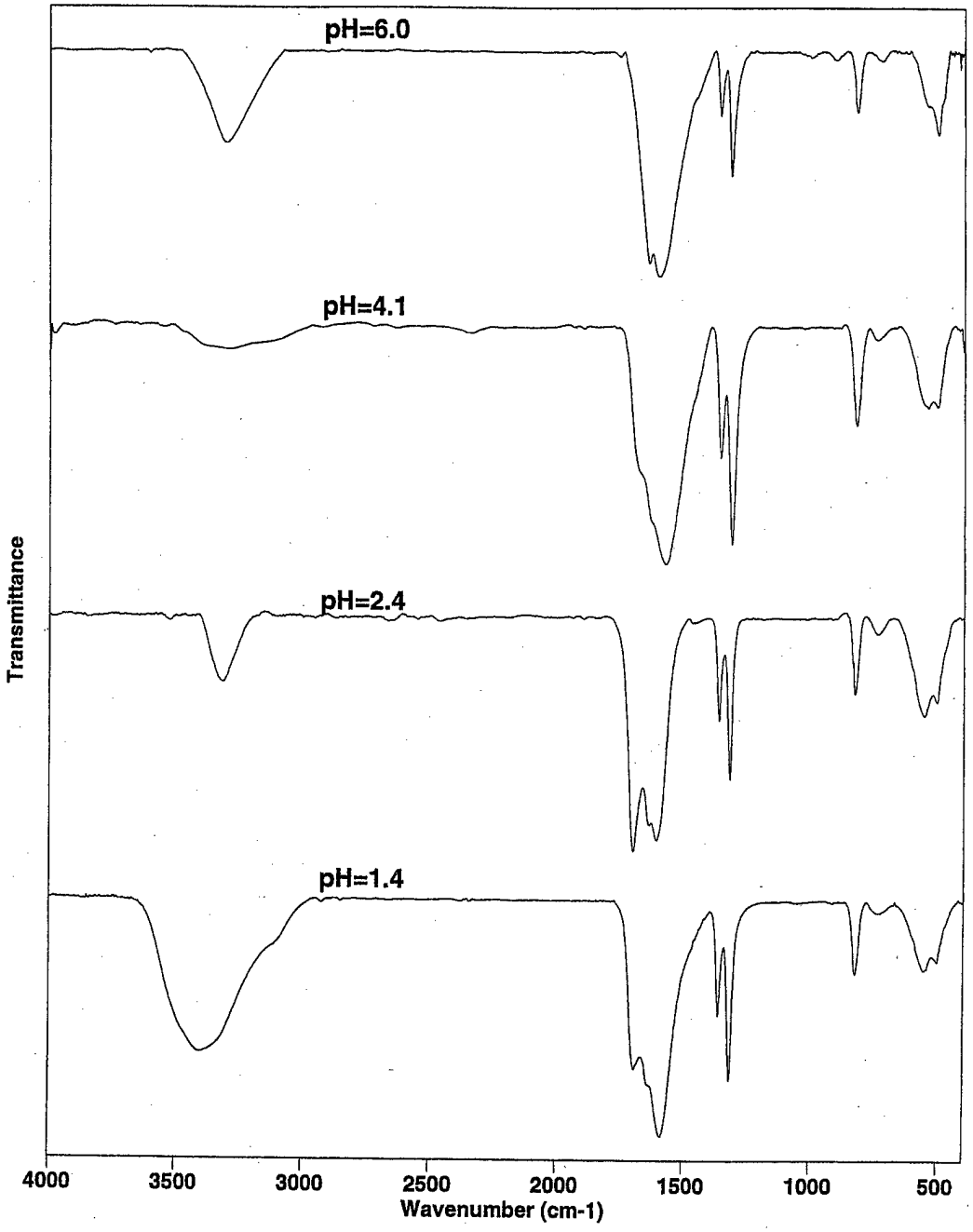

Figure 6 RAIR spectra of the interphase formed in different pH media.

no significant differences in the IR spectra of the interphase formed at different pH. The IR spectra show characteristic broad–OH absorption peaks at 3294–3403 cm^{-1}. The very strong and broad absorption duplex peak occurring at 1617–1700 cm^{-1} is due to the carbonyl group (C═O) contained in the oxalate ion. Additional sharp duplex peaks due to the C—O group occur at 1314–1364 cm^{-1}. Figure 7 shows the RAIR spectra of the interphase formed at different times during the induction period for the medium of pH 1.4. Note that the carbonyl peak and the C—O peaks were stronger at longer reaction times, as was expected. Figure 8 shows the RAIR spectra of the interphase formed at different current densities at pH 1.4. No significant difference is observed

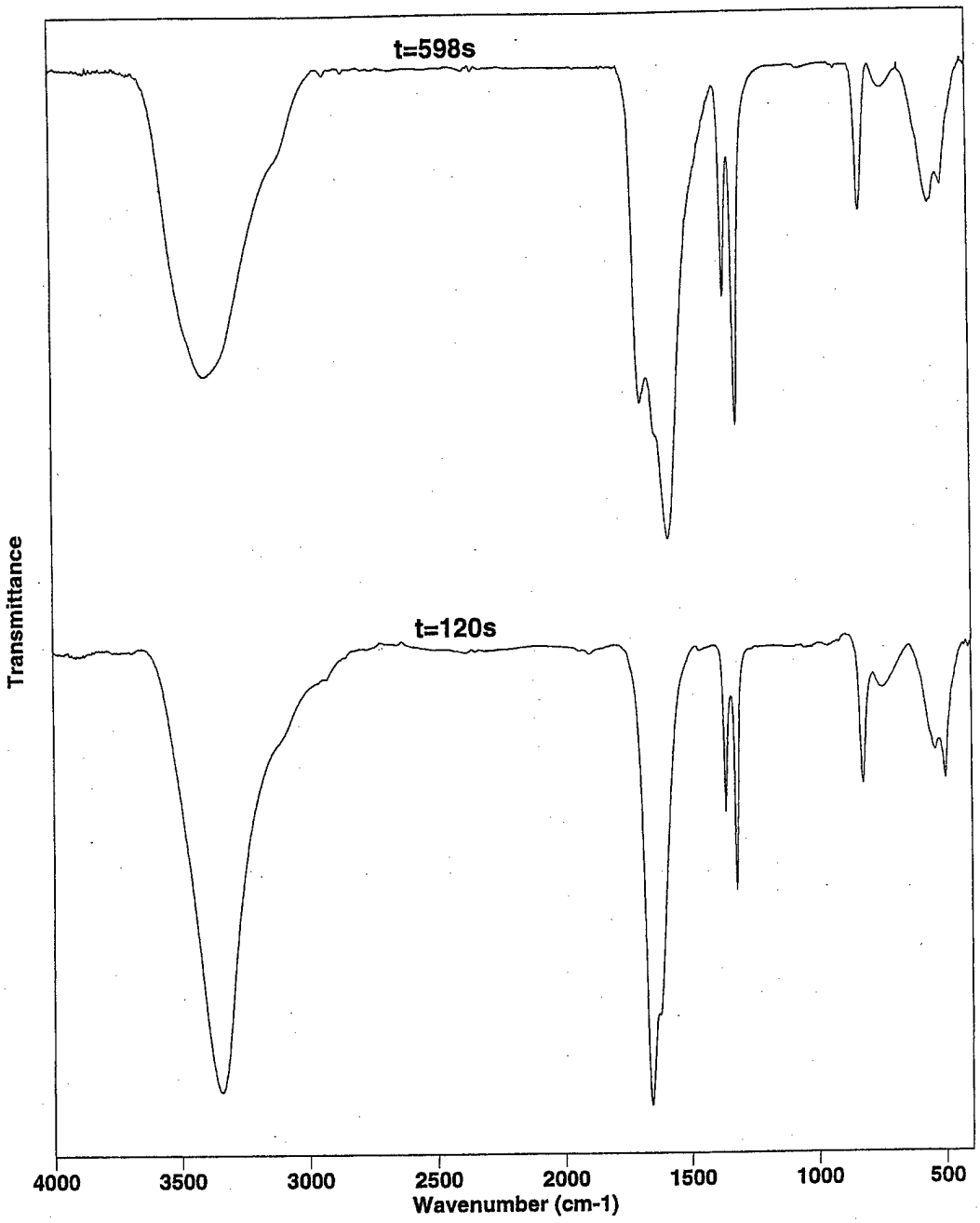

Figure 7 RAIR spectra of the interphase formed at different reaction times.

between the spectra of the interphase obtained at different reaction times or different applied current densities.

It is well known that there are two kinds of iron oxalate compounds: $FeC_2O_4 \cdot 2H_2O$ and $Fe_2(C_2O_4)_3 \cdot 6H_2O$. Figure 9 compares the IR spectra of these two model compounds with the interphase. Among them, the IR spectra of the two model compounds were done by the transmission mode. The two iron oxalate model compounds show different IR spectra. In the spectrum of $Fe_2(C_2O_4)_3 \cdot 6H_2O$, there is a very strong C—O stretch peak ~ 1264 cm^{-1} which is absent in the spectrum of $FeC_2O_4 \cdot 2H_2O$. The O—H stretch peak of $Fe_2(C_2O_4)_3 \cdot 6H_2O$ occurs ~ 3558 cm^{-1}, which is ~ 200 cm^{-1} higher than that of $FeC_2O_4 \cdot 2H_2O$. It is apparent that the IR spectrum of the interphase is very similar to that of

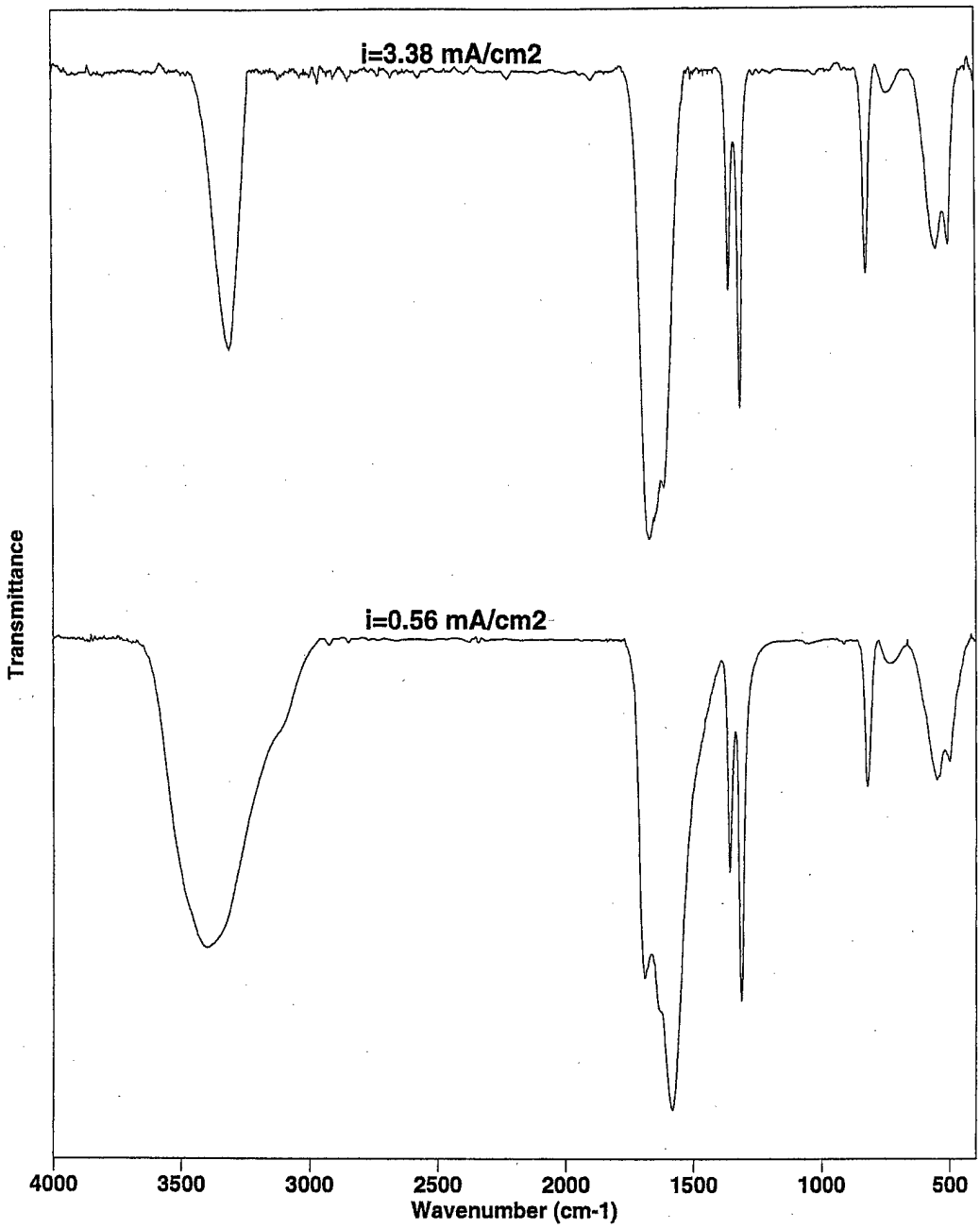

Figure 8 RAIR spectra of the interphase formed at different current densities.

$FeC_2O_4 \cdot 2H_2O$. The main absorption bands for the interphase are assigned as follows:[19–23] peaks at 3403–3294 cm^{-1}, correspond to the O—H stretch. Peaks ~ 1700–1670 cm^{-1}, 1658–1617 cm^{-1}, and 1602–1575 cm^{-1} are characteristic of the C=O stretch. Peaks located at 1364–1359 cm^{-1} and 1321–1314 cm^{-1} are due to C—O stretch. Peaks at 826–821 cm^{-1} come from O—C=O in-plane deformation. Peaks at 747–729 cm^{-1} are perhaps caused by O—C=O in-plane deformation and Fe—O stretch. Peaks at 554–540 cm^{-1} and 506–502 cm^{-1} are due to C—C—O in-plane deformation. Although the IR spectra of the interphase formed by different reaction parameters are basically the same, small differences still exist for some peaks due to polar groups. For example, the shape of the peaks due to O—H and C=O groups vary with reaction conditions. Perhaps these peaks are influenced by the size and/or orientation of the crystals.

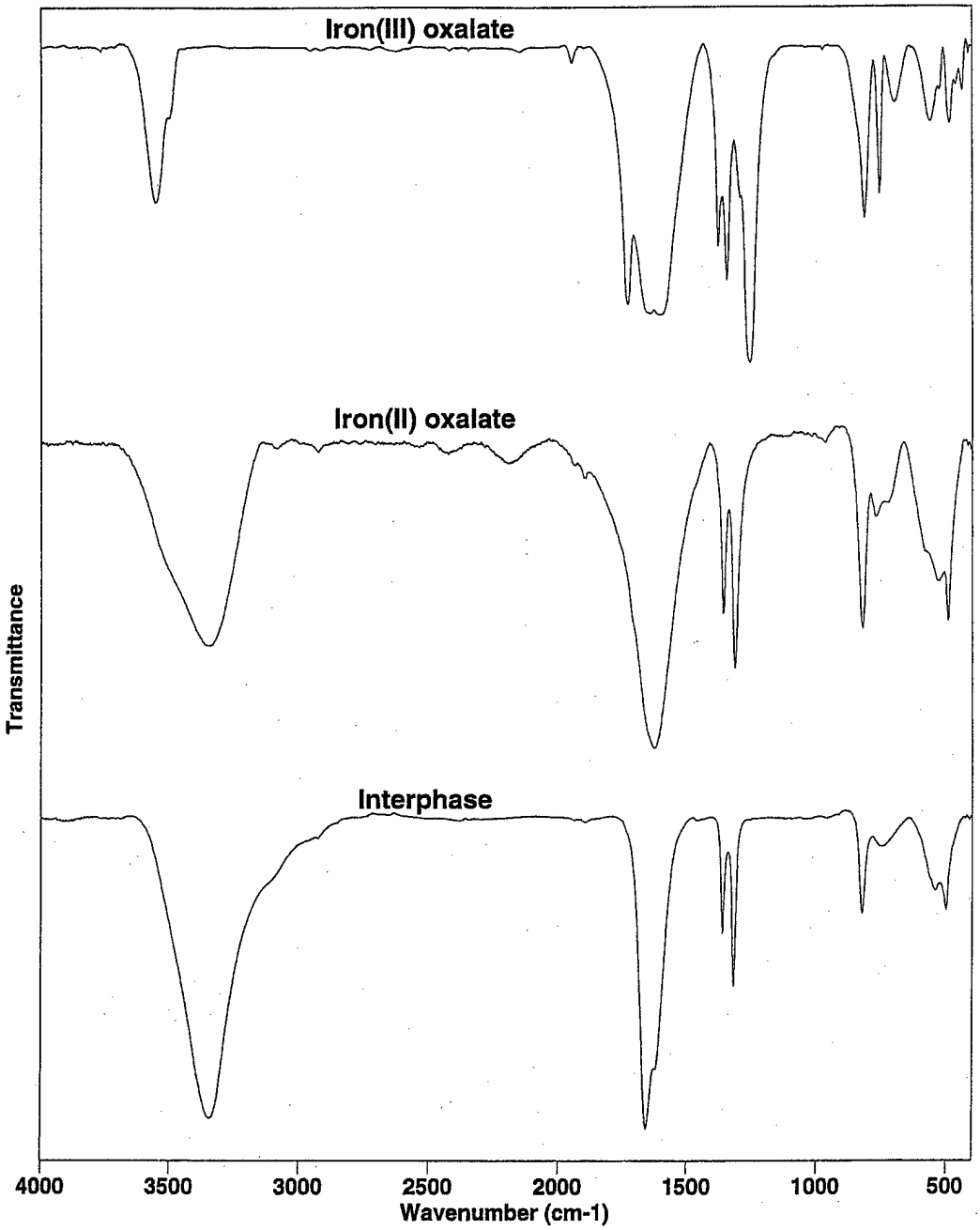

Figure 9 Comparison of IR spectra of the interphase and model compounds.

XPS technique can also be used to distinguish Fe(II) from Fe(III). Figure 10 shows the Fe(2p) spectra of the interphase formed in different pH medium. Spectra of the samples formed in acidic medium are very similar; but, they are different from the spectrum of the sample formed in basic medium. The position of the shake-up satellites in the valley between the $2p_{3/2}$ and $2p_{1/2}$ shows a large difference between the interphase formed in acidic medium and basic medium. For the interphase formed in acidic media the shake up satellites are on the lower binding energy side of the valley, which is characteristic of Fe(II).[24] For the interphase formed in basic medium, the satellite is on the higher energy side of the valley. The anodic passivation of iron in basic medium has been extensively investigated.[16] It is generally believed that passivation is due to the formation

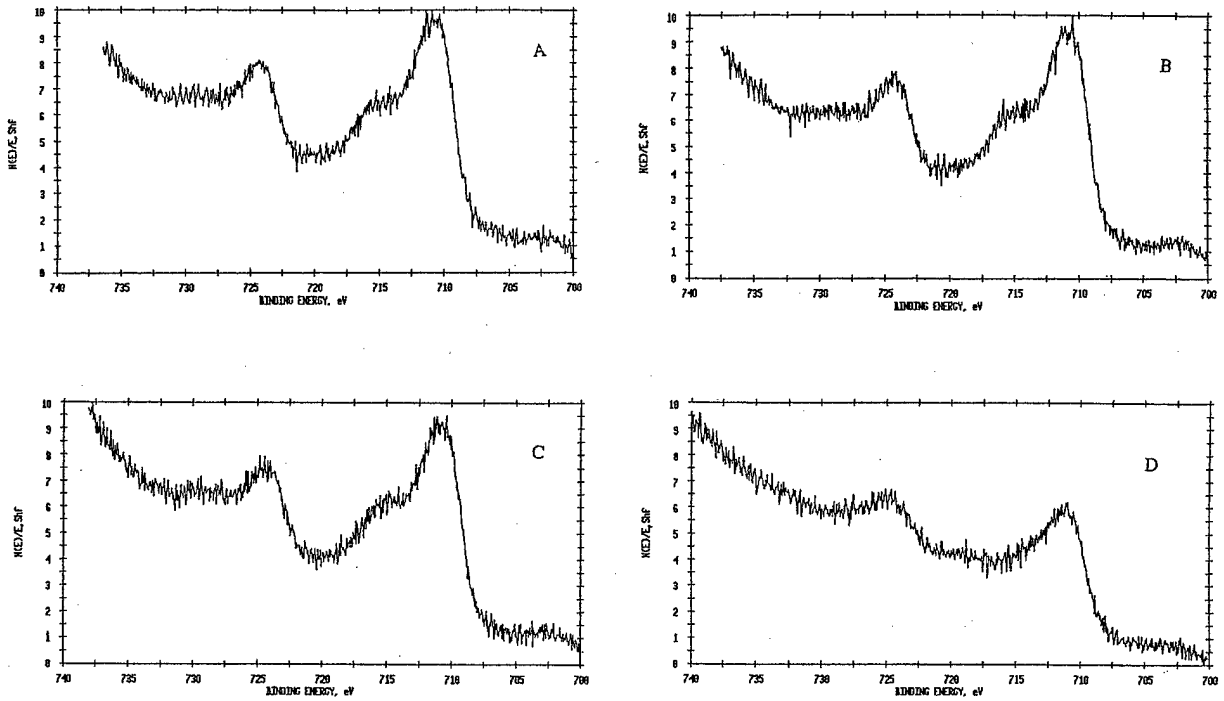

Figure 10 XPS Fe(2p) spectra of the interphase formed in different pH media. (A) pH 14. (B) pH 2.4. (C) pH 4.1. (D) pH 8.4.

of different types of iron oxides. Because pure iron oxide leads to composite XPS signals,[25] it is generally difficult to distinguish the type of oxides from XPS.

A chemical test was also used to verify the valence state of the iron atom in the interphase. No color change was observed after aqueous ammonium thiocyanate (NH_4SCN) solution was placed on the surface of the interphase. This experiment indicates that the interphase was not iron(III) oxalate. In the case of iron(III) oxalate, the color of the solution would turn red.[26]

From the above discussion, it has been shown that the passive interphase formed on steel in aqueous oxalic acid solution is crystalline iron(II) oxalate, $FeC_2O_4 \cdot 2H_2O$. This interphase compound was perhaps produced according to the following two reactions:

$$Fe - 2e \rightarrow Fe^{2+} \quad (1)$$

$$Fe^{2+} + C_2O_4^{2-} + 2H_2O \rightarrow FeC_2O_4 \cdot 2H_2O. \quad (2)$$

The anodic dissolution of iron first produced Fe^{2+} ions; these Fe^{2+} ions then reacted with the oxalate electrolyte to form the insoluble iron(II) oxalate compound, which precipitated on the steel substrate in the form of small crystals. When the substrate was completely covered by the small crystals, passivation of the steel occurred.

The fact that higher applied current density could result in shorter induction time can be easily understood by the above mechanism. More Fe^{2+} ions were produced in unit time at higher

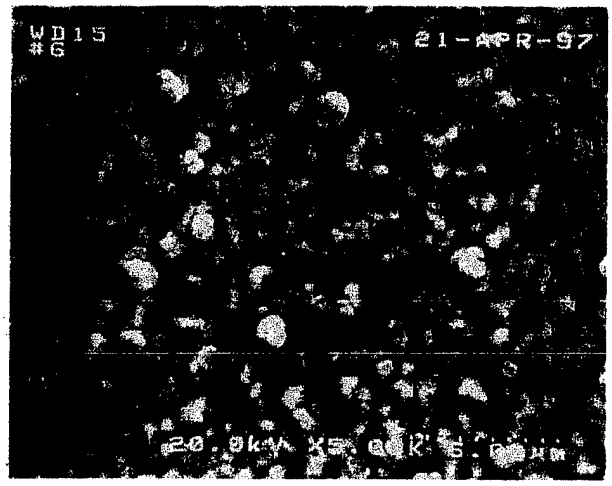

Figure 11 SEM micrograph of the polypyrrole coatings formed at 0.56 mA cm^{-2} in the medium of pH 1.4 for 20 min.

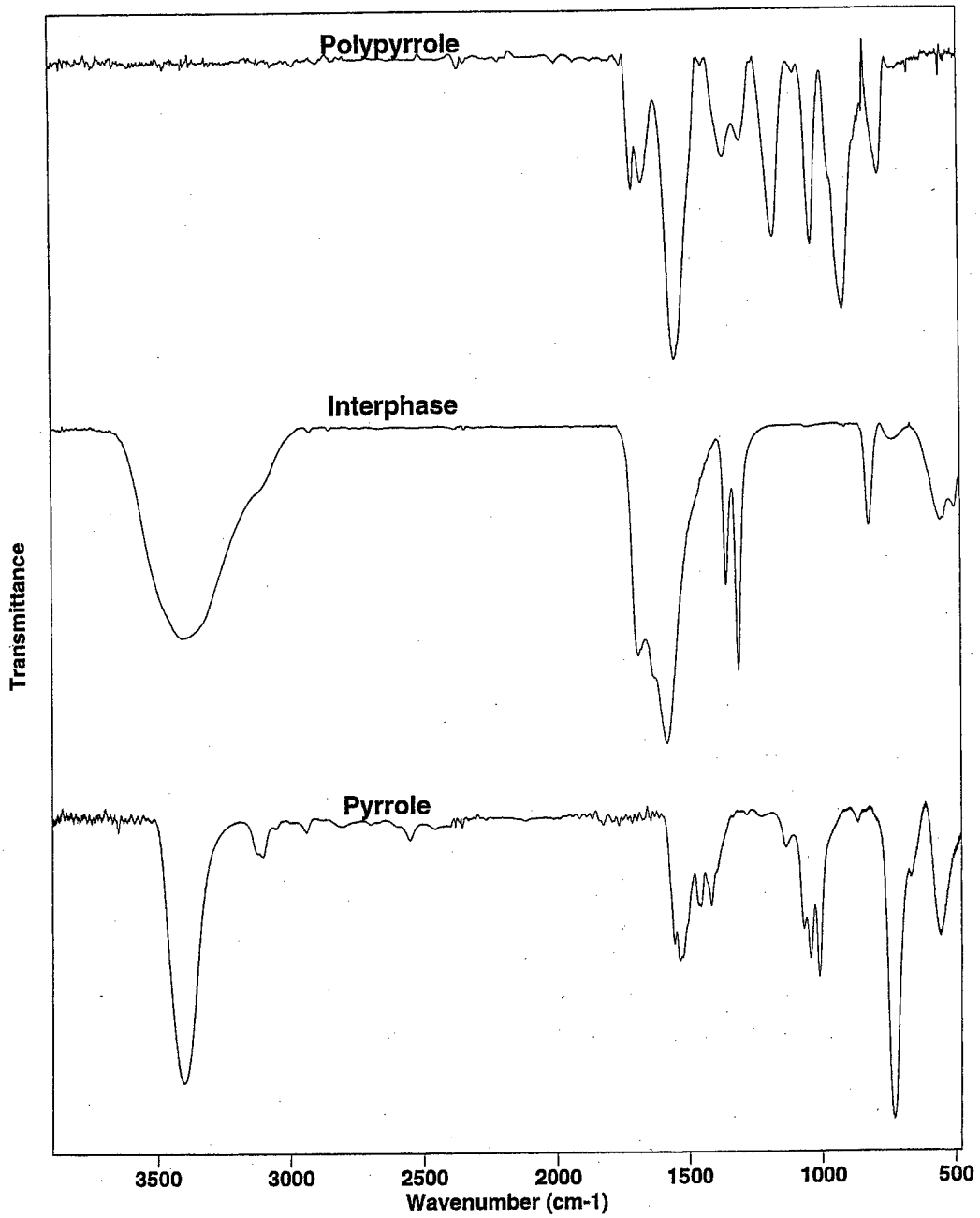

Figure 12 Comparison of IR spectra of pyrrole, interphase, and polypyrrole.

applied current density, with concomitant precipitation of more $FeC_2O_4 \cdot 2H_2O$ crystals on the substrate. Thus, the substrate could be covered by the crystals in a shorter time. Variation of the induction time with the pH of the reaction medium is not well understood so far. Perhaps the pH of the reaction medium can influence the solubility of the $FeC_2O_4 \cdot 2H_2O$ compounds. It is reported that the nearly insoluble $FeC_2O_4 \cdot 2H_2O$ can be changed into soluble oxalato complexes in the presence of excess alkali metal oxalate.[24] This perhaps can be used to explain the variation of the interphase with pH.

Morphology and Composition of Polypyrrole Coatings

Figure 11 shows the SEM micrograph of the polypyrrole coating formed at 0.56 mA cm^{-2} at pH 1.4

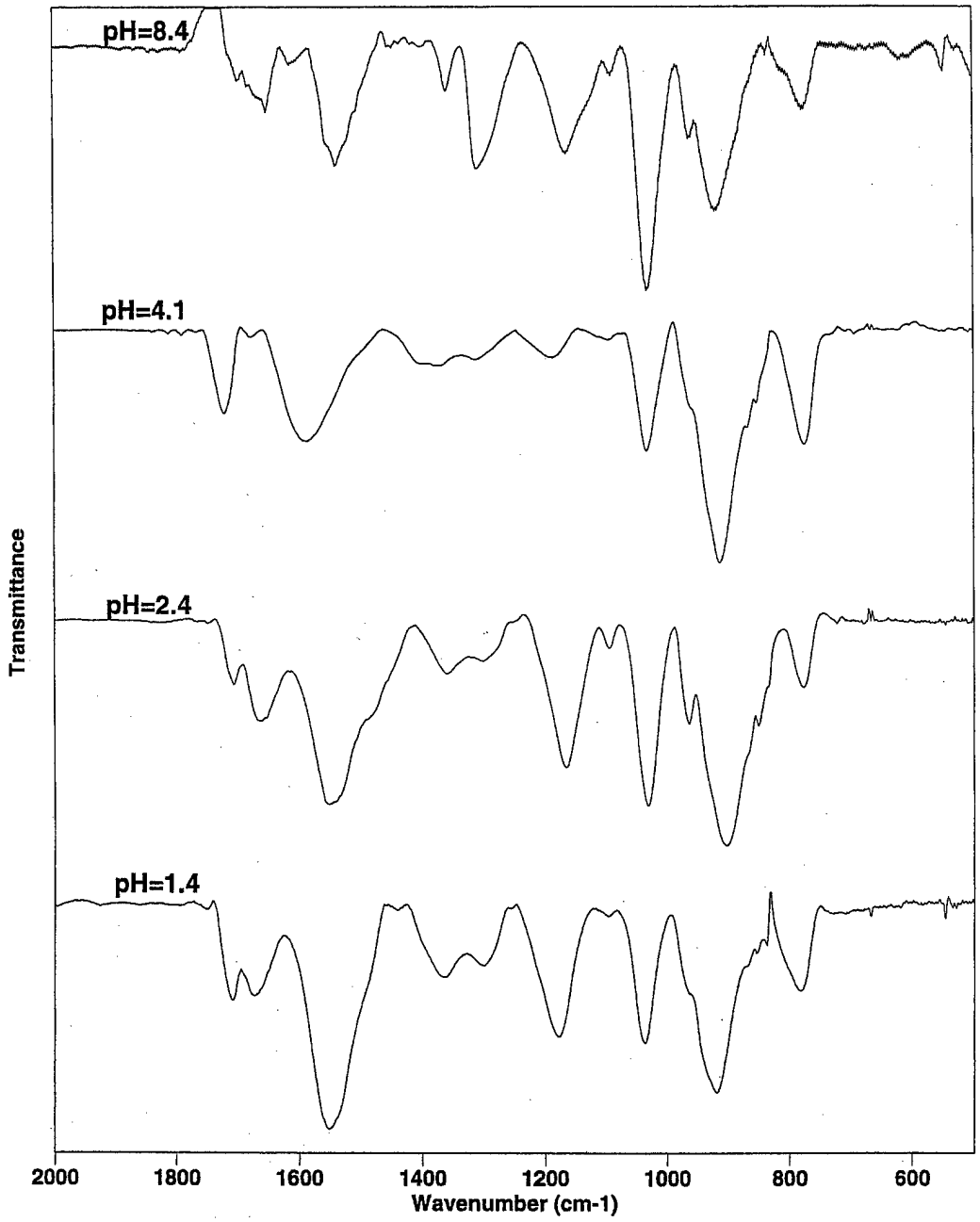

Figure 13 RAIR spectra of pyrrole coatings formed in different pH media.

in 20 min. It can be seen that the interphase was completely covered by the polypyrrole coatings after a 20-min reaction, and the polypyrrole coating obtained had a smooth surface morphology.

Figure 12 shows the IR spectra for pyrrole, the interphase, and the polypyrrole coatings obtained at pH 1.4. IR spectrum of pyrrole was obtained by transmission mode. IR results also show that the coatings formed during the induction period and polymerization period are very different. One feature of Figure 12 is that N—H or O—H stretch peaks are absent in the spectrum of polypyrrole. This phenomenon was also reported by Beck and Michaelis.[10] The detailed mechanism is not clear so far. Another feature of Figure 12 is that the strong C—H peak at 735 cm^{-1} in the pyrrole spectrum disappears in the spectrum of polypyrrole, which is due to oxidative coupling of pyrrole at the 2,5-position.

Figure 13 shows the RAIR spectra of polypyr-

role coatings formed in different pH medium. The coatings prepared in different pH medium show very similar spectra. The main absorption peaks can be assigned as follows:[19,27–30] duplex peaks at 1722–1707 cm^{-1} and 1673–1652 cm^{-1} correspond to the C═O stretch from the oxalate counterion. These duplex peaks may be due to both the carbonyl groups contained in the interphase and those incorporated into the film during doping. The peaks at 1591–1541 cm^{-1} come from the pyrrole ring C═C stretch. The duplet peaks at 1367–1361 cm^{-1} and 1310–1301 cm^{-1} were identified earlier as due to the C—O group. They have, however, become highly broadened. We believe that the broadening of these peaks is due to the fact that these peaks exist both in the interphase and in the oxalate ion-doped polypyrrole films. Peaks located at 1099–1096 cm^{-1} and 1037–1032 cm^{-1} are due to the C—H in-plane deformation of pyrrole units. Peaks at 925–903 cm^{-1} and 783–777 cm^{-1} are caused by C—H out-of-plane deformation of pyrrole units. Results of elemental analysis also confirm the incorporation of oxalate ions into polypyrrole films.[12,14]

CONCLUSIONS

Electrochemical polymerization of pyrrole coatings on steel occurred both in acidic and basic media. In acidic medium, a crystalline passive iron(II) oxalate was formed and, as a result, the electrode potential rose to a positive value of ~ 1.2 V *vs.* SCE. Consequently, electrochemical polymerization of pyrrole occurred on the passivated substrate. The passivation time was found to be dependent on the pH of the reaction medium and the applied current density. At a high pH medium, passivation was instantaneous, and the passive coatings were noncrystalline. Electropolymerization of pyrrole in the acidic medium can only occur after steel is completely covered by the crystalline passive interphase. Size and orientation of the crystalline passive interphase varied with applied current.

The authors thank the Office of Naval Research, ONR's Young Investigator Program, for financial support.

REFERENCES

1. Diaz, A. F.; Kanazawa, K. K. J Chem Soc Chem Commun 1979, 635.
2. Diaz, A. F.; Castillo, J. I. J Chem Soc Chem Commun 1980, 397.
3. Salmon, M.; Diaz, A. F.; Logan, A. J.; Krounbi, M.; Bargon, J. Mol Cryst Liq Cryst 1982, 83, 265.
4. Genies, E. M.; Bidan, G.; Diaz, A. F. J Electrochem Soc 1983, 149, 101.
5. Diaz, A. F.; Castillo, J.; Kanazawa, K. K.; Logan, J. A. J Electroanal Chem 1982, 133, 233.
6. Satoh, M.; Kaneto, K.; Yoshino, K. Synth Metals 1986, 14, 289.
7. Cheung, K. M.; Bloor, D.; Stevens, G. C. Polymer 1988, 29, 1709.
8. Ferreira, C. A.; Aeiyach, S.; Delamar, M.; Lacaze, P. C. J Electroanal Chem 1990, 284, 351.
9. Schirmeisen, M.; Beck, F. J Appl Electrochem 1989, 19, 401.
10. Beck, F.; Michaelis, R. J Coat Technol 1992, 64, 59.
11. Beck, F.; Michaelis, R.; Schloten, F.; Zinger, B. Electrochim Acta 1994, 39, 229.
12. Su, W.; Iroh, J. O. J Appl Polym Sci 1997, 65, 417.
13. Su, W.; Iroh, J. O. J Appl Polym Sci 1997, 65, 617.
14. Su, W.; Iroh, J. O. Synth Metals 1998, 95, 159.
15. Pourbaix, M. Lectures on Electrochemical Corrosion; Plenum: New York, 1973.
16. Jones, D. A. Principles and Prevention of Corrosion; Macmillan Publishing Company: New York, 1992.
17. Asavapiriyanont, S.; Chandler, G. K.; Gunawardena, G. A.; Pletcher, D. J Electroanal Chem 1984, 177, 229.
18. Otero, T. F.; Angulo, E. J Appl Electrochem 1992, 22, 369.
19. Socrates, G. Infrared Characteristic Group Frequencies, 2nd ed.; John Wiley & Sons, Inc.: New York, 1994.
20. Nakamoto, K. Infrared and Raman Spectra of Inorganic and Coordination Compounds, 4th ed.; John Wiley & Sons, Inc.: New York, 1986.
21. Nakamoto, K.; McCarthy, P. J. S J, Spectroscopy and Structure of Metal Chelate Compounds; John Wiley & Sons, Inc.: New York, 1968.
22. Fujita, J.; Nakamoto, K.; Kobayashi, M. J Phys Chem 1957, 61, 1014.
23. Schmelz, M. J.; Miyazawa, T.; Lane, T. J.; Quagliano, J. V. Spectrochim Acta 1957, 9, 51.
24. Watts, J. F. An Introduction to Surface Analysis by Electron Spectroscopy; Oxford University Press: Oxford, 1990.
25. Asami, R.; Hashimoto, K. Corros Sci 1977, 17, 559.
26. Bailar, J. C.; et al., Eds. Comprehensive Inorganic Chemistry; Pergamon Press Ltd.: New York, 1973.
27. Jones, R. A. Ed. Heterocyclic Compounds, Pyrroles, Vol. 48, Part 1; John Wiley & Sons, Inc.: New York, 990.
28. Cheung, K. M.; Bloor, D. Polymer 1988, 29, 1709.
29. Ferreira, C. A.; Aeiyach, S.; Delamar, M.; Lacaze, P. C. J Electoanal Chem 1990, 284, 351.
30. Novak, P.; Rasch, B.; Wielstich, W. J Electrochem Soc 1991, 138, 3300.

Pergamon

Electrochimica Acta, Vol. 42, No. 17, pp. 2685–2694, 1997

Printed in Great Britain
PII: S0013-4686(97)00012-1
0013–4686/97 $17.00 + 0.00

Formation of polypyrrole coatings on stainless steel in aqueous benzene sulfonate solution

Wencheng Su and Jude O. Iroh*

Department of Materials Science and Engineering, University of Cincinnati, Cincinnati, OH 45221-0012, U.S.A.

(Received 8 February 1996)

Abstract—Polypyrrole coatings with varying surface morphology have been formed on a stainless steel working electrode using benzene sulfonic acid sodium salt as the electrolyte. The morphology of the coatings varied with the current density. The amount of polypyrrole formed during electropolymerization increased with current density and monomer concentration, but was unaffected by increased electrolyte concentration. The electropolymerization potential of pyrrole increased with increased current density but the current efficiency remained relatively unchanged at 99–105%. The rate of electropolymerization of pyrrole onto stainless steel increased slightly with increased monomer concentration. The electropolymerization potential decreased with increased monomer and electrolyte concentration. © 1997 Elsevier Science Ltd

Key words: Electropolymerization, polypyrrole, benzene sulfonate, coatings current density, morphology.

INTRODUCTION

The hexavalent zinc chromate process for coating steel is hazardous and environmentally unsafe and the resulting protective coatings cannot be extended over the entire substrate [1]. This drawback can be overcome by forming oxidation-resistant polymeric coatings onto the substrate by an environmentally compatible aqueous electropolymerization. Electrochemical polymerization can play an important role in many technologies, especially in surface modification and materials processing. It is becoming increasingly attractive for preparing a range of new materials and novel microstructures [1]. This technique has been used for a variety of purposes ranging from the formation of polymers in solution [2, 3] to modification of graphite fibers [4–7] and formation of *in situ* matrix composites [8–11]. It is presently being proposed as a technique for forming new materials and novel microstructures [1]. The formation of insulating and highly crosslinked polymer coatings on steel by partial electropolymerization followed by annealing has been demonstrated [12]. Mengoli *et al.* [13] reported the electropolymerization of *o*-allyl phenol and allyl amine on steel. Their coatings showed very good corrosion resistance. One of the approaches to protecting steel against oxidation and corrosion is the application of polymeric coatings that are capable of inhibiting oxidation. Polymer coatings derived from allyl aromatic amines were shown to be very effective inhibitors for oxidation of iron [14]. Highly stable and corrosion resistant aniline–sulfur copolymer coatings have been formed on steel by electrocopolymerization of aniline and ammonium sulfide [15]. Both insulating and conductive polymer coatings have been electropolymerized onto a variety of substrates [16–20] with excellent throwing power (uniform coating of irregular and complex shapes). Berlouis and Schiffrin [21] showed that aqueous electropolymerization of pyrrole resulted in self-limiting polypyrrole film growth on steel. They noticed that sharp passivation of polymerization of pyrrole occured at about 0.09 V *vs* SCE. They suggested that the self-limiting polypyrrole film growth was due to the breakdown of conjugation [21]. It was further reported that the occurrence of passivation (increasing film resistance and electrical insulation) during electropolymerization of pyrrole and the concomitant reduction in the thickness of the polypyrrole film can be controlled by varying the pH of the reaction medium [21]. The formation of insulative polypyrrole coatings

*Author to whom correspondence should be addressed.

may offer another route to corrosion/oxidation prevention.

The kinetics and mechanism of electropolymerization of pyrrole has been investigated by various workers [22–26]. Saveant *et al.* investigated the mechanism of electropolymerization of pyrrole on platinum. They used double potential step chronoamperometry to study the early steps in electrochemical polymerization of substituted pyrrole. It was shown that radical cations coupling rather than neutral radicals coupling occurred during the electropolymerization of pyrrole. The dependence of the rate of potentiostatic polymerization of pyrrole on the reaction variables such as initial pyrrole concentration and electrolyte concentration was determined by Otero and coworkers [23, 24]. The dependence of the rate of formation of polypyrrole (on platinum electrode) on perchlorate (electrolyte) concentration and pyrrole concentration was found to be 0.5, respectively, in acetonitrile. However, the order of the reaction with respect to perchlorate increased to 0.8 in water. Iroh and Wood also studied the efficiency and kinetics of aqueous potentiostatic electropolymerization of pyrrole on carbon fibers [25, 26]. It was shown that the rate of electropolymerization of pyrrole increased with pyrrole concentration, toluene sulfonate concentration and applied voltage raised to a power of 0.8–1.0, 0.8 and 0.9–1.2, respectively [25], *ie* $Rp \propto [M]^{0.8-1.0}[SO_3Ph]^{0.8}[EPa]^{0.9-1.2}$. They showed that the efficiency of potentiostatic polymerization of pyrrole increased with pyrrole concentration and decreased with applied voltage [26].

In this paper we report our findings on the formation of polypyrrole coatings onto stainless steel by electrochemical polymerization. The kinetics of electropolymerization of pyrrole on stainless steel and the effect of reaction variables on electropolymerization potential is also reported. In a future paper, we will discuss the corrosion performance of stainless steel coated with polypyrrole. The latter will be compared with the corrosion performance of polypyrrole-coated low carbon steel.

EXPERIMENTAL

Pyrrole (98%) and benzene sulfonic acid sodium salt purchased from Aldrich Chemical Company, Inc. Tetrachloroethylene and methanol were also purchased from Aldrich Chemical Company. The reagents were dissolved in deionized water prepared in our department.

The working electrode is an 0.46 mm thick 304 stainless steel panel (2B finish) purchased from Copper Brass Sales Inc. The working electrode was degreased with tetrachloroethylene for *ca.* 60 min prior to electrochemical polymerization. The counterelectrodes comprised of two titanium alloy plates. Saturated Calomel electrode (SCE), manufactured by Corning Company, was used as reference electrode. Galvanostat electropolymerization of pyrrole was performed by an EG&G Princeton Applied Research Potentiostat/Galvanostat Model 273A.

Electropolymerization of pyrrole was carried out in a one-compartment polypropylene cell. The current densities used in this study ranged from 1.13 to 7.88 mA cm^{-2}. The electrolyte concentration was varied from 0.05 to 0.4 M, while pyrrole concentration was varied from 0.1 to 0.8 M. Electropolymerization time was varied between 300 and 1800 s.

The coated substrate was rinsed with methanol and dried at 65°C in a vacuum oven to constant weight. The weight of the coatings was determined as the difference between the coated and noncoated steel (control).

Elemental analysis of the coatings extracted from coated steel was performed by the Galbraith Laboratories, Inc. The morphology of the coated and noncoated substrate was examined by scanning electron microscopy (SEM). The samples were shadowed with carbon to enhance their conductivity.

RESULTS AND DISCUSSION

Effect of current density

The concentration of pyrrole and benzene sulfonate was kept constant at 0.25 and 0.1 M, respectively. The current density was varied from 1.13 to 7.88 mA cm^{-2}. The current density has a significant effect on the electropolymerization potential of pyrrole, E_p. The electropolymerization potential of pyrrole, increased with the current density, C_d (Fig. 1). The relationship between E_p and C_d is given by:

$$E_p = 0.61 + 0.097[C_d]. \quad (1)$$

The slope of the E_p vs i plot is the measure of the

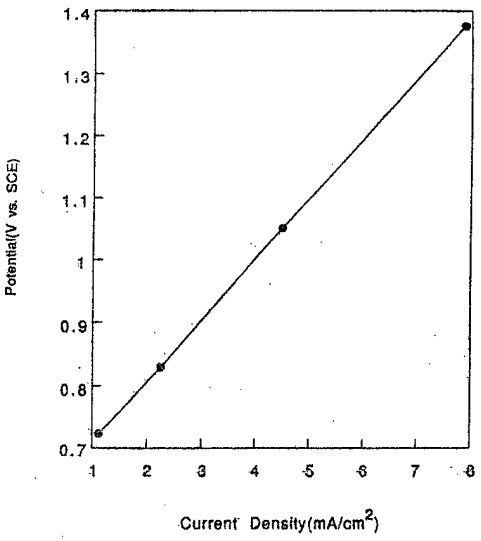

Fig. 1. Variation of electropolymerization potential with current density.

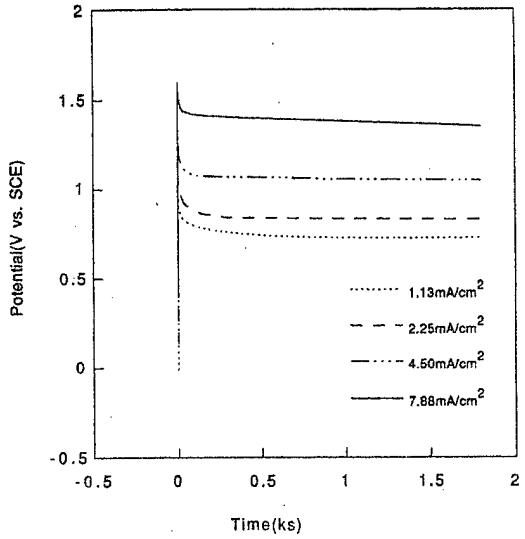

Fig. 2. Potential-time curve for electropolymerization of pyrrole on stainless steel as a function of current density and time, showing no induction time.

resistance of working electrode. Increasing the current density from 10 to 70 mA cm^{-2} (600% increase) resulted in an increase in the electropolymerization potential from 0.72 to 1.38 V (90% increase; Fig. 2). There was no induction time for electropolymerization of pyrrole on stainless steel. This maybe is due to the presence of passive Cr_2O_3 film on the steel surface [27] which prevented the dissolution of steel.

Initially, the potential difference between the reference and working electrodes steps to a positive value ($E_p \geqslant 1.5$ V) and then drops to a steady lower value $E_p \geqslant 0.6$ V (polymerization potential), without any induction time (Fig. 2). The rate of formation of polypyrrole increased proportionately by 650% (from 0.61 to 4.52 mg cm^{-2} ks^{-1}) as the current density was increased from 1.13 to 7.88 mA cm^{-2} (600% increase), however, the current efficiency remained unchanged at 99–105% [Table 1(b)], indicating that the efficiency of electropolymerization was not dependent on the current density. Table 1(b) shows the per cent current efficiency determined by using the method established by Schirmeisen and Beck [28]. Increasing the current density from 1.13 to 7.88 mA cm^{-2} (~600% increase) resulted in no significant change in the current efficiency.

Table 1(b).
Dependence of current efficiency for electrochemical polymerization of pyrrole on the current density; ([Py] = 0.25 M, [BSASS] = 0.1 M, degree of insertion, $y = 0.38$)

Current density (mA cm^{-2})	Current efficiency (%)
1.13	99
2.25	99
4.50	102
7.88	105

The amount of polypyrrole coatings formed at different current density was determined as a function of electropolymerization time (Fig. 3). As shown in Fig. 3, the weight of polypyrrole coatings formed on stainless steel is proportional to the current density and electropolymerization time. The total charge passed during the reaction increases with both the applied current and time for which the current was passed. Since the formation of polypyrrole occurs by electron transfer, which is dependent on the charge passed (current × time), increasing the latter should lead to a proportionate increase in the amount of polypyrrole formed. From the slope of the weight of coating–time curves, the rate electropolymerization of pyrrole was determined and tabulated as a function of current density (Table 1). The rate of formation of polypyrrole increased with current density. The order of the rate of electropolymerization of pyrrole with respect to the current density was determined from the slope of the Ln rate vs C_d plot (Fig. 4) to be 1.04 [equation (2)]:

$$R_p \propto [C_d]^{1.04}. \quad (2)$$

Effect of monomer concentration

The concentration of benzene sulfonic acid sodium salt and current density were kept constant at 0.1 M and 2.25 mA cm^{-2}, respectively. The concentration of pyrrole was varied from 0.05 to 0.8 M. The electropolymerization potential of pyrrole decreased with increased pyrrole concentration (Fig. 5). The chromate oxide, Cr_2O_3, film present on the stain-

Table 1(a).
Dependence of the rate electropolymerization of pyrrole onto stainless steel on the current density

Applied current (mA)	Current density (mA cm^{-2})	Electropolymerization potential (V *vs* SCE)	Rate (mg cm^{-2} ks^{-1})
10	1.13	0.72	0.61
20	2.25	0.83	1.21
40	4.50	1.05	2.51
70	7.88	1.38	4.52

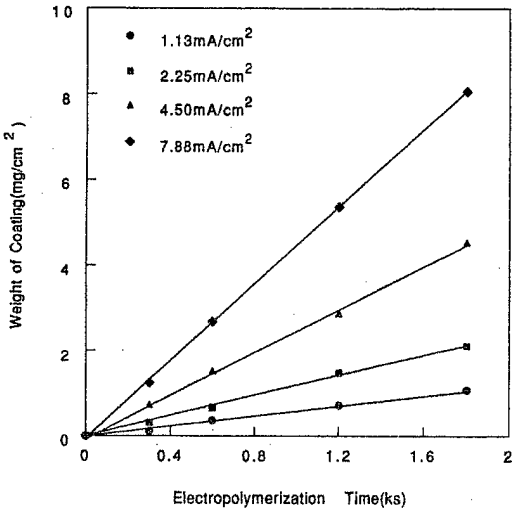

Fig. 3. Dependence of the weight of polypyrrole coatings formed onto stainless steel on the current density and reaction time.

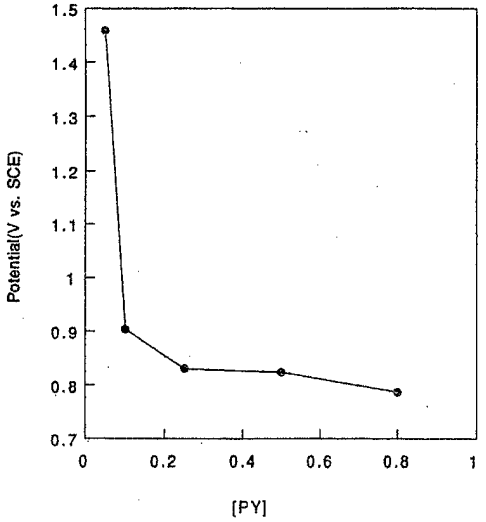

Fig. 5(a). Variation of electropolymerization potential with initial pyrrole concentration.

less steel surface (passive layer) is more insulative than the chromate oxide–polypyrrole–benzene sulfonate, Cr_2O_3–PPy–O_3Ph, composite interlayer formed during electropolymerization. A decrease in the resistance of the electrode will occur as the more conductive Cr_2O_3–PPy–O_3Ph interlayer is formed. Increasing pyrrole concentration from 0.05 to 0.1 M (100% increase) resulted in a significant decrease in the polymerization potential from 1.46 to 0.90 V (38% decrease). However, further increase in pyrrole concentration from 0.1 to 0.8 M (700% increase) resulted in only a slight decrease in the polymerization potential from 0.9 to 0.79 V (12% decrease; Fig. 5). The amount of polypyrrole coatings formed on stainless steel increased slightly with monomer concentration (Fig. 6). The increment in the amount of polypyrrole formed due to increased pyrrole concentration was significantly lower than that obtained with equivalent increase in the current density. For example, doubling the current density from 1.13 to 2.25 mA cm^{-2} resulted in the doubling of the weight of polypyrrole coatings formed from 3.2 to 5.8 mg after 10 min of reaction (Fig. 3), however, doubling the monomer concentration from 0.1 to 0.2 M resulted in a slight increase in the amount of polypyrrole formed from 11.7 to 13.1 mg [12% increase (Fig. 6)] after 20 min of reaction.

The rate of electropolymerization of pyrrole was determined from the slope of the weight of coatings vs time plots as a function of time and initial pyrrole concentration. It increased with initial pyrrole concentration (Table 2). Only a slight dependence of

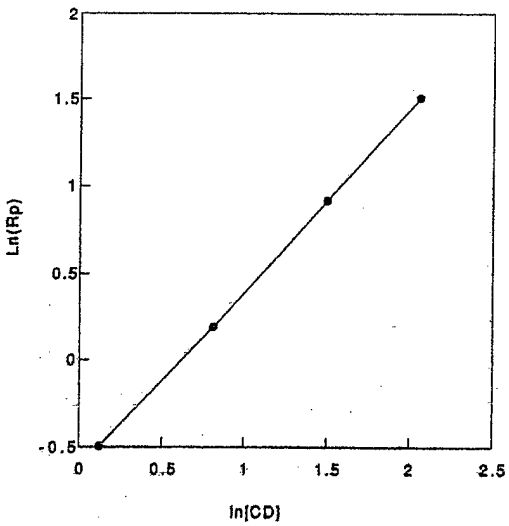

Fig. 4. Determination of the current density exponent.

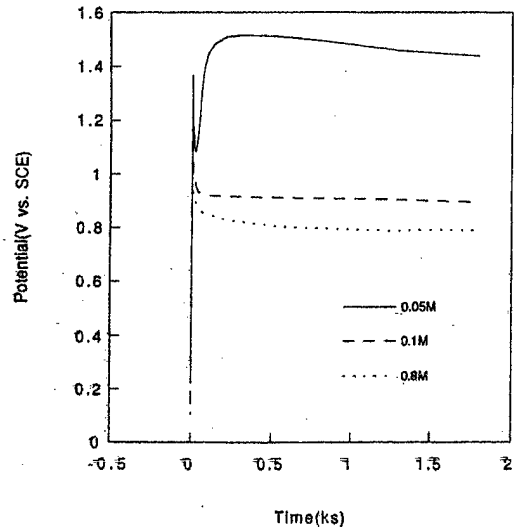

Fig. 5(b). Potential-time curve for electropolymerization of pyrrole on stainless steel as a function of pyrrole concentration and time, showing no induction time.

Table 2.
Dependence of the rate of electropolymerization of pyrrole onto stainless steel on the initial pyrrole concentration

[Py] (M)	[BSASS] (M)	Electropolymerization potential (V *vs* SCE)	Electropolymerization rate (mg cm^{-2} ks $-$ 1)
0.05	0.1	1.46	0.97
0.1	0.1	0.90	1.11
0.25	0.1	0.83	1.21
0.5	0.1	0.82	1.32
0.8	0.1	0.79	1.38

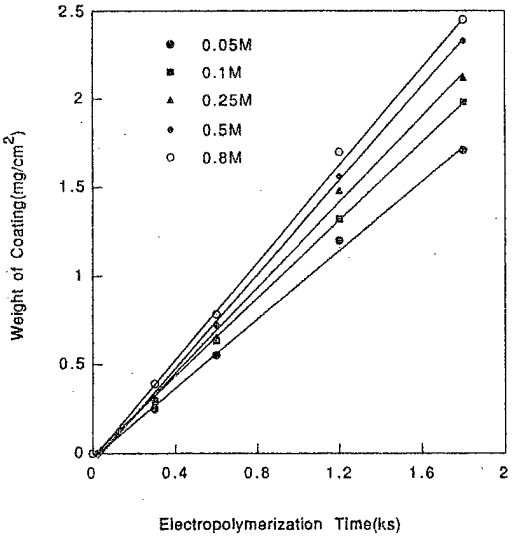

Fig. 6. Dependence of the weight of polypyrrole coatings formed onto stainless steel on the initial pyrrole concentration and reaction time.

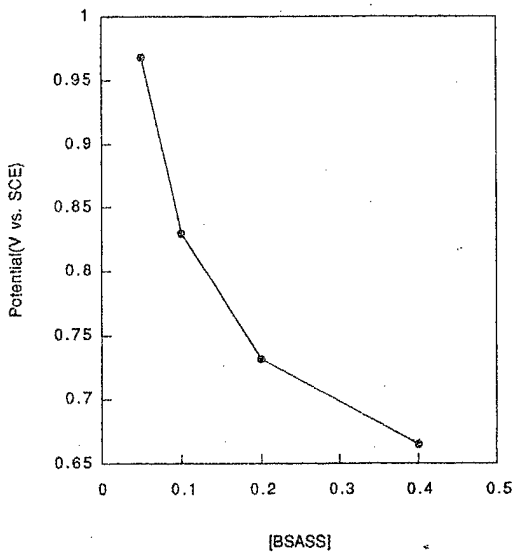

Fig. 8(a). Variation of electropolymerization potential with electrolyte concentration.

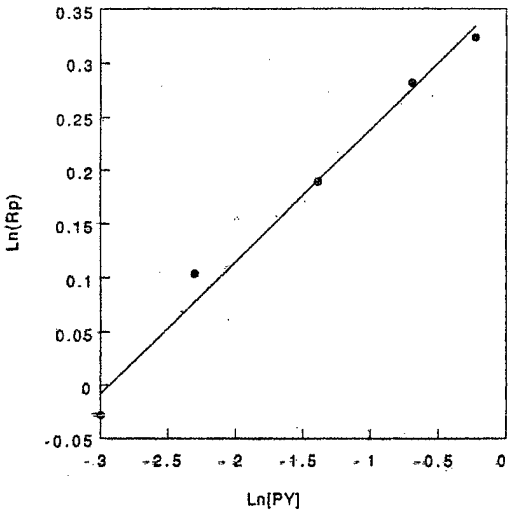

Fig. 7. Determination of the initial pyrrole concentration exponent.

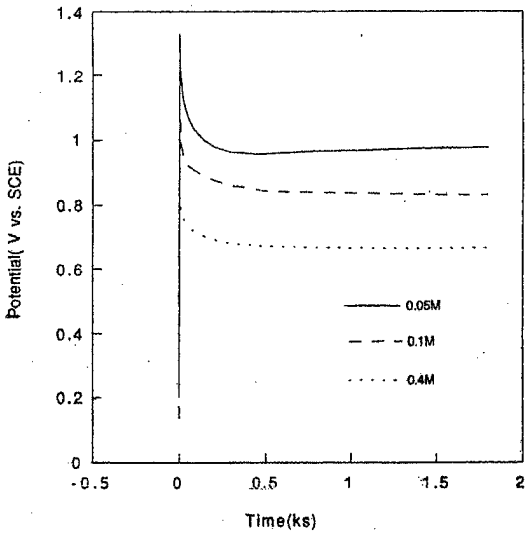

Fig. 8(b). Potential-time curve for electropolymerization of pyrrole on stainless steel as a function of electrolyte concentration and time, showing no induction time.

Table 3(a).
Dependence of the rate of electropolymerization of pyrrole on the concentration of benzene sulfonic acid sodium salt

[Py] (M)	[BSASS] (M)	Electropolymerization potential (V *vs* SCE)	Electropolymerization rate (mg cm^{-2} ks^{-1})
0.25	0.05	0.97	1.17
0.25	0.1	0.83	1.21
0.25	0.2	0.73	1.13
0.25	0.4	0.66	1.17

the rate of polypyrrole formation on initial pyrrole concentration of 0.12 is observed [equation (3)] (Fig. 7). The 0.12 dependence of the rate on pyrrole concentration is much lower than that reported for potentiostatic electropolymerization of pyrrole [23–26].

$$R_p \propto [Py]^{0.12}. \quad (3)$$

Effect of electrolyte concentration

The concentration of pyrrole was kept constant at 0.25 M and the current density was maintained at 2.25 mA cm^{-2}. The concentration of the electrolyte was varied from 0.05 to 0.4 M. The pH of the electrolyte was monitored as a function of electrolyte concentration. Increasing the electrolyte concentration from 0.05 to 0.4 M (700% increase), resulted in only a slight increase in the pH from 9.68 ($[H^+] \sim 2.09 \times 10^{-10}$ M) to 9.84 ($[H^+] \sim 1.45 \times 10^{-10}$ M) (~31% increase). The electropolymerization potential of pyrrole decreased exponentially from 0.97 to 0.66 V vs SCE (32% decrease) as the electrolyte concentration was increased from 0.05 to 0.4 M [700% increase; Figs 8(a), 8(b) and Table 3(a)]. The decrease in the polymerization potential (32%) may be attributed to the increase in the pH of the reaction medium (31%) as the electrolyte concentration was increased. Increasing the electrolyte concentration consequently increases the conductivity of the medium.

The amount of polypyrrole formed and the rate of galvanostatic electropolymerization of pyrrole on stainless steel was independent of the electrolyte concentration (Fig. 9 and Table 3) implying a zero order of dependence. The dependence of rate of polymerization on electrolyte concentration has been determined to range from 0.5 to 0.8 [23–26]. The disperity in these results may be traced to the nature of the counterions, the interaction of the counterion with the film and the technique of electropolymerization. Most of the reports that gave a higher dependence of rate on electrolyte concentration [23–26] were obtained from constant potential electropolymerization, where the current may vary with time. Higher electrolyte concentrations, [BSASS] $\geq$ 1.0 M, may show higher dependence of rate on the latter. Other factors of importance include the nature of the working electrode and the spacing of the electrodes.

Table 3(b).
Dependence of pH of the reaction medium on electrolyte concentration ([Py] = 0.25 M)

Electrolyte concentration (mol l^{-1})	pH of reaction medium
0.05	9.68
0.1	9.71
0.2	9.80
0.4	9.84

Table 4.
Elemental composition of the coatings

Elements	Composition (%)
C	57.88
H	4.11
N	11.16
S	9.83

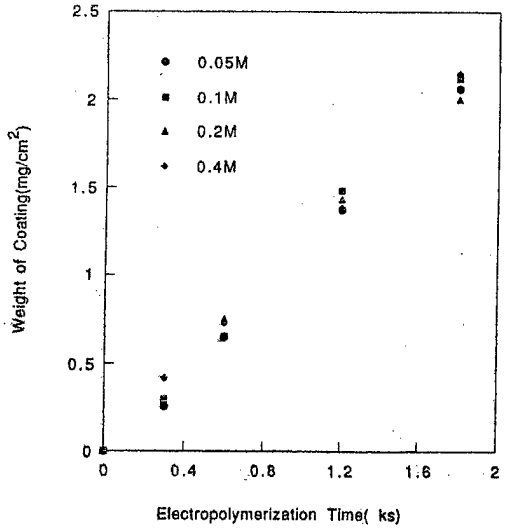

Fig. 9. Dependence of the weight of polypyrrole coatings formed onto stainless steel on electrolyte concentration and reaction time.

pyrrole concentration, [Py] and the current density, Cd, can be expressed as:

$$R_p \propto [M]^{0.12}[Cd]^{1.04} \quad (4)$$

Composition and morphology of the coatings

The elemental composition of the polypyrrole benzene sulfonate coatings formed on stainless steel is shown in Table 4. Elemental analysis shows the presence of sulfur in the coatings and indicates that the sulfonate counterion is incorporated into the polypyrrole film. The mole ratio of polypyrrole to the sulfonate ion was determined to be ~3:1.

The SEM pictures for the polypyrrole coatings

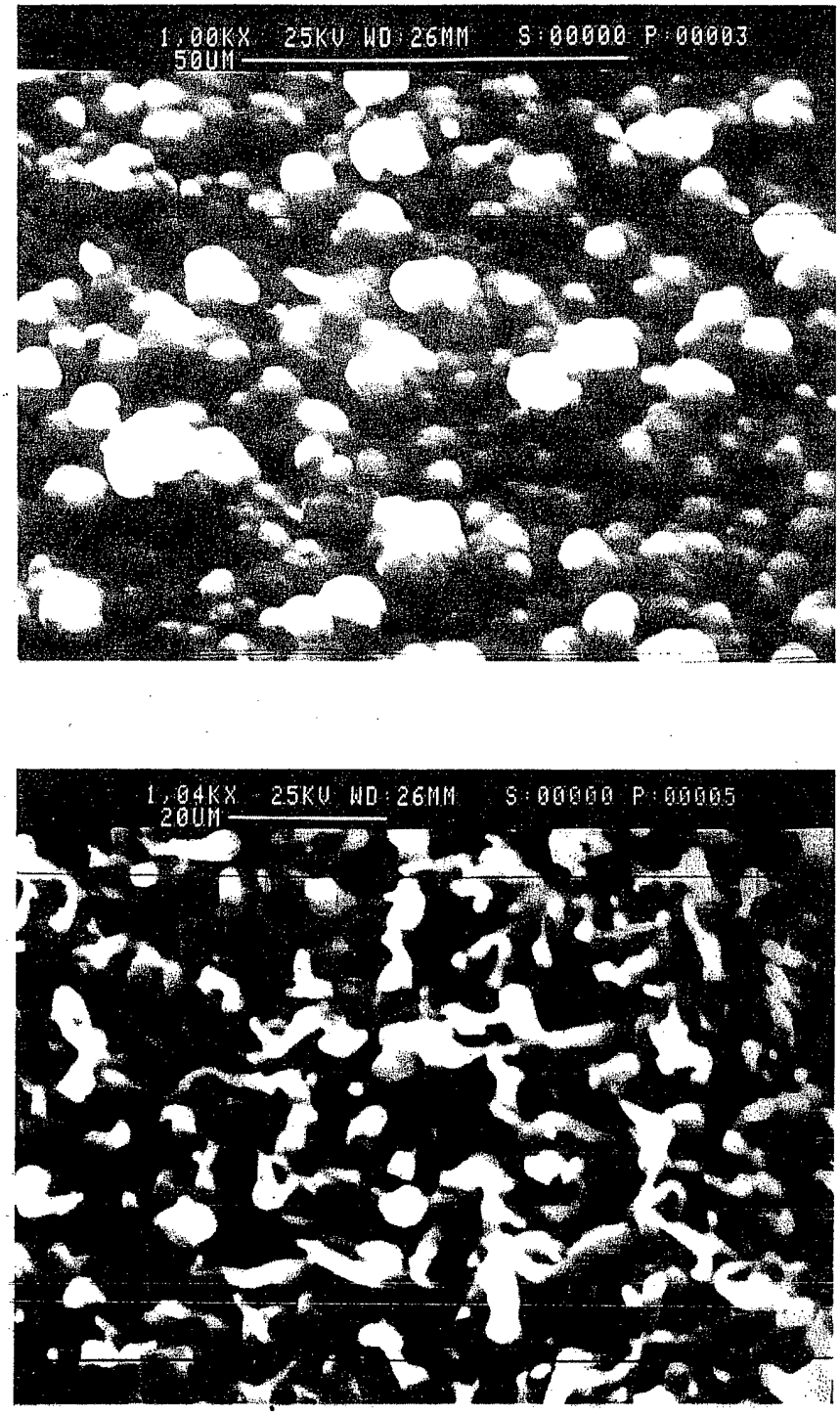

Fig. 10. SEM micrograph of stainless steel coated with polypyrrole formed by using low current density (top) and high current density (bottom).

formed on stainless steel by using different reaction parameters is shown in Figs 10–12. Overall, the surface of polypyrrole coatings is grainy and porous. The porosity of the coatings varied with the current density, monomer and electrolyte concentration, respectively. The coatings formed by passing a current density of 20 mA cm^{-2} ([M] = 0.25 M, [BSASS] = 0.1 M) was smoother and more compact than the coatings formed by using 70 mA cm^{-2} ([M] = 0.25 M. [BSASS] = 0.1 M), which is porous and leafoidal (Fig. 10). The increased porosity of the coatings formed by using a higher current density may be traced to increased deposition rate. The effect of varying monomer concentration on the morphology of the coatings is shown in Fig. 11. The polypyrrole coatings formed by using low pyrrole concentration, [M] = 0.05 M (Cd = 20 mA cm^{-2}, [BSASS] = 0.1 M), is compact and dense while the

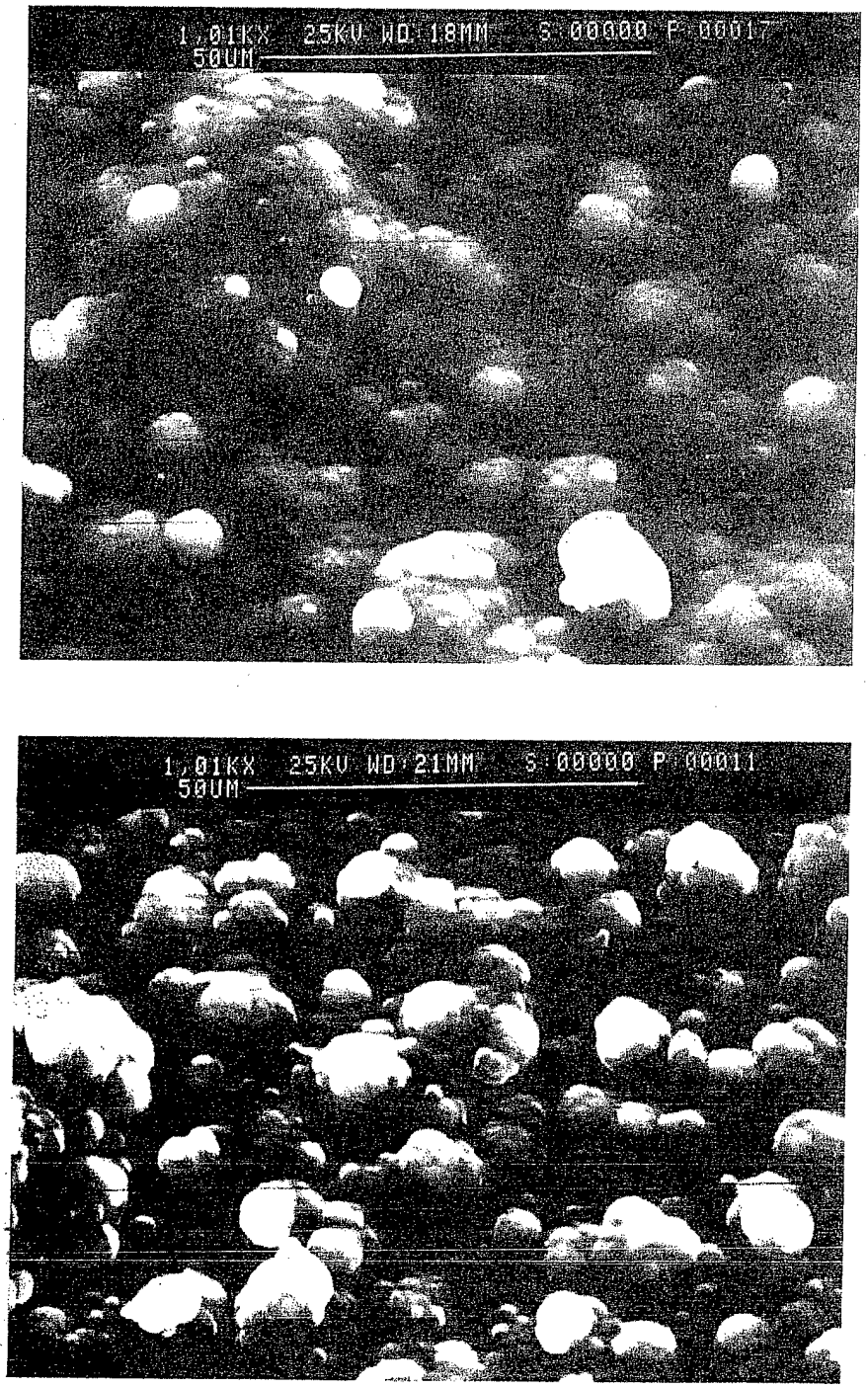

Fig. 11. SEM micrograph of stainless steel coated with polypyrrole formed by using low pyrrole concentration (top) and high pyrrole concentration (bottom).

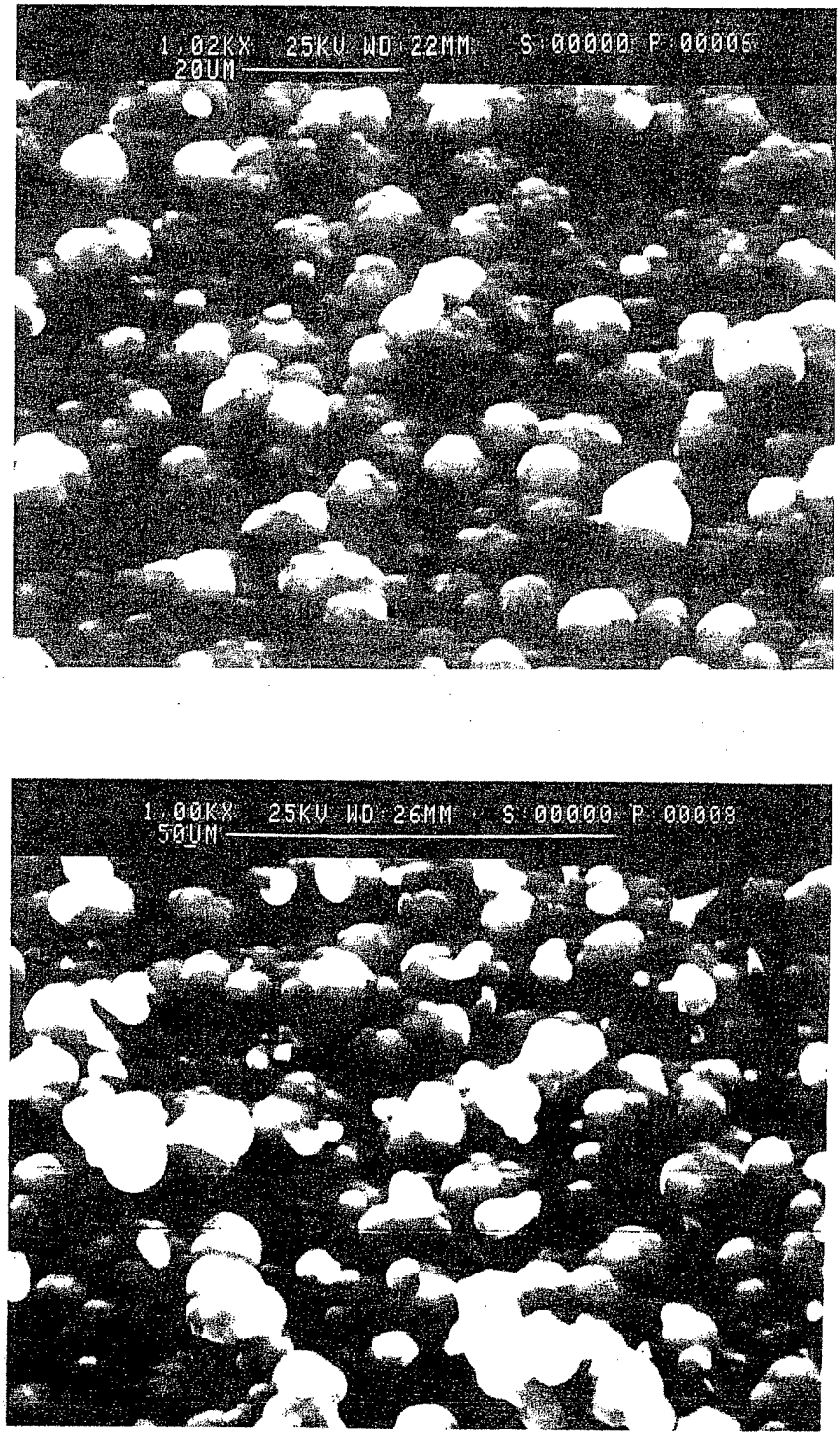

Fig. 12. SEM micrograph of stainless steel coated with polypyrrole formed by using low electrolyte concentration (top) and high electrolyte concentration (bottom).

polypyrrole coatings formed by using higher pyrrole concentration, [M] = 0.5 M (C_d = 20 mA cm^{-2}, [BSASS] = 0.1 M), is more porous and grainy. Figure 12 shows the dependence of the morphology of polypyrrole coatings on the electrolyte concentration. Smoother and compact polypyrrole coatings were formed at lower electrolyte concentration (C_d = 20 mA cm^{-2}, [M] = 0.25 M, [BSASS] = 0.05 M). Using a higher electrolyte concentration (20 mA cm^{-2}, [M] = 0.25 M, [BSASS] = 0.5 M), a less dense and porous coating is formed. It is expected that the dependence of the morphology of the coatings on the current density would be reflected in the properties of the coatings.

CONCLUSIONS

Polypeptide coatings has been formed on stainless steel by an aqueous constant current electrochemical process. The electropolymerization potential of pyrrole increased with the current density and decreased exponentially with initial pyrrole concentration and benzene sulfonate concentration. The rate of electropolymerization of pyrrole increased with the current density and slightly with initial pyrrole concentration. It, however, was unaffected by benzene sulfonate concentration. The current efficiency for galvanostatic electropolymerization of pyrrole was independent of the current density.

ACKNOWLEDGEMENTS

The authors wish to thank the Office of Naval Research, ONR's Young Investigator Program for the financial support.

REFERENCES

1. P. C. Searson and T. P. Moffat, in *Critical Review in Surface Chemistry*, (Edited by P. Sherwood) CRC Press, Boca Raton, Florida, U.S.A., Vol. 3(3,4), pp. 171–238 (1994).
2. B. L. Funt and S. N. Bhdani, *Can. J. Chem.* **42,** 2733 (1964).
3. B. L. Funt and O. G. Gray, *J. Macromol. Chem.* **1,** 625 (1966).
4. J. Chang and J. P. Bell, *SAMPE Q.* **18,** 39 (1987).
5. J. P. Bell, J. Chang, H. W. Rhee and R. Joseph, *Polym. Comp.* **8,** 46 (1987).
6. R. V. Subramanian and J. J. Jakubowoskii, *Polym. Eng. Sci.* **18,** 590 (1978).
7. R. V. Subramanian and J. J. Jakubowoskii, *Org. Coat. Plast. Chem.* **40,** 688 (1979).
8. J. O. Iroh, J. P. Bell and D. A. Scola, *J. Appl. Polym. Sci.* **41,** 735 (1990).
9. J. O. Iroh, J. P. Bell and D. A. Scola, *Chem. Mater.* **5**(1), 78 (1993).
10. J. O. Iroh, Y. Suhng and M. M. Labes, *J. Appl. Polym. Sci.* **52,** 1203 (1994).
11. J. O. Iroh, J. P. Bell, D. A. Scola and J. P. Wesson, *Polym. J.* **35**(6), 1306 (1994).
12. L. E. A. Berlouis and D. J. Schriffrin, *Trans. IMF* **64,** 42 (1986).
13. G. Mengoli, P. Bianco, S. Daolio and M. T. Munari, *J. Electrochem. Soc.* **128,** 2276 (1981).
14. G. Mengoli, S. Daolio and M. M. Musiani, *J. Appl. Electrochem.* **10,** 459 (1981).
15. G. Mengoli, S. Daolio and M. M. Musiani, B. Pelli and E. Vecchi, *J. Appl. Polym. Sci.* **28,** 1125 (1983).
16. B. Grunden and J. O. Iroh, *Polymer J.* **36,** 559 (1995).
17. A. F. Diaz and J. A. Logan, *J. Electroanal. Chem.* **111,** 111 (1980).
18. M. C. Pham, J. E. Dubois and P. C. Lacaze, *J. Electroanal. Chem.* **99,** 331 (1979).
19. F. Bruno, M. C. Pham and J. E. Dubois, *Electrochim. Acta* **22,** 451 (1977).
20. G. Mengoli, P. Bianco, S. Daolio and M. T. Munari, *J. Electrochem. Soc.* **128,** 2276 (1981).
21. L. E. A. Berlous and D. J. Schriffin, *Trans. IMF* **64,** 42 (1986).
22. J. M. Saveant, *J. Phys. Chem.* **95,** 10158 (1991).
23. T. F. Otero, J. Rodriguez, E. Angulo and C. Santamaria, *Synth. Metals* **41,** 2831 (1991).
24. T. F. Otero and E. Angulo, *J. Appl. Electrochem.* **22,** 369 (1992).
25. G. A. Wood and J. O. Iroh, Effect of Electrolytes on the Kinetics and Mechanism of the Electropolymerization of Pyrrole Onto Carbon Fibers, *Eur. Polym. J.* **33,** 107 (1997).
26. G. A. Wood and J. O. Iroh, *Synth. Metals* **80,** 73 (1996).
27. I. Sekine and C. Okano, *Corrosion* **45,** 924 (1989).
28. M. Schirmeisen and F. Beck, *J. Appl. Electrochem.* **19,** 145 (1989).

Effect of Process Parameters on the Electropolymerization Potential and Rate of Formation of Polypyrrole on Stainless Steel

JUDE O. IROH, WENCHENG SU

Department of Materials Science and Engineering, University of Cincinnati, Cincinnati, Ohio 45221-0012

Received 3 December 1996; accepted 31 January 1997

ABSTRACT: Polypyrrole coatings were formed on stainless steel working electrodes in aqueous oxalic acid solution. The rate of formation of polypyrrole coatings on stainless steel increased proportionately with the current density but increased slightly with increased pyrrole concentration. Increasing oxalic acid concentration also had no significant change in the polymerization rate. The electropolymerization potential of pyrrole decreased significantly from 1.5 to 0.8 V versus SCE when the working electrode was polished. The polymerization potential, E_p, of pyrrole, increased however, with increased current density and decreased exponentially with the initial monomer and electrolyte concentration, respectively. © 1997 John Wiley & Sons, Inc. J Appl Polym Sci **66:** 2433–2440, 1997

Key words: polypyrrole; process parameters; electropolymerization potential; electropolymerization rate; stainless steel

INTRODUCTION

Electropolymerization is used in a variety of applications, including the formation of polymers in solution,[1,2] the modification of graphite fibers,[3–6] and the formation of *in situ* matrix composites.[7–10] It is presently being proposed as a technique for forming new materials and novel microstructures.[11] The formation of insulating and highly crosslinked polymer coatings on steel by partial electropolymerization of *o*-allyl phenol and allyl amine on steel was reported.[13] Their coatings showed very good corrosion resistance. One of the approaches to protect steel against oxidation and corrosion is the application of polymeric coatings that are capable of inhibiting the oxidation of steel. Polymer coatings derived from allyl aromatic amines were shown to be very effective inhibitors for the oxidation of iron.[14] Highly stable and corrosion-resistant amine–sulfur copolymer coatings have been formed on steel by electrocopolymerization of aniline and ammonium sulfide.[15] Both insulating and conductive polymer coatings have been electropolymerized onto a variety of substrates[16–20] with excellent throwing power (uniform coating of irregular and complex shapes).

Corrosion takes place when two or more electrochemical reactions [eqs. (1) and (2)] occur on a metal surface, as follows.

$$O_2 + 2H_2O + 4e^- \rightarrow 4OH^- \ (0.4\ V) \qquad (1)$$

(reduction of oxygen)

$$M \rightarrow M^{n+} + ne^- \qquad (2)$$

(oxidation of metal)

Corrosion can be predicted from the following equation

$$\ln K = \frac{nFE_o}{RT} \qquad (3)$$

Correspondence to: J. O. Iroh.

Journal of Applied Polymer Science, Vol. 66, 2433–2440, 1997
 CCC 0021-8995/97/132438-08

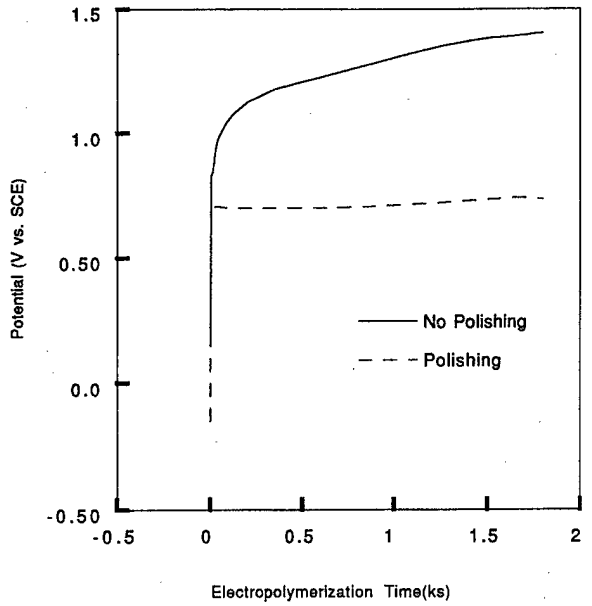

Figure 1 Potential–time curves for electropolymerization of pyrrole onto nonpolished (top) and polished (bottom) stainless steel (Cd = 2.25 mA cm^{-2}).

where n is the number of electrons, F is the Faraday's constant, E_o is the standard cell potential, and K is the equilibrium constant.

The equilibrium potential E is related to the standard potential E_o by the Nernst equation:

$$E = E_o + \frac{RT}{n\mathrm{F}} \ln[\mathrm{M}^{n+}] \qquad (4)$$

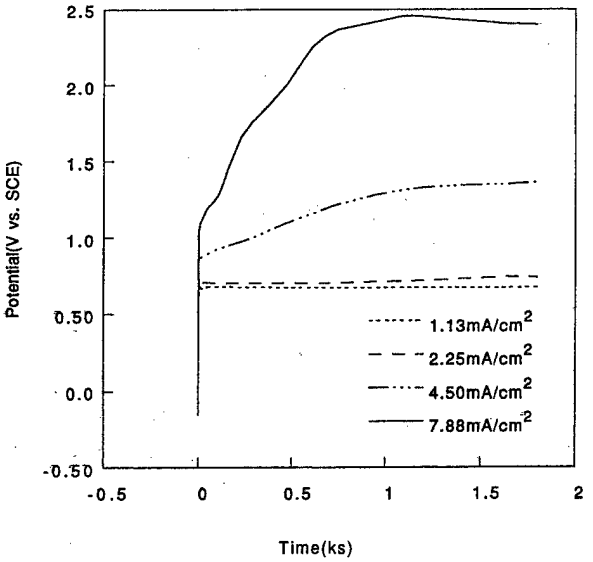

Figure 2 Potential–time curve for electropolymerization of pyrrole onto stainless steel as a function of current density and time, showing no induction time.

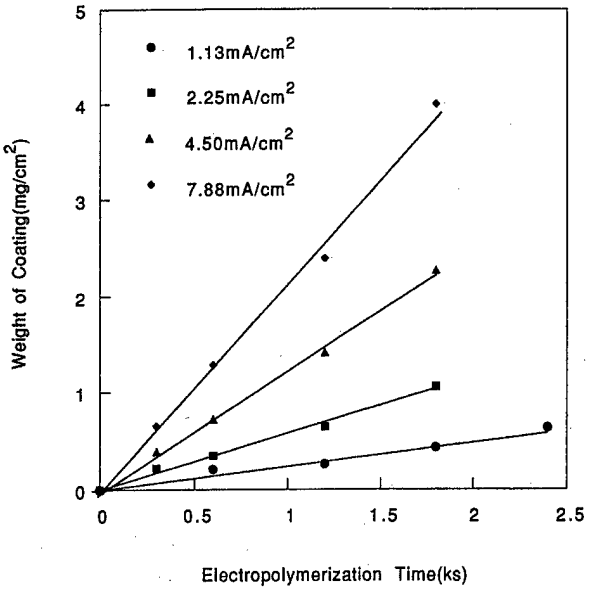

Figure 3 Dependence of the weight of polypyrrole formed onto stainless steel on the current density.

Prevention of corrosion can be achieved by applying passive nonsoluble film on the substrate, minimizing the entry of oxygen and water to the metal–film interface and keeping the oxidation power of the metal as low as possible.[21] The corrosion resistance of stainless steel in formic acid and oxalic acid solutions was investigated by Sekine and Momoi.[22,23] They showed that the room temperature corrosion resistance of stainless steel SUS 329J1 and SS 41 was very good. However, the corrosion resistance of these materials in boiling formic or oxalic acid was poor and decreased with increased acid concentration.[22,23] The formation of free-standing polypyrrole films on stainless steel is of interest because of the low cost of the substrate relative to the conventional platinum electrodes. Judiciously choosing the process variables, strongly adherent polypyrrole films can be formed on stainless steel. The corrosion performance of such coated substrates can be compared with the control. The need for a low-cost and an environmentally friendly metal protection technique has stirred renewed interest in research in this field.

Several investigators have studied the kinetics of electropolymerization of pyrrole on platinum.[24–28] Saveant et al. reported that radical cations coupling, rather than neutral radicals coupling, occurred during the electropolymerization of pyrrole.[24] The dependence of the rate of potentiostatic polymerization of pyrrole on the reaction variables, such as initial pyrrole concentration

Table I Variation of the Rate of Electropolymerization of Pyrrole with Current Density

Applied Current (mA)	Current Density (mA/cm^2)	Electropolymerization Potential (V versus SCE)	Electropolymerization rate ($mg\ cm^{-2}\ ks^{-1}$)
10	1.13	0.67	0.25
20	2.25	0.72	0.59
40	4.50	1.35	1.24
70	7.88	2.40	2.18

and electrolyte concentration, was determined by Otero and coworkers.[25,26] The dependence of the rate of formation of polypyrrole (on platinum electrode) on perchlorate (electrolyte) concentration and pyrrole concentration was found to be 0.5, respectively, in acetonitrile. However, the order of the reaction with respect to perchlorate increased to 0.8 in water. Iroh and Wood also studied the efficiency and kinetics of aqueous potentiostatic electropolymerization of pyrrole on carbon fibers.[27,28] It was shown that the rate of electropolymerization of pyrrole increased with pyrrole concentration, toluene sulfonate concentration and applied voltage raised to a power of 0.8–1.0, 0.8, and 0.9–1.2, respectively,[27] i.e., $R_p\ \alpha\ [M]^{0.8-1.0}\ [SO_3Ph]^{0.8}$, and $[EPa]^{0.9-1.2}$. They showed that the efficiency of potentiostatic polymerization of pyrrole increased with pyrrole concentration and decreased with applied voltage.[28]

In this article, we report the effect of electrochemical process variables on the electropolymerization potential and the rate of formation of polypyrrole on stainless steel. In a future article, the corrosion resistance of the polypyrrole-coated stainless steel will be evaluated and compared with that of polypyrrole-modified low-carbon steel.

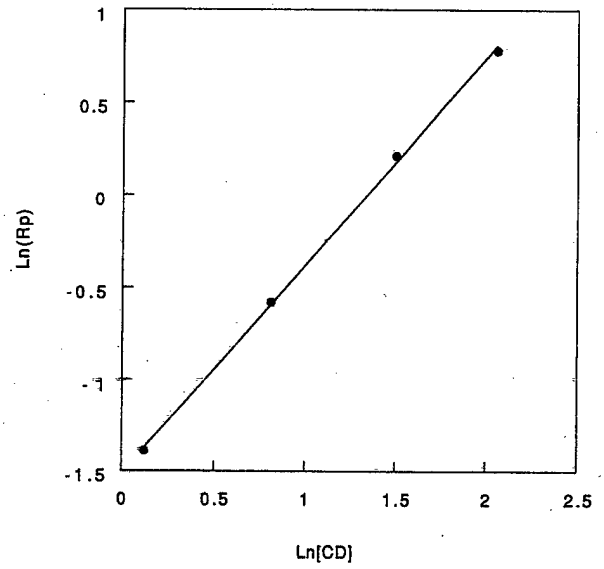

Figure 4 Determination of the current density exponent.

EXPERIMENTAL

Pyrrole (98%) and reagent-grade oxalic acid were purchased from Aldrich Chemical Company, Inc. Tetrachloroethylene and methanol were also purchased from Aldrich Chemical Company. The reagents were dissolved in deionized water prepared in our department.

The working electrode is an 0.46 mm thick 304

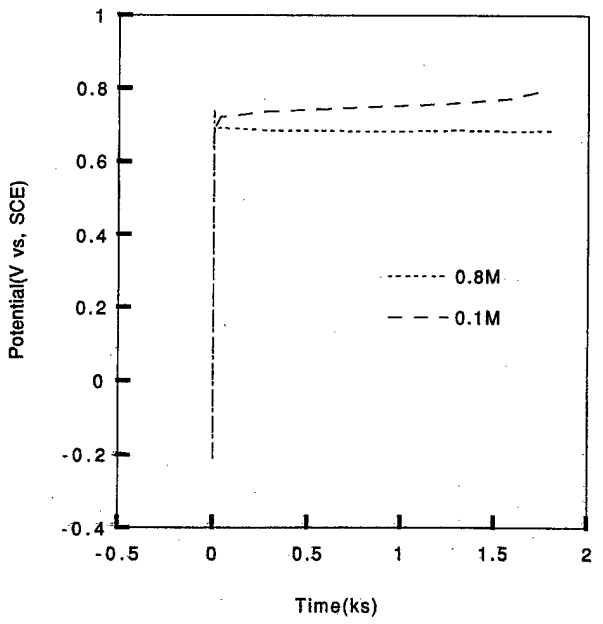

Figure 5 Potential–time curve for electropolymerization of pyrrole onto stainless steel as a function of initial pyrrole concentration and time, showing no induction time.

Table II Variation of the Rate of Electropolymerization of Pyrrole with Pyrrole Concentration

[PY] (*M*)	[OA] (*M*)	Electropolymerization Potential (V versus SCE)	Electropolymerization Rate (mg cm^{-2} ks^{-1})
0.1	0.1	0.76	0.51
0.25	0.1	0.72	0.57
0.5	0.1	0.71	0.69
0.8	0.1	0.68	0.70

stainless steel panel (2B finish) purchased from Copper Brass Sales Inc. The working electrode was degreased with tetrachloroethylene for about 60 min prior to electrochemical polymerization. The counter electrodes comprised of two titanium alloy plates. Saturated Calomel elelectrode (SCE), manufactured by Corning Company, was used as reference electrode. Galvanostatic electropolymerization of pyrrole was performed by an EG&G Princeton Applied Research Potentiostat/Galvanostat Model 273A.

Electrochemical formation of polypyrrole on stainless steel was carried out in a one-compartment polypropylene cell. The current densities used in this study ranged from 1.13 to 7.88 mA cm^{-2}. The initial electrolyte concentration was varied from 0.05 to 0.4*M*, while pyrrole concentration was varied from 0.1 to 0.8*M*. Electropolymerization time was varied between 300 and 1800 s.

The coated substrate was rinsed with methanol and dried at 65°C in a vacuum oven to constant weight. The weight of the coatings was determined as the difference between the coated and noncoated steel (control).

The infrared (IR) specimens were prepared by mixing a small quantity of the coatings with IR-grade potassium bromide (KBr) powder and subsequent pressing of the mixture into a clear pellet. Transmission IR spectroscopy was carried out using a Bio-Rad FTS-40 spectrophotometer. Elemental analysis of the coatings extracted from coated steel was performed by the Galbraith Laboratories, Inc., Knoxville, Tennessee.

RESULTS AND DISCUSSION

Effect of Current Density

The concentration of pyrrole and oxalic acid were maintained constant at 0.25 and 0.1*M*, respec-

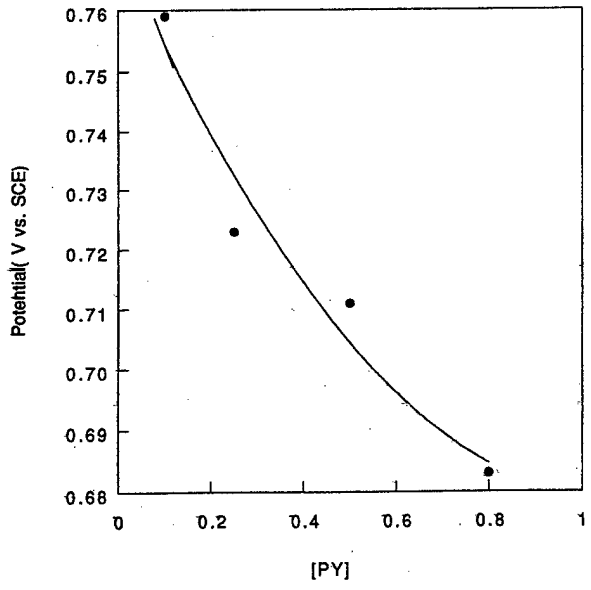

Figure 6 Variation of electropolymerization potential with initial pyrrole concentration.

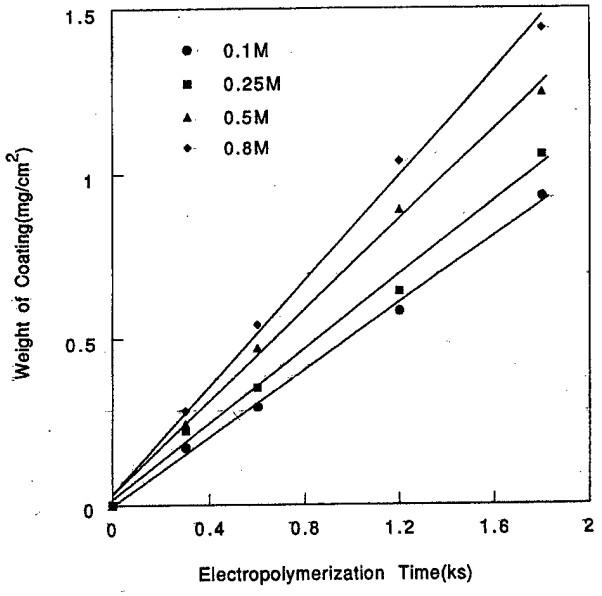

Figure 7 Dependence of the weight of polypyrrole formed onto stainless steel on pyrrole concentration.

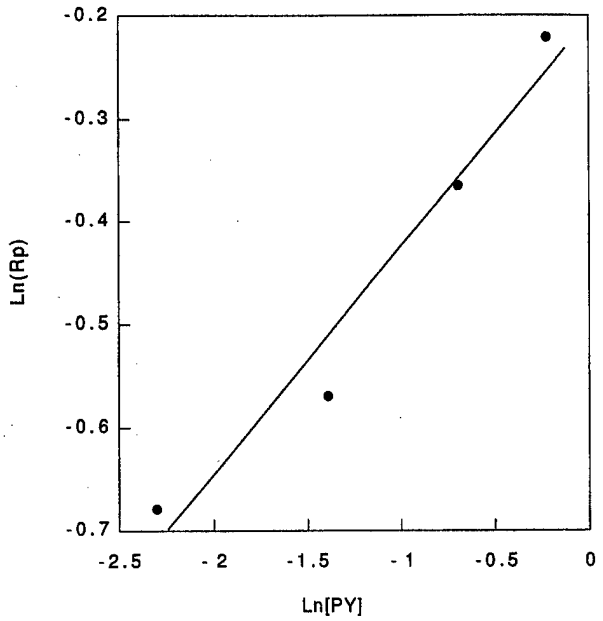

Figure 8 Determination of monomer concentration exponent.

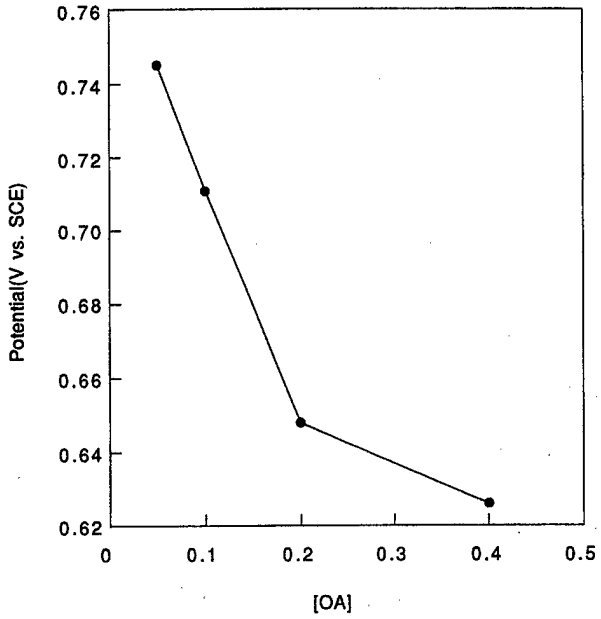

Figure 10 Variation of electropolymerization potential with electrolyte concentration.

tively, and the current density was varied from 1.13 to 7.88 mA cm^{-2}.

Figure 1 shows the dependence of the potential–time curves of pyrrole on stainless steel at 2.25 mA cm^{-2}, on the surface treatment of the substrate. When the stainless steel was polished with abrasive paper, the electropolymerization potential of pyrrole was maintained constant at $E_p \leq 0.8$ V. However, when the stainless steel was not polished, the electropolymerization potential of pyrrole became unsteady and increased sharply to $E_p = 1.5$ V.

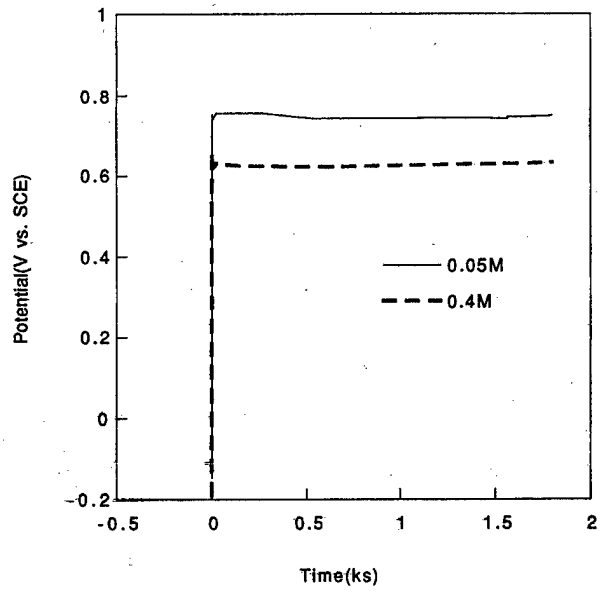

Figure 9 Potential–time curve for electropolymerization of pyrrole onto stainless steel as a function of electrolyte concentration and time, showing no induction time.

The electropolymerization potential of pyrrole increased with the current density, and the shape of the potential–time curves varied with the current density (Fig. 2). Below 2.25 mA cm^{-2}, the electropolymerization potential of pyrrole remained steady at 0.8 V versus SCE during polymerization. Significant increase in the electropolymerization potential of pyrrole to 1.5 V versus SCE occurred when the current density was raised to 4.50 mA cm^{-2}. The electropolymerization potential increased with time and attained a value of 1.35 V versus SCE in 1200 s. A further increase in the current density to 7.88 mA cm^{-2} resulted in a time-dependent increase in the electropolymerization potential for 700 s, after which it remained at 2.40 V versus SCE (Fig. 2).

Figure 3 shows the dependence of the weight of polypyrrole coatings on the current density and electropolymerization time. The weight of the coatings increased proportionately with current density and time. The rate of electropolymerization of pyrrole was determined from the slope of the weight of coating–time curves (Fig. 3). The rate of electropolymerization increased with the current density, as shown in Table I. Increasing the current density from 0.56 to 7.78 mA cm^{-2} resulted in an increase in the rate of polymeriza-

Table III Variation of the Rate of Electropolymerization of Pyrrole with Electrolyte Concentration

[PY] (*M*)	[OA] (*M*)	Electropolymerization Potential (V Versus SCE)	Electropolymerization Rate (mg cm^{-2} ks^{-1})
0.5	0.05	0.74	0.70
0.5	0.1	0.71	0.69
0.5	0.2	0.65	0.67
0.5	0.4	0.63	0.70

tion from 0.25 to 2.18 mg cm^{-2} ks^{-1}. The dependence of the rate of formation of polypyrrole on stainless steel on the current density was determined from the Ln rate versus Ln Cd plot (Fig. 4) to be 1.12 [Rp α $[Cd]^{1.12}$], indicating a first-order process.

Effect of Monomer Concentration

The concentration of oxalic acid and current density were kept constant at 0.1*M* and 2.25 mA cm^{-2}, respectively, while the concentration of pyrrole was varied from 0.1 to 0.8*M*. Figure 5 shows the electropolymerization potential–time curve as a function of initial pyrrole concentration and time. The potential–time curve rose to a maximum value at $t \sim 0$ s, after which it remains invariant with time. There was no induction period, indicating that the chromium oxide layer was effective in preventing the dissolution of iron. The electropolymerization potentials decreased exponentially (about 11% decrease; Table II) with the increased pyrrole concentration (700% increase; Fig. 6) due to increased conductivity of the PPy–C_2O_4 film. Recall that increased current density caused a proportionate increase in the polymerization potential and weight of polypyrrole coatings. The dependence of the weight of polypyrrole on the initial pyrrole concentration is shown on Figure 7. Increasing the pyrrole concentration results in a moderate increase in the weight of polypyrrole formed. For instance, increasing the pyrrole concentration from 0.1 to 0.8*M* (700% increase) resulted in an increase in the weight of coatings from 2.6 to 4.8 mg (85% increase) after 10 min of electropolymerization. The rate of polymerization was determined from the slope of the weight of coatings versus time curve and presented as a function of pyrrole concentration (Table II). The rate of electropolymerization of pyrrole increased with pyrrole concentration (Table II). The order of the electropolymerization with respect to pyrrole concentration was determined from the slope of the Ln rate of weight gain versus Ln [M] plot (Fig. 8) as 0.22 [Rp α $[PY]^{0.22}$].

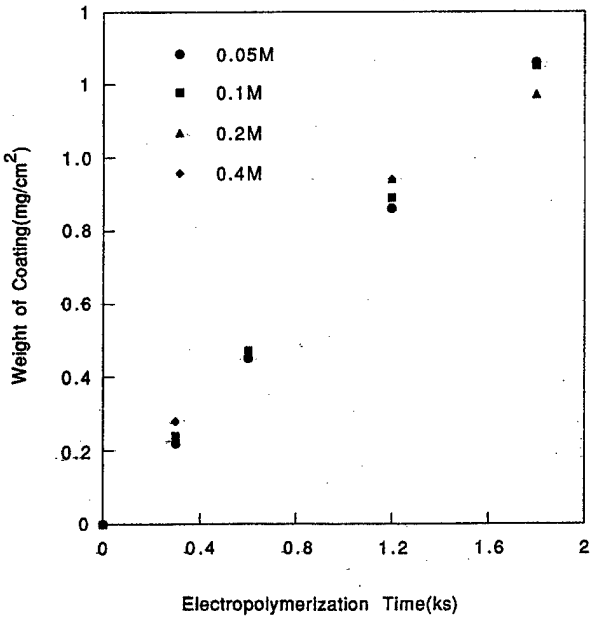

Figure 11 Dependence of the weight of polypyrrole formed onto stainless steel on oxalic acid concentration.

Effect of Electrolyte Concentration

The pyrrole concentration and current density were kept constant at 0.5*M* and 2.25 mA cm^{-2},

Table IV Elemental Composition of the Polypyrrole Coatings

Elements	Composition (%)
C	60.21
H	3.16
N	16.71
S	16.08

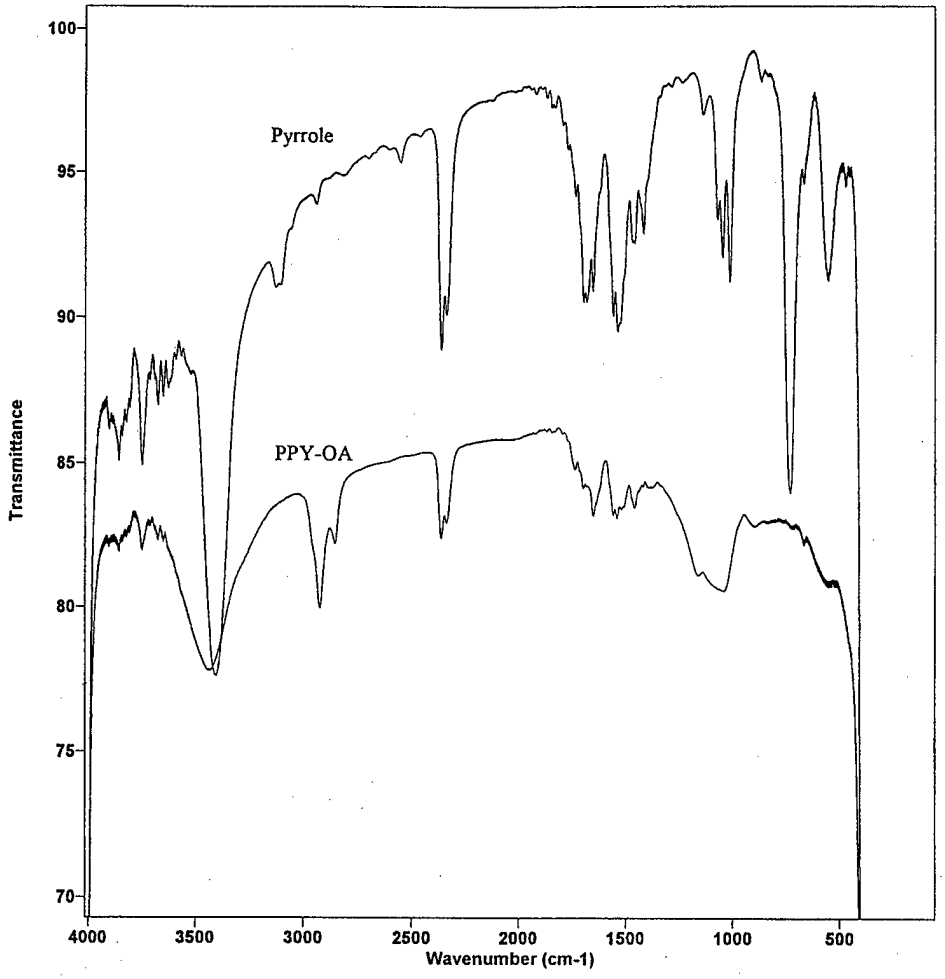

Figure 12 Infrared spectra of pyrrole (top) and polypyrrole–oxalate coatings formed on stainless steel (bottom).

respectively. The concentration of oxalic acid was varied from 0.05 to 0.4*M*. Figures 9 and 10 shows the potential–time curve for electropolymerization of pyrrole as a function of oxalic acid concentration. There was no induction time for polymerization of pyrrole onto stainless steel (Fig. 9). The steady-state polymerization potential decreased (15% decrease) with electrolyte concentration (700% increase; Table III) due to increased conductivity of the PPy-C_2O_4 layer. Generally, the electropolymerization potential decreases exponentially with the increasing electrolyte concentration (Fig. 10). The variation of the weight of polypyrrole coatings with electrolyte concentration is shown in Figure 11. The amount of polypyrrole formed per unit of time is about 0.7 mg cm^{-2} ks^{-1}, irrespective of the oxalic acid concentration (Table III), indicating a zero-order reaction with respect to the electrolyte concentration ($Rp\alpha[OA]_0$).

Elemental Composition and Analysis of the Coatings

The elemental composition of the polypyrrole oxalate coatings formed on stainless steel is shown in Table IV. Elemental analysis shows the presence of oxygen in the coatings and indicates that the hydrogen oxalate counterion is incorporated into the polypyrrole film. The mole ratio of pyrrole to the hydrogen oxalate ion in the film was determined to be $\sim 5:1$.

Fourier transform IR (FTIR) spectra of the polypyrrole coatings extracted from stainless steel show the characteristic IR peaks associated with pyrrole and the oxalate counterion. Figure 12 shows the IR spectra for pyrrole (Fig. 12, top) and that for polypyrrole coatings formed in oxalic acid solution (Fig. 12, bottom). The broad peak occurring at 3200–3500 cm^{-1} corresponds to the

N—H stretching in the pyrrole ring. The strong transmittance peak at 2923 cm^{-1} is due to the vibration of the —C—C— group from oxalic acid. The IR peaks occurring between 1650 and 1735 cm^{-1} correspond to C—C stretches, C—H deformations, C—N stretches, N—H deformation, and C=C and C=O stretches. Three distinct bands appear near 1100–1000 cm^{-1} and are due to C—H deformations. The remaining region, 1000–400 cm^{-1}, is dominated by a strong peak near 735 cm^{-1}, (Fig. 12, top), which is due to a C—H wag vibrations coming from adjacent 2,5-hydrogen atoms on the pyrrole ring. There is also a peak near 556 cm^{-1} that probably corresponds to an N—H wag vibration. The remaining peaks in this region can be assigned vibrations, such as other C—H wags, and a couple of different ring vibrations. The IR spectra of the polypyrrole coatings (Fig. 12, bottom) confirmed the presence of the oxalate ion in the coatings (2923, 1650, and 1735 cm^{-1}). One of the striking features of Figure 12 (bottom) is the disappearance of the C—H peak at 735 cm^{-1} due to oxidative coupling (anodic polymerization) of pyrrole. Overall, the IR analysis shows the presence of oxalate ions in the coatings and confirmed the elimination of the 2,5-hydrogen atoms during electropolymerization.

CONCLUSION

Polypyrrole coatings have been successfully formed on stainless steel by aqueous electrochemical polymerization using oxalic acid as the electrolyte. The rate of formation of polypyrrole increased with current density and slightly with initial pyrrole concentration but remained unchanged with electrolyte concentration. The polymerization potential increased with current density and decreased with monomer and electrolyte concentration. The polymerization potential for pyrrole in oxalic acid solution was dependent on the pretreatment of the stainless steel electrode and decreased significantly with surface polish, followed by rinse in tetrachloro ethylene. Overall, smooth and dense polypyrrole films were formed on polished substrates. IR spectra confirmed the presence of oxalate ions in the coatings and the elimination of 2,5-hydrogens during the electropolymerization of pyrrole.

Financial support from the Office of Naval Research's Young Investigators Program, Grant N00014-95-1-0485, is gratefully acknowledged.

REFERENCES

1. B. L. Funt and S. N. Bhdani, *Can. J. Chem.*, **42,** 2733 (1964).
2. B. L. Funt and O. G. Gray, *J. Macromol. Chem.*, **1,** 625 (1966).
3. J. Chang and J. P. Bell, *SAMPE Q.*, **18,** 39 (1987).
4. J. P. Bell, J. Chang, H. W. Rhee, and R. Joseph, *Polym. Comp.*, **8,** 46 (1987).
5. R. V. Subramanian and J. J. Jakubowoskii, *Polym. Eng. Sci.*, **18,** 590 (1978).
6. R. V. Subramanian and J. J. Jakubowoskii, *Org. Coat. Plast. Chem.*, **40,** 688 (1979).
7. J. O. Iroh, J. P. Bell, and D. A. Scola, *J. Appl. Polym. Sci.*, **41,** 735 (1990).
8. J. O. Iroh, J. P. Bell, and D. A. Scola, *Chem. Mater.*, **5,** 78 (1993).
9. J. O. Iroh, Y. Suhng, and M. M. Labes, *J. Appl. Polym. Sci.*, **52,** 1203 (1994).
10. J. O. Iroh, J. P. Bell, D. A. Scola, and J. P. Wesson, *Polym. J.*, **35,** 1306 (1994).
11. P. C. Searson and T. P. Moffat, in *Critical Reviews in Surface Chemistry,* P. Sherwood, Ed., Vol. 3, 1994, pp. 171–238.
12. L. E. A. Berlouis and D. J. Schiffrin, *Trans. IMF,* **64,** 42 (1986).
13. G. Mengoli, P. Bianco, S. Daolio, and M. T. Munari, *J. Electrochem. Soc.*, **128,** 2276 (1981).
14. G. Mengoli, S. Daolio, and M. M. Musiani, *J. Appl. Electrochem.*, **10,** 459, (1981).
15. G. Mengoli, S. Daolio, M. M. Musiani, B. Pelli, and E. Vecchi, *J. Appl. Polym. Sci.*, **28,** 1125 (1983).
16. B. Grunden and J. O. Iroh, *Polym. J.*, **34,** 559 (1995).
17. A. F. Diaz and J. A. Logan, *J. Electroanal. Chem.*, **111,** 111 (1980).
18. M. C. Pham, J. E. Dubois, and P. C. Lacaze, *J. Electroanal. Chem.*, **99,** 331 (1979).
19. F. Bruno, M. C. Pham, and J. E. Dubois, *Electrochim. Acta,* **22,** 451 (1977).
20. G. Mengoli, P. Bianco, S. Daolio, and M. T. Munari, *J. Electrochem. Soc.*, **128,** 2276 (1981).
21. K. B. Tator, in *Metals Handbook,* 9th ed., Vol. 13, L. J. Korb et al., Eds., 1987, pp. 399–418.
22. I. Sekine and K. Momoi, *Corrosion, NACE,* **44,** 136 (1988).
23. I. Sekine and K. Momoi, *Corrosion,* **45,** 924 (1989).
24. J. M. Saveant, *J. Phys. Chem.*, **95,** 10158 (1991).
25. T. F. Otero, J. Rodriguez, E. Angulo, and C. Santamaria, *Synth. Metals,* **41,** 2831 (1991).
26. T. F. Otero and E. Angulo, *J. Appl. Electrochem.*, **22,** 369 (1992).
27. G. A. Wood and J. O. Iroh, *Eur. Polym. J.*, **33,** 107–114 (1997).
28. G. A. Wood and J. O. Iroh, *Synth. Metals,* **80,** 73 (1996).

ELSEVIER

Synthetic Metals 97 (1998) 73–80

SYNTHETIC METALS

One-step electrochemical process for the formation of poly(*N*-methylpyrrole) coatings on steel in different media

Jude O. Iroh *, Wencheng Su

Department of Materials Science and Engineering, University of Cincinnati, Cincinnati, OH 45221-0012, USA

Received 30 June 1998; accepted 1 July 1998

Abstract

Poly(*N*-methylpyrrole) coatings have been successfully formed on steel by a one-step electrochemical process in different media. Electropolymerization was performed in aqueous medium with low monomer concentration and in a mixed aqueous/organic media with higher monomer concentrations. Ethanol (EtOH) and *N*,*N*-dimethylformamide (DMF) were chosen as the organic components of the mixed solvents and oxalic acid was used as the electrolyte. The effect of process parameters on the formation of poly(*N*-methylpyrrole) was systematically investigated. The composition and morphology of the coatings were also studied by elemental analysis, FT-IR and scanning electron microscopy (SEM). Our results reveal that the formation and properties of poly(*N*-methylpyrrole) coatings were all dependent on the solvent composition and other process parameters. The amount of poly(*N*-methylpyrrole) formed on steel increased with time and applied current for all the solvent–electrolyte systems. For the electropolymerization performed in distilled water–oxalic acid solution, the amount of polymer coatings formed decreased with increased electrolyte concentration. In contrast, the amount of polymer coatings formed on steel in distilled water:ethanol (1:1)–oxalic acid and distilled water:DMF (1:1)–oxalic acid systems, increased with increasing electrolyte concentration. By controlling the electrochemical parameters, smooth, uniform and strongly adherent coatings could be formed onto steel substrates.

Keywords: Poly(*N*-methylpyrrole) coatings; Electrochemical processes; Steel; Solvent

1. Introduction

The corrosion of metals is an enormous problem throughout the world. Many methods have been developed over the years to address the problem of corrosion of metals. Among them, polymer coatings may be the most widely used method in industry [1–3]. However, there are two major environmental problems concerning the conventional coating techniques: one is the chromate rinsing process required for the pretreatments of metals, and the other problem is the use of volatile organic solvents for the formulation of coatings [4,5]. Due to the environmental concerns about the hazardous effects of chromates and volatile organic solvents, research has been recently performed to develop environmentally friendly processes for the pretreatments of metals and formulation of coatings.

Electrochemical polymerization is perhaps an alternative coating technique which can eliminate the use of hazardous chemicals. Other merits of electropolymerization include the possibility of automation, mild production conditions and the ability to control the properties of the coatings by proper choice of the reaction parameters [6–9]. Recently, interest has been shown to form polypyrrole coatings on oxidizable metals for corrosion protection by an electropolymerization technique [10–16]. Since polypyrrole is produced by an oxidative process, formation of polypyrrole coatings can only occur on the oxidizable metals when the electrochemical conditions can lead to passivation of the metals without preventing the electropolymerization of pyrrole. It was found that only a few electrochemical systems could meet this requirement [10–16]. Compared to polypyrrole, poly(*N*-methylpyrrole) has a relatively low conductivity. Its free-standing films are stable in both oxidizable and neutral forms. In addition, the price of poly(*N*-methylpyrrole) is much lower than that of polypyrrole [17–19]. These properties of poly(*N*-methylpyrrole) make it a more attractive candidate to be considered as protective coating for metals.

In this paper, we report our investigation on the formation of poly(*N*-methylpyrrole) coatings on steel by a one-step electrochemical process. Because of the limited solubility of

* Corresponding author. Tel.: +1 513 556 3096; fax: +1 513 566 2569.

0379-6779/98/$ - see front matter
PII S0379-6779(98)00117-9

N-methylpyrrole in aqueous solution, the synthesis of poly(*N*-methylpyrrole) coatings on steel was investigated in both aqueous medium and aqueous/organic mixing media.

2. Experimental

Chemicals used in this study were all purchased from Aldrich Chemical Company. QD low carbon steel panels were provided by the Q-panel Company.

Electrochemical synthesis of poly(*N*-methylpyrrole) coatings was carried out in a one-compartment polypropylene cell. The working electrode was made from the QD low carbon steel sheets. The low carbon steel sheets were degreased with tetrachloroethylene for about 1 h prior to the electrochemical reactions. The coated surface area of the steel was 8.89 cm^2. The counter electrodes comprised of two titanium alloy plates. A saturated calomel electrode (SCE) manufactured by Corning Company was used as the reference electrode. The electrochemical reactions were performed galvanostatically. The constant current was supplied by an EG&G Princeton Applied Research 273A potentiostat/galvanostat. The working electrode and counter electrodes were used as anode and cathode respectively. After each experiment, the coated steel sheet was rinsed with deionized water and methanol, and dried in vacuum oven at 65°C to constant weight.

Elemental analysis of the coatings scraped from the substrate was done by Galbraith Laboratories, Inc. A BIO-RAD FTS-40 FT-IR spectrometer was used to measure the IR spectra of the coatings by means of potassium bromide (KBr) pellets. The morphology of the coatings was examined by scanning electron microscopy (SEM). The SEM specimens were shadowed with gold to enhance their conductivity.

3. Results and discussion

3.1. Electrodeposition of poly(N-methylpyrrole) coatings on steel in aqueous medium

In this research, oxalic acid was chosen as the electrolyte for the electrochemical synthesis of poly(*N*-methylpyrrole) coatings on steel. The formation process of poly(*N*-methylpyrrole) coatings was first investigated in aqueous medium. In this part of the study, the concentration of *N*-methylpyrrole was kept constant at 0.05 M, which is very close to the solubility of *N*-methylpyrrole in aqueous solution. The electrolyte concentrations were varied from 0.1 to 0.4 M. For each electrolyte concentration, the current density was changed from 0.5 to 4 mA/cm^2.

Figs. 1–3 show the corresponding potential–time curves for the formation reactions. The formation process of poly(*N*-methylpyrrole) on steel is somewhat different from that on inert electrodes such as platinum. When platinum was used as the electrode, the electropolymerization of *N*-methylpyrrole took place immediately after the current was supplied. However, when steel was used as the electrode, an induction period was shown before the electropolymerization of *N*-methylpyrrole took place. This phenomenon was also observed in the formation process of polypyrrole coatings on steel [13–16]. It was suggested that the following two reactions occurred during the induction period:

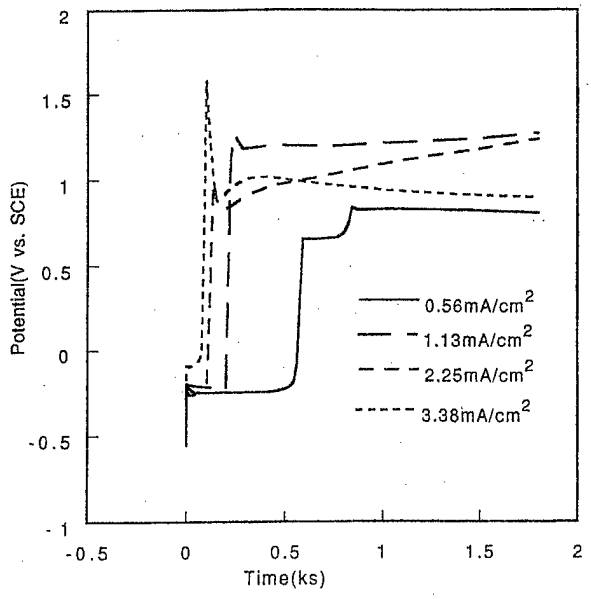

Fig. 1. Potential–time curves for the formation of poly(*N*-methylpyrrole) coatings on steel in aqueous solution, [MPy] = 0.05 M, [OA] = 0.1 M.

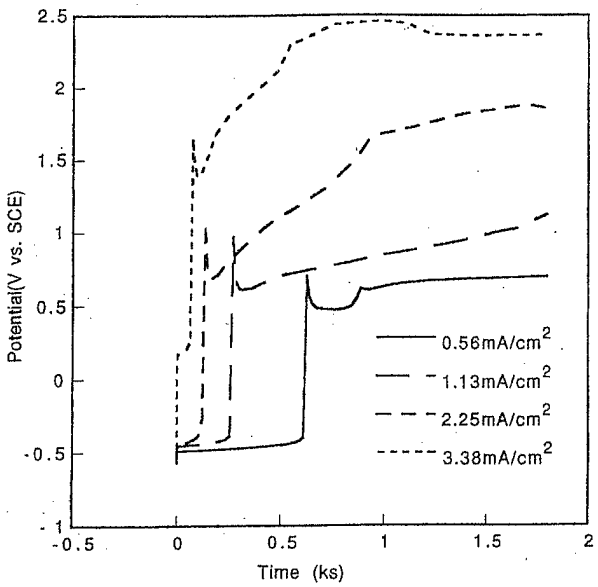

Fig. 2. Potential–time curves for the formation of poly(*N*-methylpyrrole) coatings on steel in aqueous solution, [MPy] = 0.05 M, [OA] = 0.2 M.

$$Fe - 2e \rightarrow Fe^{2+} \quad (1)$$

$$Fe^{2+} + C_2O_4^{2-} + 2H_2O \rightarrow FeC_2O_4 \cdot 2H_2O \quad (2)$$

The produced $FeC_2O_4 \cdot 2H_2O$ was almost insoluble in water and precipitated directly onto the steel substrate. At the end of the induction period, the steel substrate was completely

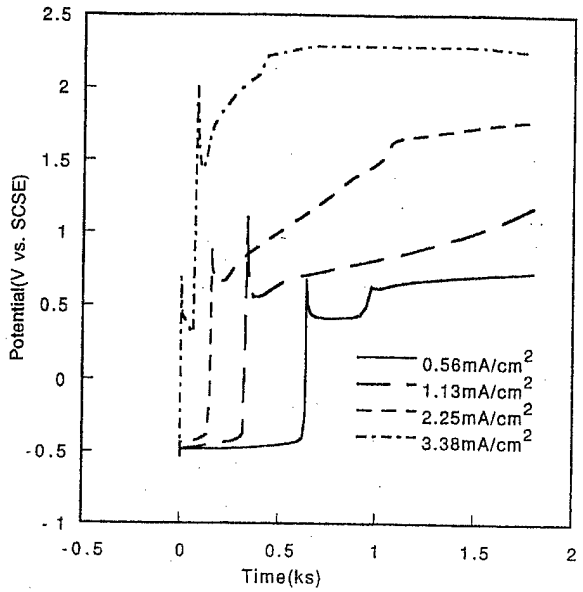

Fig. 3. Potential–time curves for the formation of poly(*N*-methylpyrrole) coatings on steel in aqueous solution, [MPy] = 0.05 M, [OA] = 0.4 M.

covered by the $FeC_2O_4 \cdot 2H_2O$, preventing further dissolution of iron. When the passivation of steel was established, the reaction potential changed from the dissolution potential of iron to the electropolymerization potential of *N*-methylpyrrole.

Fig. 4 shows the variation of the induction time with the applied current density for different electrolyte concentrations. It can be seen that the induction time decreased dramatically with increasing current density. For the same applied current density, however, induction time did not change much with electrolyte concentration. As shown in Fig. 5, ln(induction time) against ln(current density) shows a linear relationship, which can be expressed by the following equations:

$$[OA] = 0.1\ M: \ln t = 5.73 - 0.98 \ln i \quad (3)$$

$$[OA] = 0.2\ M: \ln t = 5.77 - 1.12 \ln i \quad (4)$$

$$[OA] = 0.4\ M: \ln t = 5.86 - 1.16 \ln i \quad (5)$$

When the passivation of the steel was established, black poly(*N*-methylpyrrole) coatings began to form on the steel substrate, but the electropolymerization potential of *N*-methylpyrrole and the properties of the poly(*N*-methylpyrrole) coatings were all dependent on the applied current density and the electrolyte concentration. The amount of poly(*N*-methylpyrrole) formed on steel increased with time and applied current (Table 1(a)). Increasing the applied current from 0.56 to 2.25 mA/cm^2 increased the weight of coatings from 0.07 to 0.64 mg/cm^2. The effect of increased oxalic acid concentration on the weight of polymer coatings formed on steel is shown in Table 1(b). Increasing the electrolyte concentration from 0.1 to 0.4 M resulted in decreased weight of coatings from 0.64 to 0.38 mg/cm^2 (Table 1(a)–(c)). The decreased weight of coatings at increased oxalic acid concentration may be due to increased dissolution of steel.

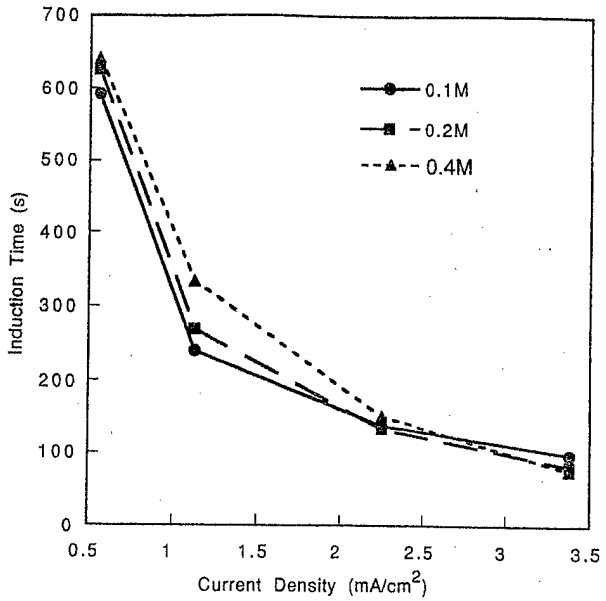

Fig. 4. Variation of induction time with applied current density for the aqueous solutions with different electrolyte concentrations.

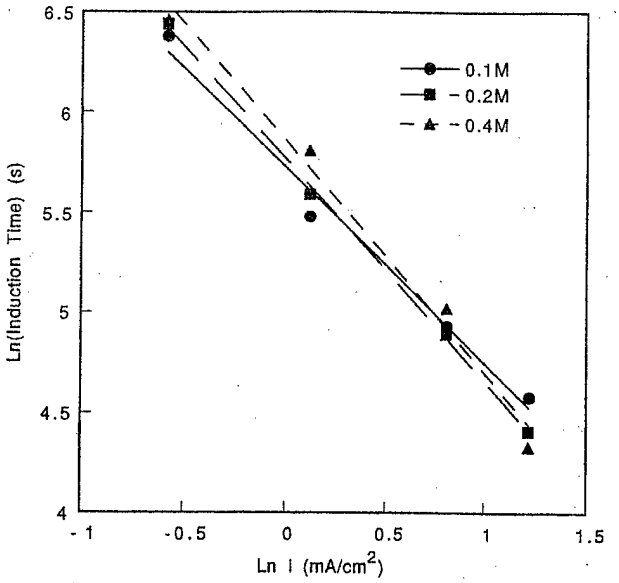

Fig. 5. Dependence of induction time on the applied current density for the aqueous solutions with different electrolyte concentrations.

The potential–time curves for the reaction are shown in Fig. 1. The polymerization potential increased from about 0.8 V to about 1.2 V when the applied current density was increased from 0.56 to 1.13 mA/cm^2. However, increasing the applied current density to 2.25 and 3.38 mA/cm^2 did not lead to further increase in the polymerization potential; on the contrary, the electropolymerization potentials at 2.25 and 3.38 mA/cm^2 were all lower than that at 1.13 mA/cm^2. However, the passivation times were significantly decreased with increased applied current. For example, increasing the applied current from 0.56 to 3.38 mA/cm^2 resulted in a decrease in the passivation time from 592 to 98 s (Table

Table 1

i (mA/cm^2)	Induction time (s)	Passivation charge (mC/cm^2)	Polymerization potential (V vs. SCE)	Weight change (mg/cm^2)
(a) Characteristics of the formation process of MPPy on steel in aqueous solution, [MPy] = 0.05 M, [OA] = 0.1 M				
0.56	592	332	0.82	0.07
1.13	240	271	1.23	0.27
2.25	138	310		0.64
3.38	98	348		−0.42
(b) Characteristics of the formation process of MPPy on steel in aqueous solution, [MPy] = 0.05 M, [OA] = 0.2 M				
0.56	625	350	0.68	0.07
1.13	269	304		0.28
2.25	133	299		0.47
3.38	82	277		0.66
(c) Characteristics of the formation process of MPPy on steel in aqueous solution, [MPy] = 0.05 M, [OA] = 0.4 M				
0.56	641	359	0.69	0.04
1.13	334	377		0.27
2.25	151	340		0.38
3.38	76	257		0.60

1(a)). The passivation charge remained nearly constant at 300 mC/cm^2 (Table 1(a)–(c)).

When the electrolyte concentration was increased to 0.2 and 0.4 M, smooth, uniform and strongly adherent coatings were obtained at applied current densities below 1.13 mA/cm^2. When the applied current densities were above 2.25 mA/cm^2, uniform coatings were obtained after 30 min reaction, but they were very brittle and could be easily peeled off from the substrates. At each applied current density, the potential–time curves showed similar characteristics between these two electrolyte concentrations. All the potential–time curves showed a sharp peak right after the induction period. This peak is perhaps related to the nucleation of poly(*N*-methylpyrrole) on the steel substrate [18]. For each reaction system, the electropolymerization potential of *N*-methylpyrrole increased with the current density for the same reaction time. When the current density was 0.56 mA/cm^2, the electropolymerization potential first reached a constant value after the sharp peak, but it only lasted about 200 to 300 s, then the potential increased rapidly to a higher value and remained roughly constant during the rest of the reaction. The steady-state electropolymerization potential of *N*-methylpyrrole was about 0.68 V for both electrolyte concentrations. At the current density of 1.13 mA/cm^2, the electropolymerization potential increased slowly with time after the sharp peak. When the applied current densities were above 2.25 mA/cm^2, the electropolymerization potentials first increased very rapidly with reaction time, then tended to level off, but higher applied current density (3.38 mA/cm^2) led to a shorter reaction time for the potential to reach the plateau. Worthy mention is that uniform and strongly adherent coatings could be obtained at high applied current densities by controlling the reaction potentials. Generally speaking, if the reaction potential exceeded 1.6 V, the adhesion of the coatings to the substrate became very poor. Perhaps the $FeC_2O_4 \cdot 2H_2O$ interlayer also began to decompose when the potential was above 1.6 V. The potential–time curves for the formation of poly(*N*-methylpyrrole) coatings on steel are also different from those for the formation of polypyrrole coatings on steel [13–16]. When pyrrole was used as monomer, the electropolymerization potential was very steady for all the current densities discussed above. This may be due to the low conductivity of poly(*N*-methylpyrrole) films.

3.2. Electrodeposition of poly(N-methylpyrrole) coatings on steel in aqueous/organic mixing media

In order to investigate the formation process of poly(*N*-methylpyrrole) coatings at higher monomer concentrations, we first chose aqueous/ethanol mixing solvent to increase the solubility of *N*-methylpyrrole. Since oxalic acid is not a good electrolyte in ethanol solution, low content of ethanol was used. For 0.1 M *N*-methylpyrrole and 0.1 M oxalic acid, about 20 vol.% ethanol was needed to dissolve the *N*-methylpyrrole completely. For this reaction system, the electrochemical reactions were investigated at different current densities. Fig. 6 shows the corresponding potential–time curves. It can be seen that the reaction at 0.56 mA/cm^2 shows an undesirable behaviour. Although the potential increased to a high positive value at the end of the induction period, it returned to the dissolution potential of iron after a very short period and changed frequently between the two potentials. No black coating was found on the substrate surface after 30 min reaction. When the current density was 1.13 mA/cm^2, uniform and strongly adherent poly(*N*-methylpyrrole) coating was obtained after 30 min reaction.

The amount of poly(*N*-methylpyrrole) formed on steel increased with the applied current (Table 2(a)). Increasing the applied current from 0.56 to 3.38 mA/cm^2 increased the weight of coatings from 0.11 to 1.27 mg/cm^2. A slight change in weight of the coatings was obtained at increased electrolyte concentration (Table 2(b)).

The electropolymerization potential of *N*-methylpyrrole did not change much with reaction time. When the current

Table 2

i (mA/cm^2)	Induction time (s)	Passivation charge (mC/cm^2)	Polymerization potential (V vs. SCE)	Weight change (mg/cm^2)
(a) Characteristics of the formation process of MPPy on steel in aqueous/ethanol solution, [MPy] = 0.1 M, [OA] = 0.1 M				
0.56	274	153		0.11
1.13	133	150	0.80	0.43
2.25	76	171		1.00
3.38	38	128		1.27
(b) Characteristics of the formation process of MPPy on steel in ethanol/aqueous solution, [MPy] = 0.1 M, [OA] = 0.4 M				
0.56	563	315		0.14

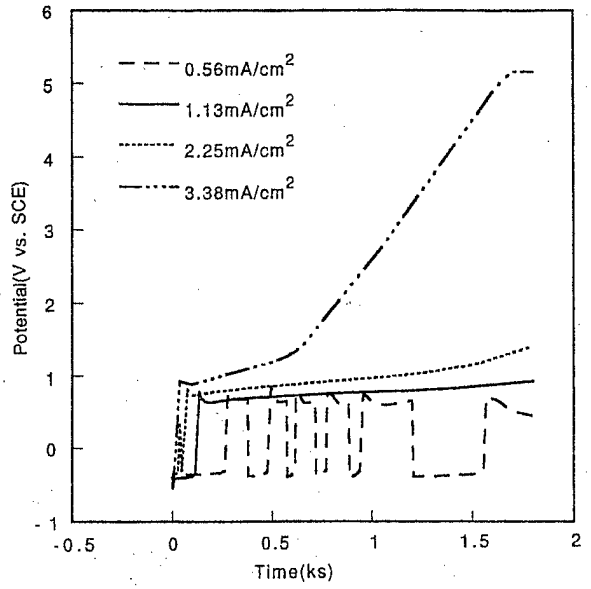

Fig. 6. Potential–time curves for the formation of poly(*N*-methylpyrrole) coatings on steel in aqueous/ethanol medium, [MPy] = 0.1 M, [OA] = 0.1 M.

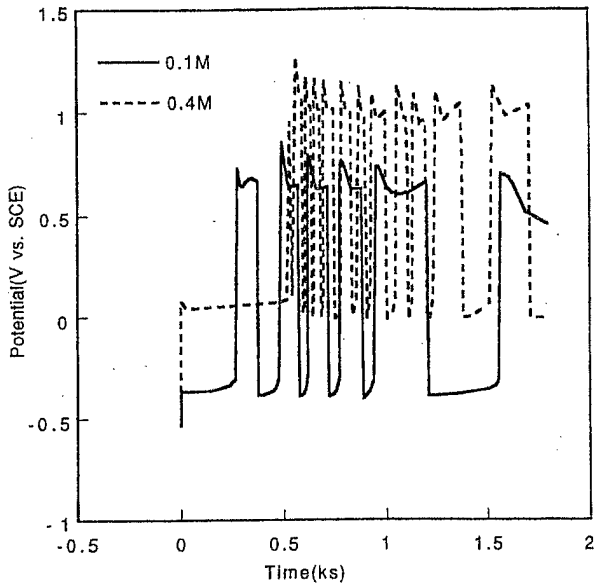

Fig. 7. Potential–time curves for the formation of poly(*N*-methylpyrrole) coatings on steel at 0.56 mA/cm^2 in aqueous/ethanol media with different electrolyte concentrations.

density was 2.25 mA/cm^2, the adhesion of the poly(*N*-methylpyrrole) coating to the steel substrate was good, but the surface of the coating became somewhat rough. The corresponding electropolymerization potential increased slowly with time. At the current density of 3.38 mA/cm^2, however, the polymerization potential of *N*-methylpyrrole first increased slowly with reaction time, and subsequently increased very rapidly after about 700 s reaction.

The concentration of oxalic acid was further increased to 0.4 M while the composition of the solvent and the concentration of the monomer remained the same as the above system. Fig. 7 shows the potential–time curve for this reaction system at applied current density of 0.56 mA/cm^2. The potential–time curve for the reaction system with 0.1 M oxalic acid concentration is also plotted in Fig. 7 for the purpose of comparison. It can be seen that the undesirable behaviour occurred again and the reaction potential changed more frequently for the reaction system with higher electrolyte concentration. The detailed mechanism is not clear so far; perhaps ethanol could interfere with the formation of the passive interlayer at low current density.

In order to overcome the above problem, the formation process of poly(*N*-methylpyrrole) coatings on steel was also investigated in aqueous/DMF mixing solvent. The composition of the reaction systems for this part of the study is shown in Table 3. Minimum content of DMF was used for each reaction system.

Figs. 8–10 show the potential–time curves for the three reaction systems. It can be seen that aqueous/DMF medium shows a different behaviour from the aqueous/ethanol medium. The characteristics of the formation process and properties of the coatings can be summarized as the following: for each solution, the induction time also decreased dramatically with increasing current density. For the reaction systems 6 and 7, smooth, uniform and strongly adherent coatings were obtained when the applied current densities were below 1.13 mA/cm^2.

The amount of poly(*N*-methylpyrrole) formed on steel increased with applied current and oxalic acid concentration (Table 4(a)–(c)). Increasing the applied current from 0.56 to 3.38 mA/cm^2 increased the weight of coatings from 0.11 and 0.07 to 0.86 and 1.20 mg/cm^2 for oxalic acid concentra-

Table 3
Composition of the solution containing DMF

No. of solution	[MPy] (M)	[OA] (M)	V_f (DMF) (%)
6	0.1	0.1	14
7	0.1	0.4	6
8	0.2	0.1	22

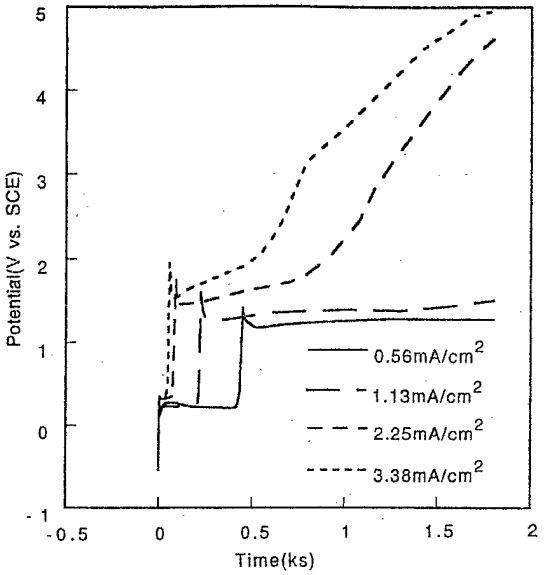

Fig. 8. Potential–time curves for the formation of poly(*N*-methylpyrrole) coatings on steel in aqueous/DMF medium, [MPy] = 0.1 M, [OA] = 0.1 M.

tions of 0.1 and 0.4 M, respectively. Note that increasing the oxalic acid concentration for this system resulted in a significant increase in the amount of polymer formed. It is believed that the dissolution of steel is minimized in the presence of DMF. Increased monomer concentration also resulted in increased amount of coatings formed on steel (Table 4(a)–(b)).

The electropolymerization potential–time curves for the polymerization of *N*-methylpyrrole in DMF were steadier than those obtained in the ethanol–water system. For reaction system 6 (Table 3), the electropolymerization potentials at 0.56 and 1.13 mA/cm^2 were 1.26 and 1.37 V, respectively. The corresponding electropolymerization potentials were 1.0 and 1.28 V for reaction system 7 (Table 3). For reaction systems 6 and 7, the quality of the coatings decreased after 30 min of reaction when the current densities were above 2.25 mA/cm^2. The corresponding polymerization potential of *N*-methylpyrrole first increased slowly with reaction time, then increased very rapidly with reaction time. For reaction system 8, smooth, uniform and strongly adherent poly(*N*-methylpyrrole) coating was formed on the steel substrate when the applied current density was 0.56 mA/cm^2. The corresponding polymerization potential of *N*-methylpyrrole was around 0.96 V. When the applied current densities were above 1.13 mA/cm^2, however, the steel substrates were only

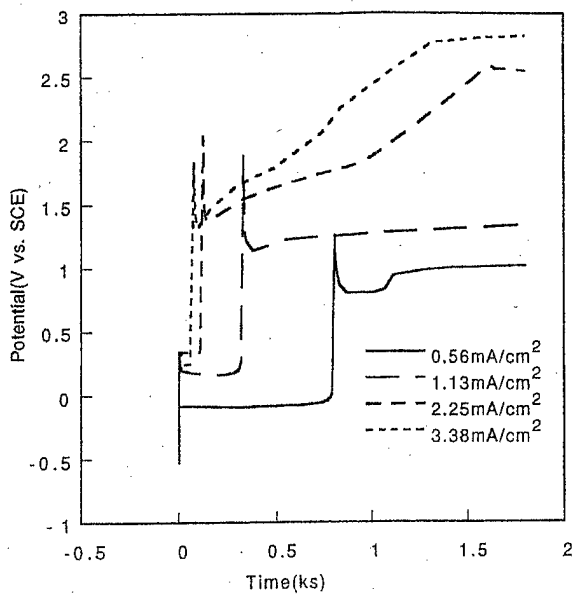

Fig. 9. Potential–time curves for the formation of poly(*N*-methylpyrrole) coatings on steel in aqueous/DFM medium, [MPy] = 0.1 M, [OA] = 0.4 M.

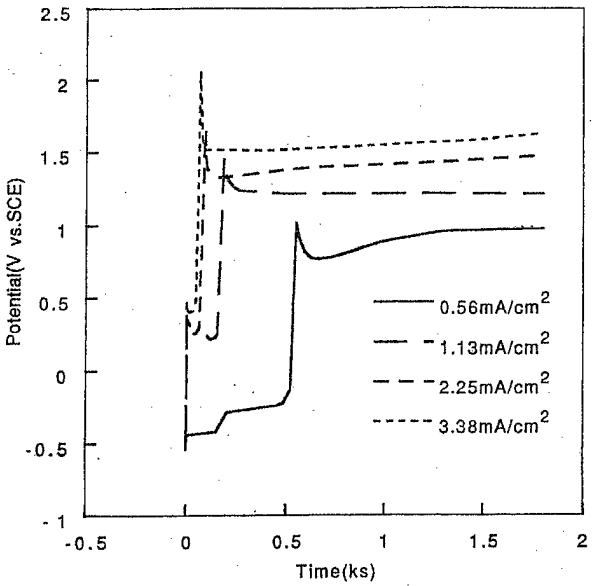

Fig. 10. Potential–time curves for the formation of poly(*N*-methylpyrrole) coatings on steel in aqueous/DFM medium, [MPy] = 0.2 M, [OA] = 0.1 M.

partially coated. The polymerization potential of *N*-methylpyrrole remained roughly constant instead of increasing with time, indicating that the passivation of the steel substrate was not well established. It seems that high content of DMF is not favorable for the passivation of steel and formation of high-quality poly(*N*-methylpyrrole) coatings.

3.3. Composition and morphology of the poly(N-methylpyrrole) coatings

The poly(*N*-methylpyrrole) coatings scraped from the steel substrates were first analyzed by elemental analysis and

Table 4

i (mA/cm^2)	Induction time (s)	Passivation charge (mC/cm^2)	Polymerization potential (V vs. SCE)	Weight change (mg/cm^2)
(a) Characteristics of the formation process of MPPy on steel in aqueous/DMF solution, [MPy] = 0.1 M, [OA] = 0.1 M				
0.56	449	251	1.26	0.11
1.13	223	252	1.37	0.26
2.25	91	205		0.56
3.38	56	189		0.86
(b) Characteristics of the formation process of MPPy on steel in aqueous/DMF solution, [MPy] = 0.2 M, [OA] = 0.1 M				
0.56	550	308	0.96	0.22
1.13	184	208	1.22	0.36
2.25	89	200	1.43	0.66
3.38	65	220	1.58	0.79
(c) Characteristics of the formation process of MPPy on steel in aqueous/DMF solution, [MPy] = 0.1 M, [OA] = 0.4 M				
0.56	805	451	1.00	0.07
1.13	331	374	1.28	0.25
2.25	123	277		0.74
3.38	74	250		1.20

the results are listed in Table 5. The results show the presence of oxygen in the coatings, indicating the electrolyte was doped into poly(*N*-methylpyrrole). Assuming that the counterion was $HC_2O_4^-$ [15], the degree of insertion of the counterions was calculated to be 0.39. This value is a little bit higher than the corresponding value of polypyrrole coatings [16].

The IR spectra of *N*-methylpyrrole, oxalic acid and poly(*N*-methylpyrrole) are shown in Fig. 11. The poly(*N*-methylpyrrole) coatings show the IR characteristic peaks

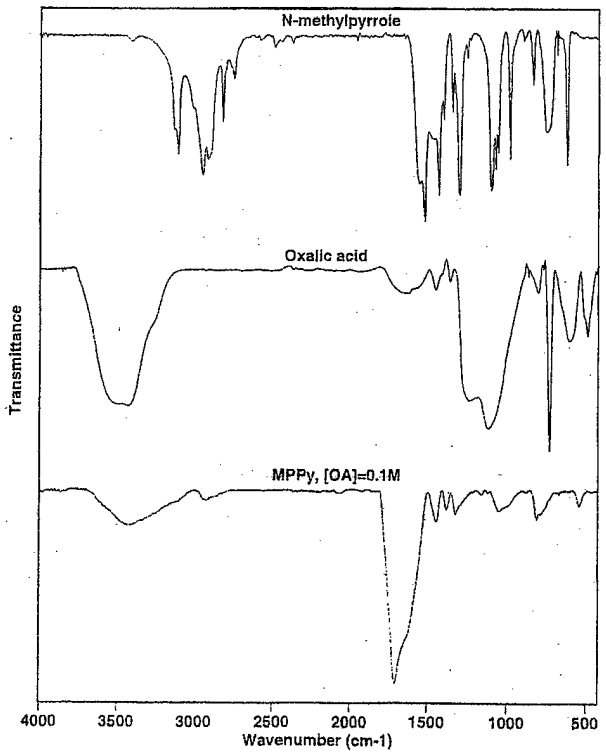

Fig. 11. IR spectra of *N*-methylpyrrole, oxalic acid and poly(*N*-methylpyrrole).

Table 5
Results of the elemental analysis of the coating

Elements	Content (%)
C	56.15
H	4.72
N	13.04
S	23.35

associated with *N*-methylpyrrole units and the oxalate counterions. The main characteristic peaks of the poly(*N*-methylpyrrole) coatings are assigned as the following [20,21]. The broad peak occurring at 3440 cm^{-1} is attributed to the O–H stretch of the counterions. The peak at 2924 cm^{-1} comes from the CH_3 stretch of the *N*-methylpyrrole unit. The strong peaks at 1717 and 1642 cm^{-1} are characteristic of C=O stretch of the counterions. The three weak peaks at 1441, 1377 and 1317 cm^{-1} are due to the ring stretch of the *N*-methylpyrrole units. The peak at 1159 cm^{-1} may correspond to C–O stretch of the counterions. The peak at 1048 cm^{-1} is assigned to the C–H in-plane deformation of the *N*-methylpyrrole units. Those peaks occurring at 873, 810 and 785 cm^{-1} are due to the C–H out-of-plane deformation of the *N*-methylpyrrole units. The peak at 589 cm^{-1} is perhaps caused by the C–C–O in-plane deformation of the counterions. Thus, the IR spectra also confirm the formation of the poly(*N*-methylpyrrole) and the incorporation of the electrolyte into the coatings.

Fig. 12 compares the SEM micrographs of the bare steel substrate and the poly(*N*-methylpyrrole) coating. The poly(*N*-methylpyrrole) coating was formed at the applied current density of 1.13 mA/cm^2 for 30 min in aqueous solution with 0.2 M electrolyte concentration. It can be seen that the steel substrate was uniformly covered by the poly(*N*-methylpyrrole) coating. Fine microspheroidal grains were

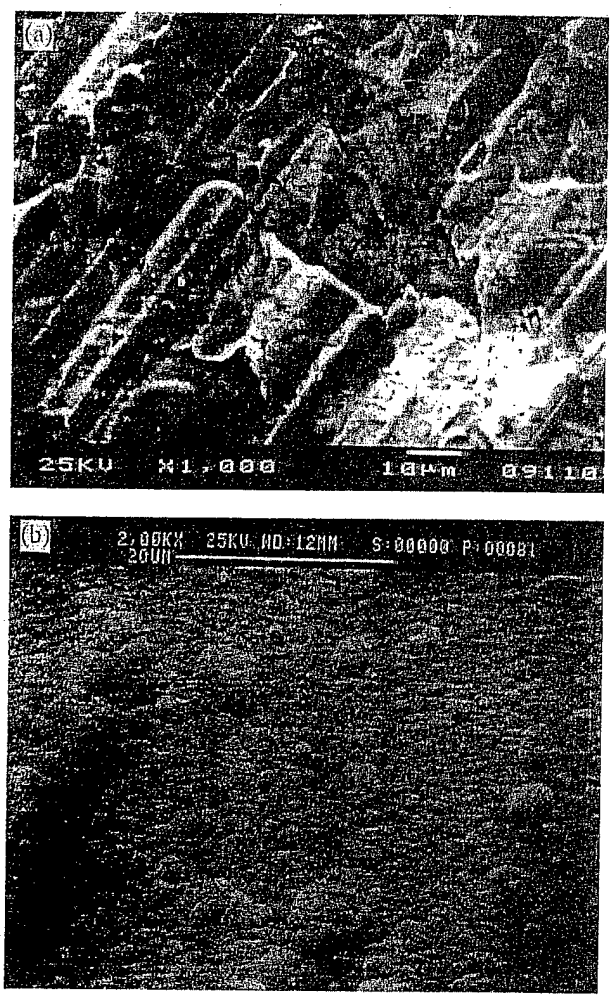

Fig. 12. SEM micrographs of (a) bare steel and (b) poly(*N*-methylpyrrole) coating.

observed on the surface of the coatings. Overall, the surface of the poly(*N*-methylpyrrole) coating was very smooth.

4. Conclusions

Poly(*N*-methylpyrrole) coatings have been successfully formed on steel by a one-step electrochemical process in aqueous medium and aqueous/organic mixing media. The formation process of poly(*N*-methylpyrrole) coatings on steel substrates turns out to be a very complex process. All electrochemical reactions were found to involve an induction period preceding the electropolymerization of *N*-methylpyrrole. All induction times decreased with increasing applied current density. The formation process and properties of the coatings were also influenced by the solvent composition and other reaction parameters. In order to obtain uniform and strongly adherent poly(*N*-methylpyrrole) coatings on steel substrate, the solvent composition and other reaction parameters must be carefully controlled.

Acknowledgements

Financial support from the Office of Naval Research, Grant N00014-95-1-0485, is gratefully acknowledged.

References

[1] G.E.F. Brew, J. Appl. Electrochem. 13 (1983) 269.
[2] G.L. Burnside, G.E.F. Brewer, J. Paint Technol. 36 (1992) 96.
[3] D.A. Jones, Principle and Prevention of Corrosion, Macmillan, London, 1992.
[4] A. Maddison, in D.E. Packham (ed.), Handbook of Adhesion, Longman Scientific & Technical, Essex, UK, 1992, p. 91.
[5] H.S. Bender, Prog. Org. Coat. 8 (1980) 241.
[6] J.O. Iroh, J.P. Bell, D.A. Scola, J. Appl. Polym. Sci. 41 (1990) 735.
[7] J.O. Iroh, J.P. Bell, D.A. Scola, Chem. Mater. 5 (1993) 78.
[8] G.A. Wood, J.O. Iroh, Synth. Met. 80 (1996) 73.
[9] W. Su, J.O. Iroh, Electrochim. Acta 42 (1997) 2685.
[10] K.M. Cheung, D. Bloor, G.C. Stevens, Polymer 29 (1988) 1709.
[11] C.A. Ferreira, S. Aeiyach, M. Delamar, P.C. Lacaze, J. Electroanal. Chem. 284 (1990) 351.
[12] M. Schirmeisen, F. Beck, J. Appl. Electrochem. 19 (1989) 401.
[13] F. Beck, R. Michaelis, J. Coat. Technol. 64 (1992) 59.
[14] F. Beck, R. Michaelis, F. Schloten, B. Zinger, Electrochim. Acta 39 (1994) 229.
[15] W. Su, J.O. Iroh, J. Appl. Polym. Sci. 65 (1997) 417.
[16] W. Su, J.O. Iroh, Synth. Met., in press.
[17] A.F. Diaz, J. Castillo, K.K. Kanazawa, J.A. Logan, J. Electroanal. Chem. 133 (1982) 233.
[18] S. Asavapiriyanont, G.K. Gunawardena, D. Pletcher, J. Electroanal. Chem. 177 (1984) 245.
[19] R.J. Mammone, M. Binder, J. Electrochem. Soc. 137 (1990) 2135.
[20] R.A. Jones (ed.), Heterocyclic Compounds, Pyrroles, Vol. 48, Part 1, Wiley, New York, 1990.
[21] G. Socrates, Infrared Characteristic Group Frequencies, Wiley, New York, 2nd edn., 1994.

Electrodeposition of Poly(*N*-methylpyrrole) Coatings on Steel from Aqueous Medium

WENCHENG SU, JUDE O. IROH

Department of Materials Science and Engineering, University of Cincinnati, Cincinnati, Ohio 45221–0012, USA

Received 14 November 1997; accepted 19 May 1998

ABSTRACT: Poly(*N*-methylpyrrole) coatings were formed on low carbon steel by an electrochemical method from aqueous oxalate solutions. The electrochemical reactions were performed in a wide range of pH of the reaction medium and applied current density. The formation of poly(*N*-methylpyrrole) on steel occurred in three stages: (i) dissolution of the steel, followed by (ii) passivation of the steel, and, finally, (iii) electropolymerization of *N*-methylpyrrole on the passivated steel. The time taken to form the passive interphase (induction time) is decreased by an increased applied current. Passivation occurred instantaneously at pH 8.4. Below pH 7, the shortest passivation time occurred at pH 2.6. The quantity of the charge consumed during passivation (passivation charge) remained independent of the applied current at pH ≈ 2.6 and decreased with the applied current at pH 4.1 and 5.7. The polymerization potential increased with the pH and the applied current. Polymerization potentials greater than 2.0 V resulted in film degradation. By controlling the electrochemical process parameters, good quality poly(*N*-methylpyrrole) was formed at a controlled induction time. © 1999 John Wiley & Sons, Inc. J Appl Polym Sci 71: 1293–1302, 1999

Key words: poly(*N*-methylpyrrole) coatings; electrodeposition; steel; aqueous medium

INTRODUCTION

Electrochemical polymerization plays an important role in many technologies, especially in surface modification and materials preparation. It has been used for a variety of purposes ranging from the formation of polymers in solution[1] to modification of graphite fibers[2] and formation of *in situ* matrix composites.[3,4] It is also being recognized as an effective technique for the synthesis of conducting polymers.[5] One of the successful examples is the electrochemical preparation of conducting polypyrrole on inert electrodes. So far, a vast number of articles can be found in the literature concerning various aspects of this material.[6–21]

Diaz et al. first prepared a series of *N*-substituted polypyrrole films on Pt electrodes in an Et_4NBF_4/CH_3CN solution.[12] Their results showed that the polymeric films are very difficult to prepare when the derivatives contain longer alkyl groups such as propyl or butyl groups. The conductivity, level of oxidation, and density of the resulting films show a decreasing trend as the size of the alkyl substituents is increased. The oxidation potential of the neutral *N*-alkyl-substituted polypyrrole is also increased by the presence of the substituents. While polypyrrole oxidizes at minus;0.2 V, the substituted polypyrrole films with *N*-alkyl substitutents oxidize in the region 0.45–0.64 V. The higher oxidation poten-

Correspondence to: J. O. Iroh.
Contract grant sponsor: Office of Naval Research.
Journal of Applied Polymer Science, Vol. 71, 1293–1302 (1999)
 CCC 0021-8995/99/081293-10

tial of *N*-alkyl-substituted pyrrole suggests a potential for enhanced corrosion resistance. Continuous poly(β-methylpyrrole) films also have been prepared by polymerizing β-methylpyrrole in acetonitrile solutions containing tetraethylammonium tetrafluoroborate.[13] The conductivity of poly(β-methylpyrrole) is intermediate between polypyrrole and poly(*N*-methylpyrrole) (MPPy). The electrodeposition of MPPy films on Pt from aqueous solutions also has been investigated. Asavapiriyanont et al. showed that nucleation and growth is the mechanism for the electrodeposition of MPPy.[14] Mammone and Binder also found that the physical properties of the resulting MPPy films were dependent on the anions used in the aqueous electrolyte.15

Recently, the electrodeposition of polypyrrole on iron substrate in an organic or aqueous solution also has been reported.[16–21] But there is not much information on the systematic formation of MPPy on steel from aqueous mediums. Aqueous electrochemical polymerization is easy to control and environmentally friendly. It is hoped that aqueous electropolymerization will replace the traditional coating technique which involves the hazardous and environmentally unsafe chromate-rinse process.[22] Other advantages of the electrochemical technique includes the possibility of forming the polymer films directly on the substrate and the ability to effectively control the properties of the polymer films by proper choice of the process parameters. The aim of this research work was to investigate the effect of the applied current, the pH of the electrolyte–monomer solution, and the electrolyte concentration on the passivation of steel and the subsequent electrodeposition of MPPy coatings on the passivated steel from aqueous medium. MPPy-coated steel is believed to have an attractive corrosion resistance.

EXPERIMENTAL

N-Methylpyrrole and oxalic acid were Aldrich products. Triethylamine (TEA) was purchased from Fisher Scientific. Aqueous solutions used in the experiments were made from deionized water.

Aqueous electrodeposition of MPPy coatings on steel was carried out in a one-compartment polypropylene cell. The working electrodes were made from 0.5-mm-thick QD low carbon steel panels provided by the Q-panel Co. The coated surface area of the steel was 8.88 cm^2. All the steel sheets were degreased with tetrachloroethylene for about 1 h prior to the electrochemical experiments. The counter electrodes comprised two titanium alloy plates. An saturated calomel electrode (SCE) manufactured by the Corning Co. was used as the reference electrode. The instrument used to electrochemically coat the low carbon steel was an EG&G Princeton Applied Research Potentiostat/Galvanostat Model 273A. Electropolymerization of *N*-methylpyrrole on the steel substrate was performed galvanostatically. The working electrode and counter electrodes were used as the anode and cathode, respectively. The current density used in this experiment was varied from 0.5 to 4 mA/cm^2. The concentration of the monomer was kept constant at 0.05*M* for all the experiments. The electrolyte concentration was varied between 0.1 and 0.2*M*. The pH of the reaction medium was varied from 1 to 9. The pH of the solution containing *N*-methylpyrrole and oxalic acid was adjusted by TEA. After each experiment, the coated steel sheet was rinsed with methanol and dried at 65°C to a constant weight.

A Bio-Rad FTS-40 FTIR spectrometer was used to measure the IR spectra of the coatings using potassium bromide (KBr) pellets. Elemental analysis of the coating scraped from the substrate was done by Galbraith Laboratories, Inc. The morphology of the coatings was examined by scanning electron microscopy (SEM). The SEM specimens were shadowed with gold to enhance their conductivity.

RESULTS AND DISCUSSION

Features of the Electrodeposition Process

The formation process of MPPy coatings on steel was first investigated with a 0.1*M* electrolyte concentration in a wide range of pH of the reaction medium and applied current density. The corresponding potential time curves are shown in Figures 1–4. As shown in Figures 1 and 2, the processes occurring in the acidic medium were quite different from those occurring in the alkaline medium. In the acidic medium, the formation process of MPPy coatings is characterized by three distinct stages: (i) dissolution of the steel, followed by (ii) passivation of the steel, and, finally, (iii) electropolymerization of *N*-methylpyrrole on the passivated steel. The time taken to form the passive interphase (induction time) is decreased

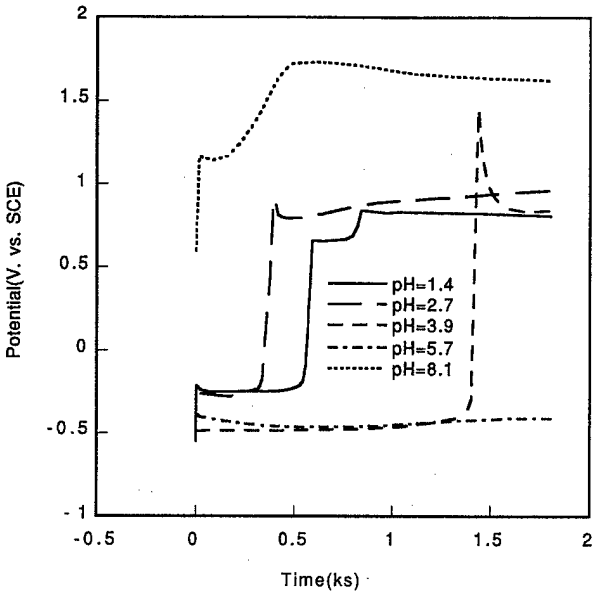

Figure 1 Potential time curves for the formation of MPPy on steel in different pH mediums, [RX] = 0.1*M*, i = 0.56 mA/cm^2.

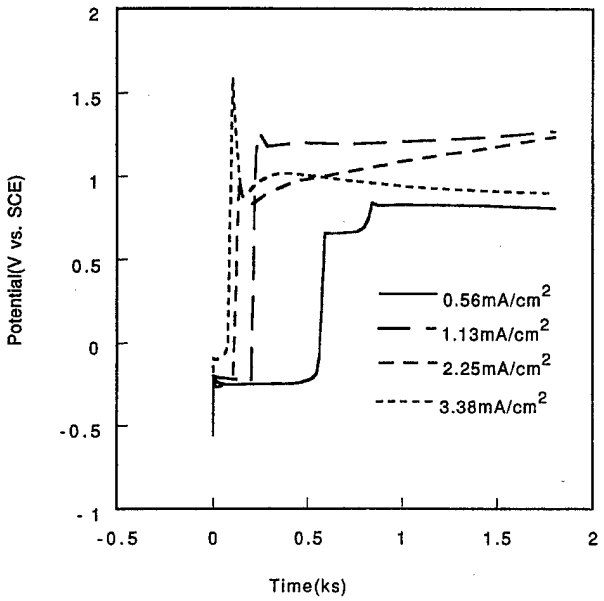

Figure 3 Potential time curves for the formatiuon of MPPy on steel at different current densities, pH 1.4, [OA] = 0.1*M*.

by an increased applied current and increased pH of the monomer–electrolyte solution. It can be seen that the pH of the reaction medium and applied current density have significant effects on the induction time (Figs. 1 and 2). When the other reaction parameters were kept constant, the induction time was the shortest at pH 2.4, and the longest, at pH 6.0. Overall, the induction time was changed according to following sequence:

$$\tau\text{pH} = 5.7 > \tau\text{pH} = 3.9 > \tau\text{pH} = 1.4 > \tau\text{pH} = 2.7 \quad (1)$$

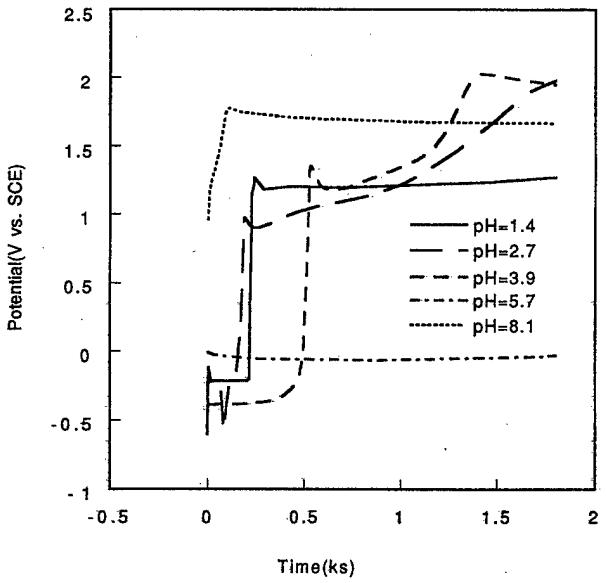

Figure 2 Potential time curves for the formation of MPPy on steel in different pH mediums, [RX] = 0.1*M*, i = 1.13 mA/cm^2.

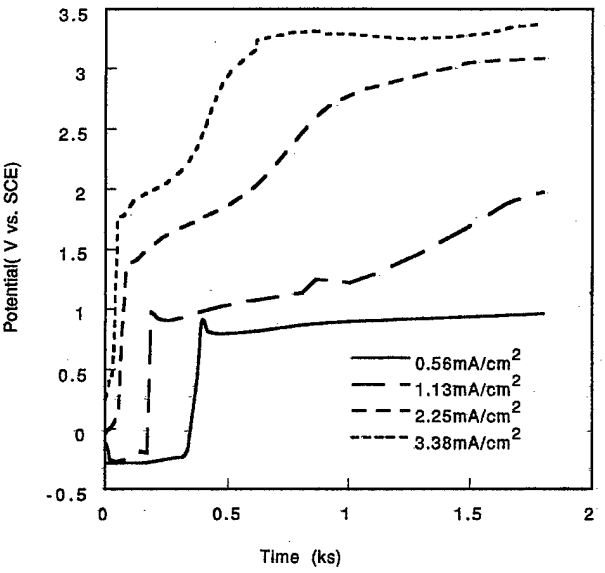

Figure 4 Potential time curves for the formatiuon of MPPy on steel at different current densities, pH 2.7, [RX] = 0.1*M*.

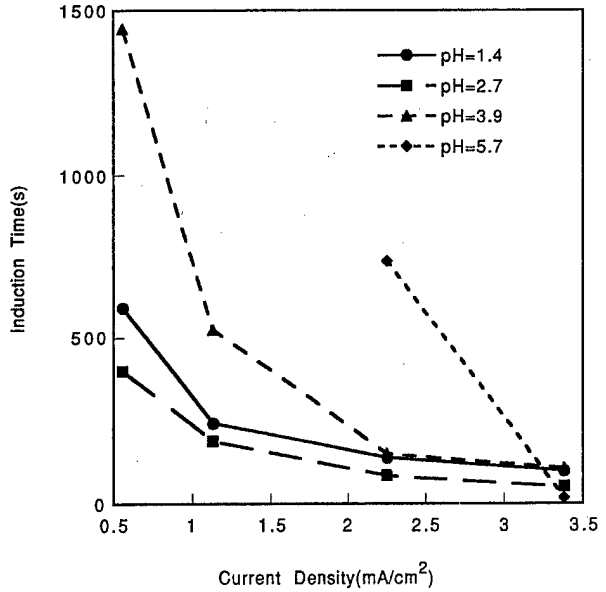

Figure 5 Relationship between induction time and applied current density at different pH, [RX] = 0.1*M*.

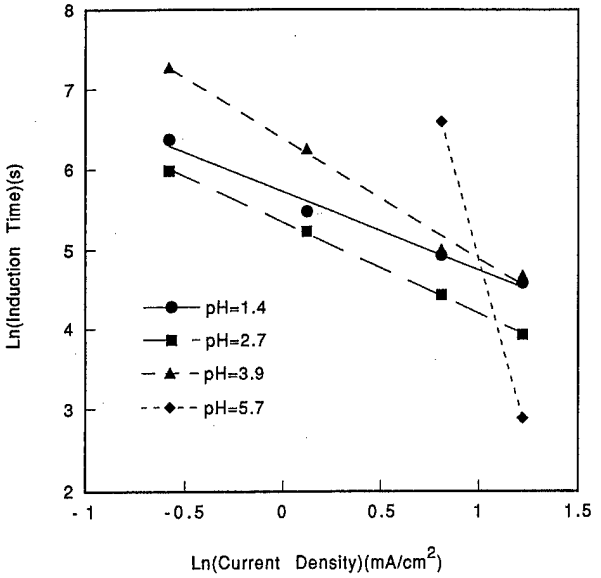

Figure 6 Dependence of induction time on applied current density at different pH, RX] = 0.1*M*.

Figure 5 shows the variation of the induction time with the applied current density at different pH. It is apparent that the induction time decreased dramatically with the applied current density for each pH medium. Because no passivation of the steel was observed in the medium of pH of 5.7 at current densities below 1.13 mA/cm^2, only the induction time corresponding to higher current densities, i = 2.25 and 3.38 mA/cm^2, is shown in Figure 5. The effects of pH on the induction time also can be seen more clearly from Figure 5. At a low applied current density, that is, 0.56 mA/cm^2, the difference in the induction time among different acidic mediums was very large. For example, the induction time was 398 s for the medium of pH of 2.7 while the induction time became 1142 s for the medium of 3.9. However, when the applied current density was increased to 3.38 mA/cm^2, the induction time became very similar for all the four reaction mediums. The dependence of the induction time on the applied current density is also plotted in Figure 6, where Ln(Induction Time) and Ln(Current Density) showed a very good linear relationship and obeyed the following equations:

$$\text{pH} = 1.4: \quad \text{Ln}\,\tau = 5.73 - 0.98\text{Ln}\,i \qquad (2)$$

$$\text{pH} = 2.7: \quad \text{Ln}\,\tau = 5.34 - 1.14\text{Ln}\,i \qquad (3)$$

$$\text{pH} = 3.9: \quad \text{Ln}\,\tau = 6.40 - 1.50\text{Ln}\,i \qquad (4)$$

$$\text{pH} = 5.7: \quad \text{Ln}\,\tau = 13.93 - 9.05\text{Ln}\,i \qquad (5)$$

Figure 7 shows the change in the charge consumed during the induction time with the applied current density for different reaction mediums. It

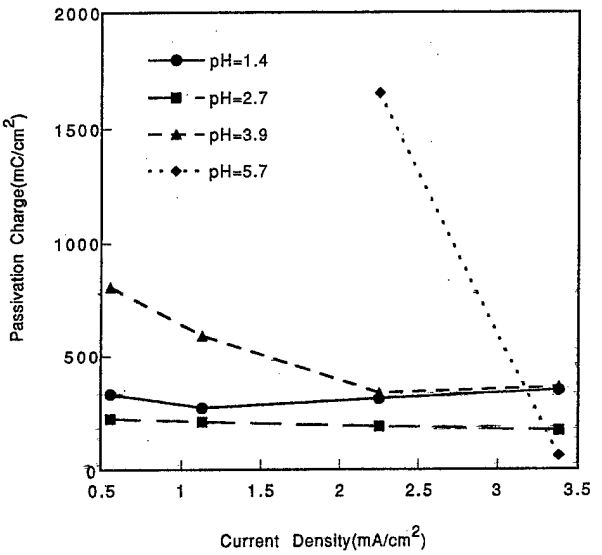

Figure 7 The relationship between passivation charge and applied current density at different pH, [RX] = 0.1*M*.

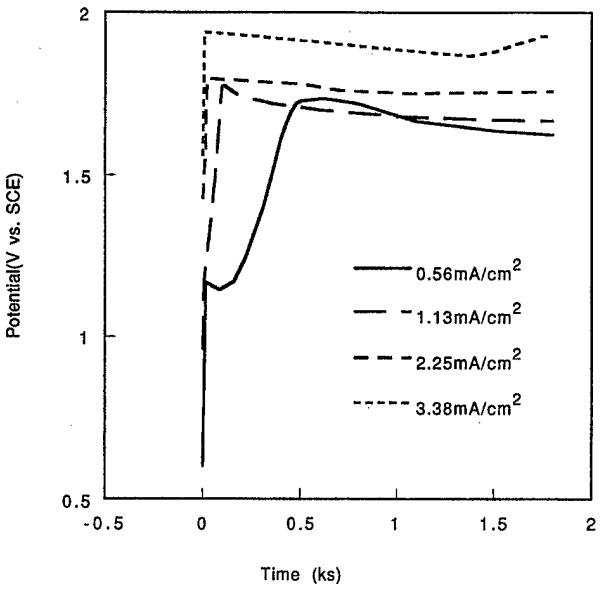

Figure 8 Potential time curves for the formatiuon of MPPy on steel at different current densities, pH 8.1, [RX] = 0.1*M*.

can be seen that the passivation charge shows a different behavior in the different mediums. The passivation charge was maintained roughly constant for the reaction mediums of pH of 1.4 and 2.7. For the medium of pH of 3.9, the passivation charge first decreased with the current density, then remained roughly constant when the current density was increased above 2.25 mA/cm^2. The passivation charge decreased sharply for the reaction medium of pH of 5.7.

In the case of the alkaline medium (Fig. 8), no induction period was observed and the reaction potential immediately attained a high positive value after the current was applied. These results are not unusual. According to Pourbaix, the application of an anodic potential to an iron immersed in alkaline medium will bring about the passivation of the iron.[22]

When the passivation of the substrate was well established, MPPy coatings began to form on the substrate. But the properties of the coatings were found to be dependent on the pH of the reaction medium and the applied current density. When the pH of the medium was 1.4, there were a few small holes on the surface of the coatings after a 30-min reaction at the current density of 0.56 or 1.13 mA/cm^2. Many small holes were observed at the current density of 2.25 mA/cm^2. The substrate was only partially coated after a 30-min reaction at 3.38 mA/cm^2; the weight of the coated substrate was even less than that of the initial substrate. Their potential time curves were also different. When the applied current density was 0.56 and 1.13 mA/cm^2, the electropolymerization potential of *N*-methylpyrrole was maintained roughly constant during the electropolymerization period. The polymerization potential increased from about 0.8 to about 1.2 V when the applied current density was increased from 0.56 to 1.13mA/cm^2. However, the electropolymerization potentials of *N*-methylpyrrole at 2.25 and 3.38 mA/cm^2 were lower than that at 1.13 mA/cm^2, indicating that the passivation of the steel was not well established.

For the reaction medium of pH of 2.7, smooth, coherent, and strongly adherent coatings were obtained when the applied current density was below 1.13 mA/cm^2. The coatings obtained at a current density above 2.25 mA/cm^2 were coherent, but they were brittle and separated from the substrate. However, smooth, coherent, and strongly adherent coatings could be obtained at shorter reaction times. The potential time curves were different from those of the reaction medium of pH of 1.4. For the reaction medium of pH of 2.7, the electropolymerization potential was maintained roughly constant around 0.89 V at the current density of 0.56 mA/cm^2. At 1.13 mA/cm^2, the polymerization potential increased slowly with time during the electropolymerization period. When the current density was increased to 2.25 and 3.38 mA/cm^2, the electropolymerization potential first increased very rapidly with the reaction time, then tended to level off. For the same reaction time, the electropolymerization potential increased with the applied current density. Generally speaking, the adhesion of the coatings to the substrate would become very poor if the reaction potential exceeded 1.5 V. The potential time curves for the electropolymerization of *N*-methylpyrrole are also different from those for the electropolymerization of pyrrole. The electropolymerization potential of pyrrole on steel is very steady at the current density discussed above.[19–21] This may be due to the low conductivity of the MPPy films.

When the pH of the reaction medium was about 3.9, black coatings were formed, but the coatings were not uniform. At 0.56 mA/cm^2, the substrate was only partially coated. For the reaction medium of pH 5.7, a thin brown coating was formed on the substrate at the current density

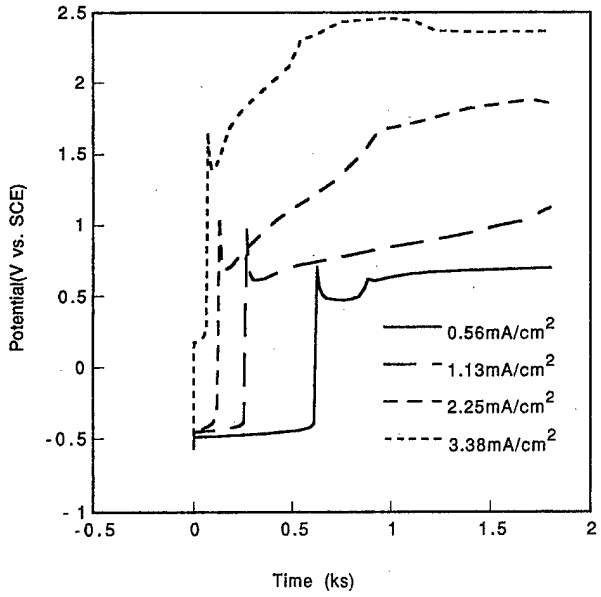

Figure 9 Potential time curves for the formation of MPPy on steel at different current densities, pH 1.2, [RX] = 0.2*M*.

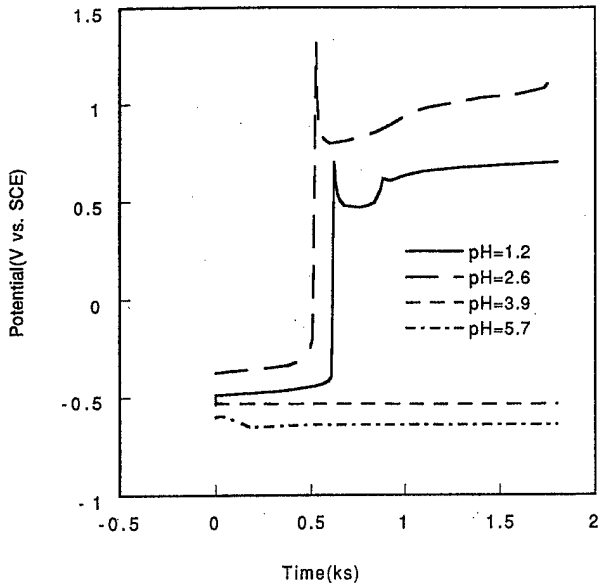

Figure 10 Potential time curves for the formation of MPPy on steel at different pH, [RX] = 0.2*M*, i = 0.56 mA/cm^2.

above 2.25mA/cm^2, but the coating was not uniform. In the alkaline medium, the coatings obtained were very similar to those formed in the medium of pH 5.7. The detailed mechanism of the above phenomenon is not clear. Perhaps a high pH medium is not advantageous for the nucleation and growth of MPPy coatings. In the alkaline medium, the corresponding polymerization potentials were basically maintained constant during the reaction period and they showed an increasing trend with the applied current density.

The effects of the pH of the acidic medium and applied current density on the formation of MPPy coatings were further investigated in a 0.2*M* electrolyte solution. The corresponding potential time curves are shown in Figures 9–12. The variation of the induction time with pH shows a similar trend to that of the above system. However, compared to the potential time curves obtained in the 0.1*M* electrolyte solution, it seems that the induction time was increased by increasing the electrolyte concentration and the difference in the induction time between these two electrolyte concentrations increased with the pH. For example, when the pH of the solution was around 1.4, the difference in the induction time was only about 30 s at 0.56 mA/cm^2. However, when the pH of the medium was around 3.9, the induction time was about 1142 s at 0.56 mA/cm^2 for the system with the 0.1*M* electrolyte concentration while the induction time was more than 1800 s for the system with the 0.2*M* electrolyte concentration.

Figures 13 and 14 show the variation of the corresponding induction time with the applied current density for different pH mediums. For

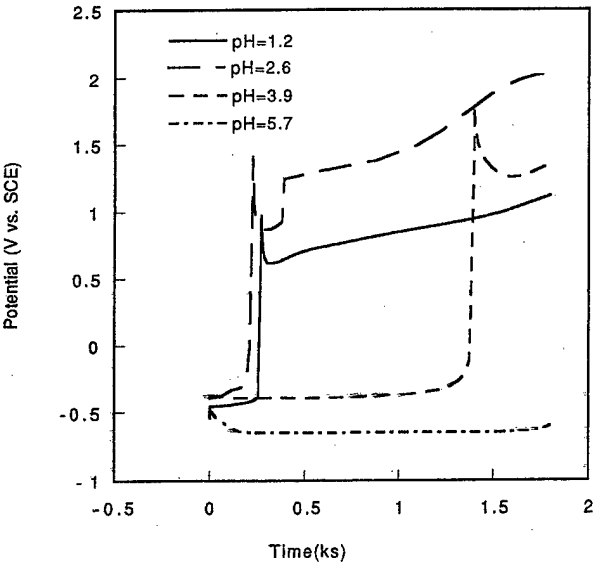

Figure 11 Potential time curves for the formation of MPPy on steel at different pH, [RX] = 0.2*M*, i = 1.13 mA/cm^2.

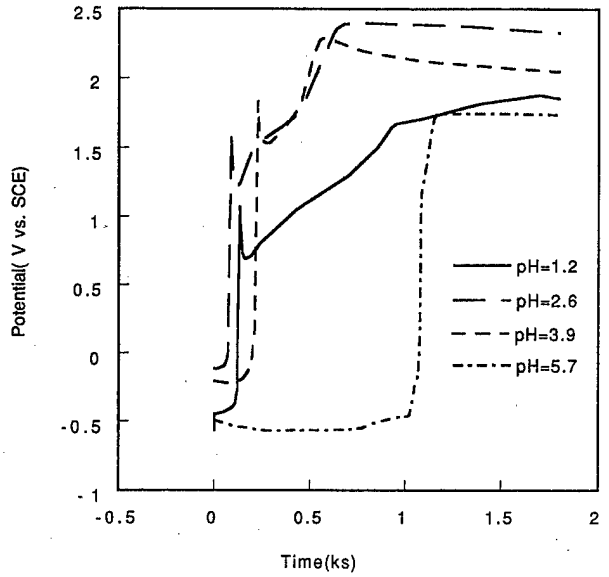

Figure 12 Potential time curves for the formation of MPPy on steel at different pH, [RX] = 0.2*M*, i = 2.25 mA/cm^2.

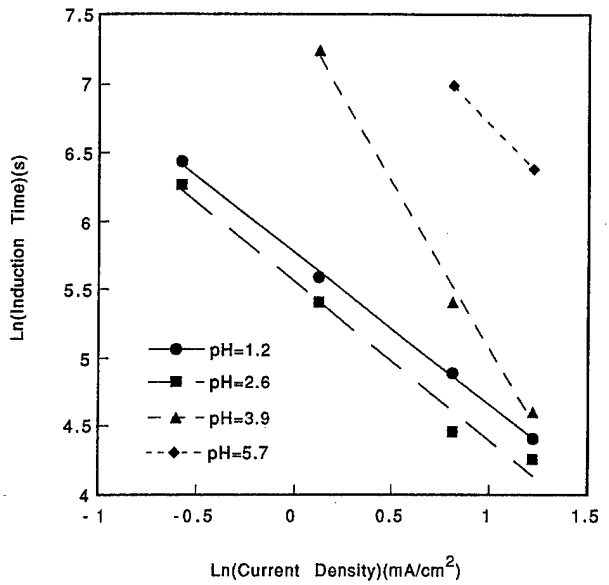

Figure 14 Dependence of induction time on applied current density at different pH, [RX] = 0.2.

each medium, the induction time also decreased dramatically with the current density. When the current density was below 2.25 mA/cm^2, the difference in the induction time was very large among the different mediums. At 3.38 mA/cm^2, the induction time of the reaction medium with a pH below 3.9 became very close, but the medium with a pH of 5.7 still had a much higher induction time than those of the other mediums. As shown in Figure 14, the Ln(Induction Time) and Ln(Current Density) also show a very good linear relationship and obey the following equations:

$$\text{pH} = 1.2: \quad \text{Ln}\,\tau = 5.77 - 1.12\text{Ln}\,i \qquad (6)$$

$$\text{pH} = 2.6: \quad \text{Ln}\,\tau = 5.56 - 1.16\text{Ln}\,i \qquad (7)$$

$$\text{pH} = 3.9: \quad \text{Ln}\,\tau = 7.49 - 2.43\text{Ln}\,i \qquad (8)$$

$$\text{pH} = 5.7: \quad \text{Ln}\,\tau = 8.20 - 1.49\text{Ln}\,i \qquad (9)$$

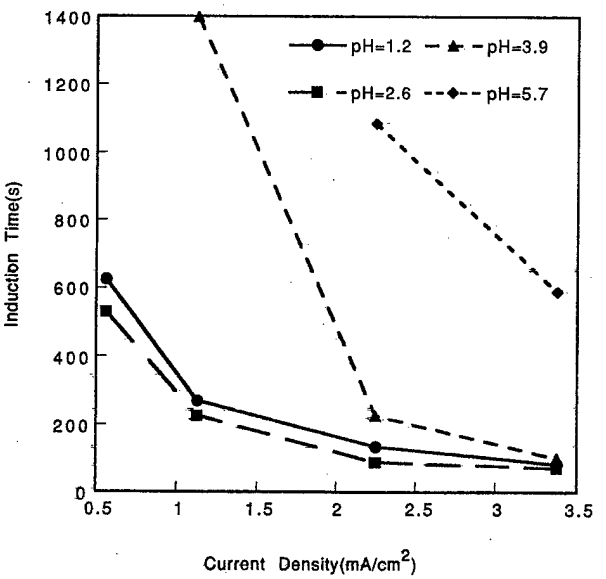

Figure 13 Relationship between induction time and applied current density at different pH, [RX] = 0.2*M*.

Figure 15 shows the change in the charge consumed during the induction time with the applied current density for the different reaction mediums. The passivation charge was maintained roughly constant for the reaction mediums of pH 1.4 and 2.4. For the mediums of pH 3.9 and 5.7, the passivation charge decreased gradually with the applied current density. Beck et al. investigated the formation of polypyrrole coatings on steel using oxalic acid as the electrolyte.[19,20] They suggested that the passivation of iron was due to the formation of an iron oxalate interlayer. But it seems that the electrochemical parameters have significant effects on the formation of the interlayer. The detailed mechanism is now being investigated in our lab.

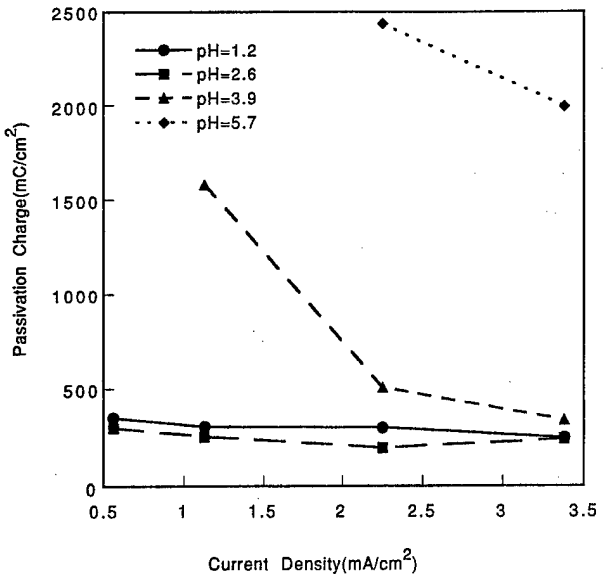

Figure 15 Relationship between passivation charge and applied current density at different pH, [RX] = 0.2*M*.

When the concentration of oxalic acid was increased to 0.2*M* (pH 1.2), smooth, coherent, and strongly adherent coatings were obtained at a current density below 1.13 mA/cm^2. When the applied current density was above 2.25 mA/cm^2, coherent coatings were obtained after a 30-min reaction, but the coatings were brittle and separated from the substrate. Coherent, smooth, and strongly adherent coatings still could be obtained at shorter reaction times. The potential time curves (Fig. 9) were very similar to those of the medium of pH 2.7 with the 0.1*M* electrolyte concentration. The properties of the coatings formed in the medium of pH 2.6 were very similar to those of the coatings formed in the medium of pH 1.2, that is, coherent and strongly adherent coatings could be obtained at a low applied current density. The quality of the coatings obtained in higher pH mediums was not very good either.

Characterization of the MPPy Coatings

The results of the elemental analysis of the costings formed in the medium of pH 1.2 are listed in Table I. The results show the presence of oxygen in the coatings, indicating that the electrolyte was doped into the MPPy coatings. Assuming that $HC_2O_4^-$ was the counterion,[15] the degree of insertion of the counterion was calculated to be 0.39.

Figure 16 shows the IR spectra of the MPPy coatings formed in different pH mediums. It can be seen that the coatings formed in the different mediums have similar IR spectra. The characteristic peaks are assigned as follows[16,17,23,24]: The broad peaks occurring at 3446–3424 cm^{-1} correspond to the O—H stretch of the counterions. The peaks at 2932–2924 cm^{-1} are attributed to the CH_3 stretch of *N*-methylpyrrole units. The strong peaks at 1712–1704 cm^{-1} and 1656–1653 cm^{-1} are characteristic of the C=O stretch of the counterions. The three weak peaks at 1442–1438, 1382–1373, and 1320–1319 cm^{-1} are due to the ring stretch of the *N*-methylpyrrole unit. The peaks at 1159–1155 cm^{-1} are perhaps caused by

Table I Results of the Elemental Analysis of the Coatings

Elements	Content (%)
C	56.15
H	4.72
N	13.04
O	23.35

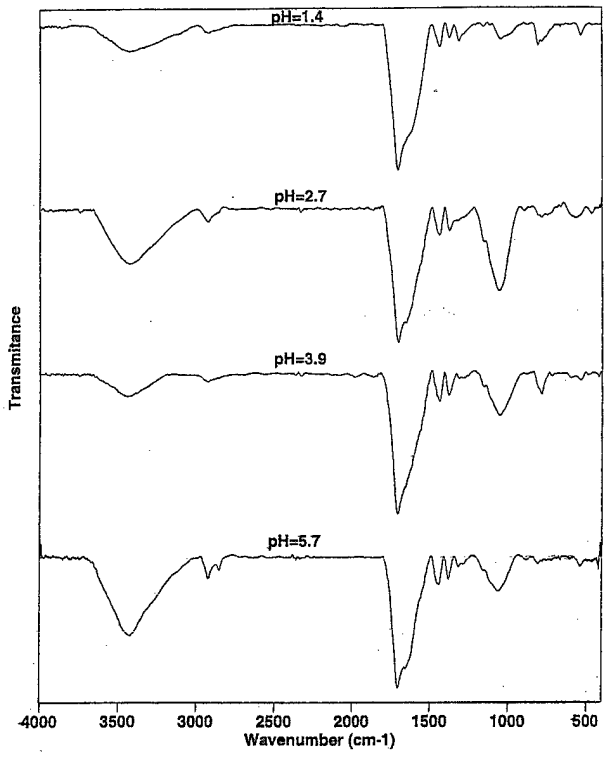

Figure 16 IR spectra of the MPPy coatings formed in different pH medium, [RX] = 0.1*M*.

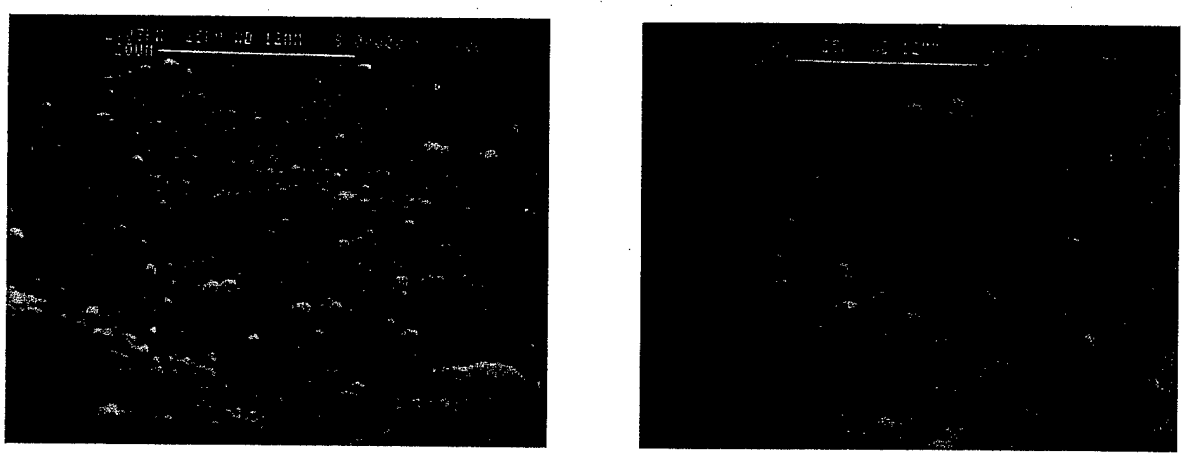

Figure 17 SEM micrograph of MPPy coatings formed at different conditions 0.56 mA/cm^2 (left), 1.13 mA/cm^2 (right).

the C—O stretch of the counterions. The peaks at 1062–1045 cm^{-1} are due to the C—H in-plane deformation of the *N*-methylpyrrole units. Those peaks occurring at 898–873, 824–807, and 786–754 cm^{-1} are due to C—H out-of-plane deformation of the *N*-methylpyrrole units. The peaks at 608–578 cm^{-1} may come from C—C—O in-plane deformation of the counterions. Thus, the IR results further confirm the formation of MPPy coatings and the doping of the counterions in the coatings.

The SEM micrograph for the the MPPy coatings formed in different conditions is shown in Figure 17. It can be seen that the steel substrate is uniformly covered by the MPPy coatings. The coatings formed in different conditions all show a fine microspheroidal surface morphology. Overall, the surface of the coatings was very smooth.

CONCLUSIONS

A process has been developed for the aqueous electrodeposition of MPPy coatings onto low carbon steel substrate. This process combines the formation of the polymeric coatings and the deposition of the coatings onto the substrate in one process. In this process, no pretreatment was performed as is the practice in traditional coating techniques. In acidic medium, the reactions were characterized by an induction period. The induction time is the time it took to form passive films on steel. It decreased dramatically with increasing current density. It was also varied with the pH. The shortest induction time was obtained at pH 2.7 while the longest induction time occurred at pH 6.0. The induction at pH 1.4 was shorter than that at pH 4.1. It was shown that the induction time was increased by increased electrolyte concentration. The properties of the coatings were also influenced by the electrochemical process parameters. To prepare coherent, smooth, and strongly adherent MPPy coatings on steel substrate, the electrochemical process parameters must be optimized.

The authors wish to thank the Office of Naval Research, ONR's Young Investigator Program, for financial support.

REFERENCES

1. Funt, B. L.; Bhdani, S. N. Can J Chem 1964, 42, 2733.
2. Bell , J. P.; Chang, J.; Rhee, H.W.; Joseph, R. Polym Compos 1987, 8, 46.
3. Iroh, J. O.; Bell, J. P.; Scola, D. A. J Appl Polym Sci 1990, 41, 735.
4. Iroh, J. O.; Bell, J. P.; Scola, D. A. Chem Mater 1993, 5(1), 78.
5. Handbook of Conducting Polymers; Marcel Dekker: New York, 1986.
6. Diaz, A. F.; Keiji Kanazawa, K. J Chem. Sci Chem Commun 1979, 635.
7. Genies, E. M.; Bidan, G.; Diaz, A. F. J Electrochem Soc 1983, 149, 101.
8. Wood, G. A.; Iroh, J. O. Synth Met 1996, 80, 73.
9. Su, W.; Iroh, J. O. Electrochim Acta 1997, 42, 2685.
10. Otero, T. F.; Angulo, E. J Appl Electrochem 1992, 22, 369.

11. Grunden, B.; Iroh, J. O. Polymer 1995, 36, 559.
12. Diaz, A. F.; Castillo, J.; Kanazawa, K. K.; Logan, J. A. J Electroanal Chem 1982, 133, 233.
13. Salmon, M.; Diaz, A. F.; Login, A. J.; Krounbi, M.; Bargon, J. Mol Cryst Liq Cryst 1982, 83, 265.
14. Asavapiriyanont, S.; Gunawardena, G. K.; Pletcher, D. J Electroanal Chem 1984, 177, 245.
15. Mammone, R. J.; Binder, M. J Electrochem Soc 1990, 137, 2135.
16. Cheung, K. M.; Bloor, D.; Stevens, G. C. Polymer 1988, 29, 1709.
17. Ferreira, C. A.; Aeiyach, S.; Delamar, M.; Lacaze, P. C. J Electroanal Chem 1990, 284, 351.
18. Schirmeisen, M.; Beck, F. J Appl Electrochem 1989, 19, 401.
19. Beck, F.; Michaelis, R. J. Coat Technol 1992, 64, 59.
20. Beck, F.; Michaelis, R.; Schloten, F.; Zinger, B. Electrochim Acta 1994, 39, 229.
21. Su, W.; Iroh, J. O. J Appl Polym Sci 1997, 65, 417.
22. Jones, D. A. Principles and Prevention of Corrosion; Macmillan: New York, 1992.
23. Heterocyclic Compounds; Jones, R. A., Ed.; Pyrroles, Vol. 48, Part 1; Wiley: New York, 1990.
24. Socrates, G. Infared Characteristic Group Frequencies, 2nd ed.; Wiley: New York, 1994.

PERGAMON

Electrochimica Acta 44 (1999) 3321–3332

ELECTROCHIMICA Acta

IR and XPS studies on the interphase and poly(*N*-methylpyrrole) coatings electrodeposited on steel substrates

Wencheng Su, Jude O. Iroh*

Department of Materials Science and Engineering, University of Cincinnati, Cincinnati, OH 45221, USA

Received 13 August 1998; received in revised form 20 December 1998

Abstract

Poly(*N*-methylpyrrole) coatings have been electrodeposited on steel substrates from aqueous oxalate solutions. The formation process of the coatings was found to be different between acidic and basic mediums. In an acidic medium, the reactions were characterized by two stages: formation of the passive interphase and electropolymerization of the *N*-methylpyrrole. The composition of the formed interphase and poly(*N*-methylpyrrole) coatings were examined by infrared spectroscopy (IR) and X-ray photoelectron spectroscopy (XPS). Our results show that the interphase formed in an acidic medium is composed of iron(II) oxalate dihydrate. The formation of poly(*N*-methylpyrrole) coatings on steel occurred after the passivation of steel was completed. Interaction between the poly(*N*-methyl pyrrole) coatings and the interphase is shown by the broadening of the –CO absorption peak.

Keywords: Poly(*n*-methylpyrrole) coatings; Steel substrate; Interphase; IR; XPS

1. Introduction

Aqueous electrochemical polymerization is now being recognized as an effective technique in many fields, especially in surface modification and materials preparation [1–9]. Among them, the most important application for the electropolymerization process is perhaps to provide metals with protective coatings [6–9]. Aqueous electropolymerization has several advantages over the traditional coatings techniques [1]. It may eliminate the hazardous and environmentally unsafe chromate rinsing process used in the traditional coating technique [2]. It combines the formation of the polymer and deposition of the coating in one process. The reaction process can be easily automated [3]. The chemical and physical properties of the coatings can be adjusted by a proper choice of the reaction parameters [4]. Aqueous solution is used and the reactions are performed at room temperature. The production costs are relatively low.

Recently, electropolymerization has also been investigated as a technique for the forming of conducting polymeric coatings on oxidizable metals [10–16]. Since most conducting polymers are produced by oxidative processes, formation of polymer coatings can only occur on the oxidizable metal substrates when the electrochemical conditions can lead to passivation of the metals without preventing electropolymerization. It was found that only a few electrochemical systems can meet this requirement [10–16]. Recently, we have developed an electrochemical process for the formation

* Corresponding author. Tel.: +1-513-556-3096; fax: +1-513-556-2569.

E-mail address: jude.iroh@uc.edu (J.O. Iroh)

0013-4686/99/$ - see front matter
PII: S0013-4686(99)00055-9

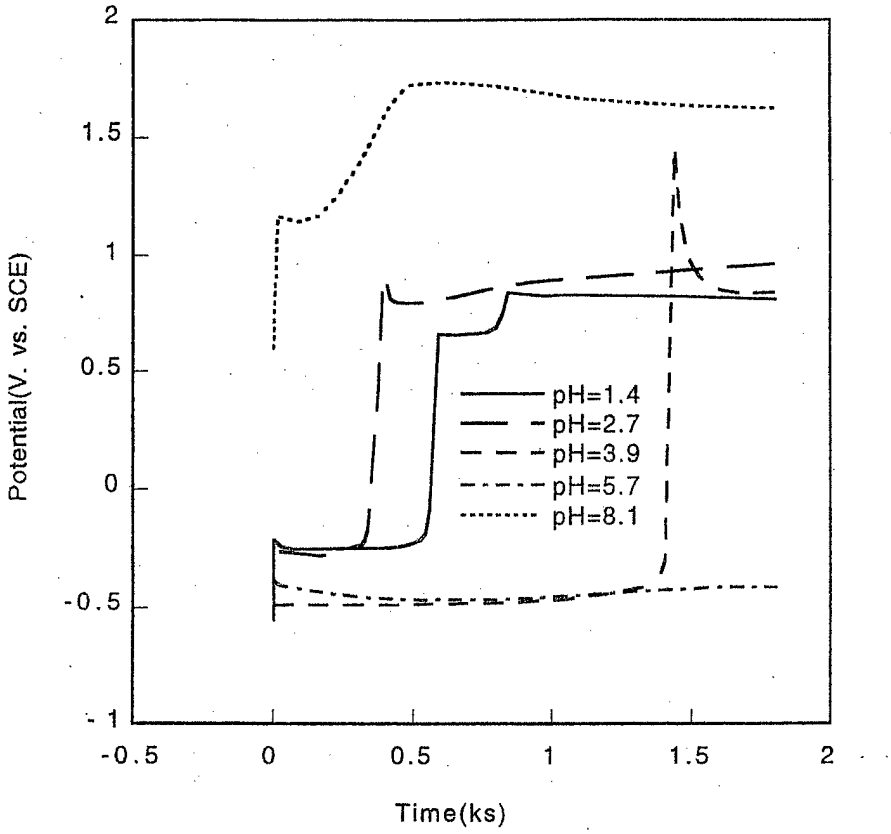

Fig. 1. Potential–time curves for the formation of MPPy on steel in different pH mediums, [RX]=0.1 M, i=0.56 mA/cm^2.

of strongly adherent poly(*N*-methylpyrrole) (MPPy) coatings from aqueous oxalate solutions. In our previous paper the effects of electrochemical parameters on the formation process have been systematically investigated [16], however, the mechanism of the electrodeposition process was not fully discussed. In this paper, we report the characterization of the interphase and the electrodeposited poly(*N*-methylpyrrole) coatings by infrared spectroscopy (IR) and X-ray photoelectron spectroscopy (XPS).

2. Experimental

2.1. Electrochemical reactions

N-methylpyrrole and oxalic acid were Aldrich products. Triethylamine was purchased from Fisher Scientific. Aqueous solutions used in the experiments were made from deionized water. QD low carbon steel panels with a thickness of 0.5 mm were provided by Q-panel Company. The as-received steel panels were first cut into small pieces, and then they were mechanically polished to a mirror finish. Finally the polished steel sheets were degreased with tetrachloroethylene for about an hour prior to the electrochemical experiments.

The electrochemical reactions were carried out in a one-compartment polypropylene cell. The working electrode used was a QD low carbon steel sheet. The counter electrodes consisted of two titanium alloy plates. A saturated calomel electrode (SCE) manufactured by Corning Company was used as the reference electrode. The electrochemical reactions were performed galvanostatically. The constant current was supplied by an EG&G Princeton Applied Research 273A Potentiostat/Galvanostat. The current density used in this experiment was varied from 0.5 to 4 mA/cm^2. The concentration of the monomer was kept constant at 0.05 M for all the experiments. The electrolyte concentration was varied between 0.1 and 0.2 M. The pH of the solutions containing *N*-methylpyrrole and oxalic acid was adjusted between 1 to 9 by addition of triethylamine (TEA). After each experiment, the coated steel sheet was rinsed thoroughly with deionized water and methanol and dried at 65°C to constant weight.

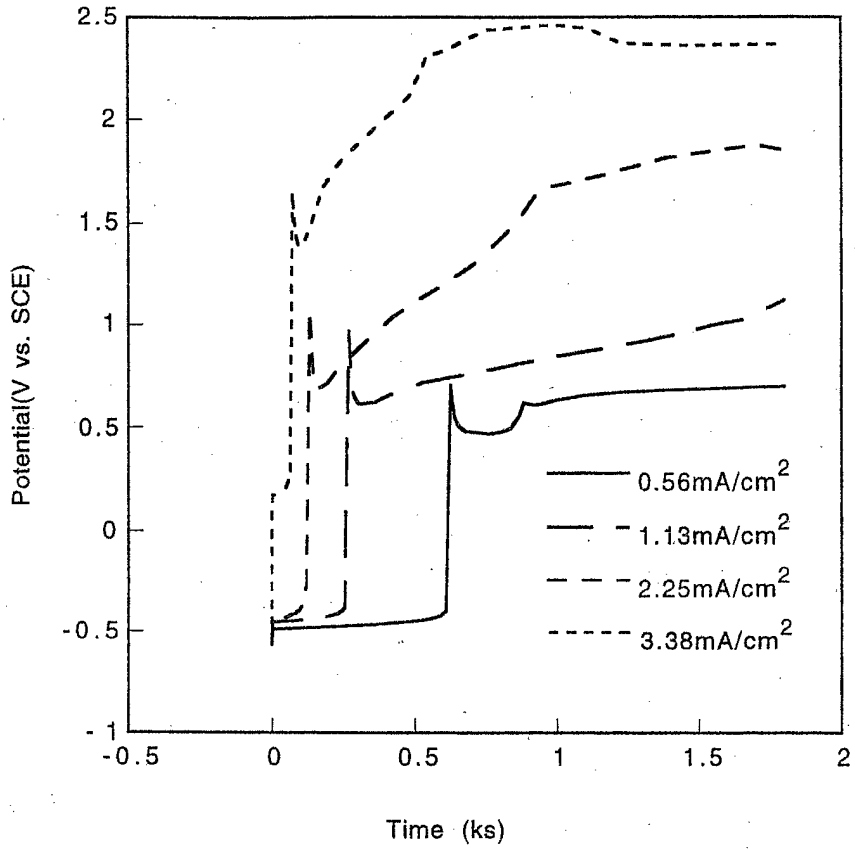

Fig. 2. Potential–time curves for the formation of MPPy on steel at different current densities, pH 1.2, [OA] = 0.2 M.

2.2. Characterization

The reflection–absorption infrared spectra (RAIR) of the samples were measured by a BIO-RAD FTS-40 FIIR spectrometer. An angular specular reflectance attachment was set to an incident angle of 65°. Spectra were obtained using a resolution of 4 cm^{-1} and were averaged over 128 scans. A background spectrum of a bare polished steel substrate was subtracted from the acquired spectra in all cases. In the case of transmission IR, the spectra were obtained by the means of potassium bromide (KBr) pellets.

A Perkin-Elmer model 5300 XPS spectrometer with Mg Ka X-rays, operating at 300 W and 15 kV dc, was used to obtain XPS spectra. An Apollo computer system with Perkin-Elmer software was used for data acquisition and processing. XPS spectra were recorded at take-off angles of 45°. The take-off angle was defined as the angle between the sample surface and the direction of propagation of the exiting photoelectrons. Binding energies are quoted relative to hydrocarbon C1s at 285.0 eV.

3. Results and discussion

3.1. Electrodeposition process

The formation process of poly(*N*-methylpyrrole) (MPPy) coatings on steel substrates was first investigated with 0.1 M electrolyte concentration in different pH mediums at the applied current density of 0.56 mA/cm^2. The corresponding potential–time curves are shown in Fig. 1. It is very interesting to note that the formation process of poly(*N*-methylpyrrole) coatings on steel is characterized by two distinct stages in acidic medium. The reaction potential remained negative in the first stage, but it rose sharply to the polymerization potential of *N*-methylpyrrole at the end of the first stage. At this current density, the polymerization potential of *N*-methylpyrrole didn't change much with time. In contrast, the reaction potential rose immediately to the polymerization potential of *N*-methylpyrrole in basic medium. The behavior of the reaction in a basic medium is expected because application of an anodic potential to iron immersed in a basic medium will bring about the passivation of the iron [17].

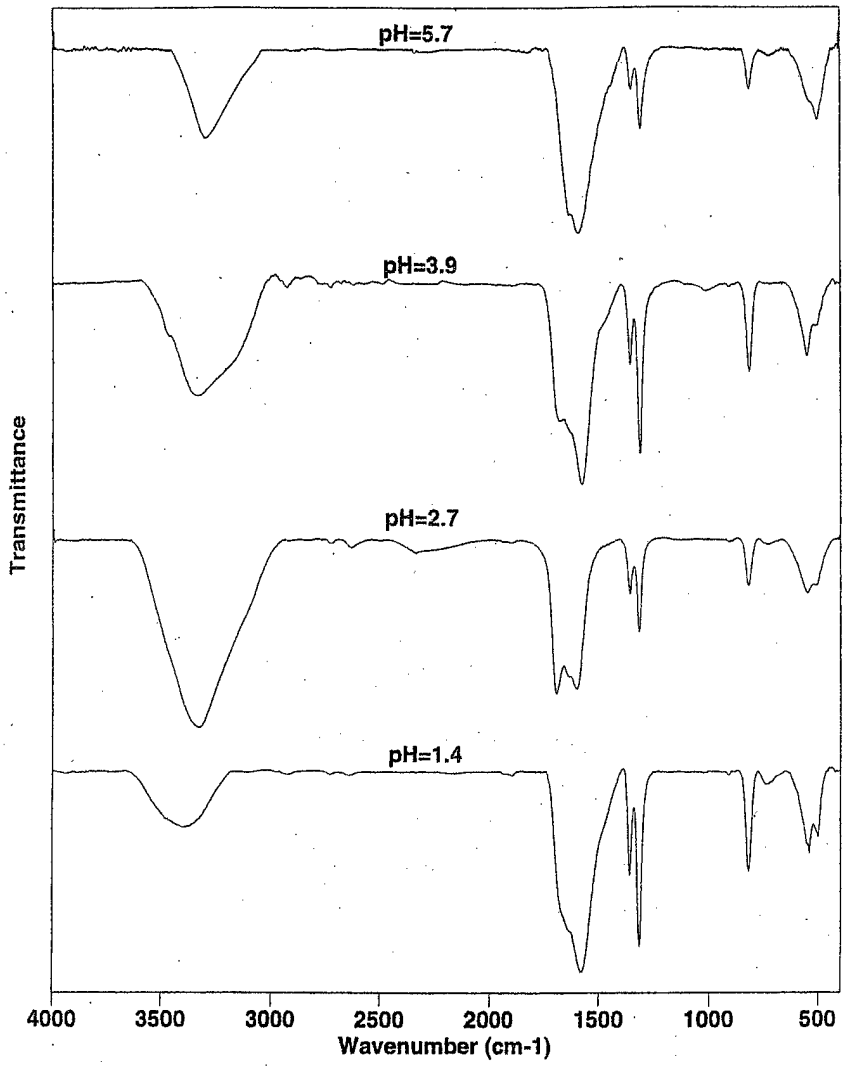

Fig. 3. RAIR spectra of the interphase formed in different pH mediums.

In an acidic medium, the first stage of the reaction can be regarded as the induction period for the polymerization of *N*-methylpyrrole. The passivation of the steel was perhaps due to the formation of an interphase at the end of the first stage. It can be seen from Fig. 1 that the pH of the acidic medium had significant effects on the induction time. When other reaction parameters were kept the same, induction time was shortest in the reaction medium of pH 2.7 while it became longest in the medium of pH 5.7. As shown in Fig. 1, no passivation of steel was established in the medium of pH 5.7 even after 30 min reaction. Overall, the induction time was changed with pH of the reaction medium according to following sequence:

$$\tau_{pH=5.7} > \tau_{pH=3.9} > \tau_{pH=1.4} > \tau_{pH=2.7}. \quad (1)$$

The effect of current density on the formation process was investigated in the reaction medium with 0.2 M oxalic acid (pH 1.2). As shown in Fig. 2, the induction time decreased dramatically with increasing current density. The electropolymerization potential maintained roughly constant at a current density of 0.56 mA/cm^2. At 1.13 mA/cm^2, the polymerization potential increased slowly with time. When the current density was increased to 2.25 and 3.38 mA/cm^2, the electropolymerization potential first increased very rapidly with reaction time, then tended to level off. The potential–time curves for the formation of poly(*N*-methylpyrrole) are different from those for the formation of polypyrrole. The polymerization potential of pyrrole was very steady during the second stage [15]. This may be due to the relatively low conductivity of

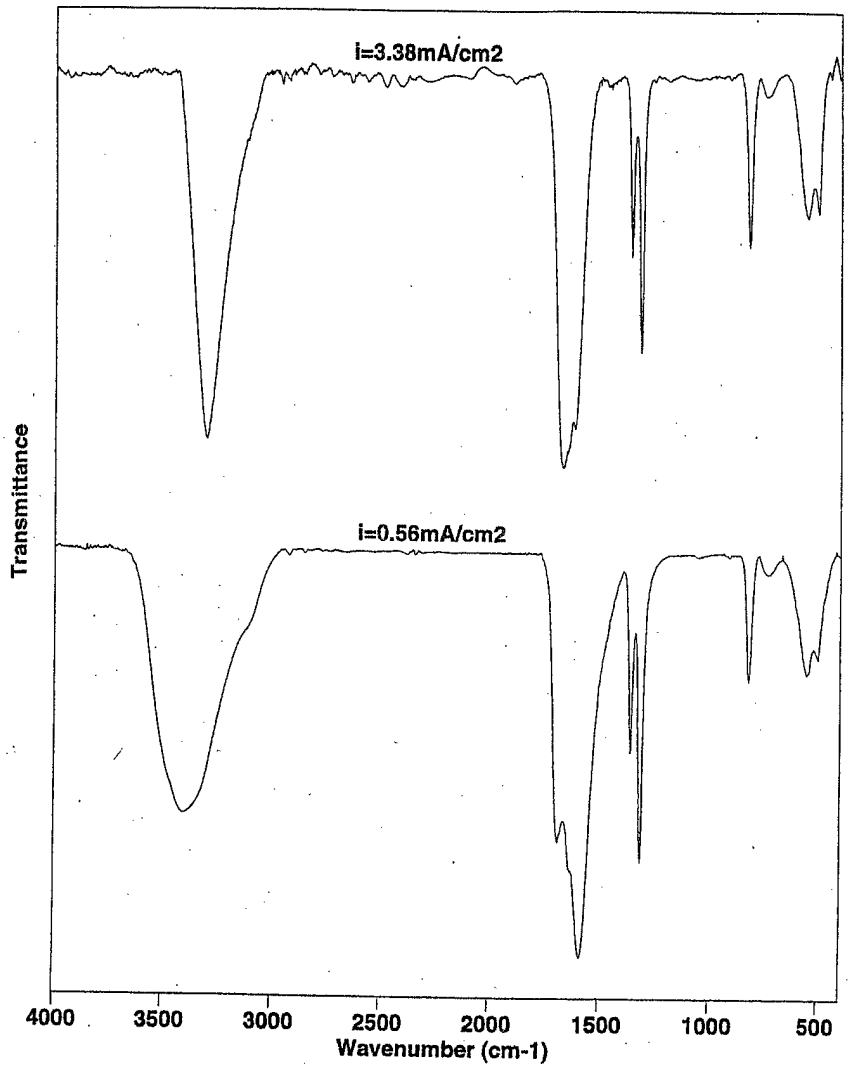

Fig. 4. RAIR spectra of the interphase formed at different current densities.

the poly(*N*-methylpyrrole) films compared to polypyrrole films.

3.2. Characterization of the interphase

The interphase samples were obtained by stopping the electrochemical reactions at the end of the induction period. Fig. 3 shows the RAIR spectra for the interphase formed at 0.56 mA/cm^2 in different pH mediums. The sample obtained in the medium of pH 6.0 was prepared at 0.56 mA/cm^2 for 30 min. There is not much difference in RAIR spectra of the interphase formed in different pH reaction mediums. Even though the passivation of the steel substrate was not established in the medium of pH 5.7, the sample still shows a spectrum similar to the other interphase. Fig. 4 shows the RAIR spectra of the interphase formed at different current densities in the medium of 0.2 M oxalic acid. The spectra of the interphase obtained at different applied current densities are also very similar. From these measurements, it seems that the interphase formed in different reaction conditions has the same composition.

Fig. 5 compares the IR spectrum of the interphase with those of $FeC_2O_4{\cdot}2H_2O$ and $Fe_2(C_2O_4)_3{\cdot}6H_2O$. The IR spectra of the two model compounds were done by transmission mode. The two iron oxalate model compounds show different IR spectra. In the spectrum of $Fe_2(C_2O_4)_3{\cdot}6H_2O$, there is a very strong C–O stretch peak around 1264 cm^{-1}, which is absent in the spectrum of $FeC_2O_4{\cdot}2H_2O$. The O–H stretch peak of $Fe_2(C_2O_4)_3{\cdot}6H_2O$ occurs around 3558 cm^{-1},

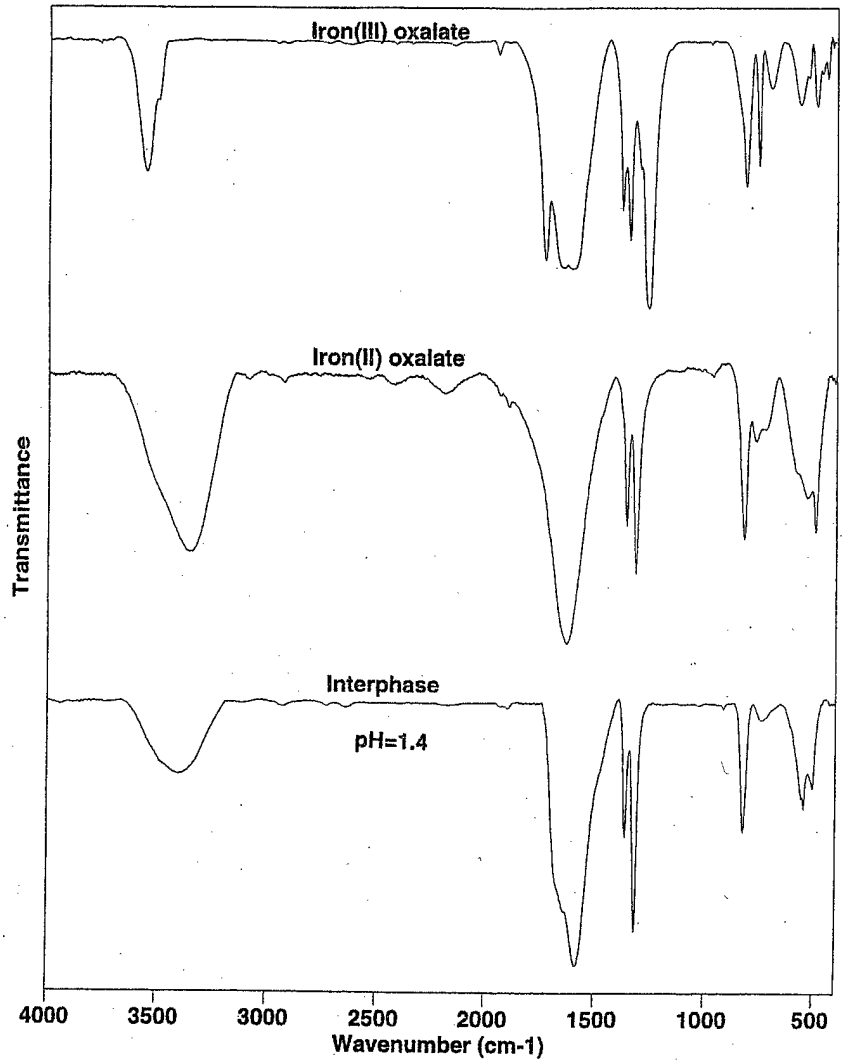

Fig. 5. IR spectra of the interphase and two model compounds.

which is about 200 cm^{-1} higher than that of $FeC_2O_4 \cdot 2H_2O$. It can be seen from Fig. 5 that the IR spectrum of the interphase is very similar to that of $FeC_2O_4 \cdot 2H_2O$. The main absorption bands for the interphase are assigned as follows [18–22]: The peaks at 3342–3304 cm^{-1}, correspond to O–H stretch. The peaks around 1695–1675, 1662–1635 and 1599–1581 cm^{-1} are characteristic of C=O stretch. The peaks located at 1364–1360 and 1322–1315 cm^{-1} are due to C–O stretch. The peaks at 828–818 cm^{-1} come from O–C=O in-plane deformation. The peaks at 743–723 cm^{-1} are perhaps caused by O–C=O in-plane deformation and Fe–O stretch. The peaks at 553–539 and 510–502 cm^{-1} are due to C–C–O in-plane deformation. Although the IR spectra of the interphase formed by different reaction parameters are basically the same, a small difference still exists for some peaks due to polar groups. For example, the shape of the peaks due to O–H and C=O groups varies with reaction conditions. The detailed mechanism is not clear so far, perhaps these peaks are influenced by the orientation of the $FeC_2O_4 \cdot 2H_2O$ molecules.

XPS measurements can also be used to distinguish Fe(II) from Fe(III). Fig. 6 shows the Fe(2p) spectra of the interphase formed at 0.56 mA/cm^2 in different pH mediums with 0.1 M electrolyte concentration. Fig. 7 shows the Fe(2p) spectra of the interphase formed at two different current densities in the medium with 0.2 M oxalic acid. The Fe(2p) spectrum of the iron(II) oxalate dihydrate is also shown in Fig. 8 for comparison. It can be seen that the Fe(2p) spectra of the interphase formed under different experimental conditions

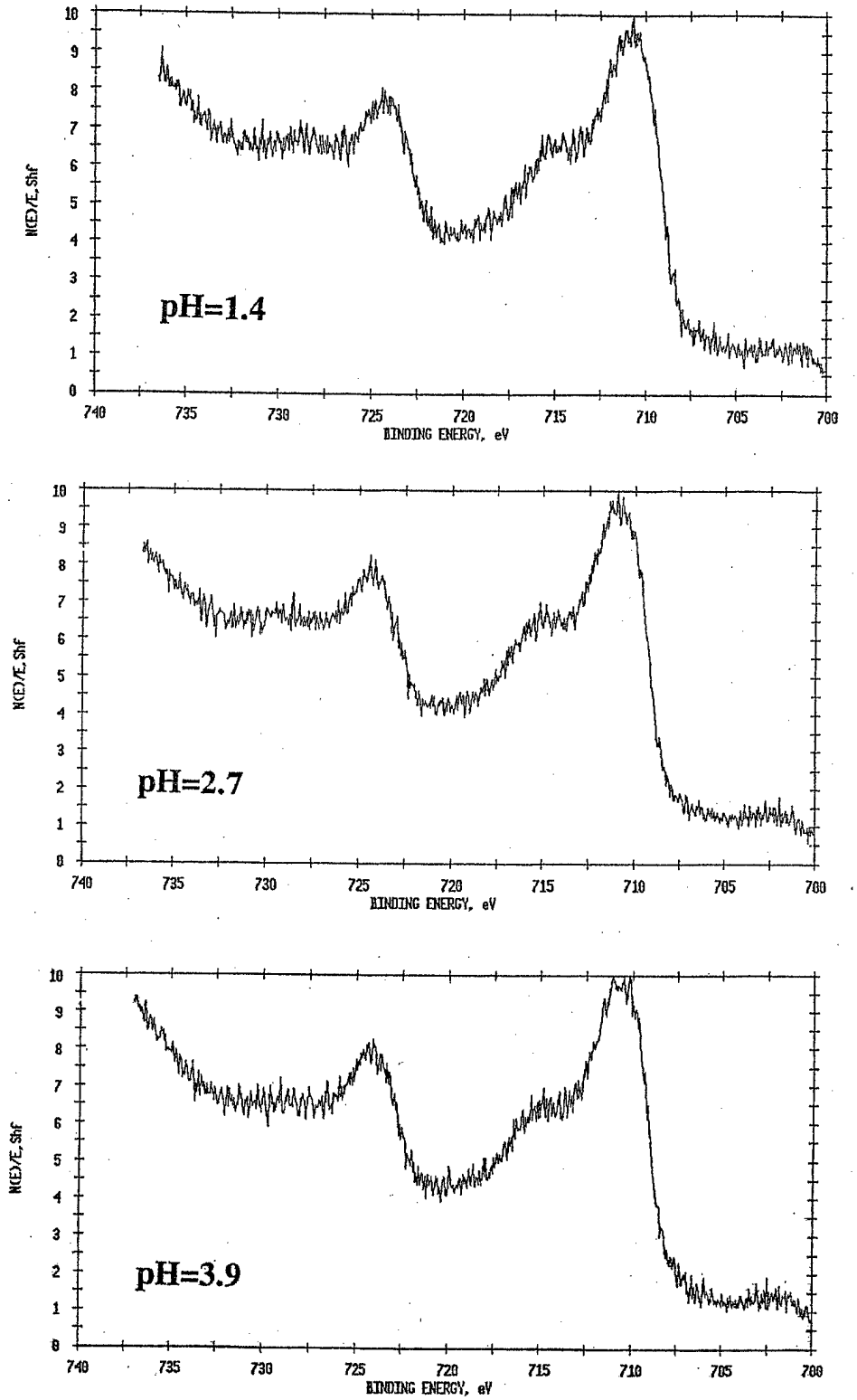

Fig. 6. Fe(2p) spectra of the interphase formed at 0.56 mA/cm^2 in different pH mediums.

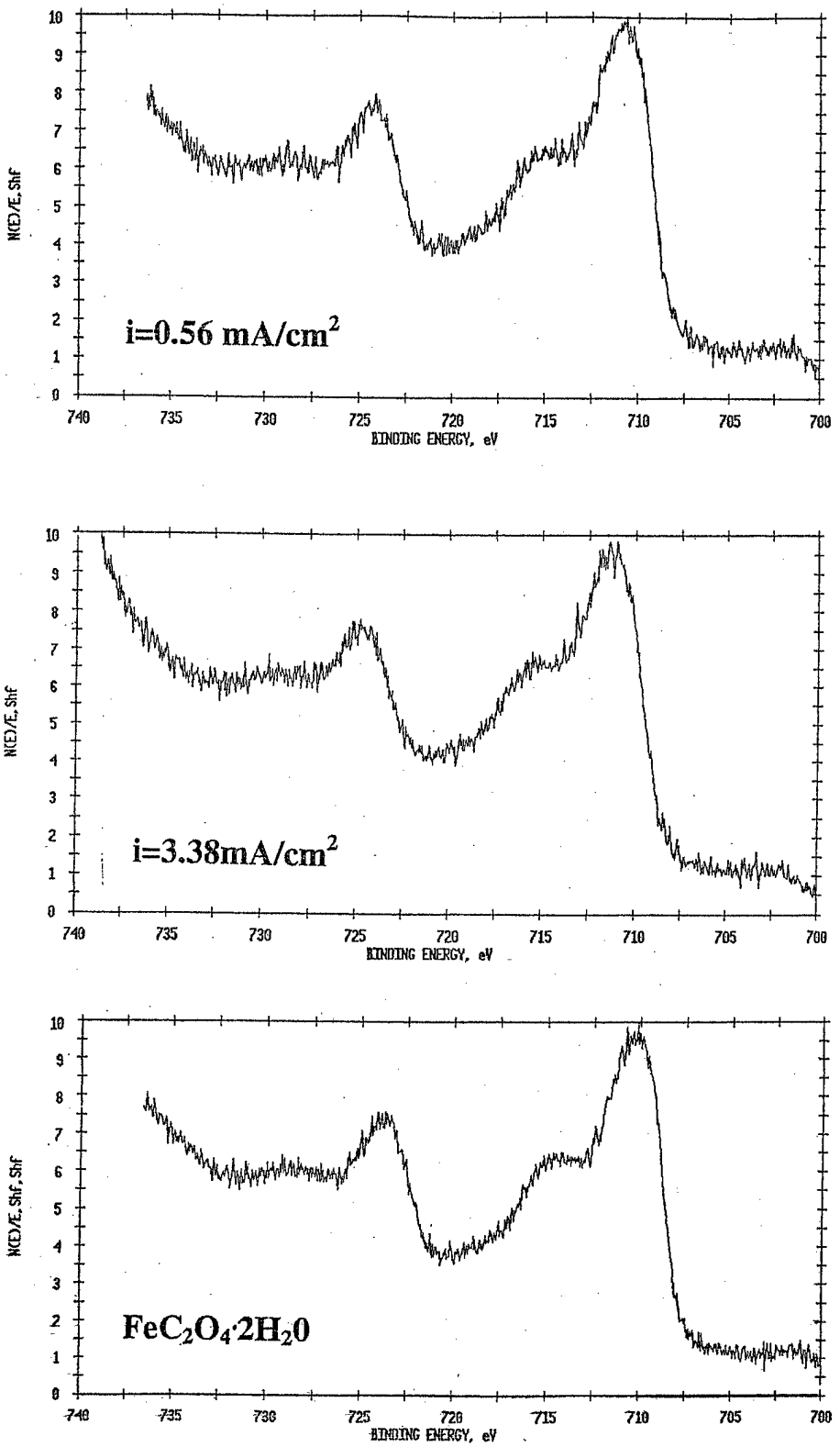

Fig. 7. Fe(2p) spectra of the interphase formed at different current densities.

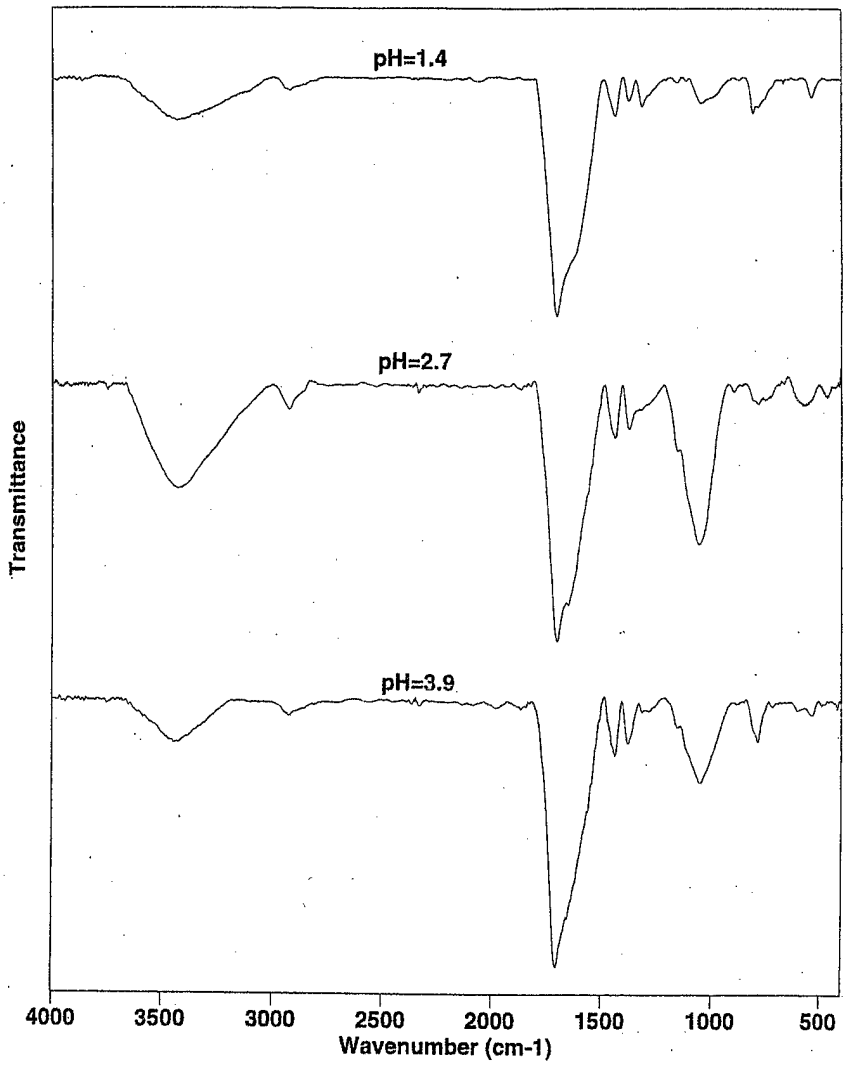

Fig. 8. IR spectra of MPPy coatings formed in different pH mediums.

are very similar and they are also very similar to that of the iron(II) oxalate dihydrate. The position of the shake-up satellites in the valley between $2p_{3/2}$ and $2p_{1/2}$ is generally used to distinguish Fe(II) from Fe(III). For the interphase formed in an acidic medium, the shake-up satellites are on the lower binding energy side of the valley, which is characteristic for Fe(II) [23]. For Fe(III), the satellite should be on the higher energy side of the valley.

From the above IR and XPS results, it can be seen that the passive interphase formed under different experimental conditions completely consists of $FeC_2O_4{\cdot}2H_2O$. The compound is perhaps produced by the following two reactions:

$$Fe - 2e \longrightarrow Fe^{2+}, \quad (2)$$

$$Fe^{2+} + C_2O_4^{2-} + 2H_2O \longrightarrow FeC_2O_4 \cdot 2H_2O. \quad (3)$$

When the steel substrate was completely covered by iron(II) oxalate dihydrate, the interphase was formed. The interphase formed insulated the steel substrate from the electrolyte solutions and passivated it. Higher current density provided a higher formation rate of $FeC_2O_4{\cdot}2H_2O$, resulting in a shorter formation time of the interphase. The effect of pH of the reaction medium on the formation time of the interphase is not well understood so far. Maybe the solubility of the $FeC_2O_4{\cdot}2H_2O$ is significantly different in different pH mediums. The solubility of $FeC_2O_4{\cdot}2H_2O$ in the medium of pH 5.7 is perhaps very large, thus it takes a very long time for $FeC_2O_4{\cdot}2H_2O$ to precipate on steel.

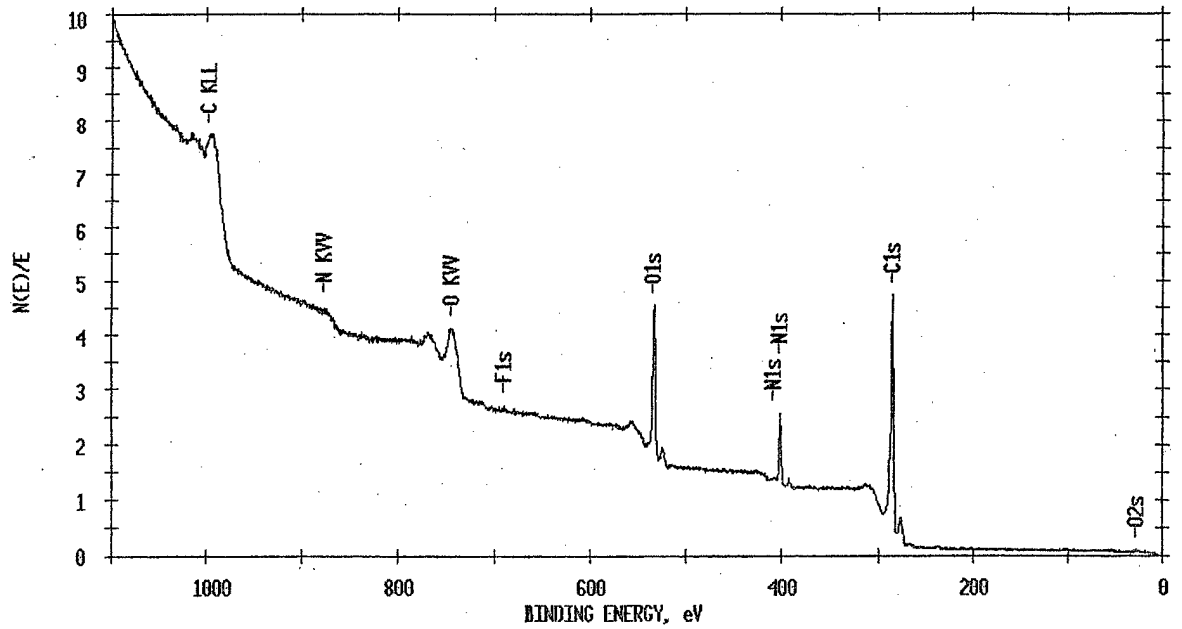

Fig. 9. XPS survey spectra of the poly(*N*-methylpyrrole) coatings.

3.3. Characterization of the poly(N-methylpyrrole) coatings

Fig. 8 shows the transmission IR spectra of the poly(*N*-methylpyrrole) coatings formed in different pH mediums. It can be seen that the coatings formed in different mediums have similar IR spectra. The characteristic peaks are assigned as follows [18,24–27]: The broad peaks occurring at 3446–3424 cm^{-1} correspond to the O–H stretch of counterions. The peaks at 2932–2924 cm^{-1} are attributed to the CH_3 stretch of the *N*-methylpyrrole units. The strong peaks at 1712–1704 cm^{-1} and 1656–1653 cm^{-1} are characteristic of the C=O stretch of the counterions. The three weak peaks at 1442–1438, 1382–1373 and 1320–1319 cm^{-1} are due to the ring stretch of the *N*-methylpyrrole unit. The peaks at 1159–1155 cm^{-1} are perhaps caused by the C–O stretch of the counterions. The peaks at 1062–1045 cm^{-1} are due to C–H in-plane deformation of the *N*-methylpyrrole units. Those peaks occurring at 898–873, 824–807 and 786–754 cm^{-1} are due to C–H out-of-plane deformation of *N*-methylpyrrole units. The peaks at 608–578 cm^{-1} maybe come from C–C–O in-plane deformation of the counterions. Thus the IR results confirm the formation of poly(*N*-methylpyrrole) coatings and the doping of the counterions in the coatings.

Fig. 9 shows the XPS survey spectra of the poly(*N*-methylpyrrole) coatings formed at 1.13 mA/cm^2 in the medium with 0.2 M oxalic acid for 30 min. It can be seen that the iron signal has completely disappeared for this sample, indicating that the substrate was completely covered by the poly(*N*-methylpyrrole) coatings. XPS analysis of the poly(*N*-methylpyrrole) coatings shows the presence of C (73.19%), O (16.77%), and N (10.01%). The O element might come from hydrogen oxalate ions which were dopped into the poly(*N*-methylpyrrole) coatings as counterions. According to the atomic concentration of the N and O elements, the degree of insertion of the counterions was estimated to be about 0.42, which is very close to the value of 0.39 obtained by elemental analysis [16].

Fig. 10 shows the curve-fitted C1s, N1s and O1s spectra of poly(*N*-methylpyrrole) coatings. Deconvolution of the C1s signal leads to four main components at 285.0, 286.4, 288.0 and 289.0 eV with relative intensities 62:21:11:6. The four components can be attributed to C–C, C–N, C=O and O=C–O groups, respectively [28]. The N1s signal consists of only one peak centered at 400.4 eV. The O1s signal is quite broad and can be decomposed into two components at 531.8 and 533.4 eV with relative intensities close to 70:30. The two components correspond to C=O and O=C–O groups, respectively [29]. The C=O and O=C–O groups mentioned above perhaps mainly come from the hydrogen oxalate counterions.

4. Conclusion

Poly(*N*-methylpyrrole) coatings have been successfully electrodeposited on steel substrate from oxalate

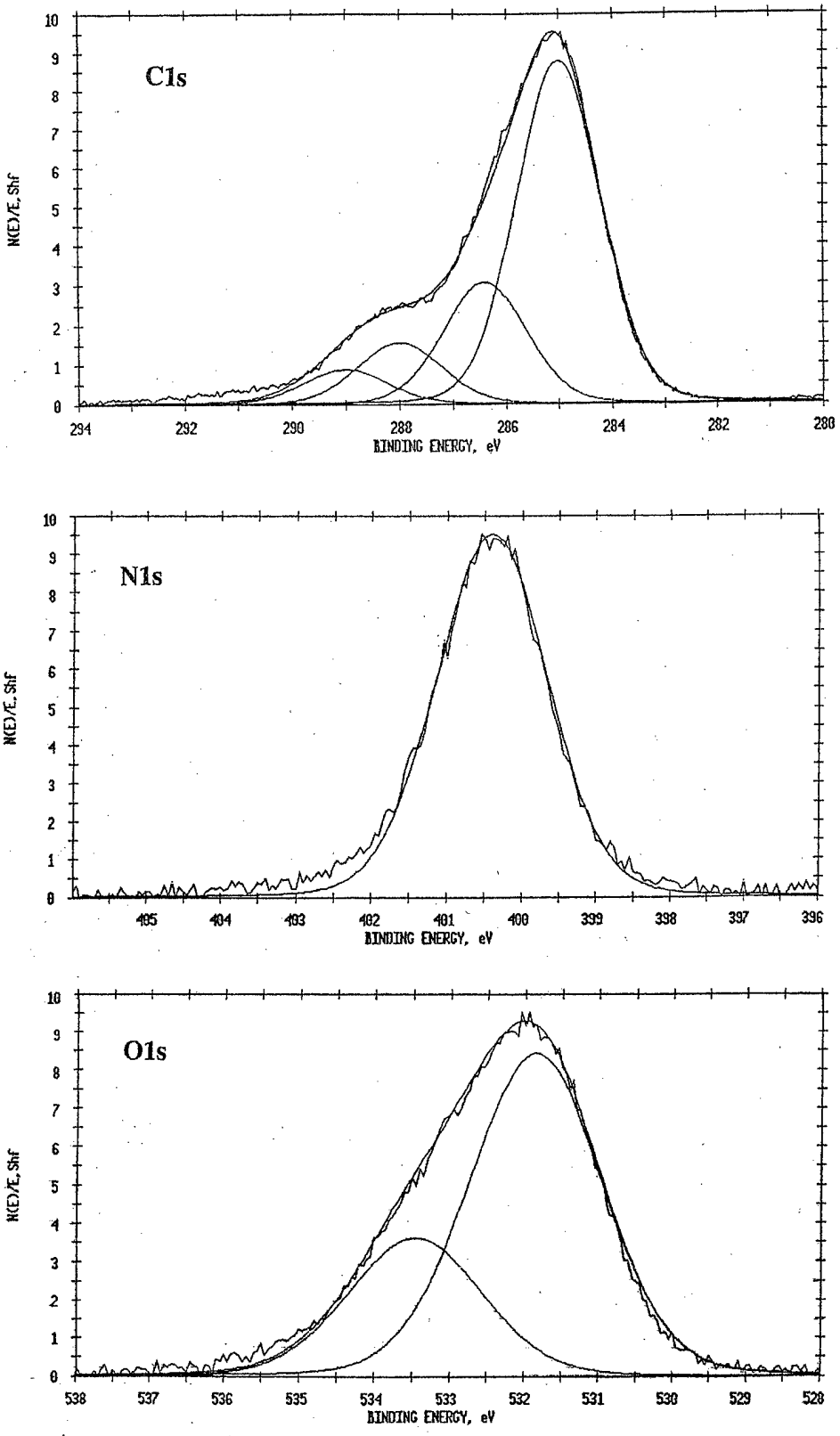

Fig. 10. Curve-fitted C1s, N1s and O1s spectra of poly(*N*-methylpyrrole) coatings.

solutions. An interphase was automatically formed on steel substrates in an acidic medium during the electrodeposition process. The composition of the interphase was found to be iron(II) oxalate dihydrate regardless of the reaction conditions. The formation time of the interphase, however, was dependent on electrochemical parameters such as the pH of the reaction medium and the applied current density. The formation of the poly(*N*-methylpyrrole) coatings and the disappearance of the interphase was also confirmed by IR and XPS. The oxalate counter ions were incorporated into the poly(*N*-methylpyrrole) coatings.

Acknowledgements

Financial support from Office of Naval Research is gratefully acknowledged.

References

[1] B.L. Funt, S.N. Bhdani, Can. J. Chem. 42 (1964) 2733.
[2] J.P. Bell, J. Chang, H.W. Rhee, R. Joseph, Polym. Composites 8 (1987) 46.
[3] J.O. Iroh, J.P. Bell, D.A. Scola, J. Appl. Polym. Sci. 41 (1990) 735.
[4] J.O. Iroh, J.P. Bell, D.A. Scola, Chem. Mater. 5 (1) (1993) 78.
[5] G.A. Wood, J.O. Iroh, Synth. Metals 80 (1996) 73.
[6] D.L. Allara, A. Baca, C.A. Pryde, Macromolecules 11 (1978) 1215.
[7] I. Curulli, A. Carelli, A. Inesi, Electrochimica Acta 30 (1985) 941.
[8] A. Chakraborty, H. Davis, M. Tirrel, J. Polym. Sci. A: Polym. Chem. 28 (1990) 3185.
[9] W. Possart, V. Schlett, J. Adhesion 48 (1995) 25.
[10] G. Mengoli, S. Daolio, M.M. Musiani. J. Appl. Polym. Sci. 28 (1983) 1125.
[11] K.M. Cheung, D. Bloor, G.C. Stevens, Polymer 29 (1988) 1709.
[12] C.A. Ferreira, S. Aeiyach, M. Delamar, P.C. Lacaze, J. Electroanal. Chem. 284 (1990) 351.
[13] M. Schirmeisen, F. Beck, J. Appl. Electrochem. 19 (1989) 401.
[14] F. Beck, R. Michaelis, F. Schloten, B. Zinger, Electrochim. Acta 39 (1994) 229.
[15] W. Su, J.O. Iroh, J. Appl. Polymer Sci. 65 (3) (1997) 417.
[16] W. Su, J.O. Iroh, J. Appl. Polym. Sci., in press.
[17] D.A. Jones, Principles and Prevention of Corrosion, Macmillan, New York, 1992.
[18] G. Socrates, Infared Characteristic Group Frequencies, John Wiley and Sons, New York, 1994.
[19] K. Nakamoto, Infrared and Raman Spectra of Inorganic and Coordination Compounds, 4th ed., John Wiley and Sons, New York.
[20] K. Nakamoto, P.J. McCarthy, Spectroscopy and Structure of Metal Chelate Compounds, John Wiley and Sons, New York, 1968.
[21] J. Fujita, K. Nakamoto, M. Kobayashi, J. Phys. Chem. 61 (1957) 1014.
[22] M.J. Schmelz, T. Miyazawa, T.J. Lane, J.V. Quagliano, Spectrochim. Acta 9 (1957) 51.
[23] J.F. Watts, An Introduction to Surface Analysis by Electron Spectroscopy, Oxford University Press, Oxford, 1990.
[24] R.A. Jones, Heterocyclic Compounds, Pyrroles, part 1, vol. 48. John Wiley and Sons, (1990).
[25] K.M. Cheung, D. Bloor, Polymer 29 (1988) 1709.
[26] C.A. Ferreira, S. Aeiyach, M. Delamar, P.C. Lacaze, J. Electoanal. Chem. 284 (1990) 351.
[27] P. Novak, B. Rasch, W. Wielstich, J. Electrochem. Soc. 138 (11) (1991) 3300.
[28] P. Pfluger, G.B. Street, J. Chem. Phys. 80 (1984) 544.
[29] D.T. Clark, A. Harrison, J. Polym. Sci. Polym. Chem. 19 (1981) 1945.